Investigation of Drug Response in Diffuse Large B-Cell Lymphoma

Due, Hanne

Publication date:
2020

Document Version
Publisher's PDF, also known as Version of record

INVESTIGATION OF DRUG RESPONSE IN DIFFUSE LARGE B-CELL LYMPHOMA

BY
HANNE DUE

DISSERTATION SUBMITTED 2020

AALBORG UNIVERSITY
DENMARK

INVESTIGATION OF DRUG RESPONSE IN DIFFUSE LARGE B-CELL LYMPHOMA

by

Hanne Due

AALBORG UNIVERSITY
DENMARK

Dissertation submitted 2020

.

Dissertation submitted: August 13, 2020

PhD supervisor: Professor Karen Dybkær,
Department of Clinical Medicine,
Aalborg University, Denmark

Assistant PhD supervisors: Professor Martin Bøgsted,
Department of Clinical Medicine,
Aalborg University, Denmark

Professor MSO Jacob Giehm Mikkelsen,
Department of Biomedicine,
Aarhus University, Denmark

Associate Professor Anne Stidsholt Roug,
Department of Hematology,
Aalborg University Hospital, Denmark

PhD committee: Professor Anne Estrup Olesen (chair)
Aalborg University

Associate Professor Lasse Sommer Kristensen
Aarhus University

Associate Professor Can Kucuk
Dokuz Eylül University

PhD Series: Faculty of Medicine, Aalborg University

Department: Department of Clinical Medicine

ISSN (online): 2246-1302
ISBN (online): 978-87-7210-690-8

Published by:
Aalborg University Press
Kroghstræde 3
DK – 9220 Aalborg Ø
Phone: +45 99407140
aauf@forlag.aau.dk
forlag.aau.dk

Printed in Denmark by Rosendahls, 2020

PREFACE

The work presented in this thesis was performed from September 2016 to August 2020 at the Department of Hematology, Aalborg University Hospital, and Department of Clinical Medicine, Aalborg University. The thesis includes two scientific papers, two systematic reviews, an introduction to the molecular aspects of diffuse large B-cell lymphoma, methodological considerations, and discussion of findings in relation to international standards. It is primarily intended for molecular biologists, bioinformaticians, and clinicians since it addresses underlying molecular response mechanisms and potential biomarkers.

The process of my PhD study has been an inspiring journey that made me grow scientifically, professionally as well as personally. I have met numerous intelligent and enthusiastic persons who have expanded my knowledge and inspired me to pursue new ideas and to adjust and optimize those already there. First and foremost, I want to express my deepest gratitude to my supervisor Professor Karen Dybkær for the opportunity to be a part of the scientific environment and for introducing me to the field of hematology research. Your extensive knowledge, scientific experience, passionate attitude, and encouragement have motivated and guided me throughout the last three years of work. Thank you for supporting and believing in me.

A special thanks to Jacob Giehm Mikkelsen and his students from the Department of Biomedicine at Aarhus University for assistance on lentiviral experiments and for making my visits comfortable and fruitful. Furthermore, I wish to thank members of the statistical group, Martin Bøgsted, Rasmus Froberg Brøndum, and Anna Amanda Schönherz, for guidance and help concerning statistical matters. I have been blessed with the best colleagues at the research unit of the Department of Hematology. Thanks to all of you. My dear previous and current fellow students Pernille, Ditte, Marijana, Issa, and Linnéa, thank you for cozy coffee breaks and for always taking your time to troubleshoot, give feedback, and support me. Moreover, I will extend my sincere gratitude to Helle Høholt and Louise Hvilshøj Madsen for your helping nature, technical assistance, and caring personality.

I acknowledge my almost long-life hobby, handball. The sport has taught me to be structured and dedicated. Combined with my parents' hardworking spirit and never-ending support, this has provided me with the drive and mindset required to obtain a PhD degree. My family is my foundation and my gratitude to you goes beyond words. Finally, I would like to express my whole-hearted gratitude to the love of my life, Martin, for his support, tolerance, and love. My beloved Ea - thank you for making me happy, grateful, and proud every day.

Hanne Due, Aalborg, August 2020

For Ea and Martin

LIST OF STUDIES

I. miR-155 as a Biomarker in B-Cell Malignancies
H. Due, P. Svendsen, J.S. Bødker, M. Bøgsted, H.E. Johnsen, T.C. Galaly, A.S. Roug, K. Dybkær.
Hindawi, BioMed**,** Research International, (2016), DOI: 10.1155/2016/9513037

II. MicroRNA-155 Controls Vincristine Sensitivity and Predicts Superior Clinical Outcome in Diffuse Large B-cell Lymphoma
H. Due, A.A. Schönherz, L. Ryø, M.N. Primo, D.S. Jespersen, E.A. Thomsen, A.S. Roug, X. Min, X. Tang, Y. Pang, K.H. Young, M. Bøgsted, J.G. Mikkelsen, K. Dybkær.
Blood Adv (2019) 3 (7): 1185–1196, DOI 10.1182/bloodadvances.2018029660

III. Aspects of vincristine-induced neuropathy in hematologic malignancies: a systematic review
M.L. Madsen, H. Due, N. Ejskjær, P. Jensen, J. Madsen, K. Dybkær.
Cancer Chemother Pharmacol 84**,** 471–485 (2019), DOI: 10.1007/s00280-019-03884-5

IV. MicroRNAs associated to single drug components of R-CHOP identifies diffuse large B-cell lymphoma patients with poor outcome and adds prognostic value to the international prognostic index
H. Due, R.F. Brøndum, K.H. Young, M. Bøgsted, K. Dybkær.
BMC Cancer **20,** 237 (2020), DOI: 10.1186/s12885-020-6643-8

The following 5 articles were also published during the PhD period; however, they are not considered as a part of the dissertation.

1. Expression of NOTCH3 exon 16 differentiates Diffuse Large B-cell Lymphoma into molecular subtypes and is associated with prognosis
D.S. Jespersen, A.A Schönherz, H. Due, M. Bøgsted, T.E. Søndergaard, K. Dybkær
Scientific Reports 9**,** 335 (2019), DOI: 10.1038/s41598-018-36680-x

2. A multiple myeloma classification system that associated normal B-cell subset phenotypes with prognosis
J.S. Bødker, A. Schmitz, R.F. Brøndum, A.A. Schönherz, M. Sønderkær, C. Vesteghem, H. Due, *et al.*
Blood Adv (2018) 2 (18): 2400–2411, DOI: 10.1182/bloodadvances.2018018564

3. Molecular classification of tissue from a transformed non-Hogkin's lymphoma case with unexpected long-time remission
J.S. Bødker, M.T. Severinsen, T.C. El-Galaly, R.F. Brøndum, M.B. Laursen, S. Falgreen, M. Nyegaard, L.H. Jacobsen, A.A Schönherz, H. Due, *et al.*
Exp Hematol Oncol 6, 3 (2017), DOI: 10.1186/s40164-016-0063-0

4. High CXCR4 expression impairs rituximab response and the prognosis of R-CHOP-treated diffuse large B-cell lymphoma patients
M.B. Laursen, L. Reinholdt, A.A. Schönherz, H. Due, D. S. Jespersen, L. Grubach, *et al.*
Oncotarget. (2019); *10*: 717-731.

5. Identification of BLNK and BTK as mediators of rituximab-induced programmed cell death by CRISPR screens in GCB-subtype diffuse large B-cell lymphoma
E.A Thomsen, A.B. Rovsin, M.V. Anderson, H. Due, J. Huang, Y. Lou, K. Dybkær, J.G. Mikkelsen.
Molecular Oncology (2020), DOI:10.1002/1878-0261.12753

ENGLISH SUMMARY

Lymphomas are a group of malignant neoplasms arising from lymphocytes. The most frequent type among adults is diffuse large B-cell lymphoma (DLBCL) with approximately 450 new patients diagnosed each year in Denmark. DLBCL is a biologic heterogeneous disease that is treated with the multidrug immuno-chemotherapy regimen R-CHOP, consisting of rituximab, cyclophosphamide, doxorubicin, vincristine, and prednisone, yet 20-50% of patients eventually die from refractory disease or relapse due to treatment resistance. Improved understanding of cellular response and resistance mechanisms of R-CHOP is pivotal for optimizing treatment efficacy in DLBCL and equally important is identification of risk markers enabling stratification of patients with efficient and poor response at time of diagnosis. The molecular heterogeneity of DLBCL is reflected in the expression profile of microRNAs (miRNAs), which are small non-coding RNA molecules with a fundamental regulatory role in various cellular processes. Deregulated miRNA expression is associated with several cancer types, including DLBCL, and the purpose of this PhD study was to investigate the role of miRNAs in chemotherapy response and resistance in DLBCL and evaluate the prognostic impact.

In paper II we focus on the anti-mitotic drug vincristine, which exerts its anti-neoplastic effect by binding to microtubules of the mitotic spindle leading to cell cycle arrest. We observed higher expression of miR-155 in vincristine sensitive DLBCL cells and showed that loss of miR-155 induces vincristine resistance. This documents that this particular miRNA is functionally involved in vincristine response in DLBCL cells. Furthermore, miR-155 displayed prognostic impact with inferior survival outcome of DLBCL patients with low levels of miR-155. The biomarker potential of miR-155 in B-cell malignancies was examined by reviewing the literature (Paper I). As DLBCL is a heterogeneous disease, paper IV attempts to improve the risk stratification of DLBCL patients by building a prognostic panel of several miRNAs whose expression is associated with response to drug components of R-CHOP. The panel consists of seven miRNAs, which in addition to miR-155 includes miR-21, miR-34a, miR-23a, miR-24-2, miR-27a, and miR-146a. Combining this panel with the clinical prognostic index (IPI) improved the prognostic performance substantially.

In clinical treatment, the aim is to obtain optimal toxic effect of a drug and at the same time minimize side effects. The dose-limiting side effect of vincristine is neuro-toxicity, caused by interference of microtubules in the neurons. In Paper III we overviewed the aspects of vincristine-induced neuropathy through literature study. In a local pilot cohort, neuropathy was reported in 37% of the patients, resulting in vincristine dose reduction or substitution to vinblastine. Clinical parameters and predicted vincristine response were examined for potential to stratify patients according to risk of vincristine-induced neurotoxicity, however, all the investigated factors were without significant association to patients with manifested neurotoxicity.

DANSK RESUMÉ

Lymfekræft opstår i den celletype af hvide blodlegemer, som hedder lymfocytter. Diffust storcellet B-celle lymfom (DLBCL) er den hyppigste form for lymfekræft hos voksne og diagnosticeres hvert år hos ca. 450 patienter i Danmark. Biologisk set er DLBCL en heterogen sygdom, som behandles med immun- og kemoterapiregimet R-CHOP bestående af rituximab, cyclofosfamid, doxorubicin, vincristin og prednisolon. Imidlertid dør 20-50% af patienterne af refraktær sygdom eller sygdomstilbagefald, fordi deres tumor er behandlingsresistent. For fremtidigt at kunne forbedre behandlingen af DLBCL-patienter er det nødvendigt at opnå en større viden om respons- og resistensmekanismer for de enkelte stoffer i R-CHOP-behandlingen. Samtidig er det også ønskværdigt, allerede på diagnosetidspunktet at kunne adskille responderende patienter fra de som ikke responderer. Den molekylære forskellighed der ses blandt DLBCL patienter afspejles i deres microRNA (miRNA) profil, som er små ikke-kodende RNA-molekyler med en fundamental rolle i regulering af mange forskellige cellulære processor. Deregulering af miRNA ekspression er associeret til mange typer af kræft, inklusiv DLBCL, og formålet med dette PhD studie var at undersøge hvilken rolle miRNA spiller i responsmekanismerne mod kemoterapeutika i DLBCL, samt om deres ekspression kan anvendes til risikovurdering af DLBCL-patienter.

I artikel II fokuserer vi på stoffet vincristin, som hæmmer tumorvækst ved at interferere med mikrotubuli i de mitotiske spindle, hvorved celledeling stoppes. Vi identificerede højt udtryk af miR-155 i vincristin sensitive DLBCL-celler og viste at tab af miR-155 gør DLBCL cellerne mere resistente imod vincristin behandling. Dette dokumenterer at denne miRNA har direkte betydning for vincrtistin respons i DLBCL. Desuden udviste miR-155 potentiale som prognostisk markør, hvor lavt niveau af miR-155 er forbundet med dårligere overlevelsessandsynlighed. Biomarkørpotentialet af miR-155 i lymfekræft blev undersøgt i et litteraturstudie (artikel I). Da DLBCL er karakteriseret ved en høj grad af biologisk variation, søger vi i artikel IV at forbedre risiko-stratificeringen af DLBCL-patienter ved at bygge et panel af miRNA, hvis ekspression er associeret til respons mod et eller flere af stofferne fra R-CHOP-behandlingen. Panelet består af syv miRNA som udover miR-155 inkluderer miR-21, miR-34a, miR-23a, miR-24-2, miR-27a, og miR-146a. Kombination af dette panel og det kliniske internationale prognostiske indeks (IPI), forbedrede den prognostiske evne væsentligt.

I kræftbehandling er målet at opnå optimal toksisk effekt og samtidig minimere bivirkninger. Den dosis-begrænsende bivirkning af vincristin er neurologisk toksicitet, hvilket skyldes interaktion med mikrotubuli i nervecellerne. I artikel III belyste vi med udgangspunkt i litteraturen flere aspekter af vincristin-induceret nerveskade. I vores lokale DLBCL-patient kohorte, var denne bivirkning rapporteret i 37%, hvilket medførte dosis reduktion eller skift til vinblastin. Kliniske parametre samt prædikteret vincristin sensitivitet blev testet for potentiale til at identificere øget risiko for udvikling af vincristin-induceret neurotoksicitet, men ingen af de undersøgte faktorer var forskellige mellem patienter med og uden neurotoksicitet.

TABLE OF CONTENTS

ABBREVIATIONS

ABC	Activated B-cell-like
AGO	Argonaute
AUC	Area under the dose response curve
BAGS	B-cell associated gene signatures
BCR	B-cell receptor
BTK	Bruton's tyrosine kinase
CRISPR	Clustered Regularly Interspaced Short Palindromic Repeats
CSR	Class-switch recombination
ddPCR	Droplet digital PCR
DGCR8	DiGeorge syndrome chromosomal region
DLBCL	Diffuse large B-cell lymphoma
DLBCL NOS	Diffuse large B-cell lymphoma not otherwise specified
DSB	Double-stranded break
ECOG	Eastern Cooperative Oncology Group
GC	Germinal center
GCB	Germinal center B-cell-like
GEP	Gene expression profiles
GFP	Green fluorescent protein
GSEA	Gene set enrichment analysis
G-model	Growth-based model
HDR	Homology-directed repair
HL	Hodgkin lymphoma
Ig	Immunoglobulin
IHC	Immunohistochemistry
IPI	International Prognostic Index
LDH	Lactate dehydrogenase
miRNA	MicroRNA
NF-κB	Nuclear factor kappa B
NHEJ	Non-homologous end-joining
NHL	Non- Hodgkin lymphoma
Nt	Nucleotide
PAM	Protospacer adjacent motif
PGK	Phosphoglycerate kinase
Pol	Polymerase
pre-miRNA	Precursor microRNA
pri-miRNA	Primary microRNA
qPCR	Quantitative PCR

REGS	Resistance gene signature
RISC	RNA-induced silencing complex
R-CHOP	Rituximab, cyclophosphamide, doxorubicin, vincristine, prednisone
sgRNA	Single guide RNA
SHM	Somatic hypermutation
shRNA	Short hairpin RNA
STR	Short tandem repeat
tAUC	Time varying area under the ROC curve
TALEN	Transcriptional activator-like effector nucleases
TGI	Total growth inhibition
TRBP	TAR RNA-binding protein
TuD	Tough Decoy
UTR	Untranslated region
VDJ	Variable, Diversity, Joining
WHO	World Health Organization
ZFN	Zinc-finger nucleases

1. INTRODUCTION

B-cell development, activation, and differentiation

B-cells are white blood cells that constitute an essential part of the adaptive immune system, which heavily relies on the humoral immune response where foreign pathogens and toxins are eliminated by antibodies produced by B-cells. Antibody diversity is important for efficient immune response and is achieved through highly organized series of developmental stages of the B-cell, where the B-cell antigen receptor (BCR) is generated and altered to achieve high-affinity antibodies (Figure 1) [1]. The BCR is composed of two heavy chain and two light chain immunoglobulin (Ig) polypeptides linked by disulfide bridges [2].

The development of B-cells initiates in the bone marrow, where pluripotent hematopoietic stem cells self-renew or differentiate into B-cell precursors [3]. During maturation in the bone marrow, B-cell precursors rearrange the Variable, Diversity, and Joining (VDJ) gene segments of the heavy and light chain Ig genes whereby specificity and diversity of the BCR are generated [3,4]. The functionality of the BCR is tested for autoreactivity, and if positive, BCRs are subjected to receptor editing to generate non-autoreactive BCRs, however, if unsuccessful the B-cell will undergo apoptosis or anergy [4]. B-cells passing this checkpoint leave the bone marrow as naïve B-cells co-expressing surface IgM and IgD and circulate between the peripheral blood and the secondary lymphoid organs, which include lymph nodes, spleen, tonsils, and mucosa-associated lymphoid tissue [2,3].

In the secondary lymphoid tissues, naïve B-cells can encounter an antigen and be activated by interaction with T-helper cells, which prime the germinal center (GC) formation [1,3]. The GCs consist of a light and a dark zone, each homing different B-cell populations (Figure 1). Naïve B-cells differentiate into centroblasts, which are large and highly proliferative cells making up the dark zone of the GC and undergo somatic hypermutation (SHM) of the V gene segment by which mutations are introduced, resulting in diversification of the antibody response. Centroblasts migrate into the light zone of the GC and differentiate into the smaller and less proliferative centrocytes. In the light zone, they reencounter the antigen in a T-cell dependent manner to ensure increased BCR affinity [1,5,6]. For most B-cells, mutations introduced by SHM will decrease affinity for the antigen and these cells will undergo apoptosis; however, centrocytes with increased affinity will be positively selected.

Each B-cell cycles between the dark and the light zone of the GC to undergo multiple rounds of SHM and cell divisions to ensure high antibody affinity [7]. This migration is mediated by chemotaxis through a gradient of chemokines produced by stromal cells in the light zone, which secrete the CXC-chemokine ligand 12 (CXCL12) attracting centroblasts as they express the CXC-chemokine receptor 4 (CXCR4). Centrocytes express CXCR5 and are attracted to the ligand CXCL13, which is abundant in the dark zone [7]. Following optimal affinity selection, centrocytes undergo class-switch DNA recombination (CSR) of the constant region of BCR to

produce antibodies of different isotype classes (IgE, IgA, or IgG) [5,6]. Mature B-cells leave the GC and differentiate into memory B-cells or plasmablasts, with the latter differentiating into antibody-producing plasma cells in the bone marrow [3].

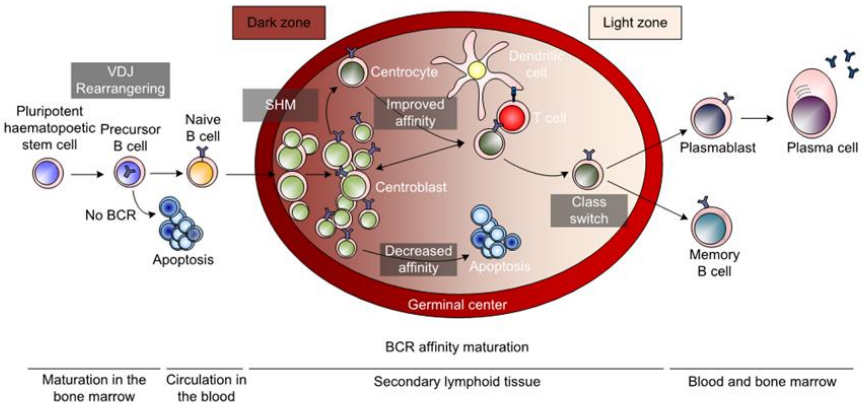

Figure 1. B-cell differentiation. Maturation of B-cells involves series of highly organized developmental stages starting in the bone marrow where hematopoietic stem cells differentiate into precursor B-cells. Precursor B-cells rearrange their Variable, Diversity, and Joining (VDJ) gene segments to generate the B-cell receptor (BCR), which subsequently are tested for autoreactivity. B-cells with non-autoreactive BCR differentiate into naïve B-cells that circulate between the peripheral blood and secondary lymphoid tissue until antigen encounter leading to B-cell activation and formation of germinal centers (GCs). GCs consist of a dark and a light zone with centroblast and centrocyte B-cells, respectively. Centroblasts undergo somatic hyper-mutation (SHM) and differentiate into centrocytes, which re-encounter antigens to select B-cells expressing a BCR with increased affinity. B-cells cycle several rounds between the dark and light zone to ensure optimal BCR affinity. Following optimal affinity, a shift in effector function by class-switch DNA recombinase takes place, and B-cells leave the GCs as memory B-cells or plasmablasts, which further can differentiate into the antibody-producing plasma cells.

Lymphoma

Cancer arises when cells acquire growth and survival benefits through epigenetic or genetic alterations. These advantages occur in different biological traits, described as the hallmarks of cancer [8]. The hallmarks of cancer include genome instability, the ability to sustain proliferative signaling, evade growth suppressors, reprogram energy metabolism, induce tumor-promoting inflammation, resist cell death, enable replicative immortality, induce angiogenesis, activate invasion and metastasis, and lastly evade immune destruction [8].

Lymphomas are a heterogeneous group of malignant neoplasms arising from lymphocytes of natural killer cell, T-cell, or B-cell origin [9]. Lymphomas are classified according to guidelines by World Health Organization (WHO), which include both clinical, morphological, histological, and genetic features of the disease entities [9]. There are two main classes of lymphoma, Hodgkin lymphoma (HL) and non-Hodgkin lymphoma (NHL), of which the latter is the most prominent (Figure 2). The majority of NHLs derive from B-cells with the most frequent being diffuse large B-cell lymphoma (DLBCL), accounting for 30-40% of all newly diagnosed adult NHL [10]. Other common types of B-cell derived NHLs include follicular lymphoma, mantle cell lymphoma, splenic marginal zone B-cell lymphoma, and chronic lymphocytic leukemia [9].

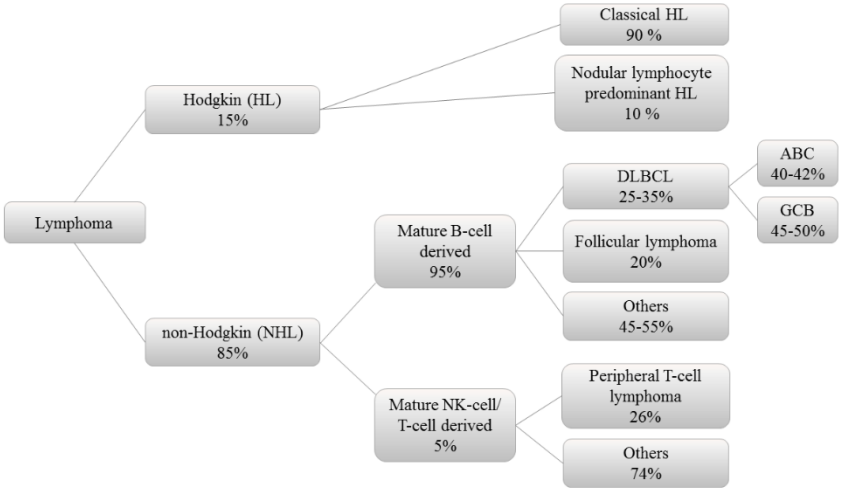

Figure 2. Lymphoma classification. Frequencies obtained from [9].

B-cell derived lymphomas can arise at multiple stages of the normal B-cell differentiation, and the stage at which the malignant clone develops is used in classification of B-cell lymphomas (Figure 3). Assessed by Ig rearrangement status, most lymphomas derive from GC B-cells or B-cells that have passed the GC [11], indicating the antigen mediated stimulation and remodeling processes of the Ig gene as important in the malignant transformation. SHM and CSR include breakage and rejoining of DNA, which increases the risk of introducing mutations and translocations, contributing to malignant transformation [2,5]. Moreover, the double-stranded DNA breaks in SHM and CSR occur in the GC wherein B-cells replicate remarkably fast, and DNA damage checkpoints are silenced by repressive activity of BCL6 [12]. Consequently, genetic alterations implicated in lymphomagenesis often derive from errors in one of the processes. Furthermore, SHM aberrantly targets some proto-oncogenes, including *PAX5, MYC, PIM1*, among others, and this mistargeting and introduction of mutations also contribute to development of DLBCL [13,14]. B-cell neoplasms often undergo clonal evolution with a gain of additional genetic alterations leading to a clinical and/or histological progression of the lymphoma [11].

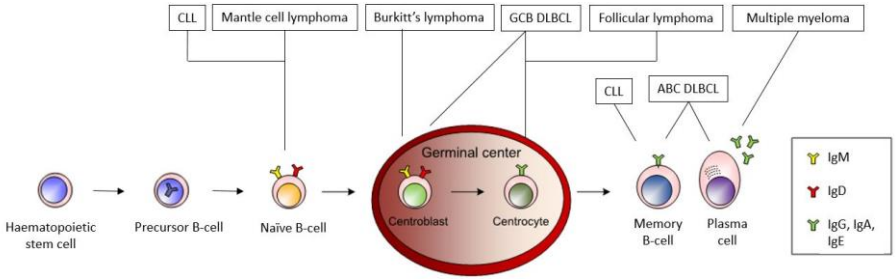

Figure 3. Cellular origin of B-cell lymphomas. B-cell malignancies can arise at various stages of the normal B-cell differentiation, and the figure depicts the cell-of-origin for selected B-cell derived malignancies.

Diffuse large B-cell lymphoma

The crude incidence of DLBCL is 3-4/100,000 in the European Union [15], which has increased during the last decades [16]. Incidence rates are increasing with age and more often men are affected than women [17]. The etiology of DLBCL remains unknown; however, autoimmune disease, underlying immunodeficiency, and a family history of lymphoma have been identified as risk factors [9,18]. DLBCL can be located in the lymph nodes or other tissues, referred to as either nodal or extranodal, respectively [9]. It can develop *de novo*, referred to as primary disease, or from progression or transformation of an indolent NHL such as follicular lymphoma [9,19]. DLBCL encompasses a clinical, morphological, and molecularly heterogeneous group of lymphomas, which by WHO is subdivided into four categories: DLBCL not otherwise specified (DLBCL NOS), other lymphomas of large B-cells, high-grade B-

cell lymphoma, and B-cell lymphoma unclassifiable. DLBCL-NOS is the most common type and has still a great morphological and molecular heterogeneity [9].

Prognostic assessment of DLBCL patients is performed using the International Prognostic Index (IPI), which has been the gold standard in clinical practice for decades [20]. IPI is a scoring system ranging from 0 to 5 based on five dichotomized clinical parameters with equal weight, and one point assigned each of the following risk factors: age at diagnosis (>60), elevated serum lactate dehydrogenase (LDH), extranodal involvement >1, Eastern Cooperative Oncology Group (ECOG) performance status ≥2, and Ann Arbor stage III or IV which is determined by tumor localization. Based on the IPI scoring system, DLBCL patients are stratified into four risk groups with different outcomes: low (score 0-1), intermediate-low (2), intermediate-high (3), and high-risk (4-5) disease [20]. Revised versions of IPI assigning patients into fewer prognostic subgroups or with inclusion of more variables have been introduced [21,22]; however, the original IPI is still the standard tool since population-based studies including clinical trials confirmed robustness of IPI despite treatment alterations [21,23].

Molecular subclasses of DLBCL

The molecular heterogeneity of DLBCL-NOS can be explained by the cell-of-origin. Gene expression profiling (GEP) enables cell-of-origin classification of DLBCL into two histologically indistinguishable subclasses: the activated B-cell-like (ABC) and the germinal center B-cell-like (GCB) of which the GCB subclass is slightly more frequent with an overall incidence of 45-50% as opposed to 40-42% for the ABC subclass (Figure 2+4) [24–27]. Cases not classifiable as ABC or GCB are defined unclassified (UC). The molecular ABC/GCB subclasses reflect a subset of the normal B-cell differentiation stages (Figure 3), where GCB resembles GC B-cells having ongoing SHM and CSR and expression of IgM or IgD, and ABC-DLBCL is similar to post-GC B-cells with aberrant CSR and expression of IgE, IgA, or IgG [2,24]. The ABC and GCB subclasses differ in pathogenesis and clinical outcome [24,25] with GCB patients having a 5-year survival rate of 69-79% compared to 52-53% for those patients classified with ABC-DLBCL when treated with standard immune-chemotherapy R-CHOP (described in a subsequent section) [28]. In addition, the molecular subclasses display distinct genetic alterations and deregulated signaling pathways [24].

Genetic abnormalities of ABC-DLBCL involve activating mutations of the BCR signaling pathway and genetic lesions, causing constitutive activation of anti-apoptotic nuclear factor kappa B (NF-κB) signaling. More than 20% of ABC-DLBCL patients harbor somatic mutations in the Ig-associated gene *CD79B*, which in complex with CD79A mediates BCR signaling. Mutations in the cytoplasmic tyrosine-based motif of this immunoreceptor circumvent negative feedback and thereby causing chronic active BCR [12,29]. Oncogenic mutations in *CARD11* occur in 7-18% of

ABC-DLBCL cases and 4-17% of GCB cases. The *CARD11* mutations impair auto-inhibition resulting in a hyperactive state that leads to constitutive NF-κB signaling [30,31], a hallmark of ABC-DLBCL tumors. Functional *in vitro* experiments documented requirement of NF-κB for proliferation and survival of ABC-DLBCL cell lines but not for GCB-DLBCL cells, and in addition, gene expression analysis identified higher expression of NF-κB transcription factors in ABC classified patients as compared to GCB-DLBCL patients [32]. Since the CARD11 protein is essential for active NF-κB pathway and most ABC tumors have wildtype *CARD11*, genetic *in vitro* screens focused on the role of BCR signaling and found that the BCR signaling component Bruton's tyrosine kinase (BTK) is required for survival of ABC-DLBCL with wildtype *CARD11* [29]. Furthermore, somatic gain-of-function mutations in *MYD88* also promote NF-κB signaling. The single amino acid substitution (L265P) of *MYD88* is specific for ABC-DLBCL and is observed in 30% of the patients [33].

Alterations characteristic of the GCB subclass of DLBCL are gain-of-function mutations of the *EZH2* oncogene, at which the Y641 residue of the catalytic domain is the mutational hotspot. These mutations are detected in 22% of GCB classified patients and are thereby one of the most frequent genetic events of GCB-DLBCL [34]. Other genetic events reported in GCB-DLBCL are protein-truncating mutations in *S1PR2* and *GNA13* (7% and 10%, respectively), which encode components of a G-coupled receptor involved in inhibitory regulation of growth and local confinement of GC B-cells [35]. In addition, activating mutations of the transcriptional activator MEF2B are observed in 11% of GCB-DLBCL cases and lead to enhanced expression of the oncogene *BCL6* [36], a characteristic of GCB-DLBCL. The transcriptional repressor BCL6 controls the B-cell differentiation of the GC and is essential for maintenance of B-cell proliferation while allowing tolerance of DNA remodeling events without inducing DNA damage responses [12]. In detail, BCL6 permits DNA remodeling events without response to DNA damage by suppression of *TP53*, allows cell cycle progression through repression of the inhibitors p21 and p27, reduces apoptosis by targeting *BCL2*, and controls differentiation into plasmablasts by repressing *PRDM1* [12].
Furthermore, chromosomal alterations are common in DLBCL and are differentially observed across molecular subclasses. Translocations affecting the BCL6 locus in band 3q27 are the most common rearrangement in DLBCL occurring in 30% of the cases and with higher frequency in ABC-DLBCL [37,38]. The t(14;18)(q32;q21.3) rearrangement of *BCL2* is present in 20-30% of DLBCL patients and more commonly in GCB cases and juxtapose *BCL2* adjacent to *IGH*, leading to constitutive expression of BCL2 [39–41]. Rearrangement of *MYC* occurs evenly in ABC and GCB-DLBCL and is detected in 5-15% of the patients [9,42,43]. Simultaneous translocations and aberrant expression of BCL2, BCL6, and MYC are associated with aggressive disease and have led to the introduction of the category high-grade lymphoma encompassing double-expressors with dual high expression of BCL2 and MYC and double-hit lymphoma with rearrangement of *MYC* and *BCL2* or less commonly *BCL6* (Figure 4) [9,41,44–47]. When all three rearrangements are present, it is denoted triple-hit

lymphoma. Co-expression of BCL2 and MYC is preferentially detected in ABC-DLBCL and dual-expressor patients have significantly inferior outcomes [41,48]. In line, double-hit lymphoma with *BCL2* and *MYC* is associated with shorter overall survival and is more frequent among GCB cases [41,49]. *BCL6-MYC* double-hit does not display subclass-specific occurrence and the prognostic significance is ambiguous [9,48]. The frequency of double-hit lymphoma in diagnostic DLBCL is 5-10%, whereas it increases to 25-30% of relapsed DLBCL, supporting the role of *MYC*, *BCL2*, and *BCL6* translocations as driver event in both treatment resistance and progression [50,51].

The molecular ABC/GCB classification has entered clinical diagnostic and prognostic evaluation, complementing IPI [9]. The gene expression-based cell-of-origin classification utilizes techniques like microarray, RNA-sequencing, and Nanostring, a digital barcode system. However, simplified and translated classification algorithms by immunohistochemistry (IHC) are commonly used (Figure 4) [52–54], and by applying the Hans algorithm with antibodies against CD10, BCL6, and IRF4/MUM1, DLBCL is classified into GCB and non-GCB subgroups leaving no cases to be unclassified [52]. IHC has the advantage of being cheap and fast, but display issues of reproducibility, accuracy, and reliability when compared between diagnostic sites [9,41].

Other transcriptional based classification systems

The ABC/GCB classification is established from a fraction of the naturally occurring B-cell subsets, specifically the GC B-cells centroblasts and centrocytes and *in vitro* activated B-cells from peripheral blood [24]. An extended cell-of-origin classification has been developed by applying subset-specific B-cell associated gene signatures (BAGS) from the normal B-cell differentiation hierarchy (Figure 4) [55]. The BAGS signature is based on fluorescence-activated cell sorting and transcriptional profiling of naïve, germinal centroblasts and centrocytes, post-germinal memory B-cells, and plasmablasts of normal human tonsils, and DLBCL patients are classified based on their GEP and assigned the subtype with highest predicted probability. The BAGS subtypes have distinct genetic profiles, differentially activated signaling pathways, and response to chemotherapeutics used in a routine clinical setting for treatment of DLBCL. In addition, BAGS subtypes display prognostic impact independent of IPI and the ABC/GCB classification, though prognostic evaluation within ABC and GCB classified patients, respectively, revealed significance exclusively in GCB-DLBCL [55].
Other prognostic transcriptional based signatures exist, reflecting multiple biological attributes of DLBCL (Figure 4). The character of the tumor microenvironment is represented by the Stromal 1/Stromal 2 signatures [26] and the Host Response signature [56]. Other biologically relevant subsets of DLBCL are based on the B-cell receptor and oxidative phosphorylation gene signatures [56], however, none of these are widely used.

None of the gene expression-based classification systems is stringent in the sense that patients assigned inferior prognostic subclasses are potentially curable, while other patients defined with favorable prognosis succumb to the disease even after aggressive treatment. Thus, studies of other molecular features of the tumors have been conducted in attempt to improve risk stratification of DLBCL patients.

Genetic classification systems

The expansion of sequencing technologies has provided comprehensive investigations of the mutational landscape of DLBCL, which revolutionized the understanding of the genetic basis of DLBCL and led to the identification of several genetic subtypes (Figure 4) [57–62]. Chapuy et al. [59] identified 158 genetic driver alterations that cluster into five distinct genetic subsets, referred to as coordinate gene signature C1-C5, and in addition a subset, C0, without detectable genetic alterations. Favorable prognostic outcome is observed for DLBCL patients with C0, C1, and C4 tumors, whereas those with C3 and C5 DLBCL exhibit adverse outcome. These coordinate gene signatures identify genetically distinct cell-of-origin subtypes, of which the C3 and C4 represent subsets of GCB-DLBCL utilizing different mechanisms to perturb common pathways and in addition, display differences in outcome. The C1 and C5 coordinate signatures define subsets of ABC-DLBCL with distinct pathogenetic mechanisms and superior outcome for patients assigned C1-ABC [59].

The genetic classifier by Schmitz et al. [58] identifies four genetic subtypes termed BN2 (*BCL6* fusions or *NOTCH2* mutations), EZB (*EZH2* mutations or *BCL2* translocations), MCD (co-occurrence of *MYD88*^{L265P} and *CD79* mutations), and N1 (*NOTCH1* mutation), of which the MCD and N1 subtypes have significantly inferior outcome than BN2 and EZB, with 5-year survival outcome of 26%, 35%, 65%, and 68%, respectively, when treated with standard immuno-chemotherapy [58]. These subtypes are included in the recently developed LymphGen algorithm, which provides a probabilistic classification of a tumor from an individual DLBCL patient into seven genetic subtypes (BN2, MCD, N1, EZB MYC+, EZB MYC-, A53, ST2) [60]. LymphGen was implemented by assigning patients to the four previously identified genetic subtypes and subsequent analysis of the remaining unassigned patients. Of these, *TP35* was the most frequently mutated gene without enrichment in one of the other subtypes, and furthermore, recurrent mutations were observed in *TET2*, *P2RY8*, *SGK1*, leading to the genetic subtypes termed A53 and ST2. LymphGen assigns 63.1% of DLBCL patients to one or more of the six genetic subtypes with BN2, MCD, and EZB being most frequent. The MCD signature is enriched for ABC-DLBCL patients, whereas GCB patients predominate the EZB subtype. As opposed, BN2, A53, and ST2 are comprised of different cell-of-origin subclasses. Patients assigned the MCD subtype have inferior overall survival probability, especially in comparison to BN2 and ST2. For GCB-DLBCL patients, the EZB subtype displays adverse prognosis; however, based on information on double hits with *BCL2* and *MYC* rearrangement, the EZB is divided into genetic MYC+ and MYC- subtypes, the latter

with superior prognosis [60]. Moreover, another five genetic subtypes termed MYD88, BCL2, SOCS1/SGK1, TET2/SGK1, and NOTCH2 have recently been published by Lacy et al. [61] in addition to a group of not elsewhere classified (NEC) encompassing 27% of the patients. Predominant mutations of the MYD88 subtype include *MYD88*^{L265P}, *PIM1*, *CD79B*, and *EVT6* and are enriched for patients of ABC origin. As opposed, GCB-DLBCL cases mainly constitute the BCL2 subtype, characterized by mutations of *EZH2*, *BCL2*, *TNFRSF14*, *KMT2D*, and *MEF2B,* and the TET2/SGK1 subtype, which beside *TET2* and *SGK1* mutations is dominated by variants in *KLHK6*, *MAP2K1*, *ZFP36L1*, *BRAF, and KRAS.* Patients of the MYD88 and NOTCH2 subtypes have inferior outcome in comparison to patients assigned TET2/SGK1, SOCS1/SGK1, and BCL2, with 5-year overall survival of 42%, 48%, 60%, 62%, and 65%, respectively, when treated with standard immuno-chemotherapy [61].

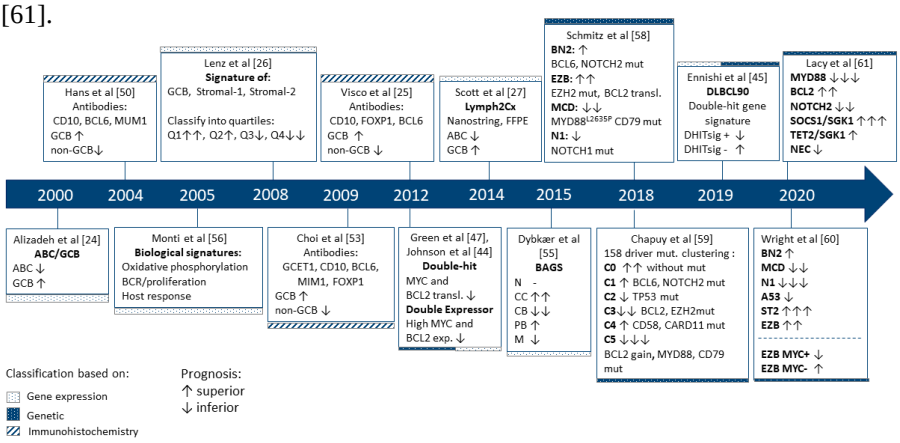

Figure 4. Timeline of the molecular subclassifications of DLBCL. A broad overview of prognostic molecular subclassifications of DLBCL. Horizontal bars (top/bottom) indicate whether the classification relies on gene expression, genetics, or immunohistochemical analysis of the tumor. Prognosis of the respective subclasses is indicated by arrows, ↑ corresponding to superior and ↓ to inferior. The more arrows, the better or worse prognosis.

Thus, targeted and global next-generation sequencing has not only revealed a compendium of common genetic alterations in DLBCL, of which several exhibit segregations by cell-of-origin, but also lead to complete new frameworks for DLBCL risk stratification based on tumor genetics [63]. These genetic classifications improve the understanding of the molecular heterogeneity of DLBCL; however, several discrepancies of these studies have to be reconciled prior to exploration of stratified treatments. Although partial overlap in genetic classes, no unambiguous link between the majority of genetic aberrations and genetic clusters has been provided, which, together with the limitation of a large number of unclassified tumors, leave the nature of the DLBCL genetic subclassification unresolved [63].

DLBCL treatment and outcome

First-line treatment of DLBCL patients is a multidrug regimen consisting of: Rituximab (R), a humanized monoclonal antibody against CD20, which is a surface protein expressed on all B-cells; Cyclophosphamide (C), a DNA alkylating agent that in addition facilitates antibody-mediated killing through cytokine release; Doxorubicin (H), a topoisomerase II inhibitor which also intercalates DNA base pairs; Vincristine (O), an ant-microtubule agent; and the steroid Prednisone (P) (R-CHOP). The mostly non-overlapping side effects permit their combined administration. Addition of rituximab to the CHOP regimen has improved DLBCL survival substantially with a 10-15% increase in 5-year overall survival to 60-70% [64]. The pharmacological principle of R-CHOP efficacy is poorly understood; however, functional genetic *in vitro* studies recently observed low cross-resistance but no synergistic interaction among the components of R-CHOP [65]. This suggests that treatment efficacy of the regimen is mediated by independently effective drugs without overlapping resistance mechanisms.

Despite treatment improvement with inclusion of rituximab, approximately 40% of DLBCL patients suffer from primary refractory disease and relapse due to drug resistance, demonstrating that standard provided treatment regimens are not sufficient to cure all patients [28,64,66]. Relapsed and refractory patients are treated with high-dose immuno-chemotherapy and autologous stem cell transplantation; however, most patients are not eligible due to their age and comorbidities, whereby only a fraction of patients with relapse are cured [67].

In the last decade, several clinical trials have been conducted in an attempt to improve the R-CHOP regimen; however, with limited benefit. Different strategies have been applied, including dose intensification, rituximab maintenance after initial treatment, consolidation with autologous transplantation [77–80], and in recent randomized phase III trials R-CHOP is combined or substituted with non-chemotherapeutic agents [68–76] (Table 1).

Study	Subclasses	No.	Regimen	Target	Result
GOYA [68]	None	1418	Obinutuzumab-CHOP	CD20	Negative
MAIN [69]	CD20+	787	R-CHOP + bevacizumab	VEGF-A	Negative
REMoDL-B [70–72]	ABC/GCB	918	R-CHOP + bortezomib	Proteasome NF-κB	Negative
PHOENIX [73,74]	non-GCB/GCB	800	R-CHOP + ibrutinib	BTK	Negative
ROBUST [75,76]	non-GCB/GCB	560	R-CHOP + lenalidomide	Immuno-modulatory	Negative

Table 1. Phase III clinical trials in DLBCL. ABC, activated B-cell; BTK, Bruton's tyrosine kinase; CHOP, cyclophosphamide, doxorubicin, vincristine, prednisone; GCB, germinal center B-cell; NF-κB, nuclear factor kappa B; R-CHOP, rituximab, cyclophosphamide, doxorubicin, vincristine, prednisone; VEGF-A, vascular endothelial growth factor A.

Moreover, molecular guided therapy using biomarkers, including ABC/GCB, double-expressor, and double-hit have been evaluated; however with inconsistent implementation in clinical trials [28,46,72,74,80]. Since the ABC subclass is the largest risk group of DLBCL, most clinical studies are focused on improving overall survival for these patients. Several genetic alterations of ABC-DLBCL dysregulate BCR signaling and NF-κB pathway at different levels, which has led to tailored treatment strategies. Single-agent treatment with the BTK inhibitor ibrutinib demonstrated selective efficacy in ABC-DLBCL, due to constitutive BTK-dependent B-cell receptor signaling [81]. Similarly, the proteasome inhibitor bortezomib has shown preferential activity in ABC-DLBCL through diminished degradation of IκBα and thereby inhibition of the chronic and required NF-κB signaling of ABC-DLBCL [82,83]. However, all randomized phase III trials testing the inclusion of targeted agents failed in improving first-line treatment, also when specific efforts have been applied to target the ABC subclass (Table 1). This can most likely be explained by the renowned biological heterogeneity of DLBCL including the recent findings of several and distinct genetical subtypes of DLBCL [58–61]. Therefore R-CHOP remains the standard treatment.

Vincristine

Vincristine (Oncovin®, O) is an antimitotic drug belonging to the group of vinca alkaloids, originally derived from the plant *Catharanthus roseus* [84]. Since the clinical approval in 1963, vincristine has been widely used in the treatment of several solid and hematological malignancies [84,85]. It is administered by intravenous infusion and has as a single agent brief and incomplete effects, however, improves clinical outcome when given in combination with other chemotherapeutics [84–86]. Cellular uptake of vincristine is mediated by multiple mechanisms, including passive diffusion and active energy- and temperature-dependent transport [87] and efflux by the ATP binding cassette (ABC)-transporter family [88].

Vincristine exerts its anti-neoplastic action by targeting β-tubulin leading to inhibition of polymerization of tubulin into microtubules (Figure 5) [89–91]. Microtubules are cytoskeletal proteins essential for several physiological cellular processes, including formation of the mitotic spindle and chromosome segregation during mitosis, cell migration, and intracellular transport. They are continuously assembled and dissembled by polymerization and depolymerization of tubulin, a dimer composed of α- and β-tubulin subunits [92].

Vincristine interferes with the mitotic spindles in a dose-dependent manner. At the lowest concentration, where cell proliferation is inhibited, vincristine stabilizes the mitotic spindle structure, whereas higher concentrations impair spindle assembly, both causing failure of chromosome segregation in the metaphase [89–91]. This activates the spindle assembly checkpoint, which prevents anaphase onset until accurate chromosome segregation, thereby causing mitotic arrest followed by apoptosis [93].

Vincristine has been considered a cornerstone of R-CHOP efficacy for several years; however, a recent comprehensive *in vitro* study shows that the effect of vincristine is antagonized in the presence of cyclophosphamide or doxorubicin [65]. Since vincristine is cell cycle phase-specific only targeting mitotic cells, the effect of vincristine could be expected to decrease in presence of doxorubicin and cyclophosphamide as these exert their action by inducing DNA damage [94,95], which prevents entry into mitosis.

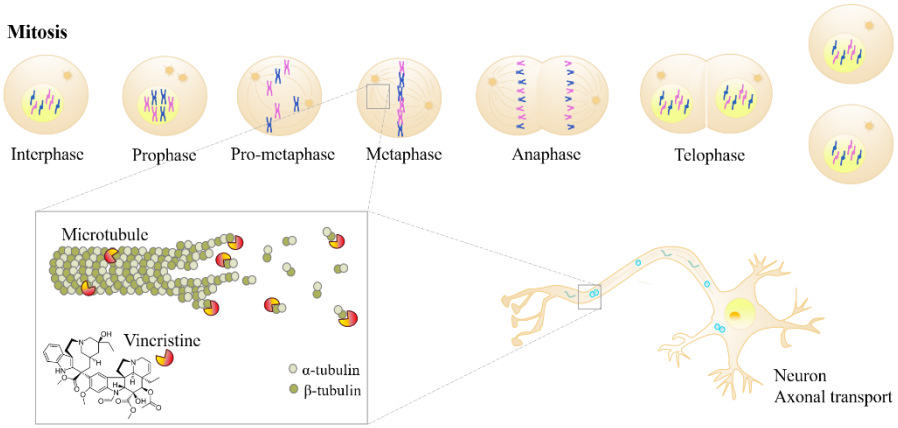

Figure 5. Vincristine mechanism of action. Vincristine exerts its anti-tumoral effect by binding to β-subunits of microtubules leading to impaired formation of mitotic spindle and metaphase arrest. Microtubules are in addition essential for axonal transports in neurons, and binding of vincristine to the microtubules blocks this transport resulting in neurotoxicity.

Neurotoxicity

The primary and dose-limiting side effect of vincristine treatment is neurotoxicity involving peripheral, autonomic, and central neuropathy [96]. The most common clinical symptoms are peripheral sensorimotor neuropathy, including paresthesia, numbness, and loss of deep tendon reflexes; however, autonomic dysfunctions characterized by constipation and urinary retention are in addition relatively often reported [97,98]. Vincristine-induced neuropathy occurs in time- and dose-dependent manner with some patients reporting clinical manifestations after the first dose, while others exhibit symptoms after treatment completion. The severity of neuropathy increases with accumulated vincristine dose and is mostly reversible [84], but can persist for months after discontinuation of treatment, and is in rare cases irreversible [99]. Symptoms of neuropathy often lead to vincristine dose reduction, discontinuation, or substitution, potentially affecting treatment efficacy of R-CHOP [100].

The mechanism underlying the toxic effect of vincristine is interference with microtubules, which causes blockage of crucial axonal transport (Figure 5) [101]. Axonal transport is a physiologic process involving transfer of molecular components, including vesicles, organelles, and proteins synthesized in the cell body, which are essential for axonal metabolism and neuronal membrane function [102]. This intracellular trafficking is mediated by microtubules, which dictates the direction of movement by polarization generated by the tubulin arrangement [103]. Impaired axonal transport caused by vincristine interference leads to neuronal degeneration that manifests distally and develops progressively [101,104].

Despite vincristine-induced neuropathy is the primary side effect and has been widely studied, no consensus about incidence, manifestations, and severity is found due to lack of consistency in neuropathy definition, assessment, and reporting. Literature review of vincristine-induced neuropathy in hematologic malignancies (Paper III) revealed a tremendously varying incidence of neuropathy with frequencies from 10% to 100% depending on patient inclusion criteria, vincristine doses and treatment cycles, and neuropathy assessment tools [96], emphasizing the inconsistency between studies. Furthermore, the absence of consensus has resulted in several conflicting studies of neuropathy, which has complicated identification of risk factors and predictive markers [96]. However, accumulated vincristine dose and preexisting neuropathy are consistently reported to predict increased risk of vincristine-induced neuropathy [98,105,106]. In addition, at the molecular level, several genes involved in the pharmacokinetics and pharmacodynamics of vincristine display potential as predictive markers [96]. Vincristine is metabolized by the cytochrome P450 3A (CYP3A) enzyme subfamily in the liver, with CYP3A4 and CYP3A5 as primary metabolizers [107]. Germline polymorphisms *CYP3A5*3* and *CYP3A5*6* introduce splice variants and protein truncation, leading to decreased CYP3A5 expression and less effective metabolism, thus, causing higher vincristine exposure and risk of neuropathy [96,108]. In addition, an inherent variant in the promotor of *CEP72* is associated with increased incidence and severity of vincristine-induced neuropathy.

This alteration leads to decreased expression of CEP72, a centrosomal protein important for microtubule formation, resulting in microtubule destabilization, and increased vincristine sensitivity [96,109].
Several strategies attempting to overcome vincristine-induced neuropathy have been examined, but currently, there is no convincing evidence of the use of pharmacologic interventions, and therefore, vincristine dose reduction, discontinuation or substitution, is the only option for diminishing neuropathy [96].

Treatment failure and drug resistance

Treatment failure of DLBCL patients is a complex problem involving many causative factors contributing to considerable inter-individual variability treatment response. Several host-related parameters influence the pharmacokinetics of a drug, including absorption, ability to reach the intended site, metabolism, and excretion in addition to dose-limiting side effects, patient co-morbidity, and performance dose-adjustments [96,110]. Furthermore, single- and multiple-drug resistance influences the overall response towards the treatment regimen. Epigenetic changes, genetic alterations, and transcriptional as well as translational aberrations all affect intracellular signaling pathways and are the underlying reason for molecular drug resistance [110].

Intrinsic resistance reflects the ability of the tumor at the time of diagnosis to circumvent the effect of a drug resulting in primary refractory disease and is caused by somatically acquired molecular aberrations of the cancer cells. As opposed, a selection process causes acquired resistance when initially responsive patients have chemo-resistant clones overgrowing the sensitive ones [110]. The third type of resistance is inherent where some patients, due to specific germline genotypes have a poor response to certain treatment regimens [111]. Thus, the treatment efficacy is affected by molecular aberrations of the cancer cells, treatment-selected resistant subpopulations, and individual germline genotypes. Furthermore, DLBCL is "addicted to the host" in terms of the tumor microenvironment modulating the disease course and sensitivity to antineoplastic drugs.

Resistance to anti-cancer drugs can be acquired by multiple intracellular mechanisms of the cancer cells and include dysregulation of pumps, modification of drug target, altered expression of detoxification mechanism, increased repair of drug-induced DNA damage, reduced susceptibility to apoptosis, and altered proliferation [110,112]. Upregulation of efflux pumps is a common mechanism of chemotherapeutic resistance, causing resistance towards multiple drugs at once, including doxorubicin and vincristine [65,113]. The function of these pumps is to transport xenobiotic drugs out of the cells leading to decreased drug retention, changed intracellular distribution, thereby affecting the availability and intracellular impact of the drug.

Chromosomal instability and aneuploidy are common characteristics of cancer, making tumor cells especially susceptible to anti-microtubule drugs like vincristine, which induces mitotic delay by activating the spindle assembly checkpoint. While most cells undergo apoptosis upon prolonged cell cycle, others appear to acquire the ability to slip through the spindle assembly checkpoint existing mitosis prematurely without proper chromosomal segregation [93,114,115]. Such mitotic slippage will contribute with even more chromosomal abnormality, and cells either die at later stages or survive and stop dividing, giving rise to a resistant clone [115].
Another adapted mechanism conferring vincristine resistance is altered tubulin isotype composition of microtubules. In humans, eight β-tubulin isotypes have been identified, which exhibit different vincristine-binding potential and dynamic properties, affecting the sensitivity [116]. Studies of solid tumors have shown perturbed isotype composition in cancer cells compared to adjacent normal tissue, involving adapted expression of one or several isotypes as well as presence of isoforms that are not typically expressed in the given tissue. Moreover, specific isotypes correlated with resistance to anti-mitotic taxanes and inferior clinical outcome [116].

microRNAs

microRNAs (miRNAs) are an abundant group of endogenous short (21-23nt) non-coding RNAs regulating gene expression at the post-transcriptional level [117]. Since the first miRNA was discovered in *Caenorhabditis elegans* in 1993 [118], the number has continuously increased, and to date, more than 2300 human miRNAs have been described and verified [119]. They are estimated to regulate up to 60% of protein-coding genes in the human genome [120] and play fundamental regulatory roles in almost every physiologic process, including development, proliferation, and apoptosis [117].

Biogenesis of miRNAs

miRNAs are encoded by inter or intragenic regions of the genome and are transcribed by RNA polymerase (pol) II or RNA pol III [121,122]. Intragenic miRNAs are processed mostly from introns and relatively few exons of protein-coding genes, whereas intergenic miRNAs have their own promoters and are transcribed independently of a host gene [123,124]. The biogenesis of miRNAs is divided into the canonical and non-canonical pathways of which the former is dominant (Figure 6).
The canonical pathway starts with transcription into the primary miRNA, designated pri-miRNA, a long transcript that either can express a single miRNA or a cluster of multiple miRNAs, which is considered a family when having similar seed sequences [125,126]. The pri-miRNA transcript comprises a 5'-cap, a hairpin region encoding the mature miRNA, and a 3'-polyadenylated tail, and is processed into precursor

miRNA (pre-miRNA) by the nuclear microprocessor complex consisting of the RNA binding protein DiGeorge syndrome chromosomal region (DGCR8) and the RNAse III enzyme Drosha [125]. When DGCR8 recognizes the precise cleavage site, the two RNAse domains of Drosha cleaves the 5'- and 3'-end of the pri-miRNA resulting in a 70 nucleotides (nts) long pre-miRNA with 2-nts overhang in the 3'-end [125,127].
The non-canonical pathway involves generation of 'mirtrons', which are intron-derived pre-miRNAs produced during splicing. When a spliced intron has the potential to form a hairpin structure resembling pre-miRNAs, it bypasses Drosha processing and follows the biogenesis of a canonical-generated pre-miRNA [128].
Once the pre-miRNA is formed, it is transported to the cytoplasm by Exportin-5 [129], where the RNAse III enzyme Dicer in complex with TAR RNA-binding protein (TRBP) cleaves the loop structure generating the mature miRNA duplex of approximately 21 nts [130,131]. The duplex is unwounded into a 5p- and 3p-strand arising from the 5'- and 3'-end of the pre-miRNA hairpin, respectively. Both strands can be incorporated into Argonaute (AGO) proteins and form the RNA-induced silencing complex (RISC) [132]. Selection of miR#-5p or miR#-3p is based on thermodynamic stability, and in general, the strand with lowest stability is loaded into AGO and is denoted the guide strand. As opposed, the unloaded strand is referred to as the passenger strand or miRNA-star (*) and is usually degraded [133,134]. Of notice, for a specific miRNA, the proportion of AGO-incorporation of miR#-5p or miR#-3p varies depending on the cell type, ranging from equilibrium to predominance of one or the other [135].

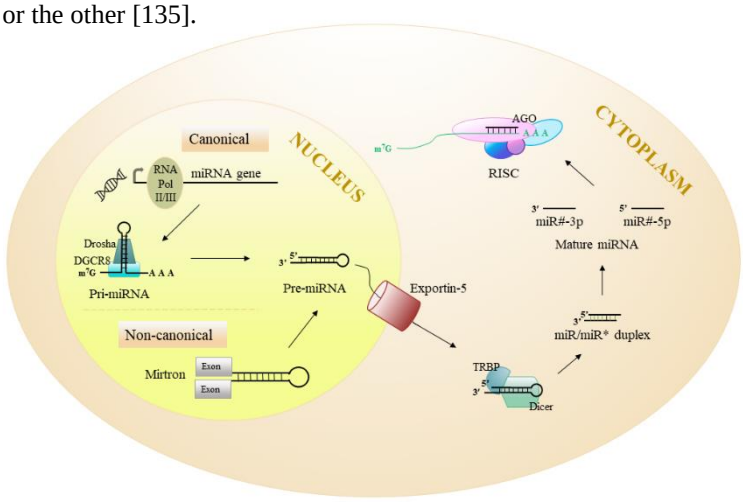

Figure 6. miRNA biogenesis. By the canonical pathway, miRNA-encoding genes are transcribed by RNA polymerase II or III into primary miRNAs (pri-miRNA), which are processed by Drosha in complex with DiGeorge syndrome chromosomal region (DGCR8), generating precursor miRNAs (pre-miRNA). By the non-canonical pathway are intron-derived pre-miRNAs generated during splicing. Exportin-5 transports pre-miRNAs to the cytoplasm where they are cleaved by Dicer in complex with TAR RNA-binding protein (TRBP), resulting in a miRNA duplex. The guide strand of the duplex is loaded into the RNA-induced silencing complex (RISC) with Argonaute (AGO) proteins, enabling binding and regulation of target mRNAs.

Function of miRNAs

The RISC complex consisting of the miRNA guide strand and AGO proteins are responsible for post-transcriptional regulation of target mRNAs [132]. RISC binds the target by complementary base pairing between the guide strand and the miRNA response element on the target mRNA. Canonical miRNA-mRNA interactions occur by full complementarity to the seed region in the 5'-end of the miRNA, which predominantly is a 6-mer sequence within position 2-8 or 7-mer from nucleotide 1-8, though extended seed regions from position 4-10 are observed [136–138]. While seed-mediated interactions constitute the majority of miRNA-mRNA interactions, only one-third of the interactions involve entirely complementary [139]. Generally, the seed interaction is accompanied by additional base pairing, which increases stability and specificity of the miRNA-mRNA interaction [139,140]. The majority of miRNA binding sites are located in the 3' untranslated region (3' UTR) of the target mRNAs; however, binding sites have also been observed in promoter regions, coding regions, and 5' UTR [139–144]. Additionally, non-canonical seedless miRNA-mRNA interactions have been identified, which alone only leads to moderate or none target regulation, but act cooperatively with seed interaction in target binding and regulation [138,139,145].

The degree of complementarity between the miRNA and target mRNA determines the mechanism of gene silencing. A fully complementary miRNA-mRNA interaction causes mRNA cleavage by the endonuclease AGO2, whereas imperfect complementarity leads to translational repression by AGO-mediated RNA interference and/or mRNA destabilization and degradation by deadenylation and decapping [136,146]. The full miRNA is rarely fully complementary to its target resulting in RNA hybrids with mismatches and characteristic bulges, preventing AGO2 endonuclease activity [136,147]. In addition to the primarily repressive function, miRNAs have been reported to mediate translational activation under specific conditions [144,148].

A miRNA can regulate several target mRNAs, and conversely, several miRNAs can cooperatively regulate a specific mRNA, and thereby miRNA-mediated gene regulation affect multiple signaling pathways [117,149]. The action of miRNAs is a dynamic process, equilibrating gene expression to a steady-state and is influenced by shuttling of RISC between intracellular compartments in addition to abundancy and availability of miRNAs and their specific target mRNAs [150]. miRNAs exhibit tissue and cell type-dependent expression patterns, specifically, the Functional Annotation of the Mammalian Genome (FANTOM) research consortium showed that one-fourth of miRNAs are broadly expressed across human cell-types, half of them are cell type enriched, and the remaining are with low expression levels [124,151]. In addition, affected mRNA targets are distinct across cell types [149], making the miRNA's targetome even more comprehensive and complex.

miRNAs in B-cell differentiation and function

The regulatory mechanism by miRNAs is important in the complex and highly regulated B-cell differentiation and activation. Each B-cell differentiation stage possesses a characteristic miRNA expression profile [152,153] and the direct impact of miRNAs in regulating differentiation is emphasized by impaired formation of normal B-cell differentiation subsets and affected antibody diversity when Dicer, the enzyme generating mature miRNAs, is removed in transgenic mice [154,155]. Specifically, Dicer ablation blocks transition into precursor B-cells in the bone marrow, formation of GC B-cells, and terminal differentiation as modeled in mice [154,155].

miRNA regulation at the specific stages of the B-cell differentiation has been extensively explored *in vitro* and *in vivo* utilizing ectopic expression and selectively targeting. The first identified hematopoietic regulator was miR-181a, of which induced expression in hematopoietic stem cells increased the fraction of cells committed to the B-cell lineage [156]. In addition, hematopoietic stem cells display higher endogenous expression of miR-181a than precursor B-cells, supporting the regulatory function in early B-cell development [152,157]. Likewise, the miR-17~92 cluster consisting of miR-17, miR-18, miR-19a, miR-19b, miR-20a, and miR-92-1 is highly expressed in hematopoietic progenitor cells and deletion of the entire miR-17~92 locus in mice impaired transition from progenitor to precursor B-cells through increased expression of the pro-apoptotic protein Bim [158]. Moreover, by restoring expression of specific miRNAs of the miR-17~92 cluster in hematopoietic stem cells isolated from miR-17~92 deficient mice, miR-17 alone was identified to rescue the progenitor to precursor B-cell transition, highlighting miR-17 as a central regulator of early hematopoiesis [159]. In addition, the miR-17~92 cluster is involved in regulation of central tolerance occurring in the bone marrow, where the BCR is tested for autoimmunity to eliminate self-reactive B-cells [159]. The model utilized for investigation of central tolerance was the IgM^b –macroself mice, engineered to ubiquitously express antigens reactive to the heavy constant region of IgM, the BCR present on immature B-cells. Therefore, as a consequence of central tolerance, these mice lack mature B-cells. Reconstituting these mice with bone marrow from transgene mice overexpressing the miR-17~92 cluster rescued B-cell development leading to occurrence of mature B-cells. Furthermore, reconstitution of individual miRNAs of the cluster lead to identification of miR-19 as the key regulator of central tolerance by targeting PTEN [159].

The most essential miRNA in regulation of the GC reaction and terminal stages of the differentiation is miR-155, which is highly expressed in GC B-cells [153]. The importance is emphasized by impaired GC formation and immune response when miR-155 is deleted in mice [160,161]. Immunization of miR-155-deficient mice resulted in fewer GC B-cells and revealed defect in immunoglobulin class switch into IgG1, evidenced by less production of antigen-specific IgG1 in contrast to normal abundance of IgM. Moreover, secondary immunization showed impaired memory response in absence of miR-155 due to reduced differentiation into plasmablasts and

memory B-cells [161,162]. In support, ectopic expression led following antigen introduction to enriched and enlarged GCs shown by immunohistochemistry and increased number of class-switched antibodies determined by fluorescent activated sorting followed by western blotting [160]. The critical role of miR-155 is mediated by regulating the gene encoding the transcription factor PU.1, which is crucial for B-cell commitment and differentiation [161]. In addition, AID is another important target of miR-155. Disruption of the miR-155 binding site in the 3' UTR of *Aicda* (AID) reduced AID expression *in vitro* as well as temporally *in vivo* and functionally affected BCR affinity maturation and immunoglobulin class switch, assessed by IgG binding efficiency and the percentage of IgG isotypes upon immunization [163]. Collectively, these studies document that miR-155 is pivotal for B-cell differentiation and effective immune response.

miRNAs in DLBCL and treatment response

As miRNAs are involved in essential cellular processes, including cancer-relevant pathways, deregulation enables cancer cells to rewire several mechanisms to provide survival advantages. Consistently, aberrant miRNA expression has been experimentally verified to be implicated in the pathogenesis of several malignancies including DLBCL [164,165]. Moreover, the regulatory network of miRNAs is affected by the 3' UTR shortening generally observed in cancer. By alternative cleavage and polyadenylation, cancer cells acquire shorter mRNA isoforms, enabling genes to avoid post-transcriptional regulation by miRNAs due to loss of miRNA-response elements [166,167].

miRNAs are recognized to act as oncogenes when their overexpression favor malignant transformation and progression by promoting proliferation and evading growth suppression and apoptosis. Likewise, miRNAs function as tumor suppressors preventing tumorigenesis through inhibition of proto-oncogenes [164,168]. However, the role of a miRNA is ambiguous, and studies of miRNAs in cancer are complicated by the genetic diversity of tumors, the fact that several miRNAs often are dysregulated in a tumor, and that miRNAs targets multiple mRNAs that furthermore is influenced by the cell-of-origin and the microenvironment surrounding the malignant cells [149,169,170]. For example, miR-148a appears to act as a tumor suppressor in skin and colorectal cancer by targeting genes involved in apoptosis, tumor invasion, and metastasis [171,172]. In contrast, high expression of miR-148a is associated with inferior outcome in DLBCL, which is suggested to be caused by attenuated immune response [173].

The underlying mechanism of dysregulated miRNA expression is not always known. However, miRNAs are often located in cancer-associated genomic regions and fragile sites, frequently leading to miRNA deletion and decreased expression in consistence with the general miRNA downregulation observed in cancer [164,174,175].

Furthermore, epigenetic silencing of miRNAs, including DNA methylation and chromatin modifications, has been documented in multiple malignancies [176–178].
The pathogenic impact of miRNAs as well as their diagnostic, prognostic, and predictive potential have been extensively studied in DLBCL. Despite highly heterogeneous miRNA expression profiles [179], several individual miRNAs and miRNA signatures have been identified to characterize different aspects of DLBCL [180,181]. Diagnostic challenges, including morphological similarity between GCB-DLBCL and high-grade FL, have been suggested to be overcome by including expression of miRNAs in the miR-17~92 cluster, and likewise, distinction between DLBCL and HL can be supported by determining the miR-155 expression [182,183]. Furthermore, distinct miRNA expression signatures divide DLBCL into the prognostic ABC and GCB subclasses, similar to GEP-based classification [180]. However, miRNA expression-based diagnostics and prognostics has not entered clinical practice, and with the field focusing on genetics, miRNAs mostly contribute with biological information rather than as a clinical tool.
Commonly deregulated miRNAs in DLBCL include the miR-17~92 cluster, miR-21, miR-34a, and miR-155, and are hence among the most thoroughly studied utilizing global miRNA profiling and functional *in vitro* and *in vivo* models.

miR-17~92 cluster

The miR-17~92 cluster is encoded by *C13orf25,* which is upregulated in DLBCL [184]. Functional evidence of oncogenic impact emerged from transgenic mice, in which overexpression of the cluster in lymphocytes led to development of lymphoproliferative disease. Furthermore, lymphocytes with ectopic expression of the miR-17~92 cluster exhibited increased proliferation and diminished activation-induced apoptosis by suppressing the tumor suppressor PTEN and pro-apoptotic factor Bim [185].
Transcription of miR-17~92 is directly activated by MYC, an oncogene frequently dysregulated and involved in the pathogenesis of DLBCL [186]. MYC and miR-17~92 cooperatively contribute to B-cell lymphomagenesis and progression, supported by suppressed tumorigenesis in MYC-driven lymphoma mice upon miR-17~92 knockout. Furthermore, genetic ablation of individual miRNAs of the cluster revealed miR-19a and miR-19b as key components for the oncogenic properties of the cluster [187].
miRNA profiling of DLBCL cell lines identified miR-17, miR-19b, and miR-20a to differentiate ABC and GCB classified cell lines, with higher expression in ABC-DLBCL [188]. Conversely, assessment of expression levels of the individual miRNAs in clinical samples did not reveal significant association to the molecular ABC/GCB subclasses but documented inferior outcome of DLBCL patients expressing low levels of miR-19a [180,189].

miR-21

The oncomiR, miR-21, has been experimentally validated to play an important role in the pathogenesis of DLBCL [190]. The oncogenic properties are supported by elevated expression levels in most cancer types [191–193] and further by functional studies of ectopic expression of miR-21 *in vivo* leading to development of lymphoma. In addition, blockage of ectopic miR-21 expression by doxycycline-dependent repression of the Cre/loxP activating system caused tumor regression, indicating miR-21 not only to be involved in malignant transformation and development but also in maintenance and progression, whereby miR-21 addiction in lymphomagenesis was suggested [190].
miR-21 has been reported to affect response to CHOP, as knockdown of miR-21 sensitized DLBCL cells to treatment by affecting PI3K/AKT signaling through regulation of PTEN [194]. In contrast, prognostic evaluation of miR-21 expression in independent clinical studies representing 157 patients revealed high levels of miR-21 in serum and DLBCL tissue to be associated with superior outcome [191,195,196], which challenges the common perception of miR-21 as an oncomiR and emphasizes the ambiguity of studying miRNAs. Moreover, several studies report miR-21 to be higher expressed in ABC-DLBCL as compared to GCB [191,196].

miR-34a

As opposed to the other commonly deregulated miRNAs described, miR-34a function as a tumor suppressor that is downregulated in DLBCL [197,198]. The gene encoding miR-34a is located in the chromosomal region 1p36.22, which frequently is deleted in cancer [174]. In addition, hypermethylation of promotor-associated CpG islands results in repression of miR-34a expression in several malignancies including DLBCL [197–199].
Tumor suppressive activity of miR-34a was evidenced in a xenograft mouse model of DLBCL, where systemic administration of miR-34a reduced tumor growth by inducing apoptosis [198]. Further examination of the underlying tumor suppressive mechanisms showed that miR-34a inhibits growth by targeting the transcription factor FoxP1 [198,200], a hematopoietic oncogene with prognostic impact in DLBCL [201]. Moreover, miR-34a expression has been documented to increase sensitivity to doxorubicin in functional studies of DLBCL cell lines and in addition being higher expressed in DLBCL patients with predicted sensitivity to doxorubicin [181]. In support, prognostic evaluation of miR-34a revealed superior clinical outcome for DLBCL patients with high miR-34a expression [181,189].

miR-155

miR-155 encoded by *BIC* (B-cell Integration Cluster, *MIR155HG*) possesses oncogenic activity in numerous solid and hematological malignancies [202]. The diagnostic, prognostic, and predictive biomarker potential of miR-155 in B-cell malignancies is reviewed in paper I [183].

Elevated expression of miR-155 is documented in DLBCL patients, with higher expression in ABC classified patients compared to GCB assessed using several technical platforms including quantitative PCR, droplet digital PCR, and microarray in a total of 370 patients [180,191,203–205]. Transcription of miR-155 is directly activated by MYB and NF-κB [206,207], both overexpressed in DLBCL [32,208]. Additionally, BCR activation induces miR-155 expression; thus, the constitutive BCR and NF-κB signaling observed in ABC-DLBCL explain why ABC classified patients exhibit high levels of miR-155 [29,30,33].

miR-155 has shown specific importance in the pathogenesis of B-cell malignancies. Ectopic expression of miR-155 in transgenic mice resulted in development of B-cell lymphoma [209–211], and subsequent withdrawal of miR-155 caused rapid tumor regression partly by apoptosis [210]. Furthermore, the potential of miR-155 as a therapeutic target has been investigated by injecting anti-miR-155 into tumor site of a miR-155 addicted lymphoma xenograft, which substantially diminished the tumor size and thereby presented promising anti-tumor effect of anti-miR-155 treatment *in vivo* [210,211]. Currently, safety, tolerability, pharmacokinetics, and potential efficacy of a miR-155 inhibitor (Cobomarsen, MRG-106) is tested in phase I clinical trial (NCT02580552) with inclusion of patients suffering from ABC-DLBCL, CLL, cutaneous T-cell lymphoma among others. For ABC-DLBCL, patients intolerant to immuno-chemotherapy or with relapsed/refractory disease are eligible for inclusion and are treated with subcutaneous or intravenous administration of Cobomarsen as monotherapy [212], but no study report has yet been posted. However, as miR-155 plays a fundamental physiological role in the hematopoiesis and immune response, systemic expression of this targeted inhibition is a challenge, potentially causing severe side effects.

2. HYPOTHESIS AND AIMS

Patients diagnosed with DLBCL very often suffer from primary refractory disease and relapse by treatment-induced immuno-chemotherapy resistance, demonstrating that standard provided R-CHOP regimens are not sufficient to cure all patients, present, 50-80% of DLBCL patients are alive after 5 years, depending on their risk profile. Early detection of drug-specific resistance is of great importance to guide individual therapy including selection of alternative treatments and sparing patients for inefficient, but still toxic therapy. Identification of underlying drug resistance mechanisms and biomarkers are therefore pivotal when attempting to overcome treatment resistance and improve clinical outcome.

The hypothesis of this PhD project was that miRNAs are important determinants in the response to immuno-chemotherapy in DLBCL and that we by functional *in vitro* studies and analysis of primary clinical samples can improve the understanding of miRNAs biological function in drug resistance and the potential of stratifying patients according to risk. Following aims were conducted to address the hypothesis:

Aim I: To obtain an overview of the potential of miR-155 as a diagnostic, prognostic, and predictive biomarker as well as target of novel treatments in B-cell malignancies.

Aim II: To pinpoint miRNAs involved in response to vincristine, a cornerstone of the R-CHOP treatment regimen, by following steps:

- Determination of differential miRNA expression between vincristine sensitive and resistant DLBCL cell lines.
- Functional manipulation of miRNA expression to validate the impact of the candidate miRNA on vincristine response in DLBCL cell lines.
- Clinical data analysis to evaluate the prognostic impact of the candidate miRNA in DLBCL and its association to cell-of-origin.

Aim III: To overview the clinical and biological risk markers of vincristine-induced neuropathy in hematological malignancies.

Aim IV: To develop a classifier predicting drug response and outcome based on expression of miRNAs associated with response to R-CHOP constituents by:

- Determination of differential miRNA expression between DLBCL cell lines categorized as sensitive, intermediate responsive, and resistant to the individual component of R-CHOP.
- Bioinformatic modeling to identify the strongest combination of single candidate miRNAs associated with chemotherapy response and outcome.

3. METHODOLOGICAL CONSIDERATIONS

Material, methods, and statistics applied in this PhD dissertation are described in material and methods sections of the respective papers, which contain all relevant information regarding setup, reagents, and experimental procedure. The following section describes the main technologies used and critically evaluates their potential, applicability, and limitations.

Cell lines as a pre-clinical model

A panel of 15 DLBCL cell lines has been used for dose-response analysis of R-CHOP constituents, and for selected cell lines functional studies has been performed including ectopic expression, targeted repression, and CRISPR-Cas9-mediated knockout.

Cell lines were passaged regularly with frequencies depending on the specific growth rate of the cell line. As the proliferative ability of cells is affected by the number of passages, the time of passaging, and the cell confluency, cell line experiments were coordinated according to passaging and to be performed when cells were growing exponentially. Cell lines were maintained in culture for no more than 20 passages to minimize the risk of microbial infection, cross-contamination, and clonal subselection of culture adjusted subpopulations. Cell line identity was confirmed when cells were thawed and at the end of the culturing period by short tandem repeat (STR) profiling of eight tetranucleotide repeat loci and the amelogenin gender-determining marker. Furthermore, cell lines were screened for mycoplasma infection, since infection could affect cellular growth, metabolism, and genetic profile [213].

In vitro human cell lines are a valuable pre-clinical model, which has been widely used in cancer research, including pharmacologic investigation of therapeutics, identification of response and resistance mechanisms as well as examination of pathogenesis. However, it is important to take into account that the genetics of a cell line resembles those in the tumor of origin and therefore, interpersonal variation between patients and the substantial heterogeneity of cancer have to be addressed by using a panel of cell lines. Panels of cell lines are useful for initial screening of drug response; however, interpretation of the degree of response combined with multi-omics data needs to be validated in functional and mechanistic studies as well as being clinically investigated.

The application of *in vitro* models has the advantage of being fast, cost-efficient, easy to handle and to genetic manipulate, and ethically beneficial in comparison to *in vivo* models. Furthermore, cell lines are an unlimited material source as they can be passaged repeatedly once they are established and recovered from cryopreservation

due to the relatively high degree of homogeneity. Thus, cell line culturing enables potentially infinite quantities for repetition of several experimental assays. However, it is important to be aware of the disadvantages. During continuous culturing, cell lines are prone to genotypic and phenotypic drift where subpopulations may arise and cause phenotypic alterations over time by selection of clones with growth advantages [214,215], which complicates the biological interpretation of results as well as the data reproducibility across facilities. However, most human cell lines grown *in vitro* retain their molecular features of their tumor of origin. Another limitation of human cell line models is the lack of complexity, as influence of the tumor microenvironment cannot be addressed in these simplified systems, requiring findings to be functionally validated in more complex systems such as *in vitro* co-cultures and animals. Several of the limitations of *in vitro* models are in this dissertation compensated for by performing technical and biological replicates, using several authenticated cell lines, and importantly by combining cellular and clinical findings.

Dose-response experiments

For each drug component of R-CHOP, dose-response experiments were conducted in biological triplicates using three independent cultures of the same cell line. Fifteen DLBCL cell lines were seeded at individual concentrations and incubated for 24 hours prior to exposure to at least 16 doses dependent on the drug for 48 hours, ensuring at least one cell cycle for all cell lines. The optimal seeding concentration was determined for each cell line prior to drug challenge to ensure exponential growth throughout the experiment in the untreated control.

An MTS assay was applied to estimate the effect of the drug by assessing the amount of metabolic active cells. This assay exploits the mitochondrial reduction of tetrazolium to formazan, a colored product directly proportional to metabolic active cells. The method is simple, rapid, and reproducible, making it ideal for comprehensive screening assays; however, cells with low metabolism as well as cells in cell cycle arrest are indistinguishable from dead cells. In addition, as cell viability is estimated indirectly by cell metabolism, no information is obtained on whether the effect of a drug is caused by cell cycle arrest, apoptosis, or both. Thus, additional methods are required to determine the mechanism of drug response. Assessment of the number of living cells can be obtained using vital dyes such as trypan blue, which is applied in the functional studies of this dissertation. As living cells possess intact cell membranes, the dye is excluded, whereas dead cells are permeable and absorb the dye resulting in a blue cytoplasm in the dead cells as opposed to a clear cytoplasm in viable cells. However, subsequent cell counting is performed using a hemocytometer, introducing the risk of counting errors and interobserver variability, thus, to ensure representable assessment two chambers and at least 100 cells were counted, and all chambers when cell number was less than 100. Further exploration of the functional effect of the drug can be conducted by investigating proliferation, cell cycle

distribution, and apoptosis by flow cytometry analysis, which however, is expensive, time-consuming and therefore not suitable for large-scale experiments.

Dose-response experiments are often analyzed by comparing cell viability between treated and untreated cells, by which the growth inhibition is estimated. Drug efficiency is subsequently reported by GI-50, the drug concentration at which the relative cell viability is 50% after a fixed time. However, response to a given drug is dependent on exposure time and cellular growth rate, thus when the drug exposure time is fixed for several cell lines, slow proliferating cells will appear less sensitive than fast proliferating ones and vice-versa.

In the high-throughput dose-response screening experiments reported in this thesis, a Growth-based dose-response model (G-model) was used, considering both drug exposure time and cell growth kinetics, to enable comparisons between drug sensitivity in the DLBCL cell lines [216]. The experimental setup consists of cell line-specific seeding in two 96-well plates in which they incubate for 24 hours before increasing drug concentrations and drug-solvent are added to each plate (Figure 7). Background absorbance is measured immediately after drug exposure for plate 1, while plate 2 is incubated for 48 hours prior to measurement. In addition, prior to dose-response analyses, the viability of each cell line in presence of the respective drug-solvents is tested, and moreover, a background control for each drug concentration is performed to correct for potential influence of the drug on absorbance.

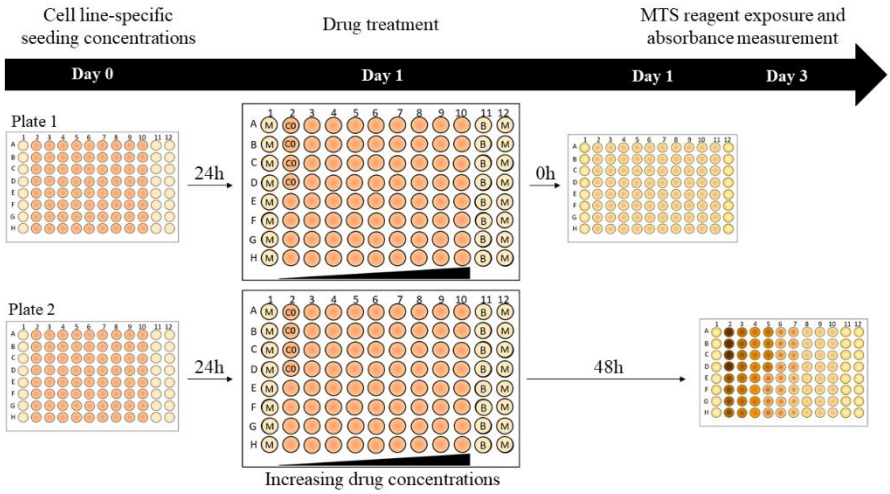

Figure 7. Dose-response screens. DLBCL cells are seeded in two plates with cell line-specific seeding concentrations on day 0. After 24 hours of incubation, increasing drug concentrations are added to both plates, and plate 1 is immediately hereafter exposed to MTS reagent for 2 hours and absorbance is subsequently measured. Plate 2 are incubated for 48 hours prior to MTS reagent exposure and measurement of absorbance. Wells labeled M contain media and are not included in the analysis, C0 wells contain drug solvent, and B denotes blank wells containing culture medium and drug solvent. Boarder wells are omitted from data analysis.

The statistical workflow of the G-model involves pre-processing of measured absorbance to account for multiplicative errors and to correct for background absorbance caused by the drug, estimation of cell line doubling times, isotonic regression modeling of dose-response curves, and a bootstrap test for estimation of confidence interval for summary statistics [216]. Summary statistics of the G-model includes GI-50, the concentration at which total growth of the cells is inhibited (TGI), the lethal concentration at which the cells decay with a halving time of 48 hours (LC_{48}), and the area under the positive part of the dose-response curve (AUC). Comparison of DLBCL cell lines was conducted by ranking them according to the AUC, which has been documented as the best summary statistics of dose-response experiments [217], followed by trichotomization into groups of sensitive, intermediate-responsive, and resistant cell lines.

Despite the entire R-CHOP regimen being used in the clinical setting, single drug screens were conducted rather than combinational studies since assessment of combination effects between drugs is far from simple when drugs have nonlinear dose–response curves like the components of the R-CHOP [181,216,218,219]. The assessed combination effect will depend on the single-dose concentration at which they are tested [220–222] and the order in which the drugs are given [219]. Despite utilizing the same ratio between drugs like the one used in the clinical setting, the actual concentration of each drug within the tumor is unknown and varies between patients influenced by drug metabolism, drug distribution, and tumor site location. Moreover, varying combinational effects occur in the clinical settings upon dose reduction or drug substitution. In experimental multi-drug screens, it is impossible to distinguish underlying response and resistance mechanisms, as both single- and multi-drug resistance could impair treatment efficacy. However, recent results from study of the mechanistic basis of R-CHOP showed no synergistic interaction between components but very low cross-resistance. Thus, the drug components of R-CHOP appear to be independently effective without overlapping resistance mechanisms [65], though with different potency complicating biological interpretation of combinational drug studies.

Functional *in vitro* studies

By combining global miRNA expression profiles of untreated DLBCL cell lines and specific drug-responses, we identified miRNAs associated with R-CHOP constituents. As the biological role and impact of miRNAs on actual drug response cannot be interpreted alone from association to drug response, functional studies including ectopic expression, targeted repression, and CRISPR-Cas9-mediated knockout of miR-155 was conducted for direct assessment of the role and impact on vincristine response.

Experimental manipulation of miRNA expression can be accomplished by direct cellular delivery of synthetic RNA molecules or by vector-based approaches. As

direct delivery approach of synthetic miRNA mimics and inhibitors potentially require recurrent delivery as well as reduced efficiency in hard-to-transfect cells such as B-cells [223], the vector-encoded approach was applied to ensure stable and persistent transgene expression. Specifically, H1 RNA polymerase III promoter-driven expression of a miRNA mimic encoding pri-miR-155 and simultaneous expression of a green fluorescent protein (GFP) driven by a phosphoglycerate kinase (PGK) promoter was utilized for upregulation of miR-155.
Suppression of miRNAs is based on full complementary antisense molecules that bind the miRNA of interest and sequester the miRNA from its target mRNA. All miRNA inhibiting strategies employ sequence complementarity and include antagomiRs, RISC-loaded shRNAs, miRNA sponges, Tough Decoys (TuDs) among others. Comparison of inhibitors documented robust and high suppressive capacity of TuD inhibitors, which consist of an RNA hairpin with two miRNA binding sites [224]. Therefore, an RNA polymerase II driven fusion transcript containing the reporter gene GFP and the TuD inhibitor directed towards miR-155 was utilized for miR-155 suppression. As functional studies were conducted in four DLBCL cell lines exhibiting various sensitivity to vincristine and endogenous levels of miR-155, both up- and down-regulation were applied. The endogenous level influences the effect of the experimental expression manipulation, as it is challenging to increase expression in cells with high intracellular levels and to reduce expression in lower-expressing cells. Furthermore, it is difficult to increase sensitivity in intrinsically sensitive cell lines and likewise, to induce resistance in intrinsically resistant cells. Thus, to ensure phenotypic effect, both up- and down-regulation were performed in all four cell lines.

Evolutionally, cells have been selected to possess defense mechanisms against acquisition of foreign genetic molecules, including naked DNA and RNA, which induce an interferon reaction by nucleic acid sensing pathways [225,226]. Thus, these mechanisms have to be overcome for delivery of vectors encoding the sequence of interest, which can be achieved by applying chemical and physical agents whereby DNA or RNA cargo can be transfected into cultured cells. However, this can be difficult and even impossible in certain cell types, including B-cells, in which introduction of sequences very often only can be obtained by viral-based transduction [227]. Most commonly used are adeno-associated virus and lentivirus, of which the latter was used for functional studies in this dissertation due to its ability to infect and integrate a transgene randomly in the genome of nearly all mammalian cell types.
Lentiviral vectors are derived from Human Immunodeficiency Virus-1 (HIV-1), a genus of the retrovirus family characterized by their RNA genome and the ability to integrate into the genome of target cells by utilizing their reverse transcriptase and integrase enzymes. This, combined with the capability of lentivirus to infect both dividing and non-dividing cells, makes these vectors optimal vehicles for gene delivery. To ensure safety of use, three generations of hybrid lentiviral systems with depleted replication of wild-type virus have been developed and encompass multiple plasmids encoding the viral proteins [228,229]. Nowadays, the third-generation system is most commonly used and consists of four plasmids encoding core

components of HIV-1 (Figure 8). The packaging **GagPol** plasmid encodes the *Gag* gene encoding structural viral components including matrix, capsid, and nucleocapsid and the *Pol* gene encoding enzymes essential for virus maturation and integration (protease, reverse transcriptase, and integrase). The **Rev** plasmid encodes the Rev proteins, which bind to viral transcripts containing the Rev responsive element (RRE), facilitating export of the viral mRNA from the nucleus to cytoplasm. The **transfer** plasmid contains the gene of interest flanked by two long terminal repeats (LTRs), which are not translated into protein but are essential for incorporation into the host genome. Lastly, the **env** plasmid encodes envelope proteins that form the outer structure of the virus. The gene encoding the envelope proteins in HIV-1 has been exchanged to the gene encoding the envelope of vesicular stomatitis virus glycoprotein (VSV-G), which targets the LDL receptor present on almost every all cell type and thereby expands the viral tropism [230,231]. In addition, VSV-G enhanced the stability of the virus particle, making high titer concentrations possible by ultracentrifugation [231]. To generate lentivirus, the four plasmids were co-transfected into HEK293T cells (Human Embryonal Kidney), which have been engineered to have high transfection efficiency and to stably express the SV40 large T-antigen.

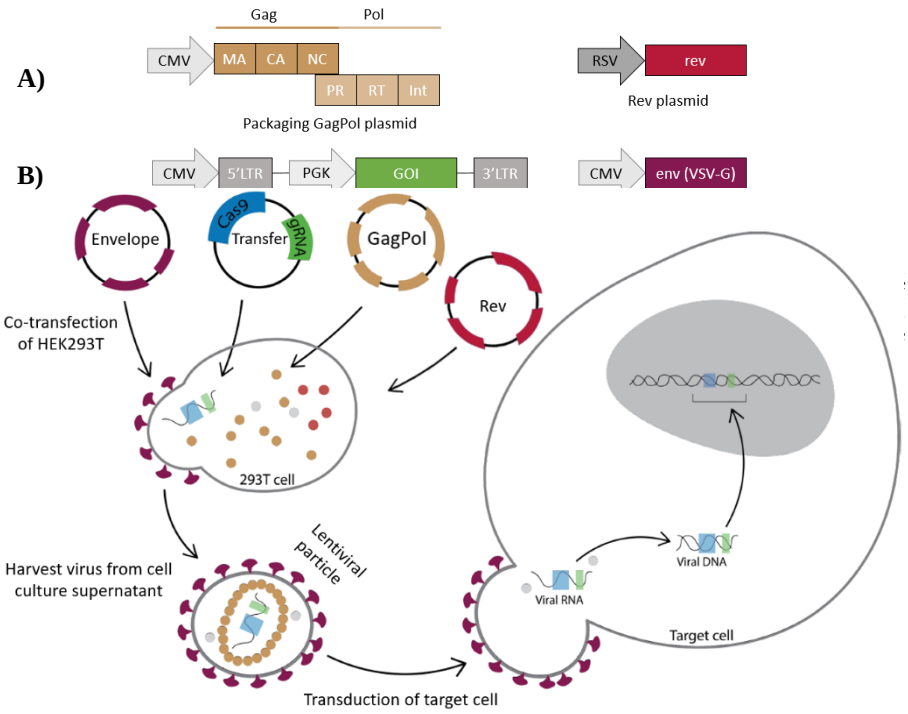

When applying functional genetic perturbation studies, it is important to consider potential cellular compensatory mechanisms attempting to maintain fitness and viability. For instance, by redundant genes, loss of one gene is compensated by expression of another gene with a similar function, leading to none or diminished phenotypic effect. Likewise, if the manipulated gene is involved in a stringently regulated pathway, the altered expression could affect the expression of other genes within the pathway to preserve its function. Moreover, induced up- and downregulation can be compensated by transcriptional adaption resulting in equilibrium. Other drawbacks of downregulation using TuD inhibitors are that it mostly leads to partial gene silencing and potentially has off-target effects, thus CRISPR-Cas9 mediated knockout of miR-155 was conducted to confirm the functional impact on vincristine response.

CRISPR-Cas9

The discovery of the CRISPR-Cas9 system revolutionized targeted genome engineering and is nowadays the most common technology in genome editing [232,233]. Originally, the Clustered Regularly Interspaced Short Palindromic Repeats (CRISPR) and CRISPR associated proteins (Cas) were identified in bacteria and archaea functioning as adaptive immune system towards bacteriophages and plasmids [234]. As the CRISPR type II system is harnessed for eukaryotic genome editing, the following section focuses on that specific type.

When bacteriophages or plasmids infect bacteria, fragments of the foreign DNA are integrated into the CRISPR loci of the bacterial genome as protospacers separated by short palindromic repeats [234]. These are subsequently transcribed and processed into trans-activating RNA (tracrRNA) and CRISPR RNAs (crRNAs), with the latter being complementary to the spacer sequences [235]. Upon reinfection, the tracrRNA assembled to the crRNA guides the Cas9 endonucleases to complementary target sites upstream a protospacer adjacent motif (PAM), whereby Cas9 activity is initiated [235]. Cas9 separates the DNA strands and induces a double-stranded break three nucleotides upstream the PAM sequence, leading to degradation of the foreign DNA [235].

By modifications of this bacterial defense system, CRISPR-Cas9 today functions as a genome-editing tool, capable of introducing double-stranded DNA break at a specific genomic location of interest [232]. The tracrRNA and crRNA have been fused to a single guide RNA (sgRNA), which can be designed to target almost all genomic loci in proximity to a PAM sequence [232,236]. Target complementarity is mediated by 20 nucleotides in the 5’end of the sgRNA, corresponding to the crRNA, and the tracrRNA functions as a scaffold for Cas9 [232]. Once the sgRNA-Cas9 complex binds to its target sequence, the Cas9 generates a double-stranded cut, which the cellular DNA repair machinery will attempt to repair by either homology-directed repair (HDR) or non-homologous end-joining (NHEJ) (Figure 9), the latter most frequently [237]. Repair by NHEJ is a highly error-prone process, resulting in

insertions or deletions (indels) of various lengths at the cut site. These indels may induce frameshift mutations altering the open reading frame or premature stop codons eliminating the production of functional protein, thereby resulting in knockout of the targeted gene [233,238]. Thus, NHEJ of Cas9-mediated double-strand break results in a heterogeneous population of cells, and therefore, clonal expansion of individual clones has to be conducted to establish a cell line with the specific knockout. The HDR pathway mediates precise repair using a homologous donor template, which can be utilized to introduce or replace specific sequences [239]. However, repair by HDR occurs in the late S and G2 phases of the cell cycle [239], making the precise insertion of a desired modification a less efficient.

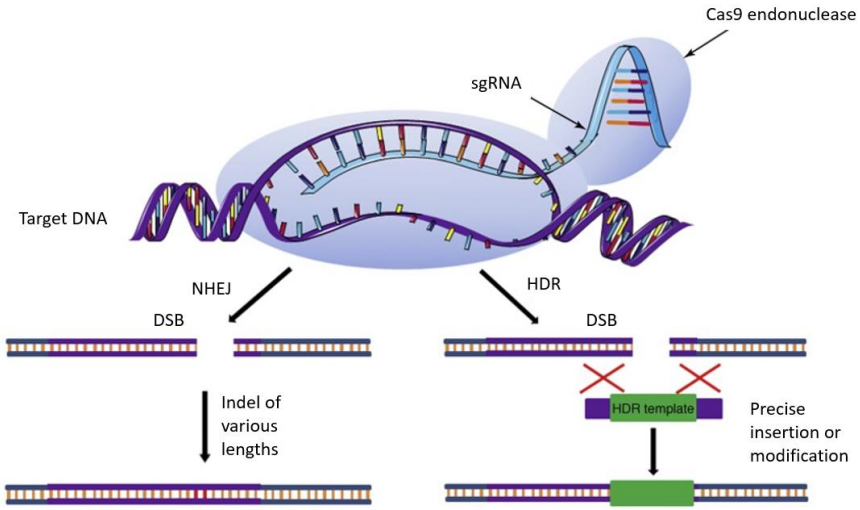

Figure 9. The CRISPR-Cas9 system. The genome-editing tool CRISPR-Cas9 is composed of two components – the Cas9 endonuclease and a sgRNA complementary to the desired target sequence. Once the sgRNA-Cas9 complex binds to the target sequence, Cas9 introduces a double-stranded break (DSB), which is repaired by non-homologous end-joining (NHEJ) or homology-directed repair (HDR). The most common repair pathway is NHEJ, which is error-prone, resulting in frequent deletions and insertions (indels) of different lengths. The HDR pathway can be employed to introduce or alter a specific sequence by delivering a donor template. Figure adapted from [240].

The major advantage of the CRISPR-Cas9 technology is the relative simplicity of design, where the sgRNA can target almost any DNA sequence, making the system easily programmable. Moreover, by applying multiplex CRISPR using multiple sgRNAs, several genes can be targeted simultaneously. In contrast, previous genome-editing tools such as zinc-finger nucleases (ZFNs) and transcriptional activator-like effector nucleases (TALENs) are based on complex DNA-protein interactions, which are difficult to design and require substantial optimization and validation [241].
A disadvantage of the CRISPR-Cas9 technology, as well as ZFN and TALEN, is that they by generating double-stranded DNA breaks are dependent on the cellular DNA repair mechanisms to function, and as indels generated by NHEJ occurs randomly,

gene knockout as a result of frameshift and nonsense mutations does not necessarily occur. Moreover, although CRISPR-Cas9 induces double-stranded break in both alleles, subsequent repair potentially results in two different indel mutations within the same cell. Off-target effects constitute another limitation of CRISPR, which, however, is challenging to predict and varies in frequency depending on the sgRNA and target sequence [238]. As breaks in non-target sites are caused by the ability of Cas9 to cleave DNA in presence of imperfect sgRNA-target complementarity, new high-fidelity Cas9 variants have been engineered to reduce off-target cleavage but retain high on-target efficiency [242–244]. Another approach limiting off-target effects is to decrease the concentration of sgRNAs and Cas9 endonucleases in the cells [242]. Since viral delivery leads to stable and persistent expression [233], alternative transient delivery methods can be utilized when attempting to reduce off-target cleavage. Besides direct delivery of sgRNA and transcribed Cas9 mRNA [245], sgRNA:Cas9 complexes can be delivered to the cells as ribonucleoproteins with the advantages of being independent of translation into Cas9 protein and the relatively short period of Cas9 activity [246,247].

Several genetic manipulation tools have been developed by utilizing the CRISPR system, and an engineered catalytically inactive Cas9 (dCas9), which can be fused to different effector domains, leading to CRISPR-based gene activation [248], gene interference [248], specific base editing [249], epigenetic modifications including DNA methylations and histone acetylation [250] among others, allowing researchers to decipher the functional implications of all genes and biological mechanisms. In addition, the simplicity of sgRNA design and the capacity to target nearly all genomic regions have led to development of genome-wide CRISPR screens utilizing thousands of unique sgRNAs targeting various genes [248,251]. By global CRISPR screens, researchers are able to identify genes regulating a desired phenotype, and the approach is especially useful for studying a phenotype where the underlying genetic alterations are poorly understood.

Even though the CRISPR-Cas9 technology is commonly described as simple, cost-efficient, and effective, a successful CRISPR gene editing experiment requires optimal designing of sgRNA directed towards a target site with high specificity and activity, efficient delivery of CRISPR-Cas9 components into target cells, determination of the CRISPR-Cas9 activity by indel quantification, and isolation and enrichment of clones. Thus, the CRISPR-Cas9 technology involves several choices of applications and experimental optimizations.

Gene expression

Gene expression profiling constitutes the second methodological part of this dissertation, including determination of both global and single gene/miRNA expression in clinical DLBCL samples.
The microarray platform has for decades been a valuable tool for identification of biological characteristics and mechanisms by capturing the transcriptional activity in a given sample. Gene expression profiling (GEP) has profoundly impacted biomarker discovery and disease characterization, emphasized by several prognostic GEP-based classification signatures in DLBCL [24–26,180]. Microarray utilizes hybridization between complementary oligonucleotides, where the hybridization intensity correlates to the concentration of target bound [252]. However, cross-hybridization, limited dynamic range due to background and saturated signals, and dependence on existing knowledge of the sequences are significant limitations of the technique. The applied GeneChip Human Genome U133 Plus 2.0 platform from Affymetrix analyzes the expression of more than 47,000 transcripts, representing 38,500 of the best characterized human genes. It consists of more than 54,000 probe sets, which each encompasses 11 oligonucleotide probes designed to detect the 3' end of a gene.

Determination of individual miRNA expressions has been conducted with two distinct methodologies, quantitative PCR (qPCR) in paper II and droplet digital PCR (ddPCR) in paper IV, which, however, rely on the same principles of PCR and enable detection and quantification of specific cDNA targets within a sample. Detection of PCR signal is achieved by TaqMan hydrolysis probes, designed with a 5' fluorescent reporter dye and a quencher in the 3' end. Upon primer extension, the DNA polymerase cleaves the probe leading to a fluorescent signal, which increases proportionally with PCR product accumulation (Figure 10A) [253].
qPCR relies on a continuous collection of PCR signals over a range of cycles, which are converted into a numerical value. Specifically, the fluorescence intensity for each sample is represented by the quantification number (Cq) corresponding to the cycle number at which the fluorescent signal crosses the threshold of quantification, with a low Cq reflecting high target quantity and vice versa. As the PCR efficiency varies between assays, thereby confounding data interpretation, standard curves were conducted at least three times on human brain reference cDNA to determine and subsequently correct for assay-specific amplification efficiency (Figure 10B). To ensure reliable and reproducible qPCR experiments, guidelines for Minimum Information for Publication of Quantitate Real-Time PCR experiments (MIQE) have been published [254]. Although the MIQE checklist is comprehensive and can be difficult to follow entirely in practice, it is important to report sufficient experimental information for other researchers to critically evaluate the quality and to reproduce results.

The ddPCR application has been developed to provide high precision and absolute quantification of nucleic acid targets in a sample. The method relies on the partitioning

of a sample into multiple discrete reaction compartments (Figure 10C), where the system by Bio-Rad partitions the sample in up to 20,000 uniform nanoliter-sized droplets [255]. A PCR run will take place in each individual droplet resulting in multiple replicates of a reaction. Upon droplet generation, target molecules in a sample will be randomly and independently distributed into the droplet; thus, some droplets will contain one or more target molecules, while others will contain none (Figure 10C). This nature of random and independent distribution follows the rules of Poisson distribution and allows the application of Poisson statistics for calculation of the number of target molecules within a sample. All droplets will contain an intrinsic fluorescence signal due to imperfect quenching of the fluorophore, however, positive droplets containing target nucleic acid will emit a strong fluorescent signal resulting from cleavage of the probe. Based on the fluorescence amplitude, a threshold is placed, and each droplet is evaluated as either positive or negative, and by applying Poisson statistics the absolute concentration can be calculated (Figure 10C) [255].

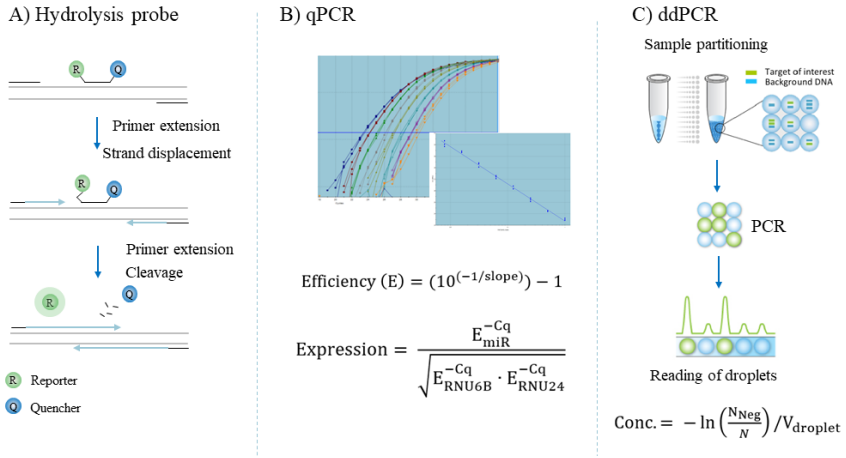

Figure 10. Quantification of gene expression. A) The principle of hydrolysis probe-based quantification. The primers and probe anneal to the complementary DNA sequences, and subsequent primer extension will cleave the probe by the 5'-3' exonuclease activity of the Taq DNA polymerase. Seperation of the fluorescent reporter (R) from the repressive quencher (Q) will result in emission of a detectable fluorescent signal. B) Illustration of a standard curve, used for qPCR, which is generated by plotting Cq-values as a function of the logarithm of reference sample concentration. miRNA expression levels were calculated by normalization to endogenous reference genes. C). Presentation of the three steps in ddPCR. The sample is partitioned into separate droplets, subjected to PCR cycling with reactions taking place in each droplet. The fluorescent signal of each droplet is analyzed. Figure adapted from [290].

The major advantage of ddPCR is the absolute quantification of target sequences, as ddPCR counts the number of molecules. For determination of gene expression, the absolute quantification is used to calculate the relative expression level of the unknown target to a reference. Proper reference genes that exhibit stable and equal cellular expression independent of samples are important for both qPCR and ddPCR. Endogenous reference genes are used for correction of potential RNA and reverse transcription efficiency biases.

Another advantage of ddPCR is the use of end-point measurements of each reaction, making the method independent of reaction efficiency, and enables nucleic acid quantification without use of standard curves. Thus, not every PCR reaction has to run perfectly, as opposed to qPCR. The massive partitioning of a sample enables detection of small fold differences in target sequence between samples to be reliable, by reducing the competition for primers and probes from background sequences. Furthermore, it facilitates detection of rare targets, which otherwise can be difficult due to dilution in a high amount of background sequences. Moreover, the multiple reactions ensure that the concentration output is not significantly affected by the position of the threshold, and results are not biased by the small fraction of droplets that do not reach endpoint. Besides gene expression, ddPCR can be applied for assessment of copy number variations, utilizing two probes designed to detect of a specific variant and wild type, respectively. For these reasons, the use of the ddPCR technology is expanding for both pre-clinical research and clinical approaches.

4. SUMMARY OF MAIN RESULTS

This section presents results generated from the experimental work of paper II [256] and paper IV [257]. As paper I is a literature review of the biomarker potential of miR-155 in B-cell malignancies [183], not including original findings, it is not considered in this section. Paper III [96] is also a review on clinical and molecular risk markers of vincristine-induced neuropathy. As follow up to this topic, a pilot study was performed from which unpublished data are presented.

Paper II

The aim of this study was to identify miRNAs involved in vincristine response in DLBCL. By vincristine dose-response analyses, twelve DLBCL cell lines were ranked according to growth inhibition and categorized as sensitive, intermediate, and resistant [256]. In order to develop prognostic tools based on pre-treatment features of tumors, baseline miRNA expression profiles of each cell line in untreated conditions were utilized for differential miRNA expression analysis between vincristine sensitive and resistant cell lines. Fifteen differentially expressed miRNAs were identified, and miR-155 displayed the largest fold-change, with significantly lower expression in vincristine resistant DLBCL cell lines. Consistent with this association, suppression of miR-155 in intrinsically vincristine-sensitive SU-DHL-5 cells induced resistance, and ectopic upregulation increased the sensitivity (Figure 11) [256].

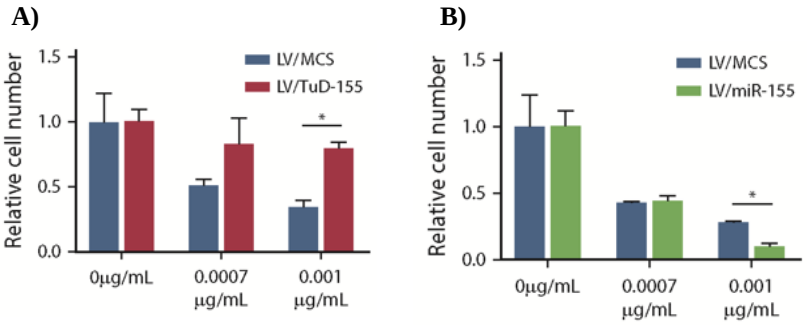

Figure 11. Selected functional assays. A) Suppression of miR-155 by Tough Decoy in SU-DHL-5 cells induced vincristine resistance. **B)** Ectopic upregulation of miR-155 in SU-DHL-5 cells increased vincristine sensitivity. Vincristine response is indicated as the number of living cells relative to drug-solvent treated control (0.0µg/mL). MCS, SU-DHL-5 cells transduced with a vector containing an empty multiple cloning site. Figure from [256]

Gene set enrichment analysis (GSEA) of SU-DHL-5 cells with induced expression of miR-155 revealed enrichment for genes involved in the G2/M checkpoint and mitotic

spindle assembly in comparison to control cells. In agreement, these gene sets were depleted in SU-DHL-5 cells with reduced miR-155 expression [256], indicating that miR-155 and the antimitotic drug vincristine affect the same biological mechanisms. Based on these findings, we hypothesized that vincristine resistance mechanisms were related to cell cycle regulation. Therefore, genes negatively correlated with miR-155 expression, which are involved in cell cycle processes, were selected and investigated for potential as miR-155 targets. The *WEE1* gene possessing a miR-155 binding site in the 3'UTR was identified [256] and has also been experimentally verified as a target by others [258,259]. Consistently, increased protein levels of Wee1 were observed in miR-155 knockout clones [256]. Notably, Wee1 is a kinase regulating cell cycle progression at the G2/M transition, which affects sensitivity to antimitotic drugs [115]. In accordance, chemical inhibition of Wee1 sensitized wild-type OCI-Ly7 cells to vincristine [256]. Together, these results document that miR-155 regulates vincristine sensitivity in cultures of GCB-DLBCL cells and further suggest a mechanism through regulation of Wee1.

Prognostic impact of miR-155 was assessed in our local cohort and verified in a large independent cohort, both of primary DLBCL patients treated with standard R-CHOP. Applying dichotomized miR-155 expression, inferior overall and progression-free survival was observed for GCB-classified patients with high miR-155 expression, whereas no prognostic stratification was obtained when analyzing all DLBCL patients or ABC cases (Figure 12) [256]. Multivariate Cox regression analysis confirmed independent prognostic effect of dichotomized and continuous miR-155 expression in GCB-DLBCL. This suggests that the functional link between miR-155 and vincristine response is strong enough to affect the clinical outcome of GCB-DLBCL patients, even though they are treated with R-CHOP combinational therapy.

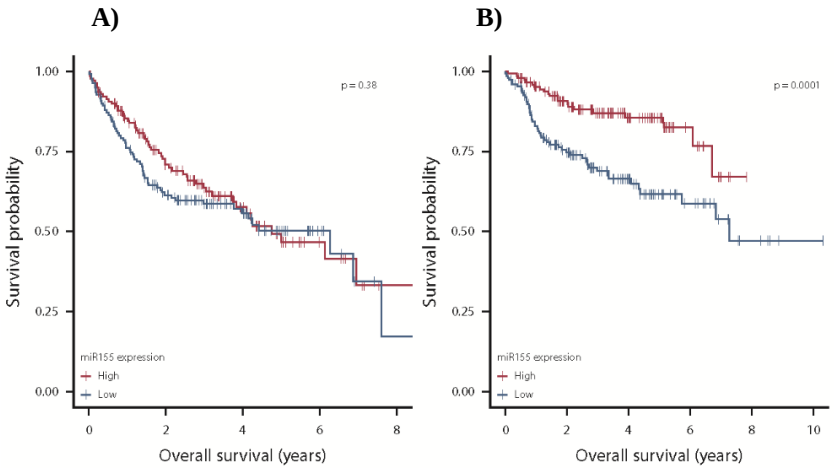

Figure 12. Prognostic impact of miR-155. Kaplan Meier analyses were conducted for **A)** ABC- and **B)** GCB-DLBCL patients. Dichotomized miR-155 expression by median split. Figure from [256].

Paper III

Systematic literature review of vincristine-induced neuropathy [96] prompted us to conduct a pilot study interrogating the dose-limiting side effect in DLBCL patients treated at Aalborg University Hospital. The study aimed at determining the incidence of vincristine-induced neuropathy and identification of potential biomarkers predicting risk of neuropathy development.

Information on clinical manifestation of neuropathy and any subsequent alteration of vincristine treatment was obtained for 92 DLBCL patients treated with CHOP or R-CHOP by examining medical records. The incidence of vincristine-induced neuropathy was 37% and led to alteration of vincristine treatment in 29 out of 34 patients (Table 2), and the remaining 5 developed neuropathy after treatment was completed. The predominant alteration was substitution to vinblastine (Table 2), another vinca alkaloid with less neurotoxicity potential [260]. Adjustments of vincristine treatment occurred at different times in the course of treatment (Table 2.B).

A)

			Treatment alteration			
		Neuropathy	Dose reduction	Substitution	Discontinuation	All
All n=92	+	34 (37%)	4 (17%)	20 (59%)	5 (17%)	29
	-	58 (63%)				
CHOP[I] n=23	+	11 (48%)	2 (30%)	6 (40%)	1 (10%)	9
	-	12 (52%)				
R-CHOP[II] n=69	+	26 (38%)	2 (10%)	14 (65%)	4 (20%)	20
	-	43 (62%)				

B)

Cycle	**1**	**2**	**3**	**4**	**5**	**6**	**7**	**8**
Dose reduction				1		1	1	1
Substitution	1	1	1	6	5	6		
Discontinuation					2	2	1	

Table 2. Vincristine-induced neuropathy. A) Incidence of neuropathy manifestation and the following adjustment of vincristine treatment. [I] CHOP, CHOEP, CNOP, COP; [II]R-CHOP, R-CEOP, R-CHOEP. + indicates neuropathy, and – no reported symptoms of neuropathy. **B)** Time outline of vincristine alteration in relation to the eight R-CHOP cycles.

Several clinical parameters, including age, performance status, creatinine levels, among others (Table 3) were examined for neuropathy risk stratification potential, however, all without significant difference between patients with and without

neuropathy manifestation. Thus, in agreement with findings of the literature review [96], none of the clinical parameters display potential as biomarkers of vincristine-induced neuropathy.

	Neuropathy	No neuropathy	*p*
n, (%)	34 (37%)	58 (63%)	
Gender			
Female	14 (41.2%)	24 (41.4%)	
Male	20 (58.8%)	34 (58.6%)	
Age			
Median	64	64	
Range	31-83	25-85	
IPI			0.36
0-1	10 (29.4%)	23 (39.7%)	
2-5	22 (64.7%)	33 (56.9%)	
NA	2 (5.9%)	2 (3.4%)	
Performance status			0.78
0-1	28 (82.3%)	49 (84.5%)	
2-5	4 (11.8%)	6 (10.3%)	
NA	2 (5.9%)	1 (1.7%)	
Diabetes mellitus			0.92
Yes	5 (14.7%)	9 (15.5%)	
No	29 (85.3%)	49 (84.5%)	
LDH			0.14
Normal	13 (38.2%)	31 (53.4%)	
Elevated	21 (61.8%)	26 (44.8%)	
NA	0	1 (1.7%)	
Alkaline phosphatase			0.14
Normal	18 (53%)	18 (31%)	
Elevated	16 (47%)	39 (67.2%)	
NA	0	1 (1.7%)	
Creatinine			0.28
Normal	26 (76.5%)	49 (84.5%)	
Elevated	7 (20.6%)	7 (12.1%)	
NA	1 (2.9%)	2 (3.4%)	

Table 3. Clinical parameters in DLBCL patients with and without neuropathy. P-values from univariate logistic regression.

As opposed to the lack of association between clinical parameters and neuropathy manifestation, multiple molecular markers were in the literature review identified to possess the ability to stratify patients according to neuropathy risk [96].

In an attempt to stratify chemotherapy resistant and sensitive patients, our research group has established predictors of response to standard multidrug regimens. We developed resistance gene signature (REGS) classifiers based on systematic *in vitro* dose response drug screens of 26 B-cell cancer cell lines, where the gene expression profiles for each cell line in untreated condition were combined with degree of dose-dependent growth inhibition after exposure to cyclophosphamide, doxorubicin, or vincristine [218]. Using REGS, each of the 92 DLBCL patients was assigned a

resistance probability for vincristine in the tumor, and subsequent analysis showed no significant difference in neuropathy frequency between patients predicted to be sensitive and resistant to vincristine (Table 4).

Vin REGS class	Neuropathy		
	+	-	In total
Sensitive	18 (56%)	14 (44%)	32
Intermediate	4 (8%)	9 (92%)	13
Resistant	11 (34%)	20 (66%)	31

Table 4. Neuropathy incidence in predicted vincristine response classes. No association between predicted vincristine response, obtained by REGS classification, and neuropathy incidence was observed (χ^2 , p=0.09). + indicates neuropathy, and – no reported symptoms of neuropathy. REGS, resistance gene signature.

Paper IV

In this study, we elucidated the predictive potential of a miRNA-panel, developed from miRNAs identified to be associated with the response of individual compounds of R-CHOP. DLBCL cell lines were analyzed with systematic single drug screens of each R-CHOP component followed by division into groups of sensitive, intermediate, and resistant cells for rituximab, cyclophosphamide, doxorubicin, and vincristine, respectively. Differential analysis of baseline miRNA expression was conducted between sensitive and resistant cell lines for each drug, resulting in identification of 43 miRNAs associated with one or more R-CHOP compounds [257].

For clinical applicability and assessment of predictive potential, miRNAs detected by probe sets of the HG-U133 GeneChip were selected for subsequent statistical modeling. Specifically, 11 probe sets covering 9 drug associated miRNAs were included. Using HG-U133 gene expression profiles and clinical outcome information of R-CHOP treated DLBCL patients, training and validation of prognostic miRNA-panel classifiers were performed for all DLBCL patients and restricted to ABC and GCB classified patients. To test both non-parametric and parametric survival analysis models, random survival forest and multivariate Cox regression were utilized for generation of classifiers. The prognostic performances were evaluated by Brier Scores, estimating the predictive accuracy, and time varying area under the ROC curves (tAUC). Multiple Cox regression-based classifiers displayed better predictive accuracy in comparison to the random survival models, which had higher prediction errors (Figure 13A). In GCB-DLBCL, the Cox miRNA-panel constituting probe sets detecting miR-21, the miR-23a~miR-27a~miR-24-2 cluster, miR-34a, miR-146a, and miR-155 (Table 5), exhibits prognostic performance comparable to IPI (Figure 13B). Furthermore, addition of the drug-response associated miRNA-panel to IPI improved the prognostic utility of IPI in GCB-DLBCL (Figure 13B).

Feature	miRNA	Hazard Ratio
IPI2–5		3.335
232504_at	miR-146a	0.857
229437_at	miR-155	0.868
220990_s_at	miR-21	0.995
1555847_a_at	miR-23a~miR-27a~miR-24-2	0.958
235571_at	miR-34a	0.776

Table 5. Probes and detected miRNAs constituting the multivariate Cox model. The miRNA panel model was trained within the GCB subclass of DLBCL patients. Only miRNA probes significant in univariate Cox regression analysis were included in this model. Table from [257].

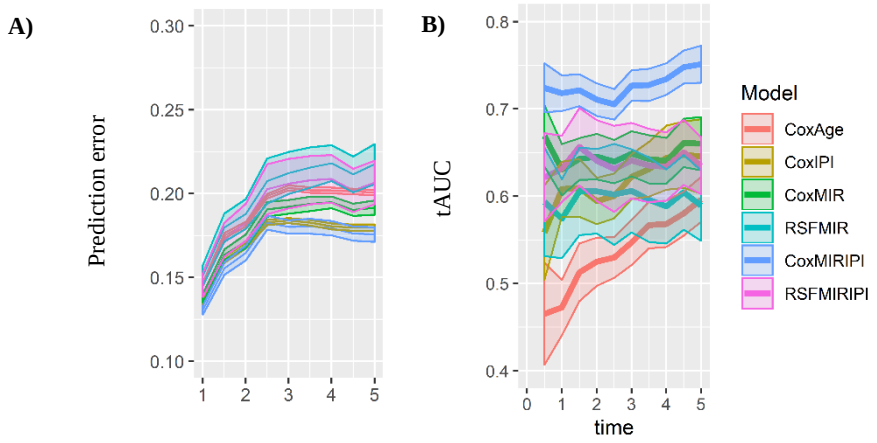

Figure 13. Evaluation of the predictive potential of generated models in GCB-DLBCL. The accuracy of predicted survival by the developed models vs. observed progression-free survival assessed by **A)** Brier Scores and **B)** time varying area under the ROC curves (tAUC). Figures depict means ± 2 standard deviations estimated across the 10 repeats of cross-validation. The predictive models include multivariate Cox regression models using either age (CoxAge), IPI (CoxIPI), expression of miRNAs (CoxMIR), or miRNA expression in combination with IPI (CoxMIRIPI), and random survival forest models using expression of miRNAs (RSFMIR) or miRNA expression combined with IPI (RSFMIRIPI). The model combining the miR-panel and IPI (CoxMIRIPI, dark blue) performed the best with the lowest prediction error in A) and the highest area under the ROC curve in B). Time in years. Figure from [257].

Utilizing the developed miRNA-panel classifier alone and in combination with IPI, a risk prediction score was calculated for each GCB classified patient. Division into groups of high-, intermediate-, and low-risk documented adverse prognosis of high-risk patients (Figure 14A+B). Thus, miRNAs associated with R-CHOP components display the potential to stratify GCB-DLBCL patients into prognostic risk groups, and combination of the miRNA panel and IPI improves the prognostic performance. All included miRNAs were initially identified to be associated with response to doxorubicin and/or vincristine, with high expression levels in sensitive cell lines. In agreement, the survival analysis revealed correlation between higher expression levels and superior prognosis.

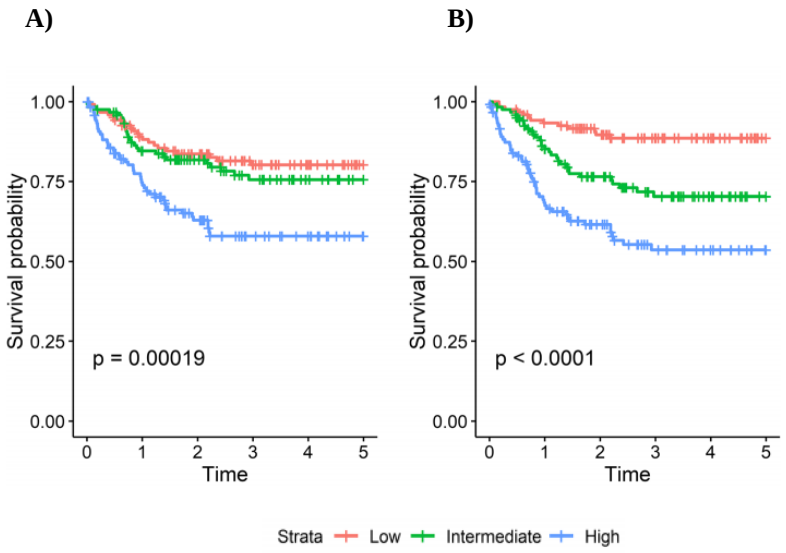

Figure 14. Kaplan Meier analysis of risk-groups of GCB-DLBCL patients. Applying the **A)** miRNA panel and **B)** miRNA panel in combination with IPI, GCB-DLBCL patients were classified as low-, intermediate-, and high-risk. P-values from log-rank test. Time in years. Figure from [257].

5. DISCUSSION

This section discusses the overall and additional considerations of presented data. Discussion of the main results of each study is included in the papers and will not be repeated except for contextual purposes.

Treatment challenges in DLBCL

Cancer therapy is shifting towards precision medicine tailoring therapeutic interventions to the individual patient characteristics by integrating clinical information and molecular features of the tumor. By moving beyond the conventional "one-fits-all" approach, precision medicine aims to identify the medical treatment that is likely to confer the greatest benefit to the individual, sparring side effects and the expense of interventions likely without efficacy [261]. In DLBCL, the significant molecular difference between ABC and GCB subclasses has been employed in clinical trials evaluating the opportunity to optimize treatment efficacy by subclass-specific targeted treatment, yet all eventually failed (Table 1) [68–76]. However, the recent genetic classifications have highlighted the extent of molecular heterogeneity of DLBCL [58–62], and only if consensus on genetic subgroups are reached a trustworthy guidance of therapeutic targeting appear realistic.

The lack of treatment improvements is multifactorial involving potentially overlapping resistance mechanisms between R-CHOP components, overlapping toxicities leading to dose reduction or omission, and biological heterogeneity of the patient population [110]. The failure of various trials emphasizes that R-CHOP constitutes a potent treatment combination that needs further investigation for an improved understanding of the underlying response and resistance mechanisms. In general, the pharmacological principles and underlying molecular mechanisms of multidrug combinations are poorly understood since they often were developed by empirical experimentation in patients without further mechanistic analysis. However, such information is pivotal for development of new treatment strategies including add on drugs. A recent investigation of the pharmacological interaction and cross-resistance among the R-CHOP compounds revealed clinical superiority by independently cytotoxic drugs having non-overlapping resistance mechanisms [65]. Therefore, identification of underlying mechanisms and factors involved in response to the individual drugs of R-CHOP is crucial for improved understanding of the entire regimen.

Vincristine-induced neuropathy

Treatment efficiency is, in addition to resistance, influenced by numerous patient-related factors, such as pharmacokinetics and treatment adjustments according to performance status, co-morbidities, and side effects. The dose-limiting side effect of vincristine is neuropathy, where severity increases by cumulative dose [96]. In our local pilot cohort, the incidence of vincristine-induced neuropathy was 37%, resulting in an alteration of vincristine treatment in all patients with manifestations during the course of R-CHOP therapy. We did not assess the impact of vincristine alteration on treatment efficacy and outcome due to limited cohort size, unequal treatment regiments (CHOP vs. R-CHOP), dose reduction concentration, substitution, and cycle number in which treatment was adjusted. Dose reduction of vincristine has been shown to confer inferior prognosis in R-CHOP treated DLBCL patients [100], in contrast, another study reported that omission of vincristine did not affect outcome [262], an inconsistency potentially caused by patient-specific vincristine alterations.
A significant limitation of the study is that information on neuropathy was obtained by clinical interview, introducing the risk inter-observatory variability. Our literature study revealed no consensus between studies in neuropathy assessment tools and scoring systems, leading to inconsistency in reported incidence, severity, and the risk stratifying potential of various clinical and molecular parameters [96]. In agreement with findings of the literature review [96], none of the clinical parameters investigated in this study exhibited association to neuropathy (Table 3).
When assessing a potential molecular marker in our pilot study, predicted vincristine sensitivity [218] did not display association to neuropathy manifestation (Table 4), an observation that could be expected as the sensitivity predictions are based on transcriptional profiles of the tumor, whereas neuropathy manifests in neurons. Molecular markers of neuropathy risk are therefore presumably germline mutations rather than somatic, and in agreement, a study analyzing normal cells isolated from acute lymphoblastic leukemia patients identified an association between polymorphisms in the drug transporters, ABCC1, ABCC2, and ABCB1, and incidence and severity of neuropathy [263,264]. Moreover, inherent mutations in the gene encoding the CYP3A5 enzyme, which metabolizes vincristine, have been shown to increase the risk of neuropathy, though with some inconsistencies between studies [96,108,265]. Unfortunately, we lack normal samples of the patients in this pilot cohort, limiting the ability to identify promising markers.

miRNA involvement in drug response

To identify miRNAs implicated in vincristine response, differential miRNA expression analysis was performed between sensitive and resistant DLBCL cell lines. Since the selected response division of cell lines may influence the output, multiple split strategies were applied to ensure a robust result. miR-155 had the highest fold-change difference irrespective of split strategy and was subsequently functionally

verified to increase vincristine sensitivity in GCB-DLBCL cells [256]. Functional analyses were conducted in two ABC and GCB cell lines, respectively, to eliminate the risk of cell line-specific effect. Although both up- and down-regulation of miR-155 was performed relative to the intrinsic vincristine response and endogenous miR-155 level, no effect on vincristine response was observed in ABC-DLBCL [256].
The rank of cell lines according to vincristine sensitivity, led to the observation that the extremes were defined by GCB cell lines, whereas ABC cells were intermediate responsive to vincristine despite having high miR-155 expression. Consequently, the involvement of miRNAs in vincristine response addressed in this study was restricted to GCB DLBCL and could explain why the manipulation of miR-155 in ABC cells did not affect vincristine sensitivity. We eliminated the possibility of technical limitations since successful transduction was documented by cellular expression of the reporter GFP. In addition, applied lentiviral vectors and the subsequent up-regulation or suppression of miR-155 had no toxic effect on either ABC or GCB cells [256]. The functional data indicate that the mechanism of miR-155-mediated vincristine response regulation is cell-of-origin selective potentially due to different targets affected depending on the cell type in which miR-155 is expressed. As the subsequent target gene analysis was restricted to GCB cells, it is arguable that further studies should have been performed in ABC cells to examine the possibility of ABC and GCB-specific targets.

Pathways affected by miR-155 was examined by GSEA and moreover, gene ontology analysis was utilized for identification of miR-155 target genes implicated in vincristine response. Although both approaches are prominent standard tools for identifying deregulated pathways of various biological states of clinical samples and cell lines [266,267], data interpretation of enriched and depleted gene sets should be conducted with caution. In GSEA, an enrichment score is calculated for an *a priori* defined set of genes having the same biological function based on their differential expression between two biological states or phenotypes [266]. Notably, overlapping genes of the respective gene sets lead to outputs with hundreds of significantly enriched gene sets, complicating the interpretation and the aim of obtaining a list with limited numbers of affected pathways. To alleviate this limitation, we restricted the analysis to the ‘Hallmark’ gene sets from the Molecular Signature Database, which consists of 50 refined gene sets derived from several founder sets to reduce the redundancy across gene sets and provide concise outputs [266,268]. With utility of GSEA, the G1/S and G2/M checkpoints and mitotic spindle assembly mechanisms were identified as putative downstream effectors of miR-155 [256]. Consistently, the E2F transcription factor and Wee1 kinase controlling G1/S and G2/M transition, respectively, are experimentally verified targets of miR-155 [258,259,269]. Likewise, we observed decreased Wee1 mRNA expression in ectopic miR-155 expressing SU-DHL-5 cells and, conversely, increased protein abundance in miR-155 knock-out clones [256]. Wee1 controls the spindle assembly checkpoint, activated upon vincristine exposure due to impaired mitotic spindle formation leading to mitotic extension and eventually apoptosis [115]. Chemical inhibition of Wee1 sensitized

DLBCL cells to vincristine [256], suggesting that the increased vincristine sensitivity observed upon high miR-155 expression is mediated by repression of Wee1, leading to continued activation of the spindle assembly checkpoint. However, further studies investigating the effect of miR-155 on cell cycle distribution, mitotic spindle assembly, and apoptosis are warranted to determine the mechanisms, which can be caused by additional targets and cellular pathways. As a specific miRNA has several target mRNAs, the phenotypic effect of deregulating the miRNA is most likely mediated via multiple targets, of which some potentially reside in the same pathway. Therefore, we investigated the pathways affected by miR-155 by GSEA prior to target gene analysis, which in addition to Wee1, identified multiple other predicted targets involved in cell cycle regulation (*CAB39*, *RPS6KB1*, *GSK3B*, *PARD3B*, *TFDP2*, *C7orf25*, *PAK2*, *RBBP4*).

Since cell lines are simplified model systems that do not reflect the complexity in patients, *in vitro* findings often need verification *in vivo* or in 2- or 3-dimensional culture assays simulating the natural setting. Alternatively, clinical investigations can be conducted to examine the clinical relevance. As the second aim in this thesis was to determine the involvement of miRNAs on vincristine response and the impact on prognosis, we performed clinical outcome analysis in primary DLBCL patients. The *in vitro* results on subclass-specific effect of miR-155 in addition to the differential expression of miR-155 between the subclasses [183,256] prompted us to investigate ABC and GCB classified patients separately. This revealed a favorable prognosis of GCB patients with high miR-155 expression, whereas no association to outcome was observed in ABC-DLBCL cases [256]. Although this finding supports the GCB-selective role of miR-155 on vincristine sensitivity, it could appear controversial when considering the known oncogenic properties of miR-155 [202,209–211]. In general, the investigation of miRNAs is complex, and studies inconsistently account as to whether a particular miRNA has oncogenic or tumor-suppressive effects [169]. However, miRNAs can display duplicity having both properties by targeting tumor suppressors and oncogenes, respectively, which furthermore can vary depending on the cell type in which it is expressed [124,149,169]. Moreover, miRNAs can modulate the tumor microenvironment [170,270–272] and, as in this study, sensitivity to treatment [256,273], why the phenotypic effect of a miRNA is a result of all these aspects.

In the past years, long non-coding RNAs and circular RNAs (circRNA) have obtained increased attention [274,275]. Like miRNAs, these exhibit tissue- and cell type-specific expression and play a role in normal cellular processes and cancer development [274–276], which, however, is largely undefined. The biological function of circRNAs is not yet fully elucidated, but miRNA sponging properties have been documented for particular circRNAs [277]. Notably, circRNAs display promising potential as biomarkers due to their stable circular structure, arising from back-splicing where the 3’ end of an exon is covalently joined to the 5’end of the same or another exon [275,278].

The DLBCL patients included for prognostic assessment have been treated with standard R-CHOP; thus, the clinical outcome is a summed effect of all drug components of the regimen. Nevertheless, prognostic evaluation of miR-155 documented increased overall and progression-free survival in GCB patients exhibiting high miR-155 expression, indicating that the regulatory role of miR-155 on vincristine is strong enough to affect the overall clinical outcome in GCB DLBCL. However, considering the complexity of miRNAs, the clinical superiority of high miR-155 expression could be caused by additional factors than through vincristine response. While the puzzling issue of why miR-155 is not associated with outcome of ABC patient remains not fully elucidated, the prognostic significance in GCB-DLBCL is compelling. Nevertheless, clinical applicability for prognostic assessment is doubtable due to the broad range of miR-155 expression.

Based on the identified prognostic impact of miR-155, we aimed at developing a panel of miRNAs associated with the individual R-CHOP compounds that could improve the predictive potential. By using several markers, the likelihood of capturing the spectra of the biology in a heterogeneous tumor is increased, strengthening the robustness [279,280]. The initial analysis in paper IV was to identify drug-response specific miRNAs. Subsequent filtering of the 43 identified miRNAs to those mapped by HG-U133 array probes led to a list of 9 candidate miRNAs, which were used as input for modeling of prognostic classifiers [257]. Although the reduction of the number of miRNAs is a significant limitation of the study, it was a strategy that allowed clinical assessment of miRNA expression in independent clinical cohorts. The multivariate Cox regression miRNA-panel model encompassing miR-21, miR-23a~miR-27a~miR-24-2 cluster, miR-34a, miR146a, and miR-155 displayed the best predictive accuracy in DLBCL patients of the GCB subclass, whereas high prediction errors were observed for all generated models in ABC classified patients [257]. As mentioned above, the study of miRNAs in vincristine response was restricted to the GCB subclass, and likewise, GCB cell lines predominate the groups of doxorubicin sensitive and resistant cells, emphasizing the different biological pathogenesis of ABC and GCB subclasses [24,25]. The majority of candidate miRNAs utilized for prognostic modeling are associated with vincristine and doxorubicin [257], which are key components of the R-CHOP regimen [84,281], explaining the better performance of developed miRNA-panel models in GCB-DLBCL in comparison to ABC-DLBCL.

In addition to the regulatory role of miR-155 on vincristine response documented in paper II [256], miR-155 was found to be associated with doxorubicin sensitivity and rituximab resistance [257]. The associations are based on statistics; thus, functional examination must be performed to determine the direct impact of miR-155 on response to these drugs. In contrast, to the identified association between doxorubicin sensitivity and high miR-155 expression, suppression of miR-155 in a lung cancer cell line increased the sensitivity to doxorubicin [282] whereas we in functional studies of DLBCL cells did not observe any effect on doxorubicin response (data not shown), in consistence with others [180]. This inconsistency is most likely a result of the tissue

and cell-type dependent effect of a miRNA and emphasizes the challenge of comparing studies of miRNAs. Of the other miRNAs in the prognostic panel, miR-34a has by lentiviral intervention been functionally verified to increase sensitivity to doxorubicin in DLBCL cells, consistent with the association we observe [181]. Contradictory, miR-21, which we found to be highly expressed in vincristine sensitive cells, has been shown to confer resistance towards combinational CHOP treatment in a DLBCL cell line [194].

The clinical applicability of the miRNA-panel classifier is limited despite prognostic impact similar to what observed for IPI and the ability to improve the prognostic performance by combining the miRNA-panel and IPI. However, as a proof of concept, it shows that molecular markers can be combined to improve clinical IPI. The primary limitation of the classifier is the restriction to the GCB subclass, whereby it is only applicable for approximately 50% of patients diagnosed with DLBCL [24,25]. In addition, recent observations of genetic heterogeneity within the ABC and GCB subclasses have led to molecular classifications based on tumor genetics [58–62] and potentially a shift in the paradigm of DLBCL subclassification from transcriptional based to rely on genetics [63]. Whether the miRNA panel is associated with the new genetic subgroups is yet to be examined.

Translation of biomarkers and classifiers into clinical practice is challenging and requires a strong correlation between biomarker and phenotype, validation in large independent cohorts, standardized material handling and detection methods, and prospective testing [283]. Moreover, classifiers often involve cohort-based normalization and clustering, whereby the assigned subtype can vary depending on the tumors included. This is an obstacle for applicability in a clinical setting where one patient is classified at a time [55,60].

Quantification of the miRNAs included in the prognostic panel can be performed by the HG-U133 probe sets or by ddPCR, which in contrast measures the mature miRNA expression. ddPCR has the advantage of being sensitive, enabling detection and quantification of rare and low abundant targets and is therefore a useful approach for liquid biopsies [284,285], where molecular markers derived from apoptotic and necrotic cancer cells are detected in blood or other body fluids. On the other hand, the HG-U133 platform has been widely used for ABC/GCB subclassification [24,25]; thus, determination of the expression of the miRNA encoding genes does not require additional experimental work. However, IHC is often used for subclassification into GCB/non-GCB [52,53], and moreover, the latest recommendation from the WHO is to perform ABC/GCB classification using the Nanostring technique [9]. Thus, this will require quantification of the seven miRNAs by ddPCR, which will be impractical despite the use of multiplex assays.

A limitation of the current work is that the drug compounds of R-CHOP potentially have additional mechanisms of actions in humans, which are not possible to assay in cultured cells. The antineoplastic effect of rituximab is mediated by direct signaling-induced apoptosis, complement-dependent cytotoxicity, and antibody-mediated

cellular toxicity [286], where we in this study only address the direct apoptotic and complement-mediated effect by performing rituximab screens in presence of human serum as a source of complement. Likewise, the antibody-mediated killing induced by cyclophosphamide through cytokine release and attraction of macrophages was not assayed [287], which, however, is a less prominent mechanisms in comparison to the alkylating cytotoxic effect. As the primary mechanism of the R-CHOP chemotherapeutics is blockage of mitosis with utility of various approaches, *in vitro* analysis was appropriate for this study.

6. CONCLUSIVE REMARKS & FUTURE PERSPECTIVES

Treatment improvements of DLBCL have been limited in the past decade despite several clinical trials based on molecular-guided targeted therapy. Notably, all trials utilizing add-on drugs to the standard immuno-chemotherapy regimen, R-CHOP, have unfortunately failed to contribute to significant improvements in survival outcome. This highlights that the standard R-CHOP regimen is still the most important and robust choice of first-line treatment, even if the underlying response and resistance mechanisms are not fully understood. This PhD study interrogated the involvement of miRNAs on response to R-CHOP components and their potential to stratify DLBCL patients according to risk. miR-155 was confirmed to regulate vincristine response in GCB-DLBCL cells, potentially by suppressing the identified target Wee1. However, further mechanistic studies unraveling the mechanism of response is warranted for complete understanding. Prognostic evaluation documented superior clinical outcomes of GCB-DLBCL patients with high expression levels of miR-155, implying that the regulatory role of miR-155 on vincristine response is powerful enough to influence the clinical output despite treatment with combinational R-CHOP therapy. Deregulation of miR-155 in ABC cells did not affect vincristine sensitivity, and the expression was without prognostic impact in ABC patients, implying subtype-specific regulation of vincristine response.
By statistical modeling, we combined miRNAs, identified to be associated with individual compounds of R-CHOP, and developed prognostic classifiers by applying multivariate Cox regression and random survival forest analysis. The Cox panel model encompassing miR-21, miR-23a~miR-27a~miR-24-2 cluster, miR-34a, miR146a, and miR-155 was documented to display the highest predictive accuracy in GCB-DLBCL, exhibiting prognostic utility comparable to IPI. Moreover, the prognostic performance was substantially improved by combining IPI and the miRNA-panel, emphasizing the importance of including both clinical and molecular features for prognostic assessment of DLBCL patients. Notably, both miR-155 expression and the miRNA-panel identified a high-risk subgroup of GCB-DLBCL patients, commonly considered as the prognostic favorable subclass of DLBCL.

The presented studies document functional impact of miRNA on drug response in DLBCL, yet the effect of miRNAs is comprehensive and complex due to the large number of target genes, which in addition is tissue- and cell-type specific. This complexity limits the clinical applicability of miRNAs as risk markers, however, as a proof of concept, we show improvement of risk stratification by combining molecular and clinical parameters. With the recent years of comprehensive investigation of the mutational landscape of DLBCL, revealing a compendium of genetic aberrations, future studies of treatment resistance should strive for functional understanding of recurrent genetic alterations and their implications in drug resistance. The CRISPR-

Cas9 technology enables scientists to edit genes with unprecedented speed and efficacy and is an indispensable tool for functional understanding of genetic alterations. The combination of next-generation sequencing data of patient tumors and functional molecular understanding by CRISPR possesses enormous potential for future individual tailored treatment and novel treatment strategies.

When the underlying mechanisms of drug resistance are poorly understood, global CRISPR library screens can be employed to identify genes that induce resistance. As DLBCL is characterized by several hallmark mutations causing constitutive activation [30–34,39,40], global CRISPR activation screens are preferable to aim at clinical relevant data. Moreover, transcriptional profiling of drug-resistant clones, expressing increased levels of respective candidate genes, can be performed to identify cellular signatures of perturbations. With support from resources such as the Connectivity Map [288], small molecule compounds antagonizing the effect of perturbation can be selected in order to test whether resistance can be overcome. This has the potential to identify actionable drug targets in treatment resistance, providing useful information for future clinical trials.

LITERATURE LIST

1. Klein U, Dalla-Favera R. Germinal centres: role in B-cell physiology and malignancy. Nat Rev Immunol. Nature Publishing Group; 2008; 8: 22–33. doi: 10.1038/nri2217.
2. Küppers R. Mechanisms of B-cell lymphoma pathogenesis. Nat Rev Cancer. Nature Publishing Group; 2005; 5: 251–62. doi: 10.1038/nrc1589.
3. Perez-Andres M, Paiva B, Nieto WG, Caraux A, Schmitz A, Almeida J, Vogt RF, Marti GE, Rawstron AC, Van Zelm MC, Van Dongen JJM, Johnsen HE, Klein B, et al. Human peripheral blood B-cell compartments: a crossroad in B-cell traffic. Cytometry B Clin Cytom. 2010; 78 Suppl 1: S47-60. doi: 10.1002/cyto.b.20547.
4. Pelanda R, Torres RM. Central B-cell tolerance: where selection begins. Cold Spring Harb Perspect Biol. Cold Spring Harbor Laboratory Press; 2012; 4: a007146. doi: 10.1101/cshperspect.a007146.
5. Basso K, Dalla-Favera R. Germinal centres and B cell lymphomagenesis. Nat Rev Immunol. Nature Publishing Group; 2015; 15: 172–84. doi: 10.1038/nri3814.
6. Xu Z, Fulop Z, Zhong Y, Evinger AJ, Zan H, Casali P. DNA lesions and repair in immunoglobulin class switch recombination and somatic hypermutation. Ann N Y Acad Sci. 2005; 1050: 146–62. doi: 10.1196/annals.1313.119.
7. Allen CDC, Ansel KM, Low C, Lesley R, Tamamura H, Fujii N, Cyster JG. Germinal center dark and light zone organization is mediated by CXCR4 and CXCR5. Nat Immunol. 2004; 5: 943–52. doi: 10.1038/ni1100.
8. Hanahan D, Weinberg RA. Hallmarks of cancer: the next generation. Cell. 2011; 144: 646–74. doi: 10.1016/j.cell.2011.02.013.
9. Swerdlow SH, Campo E, Harris NL, Jaffe ES, Pileri SA, Stein H, Thiele J, Arber DA, Hasserjian RP, Le Beau MM, Orazi A, Siebert R. WHO Classification og Tumours of Hematopoietic and Lymphoid Tissues. 4th Editio. Swerdlow SH, Campo E, Harris NL, Jaffe ES, Pileri SA, Stein H, Thiele J, editors. International Agency for Research on Cancer (IARC); 2017. 291–297 p.
10. Nogai H, Dörken B, Lenz G. Pathogenesis of non-Hodgkin's lymphoma. J Clin Oncol. 2011; 29: 1803–11. doi: 10.1200/JCO.2010.33.3252.
11. Swerdlow SH, Campo E, Harris NL, Jaffe ES, Pileri S, Stein H, Thiele J, Vardiman JW. WHO Classification of Tumours of Haematopoietic and Lymphoid Tissues. 2008.
12. Pasqualucci L, Dalla-Favera R. The Genetic Landscape of Diffuse Large B-Cell Lymphoma. Seminars in Hematology. W.B. Saunders; 2015. p. 67–76. doi: 10.1053/j.seminhematol.2015.01.005.
13. Pasqualucci L, Neumeister P, Goossens T, Nanjangud G, Chaganti RSK, Küppers R, Dalla-Favera R. Hypermutation of multiple proto-oncogenes in

B-cell diffuse large-cell lymphomas. Nature. Nature Publishing Group; 2001; 412: 341–6. doi: 10.1038/35085588.

14. Khodabakhshi AH, Morin RD, Fejes AP, Mungall AJ, Mungall KL, Bolger-Munro M, Johnson NA, Connors JM, Gascoyne RD, Marra MA, Birol I, Jones SJM. Recurrent targets of aberrant somatic hypermutation in lymphoma. Oncotarget. Oncotarget; 2012; 3: 1308–19. doi: 10.18632/oncotarget.653.
15. Tilly H, Gomes da Silva M, Vitolo U, Jack A, Meignan M, Lopez-Guillermo A, Walewski J, André M, Johnson PW, Pfreundschuh M, Ladetto M. Diffuse large B-cell lymphoma (DLBCL): ESMO Clinical Practice Guidelines for diagnosis, treatment and follow-up. Ann Oncol. Oxford University Press; 2015; 26: v116–25. doi: 10.1093/annonc/mdv304.
16. Morgan G, Vornanen M, Puitinen J, Naukkarinen A, Brincker H, Olsen J, Coeburgh JW, Vrints LW, Clayden D, McNally R, Jack A, Carli PM, Petrella T, et al. Changing trends in the incidence of non-Hodgkin's lymphoma in Europe. Biomed Study Group. Ann Oncol. 1997; 8 Suppl 2: 49–54.
17. Lenz G, Staudt LM. Aggressive lymphomas. N Engl J Med. 2010; 362: 1417–29. doi: 10.1056/NEJMra0807082.
18. Morton LM, Slager SL, Cerhan JR, Wang SS, Vajdic CM, Skibola CF, Bracci PM, de Sanjose S, Smedby KE, Chiu BCH, Zhang Y, Mbulaiteye SM, Monnereau A, et al. Etiologic Heterogeneity Among Non-Hodgkin Lymphoma Subtypes: The InterLymph Non-Hodgkin Lymphoma Subtypes Project. JNCI Monogr. Oxford University Press; 2014; 2014: 130–44. doi: 10.1093/jncimonographs/lgu013.
19. Montoto S, Fitzgibbon J. Transformation of indolent B-cell lymphomas. J Clin Oncol. 2011; 29: 1827–34. doi: 10.1200/JCO.2010.32.7577.
20. A predictive model for aggressive non-Hodgkin's lymphoma. The International Non-Hodgkin's Lymphoma Prognostic Factors Project. N Engl J Med. 1993; 329: 987–94. doi: 10.1056/NEJM199309303291402.
21. Sehn LH, Berry B, Chhanabhai M, Fitzgerald C, Gill K, Hoskins P, Klasa R, Savage KJ, Shenkier T, Sutherland J, Gascoyne RD, Connors JM. The revised International Prognostic Index (R-IPI) is a better predictor of outcome than the standard IPI for patients with diffuse large B-cell lymphoma treated with R-CHOP. Blood. 2007; 109: 1857–61. doi: 10.1182/blood-2006-08-038257.
22. Zhou Z, Sehn LH, Rademaker AW, Gordon LI, Lacasce AS, Crosby-Thompson A, Vanderplas A, Zelenetz AD, Abel GA, Rodriguez MA, Nademanee A, Kaminski MS, Czuczman MS, et al. An enhanced International Prognostic Index (NCCN-IPI) for patients with diffuse large B-cell lymphoma treated in the rituximab era. Blood. 2014; 123: 837–42. doi: 10.1182/blood-2013-09-524108.
23. Ziepert M, Hasenclever D, Kuhnt E, Glass B, Schmitz N, Pfreundschuh M, Loeffler M. Standard international prognostic index remains a valid predictor of outcome for patients with aggressive CD20+ B-cell lymphoma in the rituximab era. J Clin Oncol. 2010; 28: 2373–80. doi: 10.1200/JCO.2009.26.2493.

24. Alizadeh AA, Eisen MB, Davis RE, Ma C, Lossos IS, Rosenwald A, Boldrick JC, Sabet H, Tran T, Yu X, Powell JI, Yang L, Marti GE, et al. Distinct types of diffuse large B-cell lymphoma identified by gene expression profiling. Nature. Nature Publishing Group; 2000; 403: 503–11. doi: 10.1038/35000501.
25. Visco C, Li Y, Xu-Monette ZY, Miranda RN, Green TM, Li Y, Tzankov A, Wen W, Liu W, Kahl BS, D'Amore ESG, Montes-Moreno S, Dybkær K, et al. Comprehensive gene expression profiling and immunohistochemical studies support application of immunophenotypic algorithm for molecular subtype classification in diffuse large B-cell lymphoma: a report from the International DLBCL Rituximab-CHOP Consortiu. Leukemia. 2012; 26: 2103–13.
26. Lenz G, Wright G, Dave SS, Xiao W, Powell J, Zhao H, Xu W, Tan B, Goldschmidt N, Iqbal J, Vose J, Bast M, Fu K, et al. Stromal Gene Signatures in Large-B-Cell Lymphomas. N Engl J Med. 2008; 359: 2313–23. doi: 10.1056/NEJMoa0802885.
27. Scott DW, Wright GW, Williams PM, Lih CJ, Walsh W, Jaffe ES, Rosenwald A, Campo E, Chan WC, Connors JM, Smeland EB, Mottok A, Braziel RM, et al. Determining cell-of-origin subtypes of diffuse large B-cell lymphoma using gene expression in formalin-fixed paraffin-embedded tissue. Blood. American Society of Hematology; 2014; 123: 1214–7. doi: 10.1182/blood-2013-11-536433.
28. Coiffier B, Lepage E, Briere J, Herbrecht R, Tilly H, Bouabdallah R, Morel P, Van Den Neste E, Salles G, Gaulard P, Reyes F, Lederlin P, Gisselbrecht C. CHOP chemotherapy plus rituximab compared with CHOP alone in elderly patients with diffuse large-B-cell lymphoma. N Engl J Med. 2002; 346: 235–42. doi: 10.1056/NEJMoa011795.
29. Davis RE, Ngo VN, Lenz G, Tolar P, Young RM, Romesser PB, Kohlhammer H, Lamy L, Zhao H, Yang Y, Xu W, Shaffer AL, Wright G, et al. Chronic active B-cell-receptor signalling in diffuse large B-cell lymphoma. Nature. Nature Publishing Group; 2010; 463: 88–92. doi: 10.1038/nature08638.
30. Lenz G, Davis RE, Ngo VN, Lam L, George TC, Wright GW, Dave SS, Zhao H, Xu W, Rosenwald A, Ott G, Muller-Hermelink HK, Gascoyne RD, et al. Oncogenic CARD11 mutations in human diffuse large B cell lymphoma. Science (80-). American Association for the Advancement of Science; 2008; 319: 1676–9. doi: 10.1126/science.1153629.
31. Miao Y, Medeiros LJ, Li Y, Li J, Young KH. Genetic alterations and their clinical implications in DLBCL. Nature Reviews Clinical Oncology. Nature Publishing Group; 2019. p. 634–52. doi: 10.1038/s41571-019-0225-1.
32. Davis RE, Brown KD, Siebenlist U, Staudt LM. Constitutive nuclear factor kappaB activity is required for survival of activated B cell-like diffuse large B cell lymphoma cells. J Exp Med. Rockefeller University Press; 2001; 194: 1861–74. doi: 10.1084/JEM.194.12.1861.
33. Ngo VN, Young RM, Schmitz R, Jhavar S, Xiao W, Lim K-H, Kohlhammer

H, Xu W, Yang Y, Zhao H, Shaffer AL, Romesser P, Wright G, et al. Oncogenically active MYD88 mutations in human lymphoma. Nature. 2010; 470: 115–9. doi: 10.1038/nature09671.

34. Morin RD, Johnson NA, Severson TM, Mungall AJ, An J, Goya R, Paul JE, Boyle M, Woolcock BW, Kuchenbauer F, Yap D, Humphries RK, Griffith OL, et al. Somatic mutations altering EZH2 (Tyr641) in follicular and diffuse large B-cell lymphomas of germinal-center origin. Nat Genet. Nature Publishing Group; 2010; 42: 181–5. doi: 10.1038/ng.518.
35. Muppidi JR, Schmitz R, Green JA, Xiao W, Larsen AB, Braun SE, An J, Xu Y, Rosenwald A, Ott G, Gascoyne RD, Rimsza LM, Campo E, et al. Loss of signalling via Gα13 in germinal centre B-cell-derived lymphoma. Nature. NIH Public Access; 2014; 516: 254–8. doi: 10.1038/nature13765.
36. Ying CY, Dominguez-Sola D, Fabi M, Lorenz IC, Hussein S, Bansal M, Califano A, Pasqualucci L, Basso K, Dalla-Favera R. MEF2B mutations lead to deregulated expression of the oncogene BCL6 in diffuse large B cell lymphoma. Nat Immunol. Nature Publishing Group; 2013; 14: 1084–92. doi: 10.1038/ni.2688.
37. Barrans SL, O'Connor SJM, Evans PAS, Davies FE, Owen RG, Haynes AP, Morgan GJ, Jack AS. Rearrangement of the BCL6 locus at 3q27 is an independent poor prognostic factor in nodal diffuse large B-cell lymphoma. Br J Haematol. John Wiley & Sons, Ltd; 2002; 117: 322–32. doi: 10.1046/j.1365-2141.2002.03435.x.
38. Iqbal J, Greiner TC, Patel K, Dave BJ, Smith L, Ji J, Wright G, Sanger WG, Pickering DL, Jain S, Horsman DE, Shen Y, Fu K, et al. Distinctive patterns of BCL6 molecular alterations and their functional consequences in different subgroups of diffuse large B-cell lymphoma. Leukemia. Nature Publishing Group; 2007; 21: 2332–43. doi: 10.1038/sj.leu.2404856.
39. Huang JZ, Sanger WG, Greiner TC, Staudt LM, Weisenburger DD, Pickering DL, Lynch JC, Armitage JO, Warnke RA, Alizadeh AA, Lossos IS, Levy R, Chan WC. The t(14;18) defines a unique subset of diffuse large B-cell lymphoma with a germinal center B-cell gene expression profile. Blood. 2002; 99: 2285–90.
40. Barrans SL, Evans PAS, O'Connor SJM, Kendall SJ, Owen RG, Haynes AP, Morgan GJ, Jack AS. The t(14;18) is associated with germinal center-derived diffuse large B-cell lymphoma and is a strong predictor of outcome. Clin Cancer Res. American Association for Cancer Research; 2003; 9: 2133–9.
41. Scott DW, Mottok A, Ennishi D, Wright GW, Farinha P, Ben-Neriah S, Kridel R, Barry GS, Hother C, Abrisqueta P, Boyle M, Meissner B, Telenius A, et al. Prognostic significance of diffuse large B-cell lymphoma cell of origin determined by digital gene expression in formalin-fixed paraffin-embedded tissue biopsies. J Clin Oncol. American Society of Clinical Oncology; 2015; 33: 2848–56. doi: 10.1200/JCO.2014.60.2383.
42. Barrans S, Crouch S, Smith A, Turner K, Owen R, Patmore R, Roman E, Jack A. Rearrangement of MYC is associated with poor prognosis in patients with

diffuse large B-cell lymphoma treated in the era of rituximab. J Clin Oncol. 2010; 28: 3360–5. doi: 10.1200/JCO.2009.26.3947.

43. Savage KJ, Johnson NA, Ben-Neriah S, Connors JM, Sehn LH, Farinha P, Horsman DE, Gascoyne RD. MYC gene rearrangements are associated with a poor prognosis in diffuse large B-cell lymphoma patients treated with R-CHOP chemotherapy. Blood. American Society of Hematology; 2009; 114: 3533–7. doi: 10.1182/blood-2009-05-220095.
44. Johnson NA, Slack GW, Savage KJ, Connors JM, Ben-Neriah S, Rogic S, Scott DW, Tan KL, Steidl C, Sehn LH, Chan WC, Iqbal J, Meyer PN, et al. Concurrent expression of MYC and BCL2 in diffuse large B-cell lymphoma treated with rituximab plus cyclophosphamide, doxorubicin, vincristine, and prednisone. J Clin Oncol. 2012; 30: 3452–9. doi: 10.1200/JCO.2011.41.0985.
45. Ennishi D, Jiang A, Boyle M, Collinge B, Grande BM, Ben-Neriah S, Rushton C, Tang J, Thomas N, Slack GW, Farinha P, Takata K, Miyata-Takata T, et al. Double-hit gene expression signature defines a distinct subgroup of germinal center B-cell-like diffuse large B-cell lymphoma. Journal of Clinical Oncology. 2019. doi: 10.1200/JCO.18.01583.
46. Hu S, Xu-Monette ZY, Tzankov A, Green T, Wu L, Balasubramanyam A, Liu WM, Visco C, Li Y, Miranda RN, Montes-Moreno S, Dybkaer K, Chiu A, et al. MYC/BCL2 protein coexpression contributes to the inferior survival of activated B-cell subtype of diffuse large B-cell lymphoma and demonstrates high-risk gene expression signatures: A report from the International DLBCL Rituximab-CHOP Consortium Program. Blood. American Society of Hematology; 2013; 121: 4021–31. doi: 10.1182/blood-2012-10-460063.
47. Green TM, Young KH, Visco C, Xu-Monette ZY, Orazi A, Go RS, Nielsen O, Gadeberg O V., Mourits-Andersen T, Frederiksen M, Pedersen LM, Møller MB. Immunohistochemical double-hit score is a strong predictor of outcome in patients with diffuse large B-cell lymphoma treated with rituximab plus cyclophosphamide, doxorubicin, vincristine, and prednisone. J Clin Oncol. J Clin Oncol; 2012; 30: 3460–7. doi: 10.1200/JCO.2011.41.4342.
48. Ye Q, Xu-Monette ZY, Tzankov A, Deng L, Wang X, Manyam GC, Visco C, Montes-Moreno S, Zhang L, Dybkær K, Chiu A, Orazi A, Zu Y, et al. Prognostic impact of concurrent MYC and BCL6 rearrangements and expression in de novo diffuse large B-cell lymphoma. Oncotarget. Impact Journals LLC; 2016; 7: 2401–16. doi: 10.18632/oncotarget.6262.
49. Aukema SM, Siebert R, Schuuring E, Van Imhoff GW, Kluin-Nelemans HC, Boerma EJ, Kluin PM. Double-hit B-cell lymphomas. Blood. American Society of Hematology; 2011. p. 2319–31. doi: 10.1182/blood-2010-09-297879.
50. Epperla N, Maddocks KJ, Salhab M, Chavez JC, Reddy N, Karmali R, Umyarova E, Bachanova V, Costa C, Glenn M, Calzada O, Xavier AC, Zhou Z, et al. C-MYC-positive relapsed and refractory, diffuse large B-cell lymphoma: Impact of additional “hits” and outcomes with subsequent therapy. Cancer. John Wiley and Sons Inc.; 2017; 123: 4411–8. doi:

10.1002/cncr.30895.

51. Cuccuini W, Briere J, Mounier N, Voelker H-U, Rosenwald A, Sundstrom C, Cogliatti S, Bron D, Hirchaud E, Soulier J, Gaulard P, Houlgatte R, Gisselbrecht C, et al. MYC + Diffuse Large B Cell Lymphomas (DLBCL) Treated in Randomized Prospective Salvage Therapy, RICE or RDHAP Followed by BEAM Plus Autologous Stem Cell Transplantation (ASCT). A BioCORAL Report. Blood. American Society of Hematology; 2011; 118: 594–594. doi: 10.1182/blood.v118.21.594.594.
52. Hans CP, Weisenburger DD, Greiner TC, Gascoyne RD, Delabie J, Ott G, Müller-Hermelink HK, Campo E, Braziel RM, Jaffe ES, Pan Z, Farinha P, Smith LM, et al. Confirmation of the molecular classification of diffuse large B-cell lymphoma by immunohistochemistry using a tissue microarray. Blood. 2004; 103: 275–82. doi: 10.1182/blood-2003-05-1545.
53. Choi WWL, Weisenburger DD, Greiner TC, Piris MA, Banham AH, Delabie J, Braziel RM, Geng H, Iqbal J, Lenz G, Vose JM, Hans CP, Fu K, et al. A new immunostain algorithm classifies diffuse large B-cell lymphoma into molecular subtypes with high accuracy. Clin Cancer Res. 2009; 15: 5494–502. doi: 10.1158/1078-0432.CCR-09-0113.
54. Read JA, Koff JL, Nastoupil LJ, Williams JN, Cohen JB, Flowers CR. Evaluating cell-of-origin subtype methods for predicting diffuse large B-cell lymphoma survival: a meta-analysis of gene expression profiling and immunohistochemistry algorithms. Clin Lymphoma Myeloma Leuk. 2014; 14: 460-467.e2. doi: 10.1016/j.clml.2014.05.002.
55. Dybkær K, Bøgsted M, Falgreen S, Bødker JS, Kjeldsen MK, Schmitz A, Bilgrau AE, Xu-Monette ZY, Li L, Bergkvist KS, Laursen MB, Rodrigo-Domingo M, Marques SC, et al. Diffuse large B-cell lymphoma classification system that associates normal B-cell subset phenotypes with prognosis. J Clin Oncol. American Society of Clinical Oncology; 2015; 33: 1379–88. doi: 10.1200/JCO.2014.57.7080.
56. Monti S, Savage KJ, Kutok JL, Feuerhake F, Kurtin P, Mihm M, Wu B, Pasqualucci L, Neuberg D, Aguiar RCT, Cin PD, Ladd C, Pinkus GS, et al. Molecular profiling of diffuse large B-cell lymphoma identifies robust subtypes including one characterized by host inflammatory response. Blood. American Society of Hematology; 2005; 105: 1851–61. doi: 10.1182/blood-2004-07-2947.
57. Reddy A, Zhang J, Davis NS, Moffitt AB, Love CL, Waldrop A, Leppa S, Pasanen A, Meriranta L, Karjalainen-Lindsberg ML, Nørgaard P, Pedersen M, Gang AO, et al. Genetic and Functional Drivers of Diffuse Large B Cell Lymphoma. Cell. Cell Press; 2017; 171: 481-494.e15. doi: 10.1016/j.cell.2017.09.027.
58. Schmitz R, Wright GW, Huang DW, Johnson CA, Phelan JD, Wang JQ, Roulland S, Kasbekar M, Young RM, Shaffer AL, Hodson DJ, Xiao W, Yu X, et al. Genetics and Pathogenesis of Diffuse Large B-Cell Lymphoma. N Engl J Med. Massachussetts Medical Society; 2018; 378: 1396–407. doi:

10.1056/NEJMoa1801445.

59. Chapuy B, Stewart C, Dunford AJ, Kim J, Kamburov A, Redd RA, Lawrence MS, Roemer MGM, Li AJ, Ziepert M, Staiger AM, Wala JA, Ducar MD, et al. Molecular subtypes of diffuse large B cell lymphoma are associated with distinct pathogenic mechanisms and outcomes. Nat Med. Nature Publishing Group; 2018; 24: 679–90. doi: 10.1038/s41591-018-0016-8.
60. Wright GW, Huang DW, Phelan JD, Coulibaly ZA, Roulland S, Young RM, Wang JQ, Schmitz R, Morin RD, Tang J, Jiang A, Bagaev A, Plotnikova O, et al. A Probabilistic Classification Tool for Genetic Subtypes of Diffuse Large B Cell Lymphoma with Therapeutic Implications. Cancer Cell. Cell Press; 2020; 37: 551-568.e14. doi: 10.1016/j.ccell.2020.03.015.
61. Lacy SE, Barrans SL, Beer PA, Painter D, Smith AG, Roman E, Cooke SL, Ruiz C, Glover P, Van Hoppe SJL, Webster N, Campbell PJ, Tooze RM, et al. Targeted sequencing in DLBCL, molecular subtypes, and outcomes: a Haematological Malignancy Research Network report. Blood. NLM (Medline); 2020; 135: 1759–71. doi: 10.1182/blood.2019003535.
62. Xu-Monette ZY, Zhang H, Zhu F, Tzankov A, Bhagat G, Visco C, Dybkaer K, Chiu A, Tam W, Zu Y, Hsi ED, You H, Huh J, et al. A refined cell-of-origin classifier with targeted NGS and artificial intelligence shows robust predictive value in DLBCL. Blood Adv. American Society of Hematology; 2020; 4: 3391–404. doi: 10.1182/bloodadvances.2020001949.
63. Morin RD, Scott DW. DLBCL subclassification: divide and conquer? Blood. NLM (Medline); 2020; 135: 1722–4. doi: 10.1182/blood.2020005335.
64. Friedberg JW. Relapsed/refractory diffuse large B-cell lymphoma. Hematology Am Soc Hematol Educ Program. 2011; 2011: 498–505. doi: 10.1182/asheducation-2011.1.498.
65. Palmer AC, Chidley C, Sorger PK. A curative combination cancer therapy achieves high fractional cell killing through low cross resistance and drug Additivity. Elife. eLife Sciences Publications Ltd; 2019; 8. doi: 10.7554/eLife.50036.
66. Sehn LH, Donaldson J, Chhanabhai M, Fitzgerald C, Gill K, Klasa R, MacPherson N, O'Reilly S, Spinelli JJ, Sutherland J, Wilson KS, Gascoyne RD, Connors JM. Introduction of combined CHOP plus rituximab therapy dramatically improved outcome of diffuse large B-cell lymphoma in British Columbia. J Clin Oncol. 2005; 23: 5027–33. doi: 10.1200/JCO.2005.09.137.
67. Gisselbrecht C, Glass B, Mounier N, Singh Gill D, Linch DC, Trneny M, Bosly A, Ketterer N, Shpilberg O, Hagberg H, Ma D, Brière J, Moskowitz CH, et al. Salvage regimens with autologous transplantation for relapsed large B-cell lymphoma in the rituximab era. J Clin Oncol. American Society of Clinical Oncology; 2010; 28: 4184–90. doi: 10.1200/JCO.2010.28.1618.
68. Vitolo U, Trněný M, Belada D, Carella AM, Chua N, Abrisqueta P, Demeter J, Flinn IW, Hong X, Kim WS, Pinto A, Burke JM, Shi Y, et al. Obinutuzumab or Rituximab Plus CHOP in Patients with Previously Untreated Diffuse Large B-Cell Lymphoma: Final Results from an Open-Label, Randomized Phase 3

Study (GOYA). Blood. 2016; . doi: 10.1182/blood.v128.22.470.470.

69. Seymour JF, Pfreundschuh M, Trněný M, Sehn LH, Catalano J, Csinady E, Moore N, Coiffier B, MAIN Study Investigators. R-CHOP with or without bevacizumab in patients with previously untreated diffuse large B-cell lymphoma: final MAIN study outcomes. Haematologica. Haematologica; 2014; 99: 1343–9. doi: 10.3324/haematol.2013.100818.
70. Davies AJ, Caddy J, Maishman T, Barrans S, Mamot C, Care M, Pocock C, Stanton L, Hamid D, Pugh K, McMillan A, Fields P, Kruger A, et al. A Prospective Randomised Trial of Targeted Therapy for Diffuse Large B-Cell Lymphoma (DLBCL) Based upon Real-Time Gene Expression Profiling: The Remodl-B Study of the UK NCRI and SAKK Lymphoma Groups (ISRCTN51837425). Blood. 2015; . doi: 10.1182/blood.v126.23.812.812.
71. Davies AJ, Barrans S, Maishman T, Cummin TE, Bentley M, Mamot C, Novak U, Caddy J, Hamid D, Kazmi-Stokes SH, McMillan A, Fields PA, Pocock C, et al. Differential efficacy of bortezomib in subtypes of diffuse large B-cell lymphoma (DLBL): A prospective randomised study stratified by transcriptome profiling: REMoDL-B. Hematol Oncol. 2017; . doi: 10.1002/hon.2437.
72. Davies A, Cummin TE, Barrans S, Maishman T, Mamot C, Novak U, Caddy J, Stanton L, Kazmi-Stokes S, McMillan A, Fields P, Pocock C, Collins GP, et al. Gene-expression profiling of bortezomib added to standard chemoimmunotherapy for diffuse large B-cell lymphoma (REMoDL-B): an open-label, randomised, phase 3 trial. Lancet Oncol. Lancet Publishing Group; 2019; 20: 649–62. doi: 10.1016/S1470-2045(18)30935-5.
73. Younes A, Zinzani PL, Sehn LH, Johnson PWM, Gascoyne RD, Ahmadi T, Bellew KM, Vermeulen J, Zhuang SH, Sun S, Staudt LM, Wilson WH. A randomized, double-blind, placebo-controlled phase 3 study of ibrutinib in combination with rituximab, cyclophosphamide, doxorubicin, vincristine, and prednisone (R-CHOP) in subjects with newly diagnosed nongerminal center B-cell subtype of diffuse larg. J Clin Oncol. 2014; . doi: 10.1200/jco.2014.32.15_suppl.tps8615.
74. Younes A, Sehn LH, Johnson P, Zinzani PL, Hong X, Zhu J, Patti C, Belada D, Samoilova O, Suh C, Leppä S, Rai S, Turgut M, et al. Randomized phase III trial of ibrutinib and rituximab plus cyclophosphamide, doxorubicin, vincristine, and prednisone in non–germinal center B-cell diffuse large B-cell lymphoma. J Clin Oncol. 2019; . doi: 10.1200/JCO.18.02403.
75. Nowakowski GS, Chiappella A, Witzig TE, Spina M, Gascoyne RD, Zhang L, Flament J, Repici J. ROBUST: Lenalidomide-R-CHOP versus placebo-R-CHOP in previously untreated ABC-type diffuse large B-cell lymphoma. Future Oncology. 2016.
76. Vitolo U, Witzig TE, Gascoyne RD, Scott DW, Zhang Q, Jurczak W, Özcan M, Hong X, Zhu J, Jin J, Belada D, Bergua JM, Piazza F, et al. ROBUST: First report of phase III randomized study of lenalidomide/R-CHOP (R^2-CHOP) vs placebo/R-CHOP in previously untreated ABC-type diffuse large

B-cell lymphoma. Hematol Oncol. 2019; 37: 36–7. doi: 10.1002/hon.5_2629.

77. Cunningham D, Hawkes EA, Jack A, Qian W, Smith P, Mouncey P, Pocock C, Ardeshna KM, Radford JA, McMillan A, Davies J, Turner D, Kruger A, et al. Rituximab plus cyclophosphamide, doxorubicin, vincristine, and prednisolone in patients with newly diagnosed diffuse large B-cell non-Hodgkin lymphoma: A phase 3 comparison of dose intensification with 14-day versus 21-day cycles. Lancet. Lancet Publishing Group; 2013; 381: 1817–26. doi: 10.1016/S0140-6736(13)60313-X.
78. Jaeger U, Trneny M, Melzer H, Praxmarer M, Nawarawong W, Ben Yehuda D, Goldstein D, Mihaljevic B, Ilhan O, Ballova V, Hedenus M, Hsiao L-T, Au W-Y, et al. Rituximab maintenance for patients with aggressive B-cell lymphoma in first remission: results of the randomized NHL13 trial. Haematologica. Haematologica; 2015; 100: 955–63. doi: 10.3324/haematol.2015.125344.
79. Stiff PJ, Unger JM, Cook JR, Constine LS, Couban S, Stewart DA, Shea TC, Porcu P, Winter JN, Kahl BS, Miller TP, Tubbs RR, Marcellus D, et al. Autologous transplantation as consolidation for aggressive non-Hodgkin's lymphoma. N Engl J Med. Massachussetts Medical Society; 2013; 369: 1681–90. doi: 10.1056/NEJMoa1301077.
80. Petrich AM, Gandhi M, Jovanovic B, Castillo JJ, Rajguru S, Yang DT, Shah KA, Whyman JD, Lansigan F, Hernandez-Ilizaliturri FJ, Lee LX, Barta SK, Melinamani S, et al. Impact of induction regimen and stem cell transplantation on outcomes in double-hit lymphoma: A multicenter retrospective analysis. Blood. American Society of Hematology; 2014; 124: 2354–61. doi: 10.1182/blood-2014-05-578963.
81. Wilson WH, Young RM, Schmitz R, Yang Y, Pittaluga S, Wright G, Lih C-J, Williams M, Shaffer AL, Gerecitano J, De Vos S, Goy A, Kenkre VP, et al. Targeting B cell receptor signaling with ibrutinib in diffuse large B cell lymphoma. 2015; 21. doi: 10.1038/nm.3884.
82. Dunleavy K, Pittaluga S, Czuczman MS, Dave SS, Wright G, Grant N, Shovlin M, Jaffe ES, Janik JE, Staudt LM, Wilson WH. Differential efficacy of bortezomib plus chemotherapy within molecular subtypes of diffuse large B-cell lymphoma. Blood. 2009; 113: 6069–76. doi: 10.1182/blood-2009-01-199679.
83. Leonard JP, Kolibaba KS, Reeves JA, Tulpule A, Flinn IW, Kolevska T, Robles R, Flowers CR, Collins R, DiBella NJ, Papish SW, Venugopal P, Horodner A, et al. Randomized Phase II Study of R-CHOP With or Without Bortezomib in Previously Untreated Patients With Non-Germinal Center B-Cell-Like Diffuse Large B-Cell Lymphoma. J Clin Oncol. American Society of Clinical Oncology; 2017; 35: 3538–46. doi: 10.1200/JCO.2017.73.2784.
84. Gidding C. Vincristine revisited. Crit Rev Oncol Hematol. 1999; 29: 267–87. doi: 10.1016/S1040-8428(98)00023-7.
85. Vincristine Sulfate Monograph for Professionals - Drugs.com [Internet]. Available 2020 Mar 31, from https://www.drugs.com/monograph/vincristine-

sulfate.html

86. Said R, Tsimberidou AM. Pharmacokinetic evaluation of vincristine for the treatment of lymphoid malignancies. Expert Opin Drug Metab Toxicol. 2014; 10: 483–94. doi: 10.1517/17425255.2014.885016.
87. Zhou XJ, Rahmani R. Preclinical and Clinical Pharmacology of Vinca Alkaloids. Drugs. Springer; 1992; 44: 1–16. doi: 10.2165/00003495-199200444-00002.
88. Huang R, Murry DJ, Kolwankar D, Hall SD, Foster DR. Vincristine transcriptional regulation of efflux drug transporters in carcinoma cell lines. Biochem Pharmacol. Elsevier; 2006; 71: 1695–704. doi: 10.1016/j.bcp.2006.03.009.
89. Correia JJ. Effects of antimitotic agents on tubulin-nucleotide interactions. Pharmacol Ther. 1991; 52: 127–47. doi: 10.1016/0163-7258(91)90004-6.
90. Binet S, Chaineau E, Fellous A, Lataste H, Krikorian A, Couzinier J-P, Meininger V. Immunofluorescence study of the action of navelbine, vincristine and vinblastine on mitotic and axonal microtubules. Int J Cancer. 1990; 46: 262–6. doi: 10.1002/ijc.2910460220.
91. Jordan MA, Thrower D, Wilson L. Mechanism of inhibition of cell proliferation by Vinca alkaloids. Cancer Res. 1991; 51: 2212–22. Available from http://www.ncbi.nlm.nih.gov/pubmed/2009540
92. Brouhard GJ, Rice LM. Microtubule dynamics: An interplay of biochemistry and mechanics. Nature Reviews Molecular Cell Biology. Nature Publishing Group; 2018. p. 451–63. doi: 10.1038/s41580-018-0009-y.
93. Musacchio A, Salmon ED. The spindle-assembly checkpoint in space and time. Nat Rev Mol Cell Biol. Nature Publishing Group; 2007; 8: 379–93. doi: 10.1038/nrm2163.
94. Yang F, Teves SS, Kemp CJ, Henikoff S. Doxorubicin, DNA torsion, and chromatin dynamics. Biochimica et Biophysica Acta - Reviews on Cancer. NIH Public Access; 2014. p. 84–9. doi: 10.1016/j.bbcan.2013.12.002.
95. Cyclophosphamide - DrugBank [Internet]. Available 2020 Mar 31, from https://www.drugbank.ca/drugs/DB00531
96. Madsen ML, Due H, Ejskjær N, Jensen P, Madsen J, Dybkær K. Aspects of vincristine-induced neuropathy in hematologic malignancies: a systematic review. Cancer Chemotherapy and Pharmacology. 2019. doi: 10.1007/s00280-019-03884-5.
97. Kavcic M, Koritnik B, Krzan M, Velikonja O, Prelog T, Stefanovic M, Debeljak M, Jazbec J. Electrophysiological Studies to Detect Peripheral Neuropathy in Children Treated with Vincristine. J Pediatr Hematol Oncol. Lippincott Williams and Wilkins; 2017; 39: 266–71. doi: 10.1097/MPH.0000000000000825.
98. Haim N, Epelbaum R, Ben-Shahar M, Yarnitsky D, Simri W, Robinson E. Full dose vincristine (without 2-mg dose limit) in the treatment of lymphomas. Cancer. 1994; 73: 2515–9. doi: 10.1002/1097-0142(19940515)73:10<2515::AID-CNCR2820731011>3.0.CO;2-G.

99. Lehtinen SS, Huuskonen UE, Harila-Saari AH, Tolonen U, Vainionpää LK, Lanning BM. Motor nervous system impairment persists in long-term survivors of childhood acute lymphoblastic leukemia. Cancer. 2002; 94: 2466–73. doi: 10.1002/cncr.10503.
100. Utsu Y, Takaishi K, Inagaki S, Arai H, Yuasa H, Masuda S, Matsuura Y, Aotsuka N, Wakita H. Influence of dose reduction of vincristine in R-CHOP on outcomes of diffuse large B cell lymphoma. Ann Hematol. Springer Verlag; 2016; 95: 41–7. doi: 10.1007/s00277-015-2514-9.
101. Donoso JA, Green LS, Heller-Bettinger IE, Samson FE. Action of the vinca alkaloids vincristine, vinblastine, and desacetyl vinblastine amide on axonal fibrillar organelles in vitro. Cancer Res. 1977; 37: 1401–7. Available from http://www.ncbi.nlm.nih.gov/pubmed/558047
102. Morfini GA, Burns MR, Stenoien DL, Brady ST. Axonal Transport. Basic Neurochemistry. Elsevier; 2012. p. 146–64. doi: 10.1016/B978-0-12-374947-5.00008-0.
103. De Vos KJ, Hafezparast M. Neurobiology of axonal transport defects in motor neuron diseases: Opportunities for translational research? Neurobiology of Disease. Academic Press Inc.; 2017. p. 283–99. doi: 10.1016/j.nbd.2017.02.004.
104. Chan SY, Worth R, Ochs S. Block of axoplasmic transportin vitro by vinca alkaloids. J Neurobiol. 1980; 11: 251–64. doi: 10.1002/neu.480110304.
105. Verstappen CCP, Koeppen S, Heimans JJ, Huijgens PC, Scheulen ME, Strumberg D, Kiburg B, Postma TJ. Dose-related vincristine-induced peripheral neuropathy with unexpected off-therapy worsening. Neurology. Lippincott Williams and Wilkins; 2005; 64: 1076–7. doi: 10.1212/01.WNL.0000154642.45474.28.
106. Ibañez-Juliá MJ, Berzero G, Reyes-Botero G, Maisonobe T, Lenglet T, Slim M, Louis S, Balaguer A, Sanson M, Le Guern E, Latour P, Ricard D, Stojkovic T, et al. Antineoplastic agents exacerbating Charcot Marie Tooth disease: red flags to avoid permanent disability. Acta Oncol (Madr). Taylor and Francis Ltd; 2018; 57: 403–11. doi: 10.1080/0284186X.2017.1415462.
107. Dennison JB, Kulanthaivel P, Barbuch RJ, Renbarger JL, Ehlhardt WJ, Hall SD. Selective metabolism of vincristine in vitro by CYP3A5. Drug Metab Dispos. American Society for Pharmacology and Experimental Therapeutics; 2006; 34: 1317–27. doi: 10.1124/dmd.106.009902.
108. Kuehl P, Zhang J, Lin Y, Lamba J, Assem M, Schuetz J, Watkins PB, Daly A, Wrighton SA, Hall SD, Maurel P, Relling M, Brimer C, et al. Sequence diversity in CYP3A promoters and characterization of the genetic basis of polymorphic CYP3A5 expression. Nat Genet. Nature Publishing Group; 2001; 27: 383–91. doi: 10.1038/86882.
109. Diouf B, Crews KR, Lew G, Pei D, Cheng C, Bao J, Zheng JJ, Yang W, Fan Y, Wheeler HE, Wing C, Delaney SM, Komatsu M, et al. Association of an Inherited Genetic Variant With Vincristine-Related Peripheral Neuropathy in Children With Acute Lymphoblastic Leukemia. JAMA. American Medical

Association; 2015; 313: 815. doi: 10.1001/jama.2015.0894.
110. Gottesman MM. Mechanisms of cancer drug resistance. Annu Rev Med. 2002; 53: 615–27. doi: 10.1146/annurev.med.53.082901.103929.
111. Cheng EH, Sawyers CL. In cancer drug resistance, germline matters too. Nature Medicine. Nature Publishing Group; 2012. p. 494–6. doi: 10.1038/nm.2725.
112. Cree IA, Charlton P. Molecular chess? Hallmarks of anti-cancer drug resistance. BMC Cancer. BioMed Central Ltd.; 2017. p. 10. doi: 10.1186/s12885-016-2999-1.
113. Beck WT. Cellular pharmacology of vinca alkaloid resistance and its circumvention. Adv Enzyme Regul. 1984; 22: 207–27. doi: 10.1016/0065-2571(84)90015-3.
114. Rieder CL, Maiato H. Stuck in Division or Passing through: What Happens When Cells Cannot Satisfy the Spindle Assembly Checkpoint. Dev Cell. Cell Press; 2004; 7: 637–51. doi: 10.1016/J.DEVCEL.2004.09.002.
115. Visconti R, Della Monica R, Palazzo L, D'Alessio F, Raia M, Improta S, Villa MR, Del Vecchio L, Grieco D. The Fcp1-Wee1-Cdk1 axis affects spindle assembly checkpoint robustness and sensitivity to antimicrotubule cancer drugs. Cell Death Differ. 2015; 22: 1551–60. doi: 10.1038/cdd.2015.13.
116. Parker AL, Teo WS, McCarroll JA, Kavallaris M. An emerging role for tubulin isotypes in modulating cancer biology and chemotherapy resistance. International Journal of Molecular Sciences. MDPI AG; 2017. p. 1434. doi: 10.3390/ijms18071434.
117. Bartel DP. MicroRNAs: Genomics, Biogenesis, Mechanism, and Function. Cell. Cell Press; 2004; 116: 281–97. doi: 10.1016/S0092-8674(04)00045-5.
118. Lee RC, Feinbaum RL, Ambros V. The C. elegans heterochronic gene lin-4 encodes small RNAs with antisense complementarity to lin-14. Cell. Cell Press; 1993; 75: 843–54. doi: 10.1016/0092-8674(93)90529-Y.
119. Alles J, Fehlmann T, Fischer U, Backes C, Galata V, Minet M, Hart M, Abu-Halima M, Grässer FA, Grässer G, Lenhof H-P, Keller A, Meese E. An estimate of the total number of true human miRNAs. Nucleic Acids Res. 2019; 47: 3353–64. doi: 10.1093/nar/gkz097.
120. Friedman RC, Farh KKH, Burge CB, Bartel DP. Most mammalian mRNAs are conserved targets of microRNAs. Genome Res. Cold Spring Harbor Laboratory Press; 2009; 19: 92–105. doi: 10.1101/gr.082701.108.
121. Lee Y, Kim M, Han J, Yeom K-H, Lee S, Baek SH, Kim VN. MicroRNA genes are transcribed by RNA polymerase II. EMBO J. 2004; 23: 4051–60. doi: 10.1038/sj.emboj.7600385.
122. Borchert GM, Lanier W, Davidson BL. RNA polymerase III transcribes human microRNAs. Nat Struct Mol Biol. 2006; 13: 1097–101. doi: 10.1038/nsmb1167.
123. Kim YK, Kim VN. Processing of intronic microRNAs. EMBO J. 2007; 26: 775–83. doi: 10.1038/sj.emboj.7601512.
124. De Rie D, Abugessaisa I, Alam T, Arner E, Arner P, Ashoor H, Åström G,

Babina M, Bertin N, Burroughs AM, Carlisle AJ, Daub CO, Detmar M, et al. An integrated expression atlas of miRNAs and their promoters in human and mouse. Nat Biotechnol. Nature Publishing Group; 2017; 35: 872–8. doi: 10.1038/nbt.3947.

125. Cai X, Hagedorn CH, Cullen BR. Human microRNAs are processed from capped, polyadenylated transcripts that can also function as mRNAs. RNA. Cold Spring Harbor Laboratory Press; 2004; 10: 1957–66. doi: 10.1261/rna.7135204.
126. Tanzer A, Stadler PF. Molecular evolution of a microRNA cluster. J Mol Biol. Academic Press; 2004; 339: 327–35. doi: 10.1016/j.jmb.2004.03.065.
127. Han J, Lee Y, Yeom KH, Nam JW, Heo I, Rhee JK, Sohn SY, Cho Y, Zhang BT, Kim VN. Molecular Basis for the Recognition of Primary microRNAs by the Drosha-DGCR8 Complex. Cell. 2006; 125: 887–901. doi: 10.1016/j.cell.2006.03.043.
128. Sibley CR, Seow Y, Saayman S, Dijkstra KK, El Andaloussi S, Weinberg MS, Wood MJA. The biogenesis and characterization of mammalian microRNAs of mirtron origin. Nucleic Acids Res. 2012; 40: 438–48. doi: 10.1093/nar/gkr722.
129. Yi R, Qin Y, Macara IG, Cullen BR. Exportin-5 mediates the nuclear export of pre-microRNAs and short hairpin RNAs. Genes Dev. 2003; 17: 3011–6. doi: 10.1101/gad.1158803.
130. Hutvágner G, McLachlan J, Pasquinelli AE, Bálint É, Tuschl T, Zamore PD. A cellular function for the RNA-interference enzyme dicer in the maturation of the let-7 small temporal RNA. Science (80-). 2001; 293: 834–8. doi: 10.1126/science.1062961.
131. Kok KH, Ng M-HJ, Ching Y-P, Jin D-Y. Human TRBP and PACT directly interact with each other and associate with dicer to facilitate the production of small interfering RNA. J Biol Chem. 2007; 282: 17649–57. doi: 10.1074/jbc.M611768200.
132. Kawamata T, Tomari Y. Making RISC. Trends in Biochemical Sciences. Elsevier Current Trends; 2010. p. 368–76. doi: 10.1016/j.tibs.2010.03.009.
133. Khvorova A, Reynolds A, Jayasena SD. Functional siRNAs and miRNAs exhibit strand bias. Cell. Cell Press; 2003; 115: 209–16. doi: 10.1016/S0092-8674(03)00801-8.
134. Ha M, Kim VN. Regulation of microRNA biogenesis. Nature Reviews Molecular Cell Biology. Nature Publishing Group; 2014. p. 509–24. doi: 10.1038/nrm3838.
135. Meijer HA, Smith EM, Bushell M. Regulation of miRNA strand selection: Follow the leader? Biochemical Society Transactions. Portland Press Ltd; 2014. p. 1135–40. doi: 10.1042/BST20140142.
136. Jo MH, Shin S, Jung SR, Kim E, Song JJ, Hohng S. Human Argonaute 2 Has Diverse Reaction Pathways on Target RNAs. Mol Cell. Cell Press; 2015; 59: 117–24. doi: 10.1016/j.molcel.2015.04.027.
137. Lewis BP, Shih IH, Jones-Rhoades MW, Bartel DP, Burge CB. Prediction of

Mammalian MicroRNA Targets. Cell. Cell Press; 2003; 115: 787–98. doi: 10.1016/S0092-8674(03)01018-3.
138. Wang X. Composition of seed sequence is a major determinant of microRNA targeting patterns. 2014; 30: 1377–83. doi: 10.1093/bioinformatics/btu045.
139. Helwak A, Kudla G, Dudnakova T, Tollervey D. Mapping the human miRNA interactome by CLASH reveals frequent noncanonical binding. Cell. Elsevier; 2013; 153: 654–65. doi: 10.1016/j.cell.2013.03.043.
140. Broughton JP, Lovci MT, Huang JL, Yeo GW, Pasquinelli AE. Pairing beyond the Seed Supports MicroRNA Targeting Specificity. Mol Cell. Cell Press; 2016; 64: 320–33. doi: 10.1016/j.molcel.2016.09.004.
141. Lytle JR, Yario TA, Steitz JA. Target mRNAs are repressed as efficiently by microRNA-binding sites in the 5' UTR as in the 3' UTR. Proc Natl Acad Sci U S A. 2007; 104: 9667–72. doi: 10.1073/pnas.0703820104.
142. Moretti F, Thermann R, Hentze MW. Mechanism of translational regulation by miR-2 from sites in the 5' untranslated region or the open reading frame. RNA. 2010; 16: 2493–502. doi: 10.1261/rna.2384610.
143. Forman JJ, Legesse-Miller A, Coller HA. A search for conserved sequences in coding regions reveals that the let-7 microRNA targets Dicer within its coding sequence. Proc Natl Acad Sci U S A. 2008; 105: 14879–84. doi: 10.1073/pnas.0803230105.
144. Place RF, Li LC, Pookot D, Noonan EJ, Dahiya R. MicroRNA-373 induces expression of genes with complementary promoter sequences. Proc Natl Acad Sci U S A. National Academy of Sciences; 2008; 105: 1608–13. doi: 10.1073/pnas.0707594105.
145. Flamand MN, Gan HH, Mayya VK, Gunsalus KC, Duchaine TF. A non-canonical site reveals the cooperative mechanisms of microRNA-mediated silencing. Nucleic Acids Res. 2017; 45: 7212–25. doi: 10.1093/nar/gkx340.
146. Huntzinger E, Izaurralde E. Gene silencing by microRNAs: Contributions of translational repression and mRNA decay. Nature Reviews Genetics. Nature Publishing Group; 2011. p. 99–110. doi: 10.1038/nrg2936.
147. Bartel DP. MicroRNAs: target recognition and regulatory functions. Cell. 2009; 136: 215–33. doi: 10.1016/j.cell.2009.01.002.
148. Truesdell SS, Mortensen RD, Seo M, Schroeder JC, Lee JH, Letonqueze O, Vasudevan S V. MicroRNA-mediated mRNA translation activation in quiescent cells and oocytes involves recruitment of a nuclear microRNP. Sci Rep. Nature Publishing Group; 2012; 2: 1–12. doi: 10.1038/srep00842.
149. Clark PM, Loher P, Quann K, Brody J, Londin ER, Rigoutsos I. Argonaute CLIP-Seq reveals miRNA targetome diversity across tissue types. Sci Rep. Nature Publishing Group; 2015; 4: 5947. doi: 10.1038/srep05947.
150. Barman B, Bhattacharyya SN. mRNA targeting to endoplasmic reticulum precedes ago protein interaction and MicroRNA (miRNA)-mediated translation repression in mammalian cells. J Biol Chem. American Society for Biochemistry and Molecular Biology Inc.; 2015; 290: 24650–6. doi: 10.1074/jbc.C115.661868.

151. Ludwig N, Leidinger P, Becker K, Backes C, Fehlmann T, Pallasch C, Rheinheimer S, Meder B, Meese E, Keller A. Distribution of miRNA expression across human tissues. Nucleic Acids Res. 2016; 44: 3865–77. doi: 10.1093/nar/gkw116.
152. Zhang J, Jima DD, Jacobs C, Fischer R, Gottwein E, Huang G, Lugar PL, Lagoo AS, Rizzieri DA, Friedman DR, Weinberg JB, Lipsky PE, Dave SS. Patterns of microRNA expression characterize stages of human B-cell differentiation. Blood. 2009; 113: 4586–94. doi: 10.1182/blood-2008-09-178186.
153. Jima DD, Zhang J, Jacobs C, Richards KL, Dunphy CH, Choi WWL, Au WY, Srivastava G, Czader MB, Rizzieri DA, Lagoo AS, Lugar PL, Mann KP, et al. Deep sequencing of the small RNA transcriptome of normal and malignant human B cells identifies hundreds of novel microRNAs. Blood. American Society of Hematology; 2010; 116: e118-27. doi: 10.1182/blood-2010-05-285403.
154. Xu S, Guo K, Zeng Q, Huo J, Lam K-P. The RNase III enzyme Dicer is essential for germinal center B-cell formation. Blood. 2012; 119: 767–76. doi: 10.1182/blood-2011-05-355412.
155. Koralov SB, Muljo SA, Galler GR, Krek A, Chakraborty T, Kanellopoulou C, Jensen K, Cobb BS, Merkenschlager M, Rajewsky N, Rajewsky K. Dicer ablation affects antibody diversity and cell survival in the B lymphocyte lineage. Cell. 2008; 132: 860–74. doi: 10.1016/j.cell.2008.02.020.
156. Chen C-Z, Li L, Lodish HF, Bartel DP. MicroRNAs modulate hematopoietic lineage differentiation. Science. 2004; 303: 83–6. doi: 10.1126/science.1091903.
157. Jensen K, Brusletto BS, Da Aass HC, Olstad OK, Kierulf P, Gautvik KM. Transcriptional Profiling of mRNAs and microRNAs in Human Bone Marrow Precursor B Cells Identifies Subset- and Age-Specific Variations. PLoS One. Public Library of Science; 2013; 8. doi: 10.1371/journal.pone.0070721.
158. Ventura A, Young AG, Winslow MM, Lintault L, Meissner A, Erkeland SJ, Newman J, Bronson RT, Crowley D, Stone JR, Jaenisch R, Sharp PA, Jacks T. Targeted Deletion Reveals Essential and Overlapping Functions of the miR-17~92 Family of miRNA Clusters. Cell. Cell Press; 2008; 132: 875–86. doi: 10.1016/j.cell.2008.02.019.
159. Lai M, Gonzalez-Martin A, Cooper AB, Oda H, Jin HY, Shepherd J, He L, Zhu J, Nemazee D, Xiao C. Regulation of B-cell development and tolerance by different members of the miR-17~1/492 family microRNAs. Nat Commun. Nature Publishing Group; 2016; 7. doi: 10.1038/ncomms12207.
160. Thai T-H, Calado DP, Casola S, Ansel KM, Xiao C, Xue Y, Murphy A, Frendewey D, Valenzuela D, Kutok JL, Schmidt-Supprian M, Rajewsky N, Yancopoulos G, et al. Regulation of the germinal center response by microRNA-155. Science. 2007; 316: 604–8. doi: 10.1126/science.1141229.
161. Vigorito E, Perks KL, Abreu-Goodger C, Bunting S, Xiang Z, Kohlhaas S, Das PP, Miska EA, Rodriguez A, Bradley A, Smith KGC, Rada C, Enright

AJ, et al. microRNA-155 regulates the generation of immunoglobulin class-switched plasma cells. Immunity. 2007; 27: 847–59. doi: 10.1016/j.immuni.2007.10.009.

162. Rodriguez A, Vigorito E, Clare S, Warren M V., Couttet P, Soond DR, Van Dongen S, Grocock RJ, Das PP, Miska EA, Vetrie D, Okkenhaug K, Enright AJ, et al. Requirement of bic/microRNA-155 for normal immune function. Science (80-). American Association for the Advancement of Science; 2007; 316: 608–11. doi: 10.1126/science.1139253.
163. Teng G, Hakimpour P, Landgraf P, Rice A, Tuschl T, Casellas R, Papavasiliou FN. MicroRNA-155 is a negative regulator of activation-induced cytidine deaminase. Immunity. 2008; 28: 621–9. doi: 10.1016/j.immuni.2008.03.015.
164. Jansson MD, Lund AH. MicroRNA and cancer. Mol Oncol. 2012; 6: 590–610. doi: 10.1016/j.molonc.2012.09.006.
165. Eis PS, Tam W, Sun L, Chadburn A, Li Z, Gomez MF, Lund E, Dahlberg JE. Accumulation of miR-155 and BIC RNA in human B cell lymphomas. Proc Natl Acad Sci U S A. National Academy of Sciences; 2005; 102: 3627–32. doi: 10.1073/pnas.0500613102.
166. Mayr C, Bartel DP. Widespread shortening of 3′UTRs by alternative cleavage and polyadenylation activates oncogenes in cancer cells. doi: 10.1016/j.cell.2009.06.016.
167. Li L, Wang D, Xue M, Mi X, Liang Y, Wang P. 3'UTR shortening identifies high-risk cancers with targeted dysregulation of the ceRNA network. Sci Rep. Nature Publishing Groups; 2014; 4: 1–7. doi: 10.1038/srep05406.
168. Zhang B, Pan X, Cobb GP, Anderson TA. microRNAs as oncogenes and tumor suppressors. Dev Biol. Academic Press; 2007; 302: 1–12. doi: 10.1016/J.YDBIO.2006.08.028.
169. Svoronos AA, Engelman DM, Slack FJ. OncomiR or tumor suppressor? The duplicity of MicroRNAs in cancer [Internet]. Cancer Research. American Association for Cancer Research Inc.; 2016. p. 3666–70. doi: 10.1158/0008-5472.CAN-16-0359.
170. Cui B, Chen L, Zhang S, Mraz M, Fecteau JF, Yu J, Ghia EM, Zhang L, Bao L, Rassenti LZ, Messer K, Calin GA, Croce CM, et al. Micro RNA-155 influences B-cell receptor signaling and associates with aggressive disease in chronic lymphocytic leukemia. Blood. American Society of Hematology; 2014; 124: 546–54. doi: 10.1182/blood-2014-03-559690.
171. Tian Y, Wei W, Li L, Yang R. Down-Regulation of miR-148a Promotes Metastasis by DNA Methylation and is Associated with Prognosis of Skin Cancer by Targeting TGIF2. Med Sci Monit. 2015; 21: 3798–805.
172. Zhang H, Li Y, Huang Q, Ren X, Hu H, Sheng H, Lai M. MiR-148a promotes apoptosis by targeting Bcl-2 in colorectal cancer. Cell Death Differ. Nature Publishing Group; 2011; 18: 1702–10. doi: 10.1038/cdd.2011.28.
173. Lim EL, Trinh DL, Scott DW, Chu A, Krzywinski M, Zhao Y, Robertson AG, Mungall AJ, Schein J, Boyle M, Mottok A, Ennishi D, Johnson NA, et al.

Comprehensive miRNA sequence analysis reveals survival differences in diffuse large B-cell lymphoma patients. Genome Biol. BioMed Central; 2015; 16: 18. doi: 10.1186/s13059-014-0568-y.

174. Calin GA, Sevignani C, Dumitru CD, Hyslop T, Noch E, Yendamuri S, Shimizu M, Rattan S, Bullrich F, Negrini M, Croce CM. Human microRNA genes are frequently located at fragile sites and genomic regions involved in cancers. Proc Natl Acad Sci U S A. 2004; 101: 2999–3004. doi: 10.1073/pnas.0307323101.
175. Calin GA, Dumitru CD, Shimizu M, Bichi R, Zupo S, Noch E, Aldler H, Rattan S, Keating M, Rai K, Rassenti L, Kipps T, Negrini M, et al. Frequent deletions and down-regulation of micro- RNA genes miR15 and miR16 at 13q14 in chronic lymphocytic leukemia. Proc Natl Acad Sci U S A. 2002; 99: 15524–9. doi: 10.1073/pnas.242606799.
176. Baer C, Claus R, Frenzel LP, Zucknick M, Park YJ, Gu L, Weichenhan D, Fischer M, Pallasch CP, Herpel E, Rehli M, Byrd JC, Wendtner C-M, et al. Extensive promoter DNA hypermethylation and hypomethylation is associated with aberrant microRNA expression in chronic lymphocytic leukemia. Cancer Res. 2012; 72: 3775–85. doi: 10.1158/0008-5472.CAN-12-0803.
177. Wong K-Y, Yim RL-H, Kwong Y-L, Leung C-Y, Hui P-K, Cheung F, Liang R, Jin D-Y, Chim C-S. Epigenetic inactivation of the MIR129-2 in hematological malignancies. J Hematol Oncol. 2013; 6: 16. doi: 10.1186/1756-8722-6-16.
178. Lv L V, Zhou J, Lin C, Hu G, Yi LU, DU J, Gao K, Li X. DNA methylation is involved in the aberrant expression of miR-133b in colorectal cancer cells. Oncol Lett. 2015; 10: 907–12. doi: 10.3892/ol.2015.3336.
179. Di Lisio L, Sánchez-Beato M, Gómez-López G, Rodríguez ME, Montes-Moreno S, Mollejo M, Menárguez J, Martínez MA, Alves FJ, Pisano DG, Piris MA, Martínez N. MicroRNA signatures in B-cell lymphomas. Blood Cancer J. 2012; 2: e57. doi: 10.1038/bcj.2012.1.
180. Iqbal J, Shen Y, Huang X, Liu Y, Wake L, Liu C, Deffenbacher K, Lachel CM, Wang C, Rohr J, Guo S, Smith LM, Wright G, et al. Global microRNA expression profiling uncovers molecular markers for classification and prognosis in aggressive B-cell lymphoma. Blood. American Society of Hematology; 2015; 125: 1137–45. doi: 10.1182/blood-2014-04-566778.
181. Marques SC, Ranjbar B, Laursen MB, Falgreen S, Bilgrau AE, Bødker JS, Jørgensen LK, Primo MN, Schmitz A, Ettrup MS, Johnsen HE, Bøgsted M, Mikkelsen JG, et al. High miR-34a expression improves response to doxorubicin in diffuse large B-cell lymphoma. Exp Hematol. 2016; 44: 238-246.e2. doi: 10.1016/j.exphem.2015.12.007.
182. Fassina A, Marino F, Siri M, Zambello R, Ventura L, Fassan M, Simonato F, Cappellesso R. The miR-17-92 microRNA cluster: A novel diagnostic tool in large B-cell malignancies. Lab Investig. Nature Publishing Group; 2012; 92: 1574–82. doi: 10.1038/labinvest.2012.129.

183. Due H, Svendsen P, Bødker JS, Schmitz A, Bøgsted M, Johnsen HE, El-Galaly TC, Roug AS, Dybkær K, El-Galaly TC, Roug AS, Dybkær K. miR-155 as a Biomarker in B-Cell Malignancies. Biomed Res Int. Hindawi Publishing Corporation; 2016; 2016: 1–14. doi: 10.1155/2016/9513037.
184. Ota A, Tagawa H, Karnan S, Tsuzuki S, Karpas A, Kira S, Yoshida Y, Seto M. Identification and Characterization of a Novel Gene, C13orf25, as a Target for 13q31-q32 Amplification in Malignant Lymphoma. Cancer Res. Cancer Res; 2004; 64: 3087–95. doi: 10.1158/0008-5472.CAN-03-3773.
185. Xiao C, Srinivasan L, Calado DP, Patterson HC, Zhang B, Wang J, Henderson JM, Kutok JL, Rajewsky K. Lymphoproliferative disease and autoimmunity in mice with increased miR-17-92 expression in lymphocytes. Nat Immunol. Nature Publishing Group; 2008; 9: 405–14. doi: 10.1038/ni1575.
186. Ott G, Rosenwald A, Campo E. Understanding MYC-driven aggressive B-cell lymphomas: Pathogenesis and classification. Blood. American Society of Hematology; 2013. p. 3884–91. doi: 10.1182/blood-2013-05-498329.
187. Mu P, Han YC, Betel D, Yao E, Squatrito M, Ogrodowski P, De Stanchina E, D'Andrea A, Sander C, Ventura A. Genetic dissection of the miR-17-92 cluster of microRNAs in Myc-induced B-cell lymphomas. Genes Dev. Cold Spring Harbor Laboratory Press; 2009; 23: 2806–11. doi: 10.1101/gad.1872909.
188. Mainou-Fowler. A 9 series microRNA signature differentiates between germinal centre and activated B-cell-like diffuse large B-cell lymphoma cell lines. Int J Oncol. Spandidos Publications; 2010; 37. doi: 10.3892/ijo_00000685.
189. Roehle A, Hoefig KP, Repsilber D, Thorns C, Ziepert M, Wesche KO, Thiere M, Loeffler M, Klapper W, Pfreundschuh M, Matolcsy A, Bernd H-W, Reiniger L, et al. MicroRNA signatures characterize diffuse large B-cell lymphomas and follicular lymphomas. Br J Haematol. 2008; 142: 732–44. doi: 10.1111/j.1365-2141.2008.07237.x.
190. Medina PP, Nolde M, Slack FJ. OncomiR addiction in an in vivo model of microRNA-21-induced pre-B-cell lymphoma. Nature. Nature; 2010; 467: 86–90. doi: 10.1038/nature09284.
191. Lawrie CH, Soneji S, Marafioti T, Cooper CDO, Palazzo S, Paterson JC, Cattan H, Enver T, Mager R, Boultwood J, Wainscoat JS, Hatton CSR. MicroRNA expression distinguishes between germinal center B cell-like and activated B cell-like subtypes of diffuse large B cell lymphoma. Int J Cancer. 2007; 121: 1156–61. doi: 10.1002/ijc.22800.
192. Wang H, Tan Z, Hu H, Liu H, Wu T, Zheng C, Wang X, Luo Z, Wang J, Liu S, Lu Z, Tu J. MicroRNA-21 promotes breast cancer proliferation and metastasis by targeting LZTFL1. BMC Cancer. BioMed Central Ltd.; 2019; 19: 738. doi: 10.1186/s12885-019-5951-3.
193. Wu Y, Song Y, Xiong Y, Wang X, Xu K, Han B, Bai Y, Li L, Zhang Y, Zhou L. MicroRNA-21 (Mir-21) Promotes Cell Growth and Invasion by Repressing Tumor Suppressor PTEN in Colorectal Cancer. Cell Physiol Biochem. S.

Karger AG; 2017; 43: 945–58. doi: 10.1159/000481648.
194. Bai H, Wei J, Deng C, Yang X, Wang C, Xu R. MicroRNA-21 regulates the sensitivity of diffuse large B-cell lymphoma cells to the CHOP chemotherapy regimen. Int J Hematol. 2013; 97: 223–31. doi: 10.1007/s12185-012-1256-x.
195. Lawrie CH, Gal S, Dunlop HM, Pushkaran B, Liggins AP, Pulford K, Banham AH, Pezzella F, Boultwood J, Wainscoat JS, Hatton CSR, Harris AL. Detection of elevated levels of tumour-associated microRNAs in serum of patients with diffuse large B-cell lymphoma. Br J Haematol. 2008; 141: 672–5. doi: 10.1111/j.1365-2141.2008.07077.x.
196. Chen W, Wang H, Chen H, Liu S, Lu H, Kong D, Huang X, Kong Q, Lu Z. Clinical significance and detection of microRNA-21 in serum of patients with diffuse large B-cell lymphoma in Chinese population. Eur J Haematol. Blackwell Publishing Ltd; 2014; 92: 407–12. doi: 10.1111/ejh.12263.
197. Craig VJ, Cogliatti SB, Imig J, Renner C, Neuenschwander S, Rehrauer H, Schlapbach R, Dirnhofer S, Tzankov A, Müller A. Myc-mediated repression of microRNA-34a promotes high-grade transformation of B-cell lymphoma by dysregulation of FoxP1. Blood. American Society of Hematology; 2011; 117: 6227–36. doi: 10.1182/blood-2010-10-312231.
198. Craig VJ, Tzankov A, Flori M, Schmid CA, BaDer AG, Müller A. Systemic microRNA-34a delivery induces apoptosis and abrogates growth of diffuse large B-cell lymphoma in vivo. Leukemia. Nature Publishing Group; 2012. p. 2421–4. doi: 10.1038/leu.2012.110.
199. Lodygin D, Tarasov V, Epanchintsev A, Berking C, Knyazeva T, Körner H, Knyazev P, Diebold J, Hermeking H. Inactivation of miR-34a by aberrant CpG methylation in multiple types of cancer. Cell Cycle. Taylor and Francis Inc.; 2008; 7: 2591–600. doi: 10.4161/cc.7.16.6533.
200. Rao DS, O'Connell RM, Chaudhuri AA, Garcia-Flores Y, Geiger TL, Baltimore D. MicroRNA-34a perturbs B lymphocyte development by repressing the forkhead box transcription factor Foxp1. Immunity. Cell Press; 2010; 33: 48–59. doi: 10.1016/j.immuni.2010.06.013.
201. Banham AH, Connors JM, Brown PJ, Cordell JL, Ott G, Sreenivasan G, Farinha P, Horsman DE, Gascoyne RD. Expression of the FOXP1 transcription factor is strongly associated with inferior survival in patients with diffuse large B-cell lymphoma. Clin Cancer Res. American Association for Cancer Research Inc.; 2005; 11: 1065–72.
202. He J, Zhang F, Wu Y, Zhang W, Zhu X, He X, Zhao Y, Zhao Y. Prognostic role of microRNA-155 in various carcinomas: results from a meta-analysis. Dis Markers. 2013; 34: 379–86. doi: 10.3233/DMA-130984.
203. Lawrie CH, Chi J, Taylor S, Tramonti D, Ballabio E, Palazzo S, Saunders NJ, Pezzella F, Boultwood J, Wainscoat JS, Hatton CSR. Expression of microRNAs in diffuse large B cell lymphoma is associated with immunophenotype, survival and transformation from follicular lymphoma. J Cell Mol Med. 2009; 13: 1248–60. doi: 10.1111/j.1582-4934.2008.00628.x.
204. Zhong H, Xu L, Zhong J-H, Xiao F, Liu Q, Huang H-H, Chen F-Y. Clinical

and prognostic significance of miR-155 and miR-146a expression levels in formalin-fixed/paraffin-embedded tissue of patients with diffuse large B-cell lymphoma. Exp Ther Med. 2012; 3: 763–70. doi: 10.3892/etm.2012.502.

205. Beheshti A, Stevenson K, Vanderburg C, Ravi D, McDonald JT, Christie AL, Shigemori K, Jester H, Weinstock DM, Evens AM. Identification of Circulating Serum Multi-MicroRNA Signatures in Human DLBCL Models. Sci Rep. Nature Research; 2019; 9: 1–11. doi: 10.1038/s41598-019-52985-x.
206. Thompson RC, Vardinogiannis I, Gilmore TD. Identification of an NF-κB p50/p65-responsive site in the human MIR155HG promoter. BMC Mol Biol. 2013; 14: 24. doi: 10.1186/1471-2199-14-24.
207. Vargova K, Curik N, Burda P, Basova P, Kulvait V, Pospisil V, Savvulidi F, Kokavec J, Necas E, Berkova A, Obrtlikova P, Karban J, Mraz M, et al. MYB transcriptionally regulates the miR-155 host gene in chronic lymphocytic leukemia. Blood. 2011; 117: 3816–25. doi: 10.1182/blood-2010-05-285064.
208. Ma M, Zhao R, Yang X, Zhao L, Liu L, Zhang C, Wang X, Shan B. The clinical significance of mda-7/il-24 and c-myb expression in tumor tissues of patients with diffuse large b cell lymphoma. Exp Ther Med. Spandidos Publications; 2018; 16: 649–56. doi: 10.3892/etm.2018.6230.
209. Costinean S, Zanesi N, Pekarsky Y, Tili E, Volinia S, Heerema N, Croce CM. Pre-B cell proliferation and lymphoblastic leukemia/high-grade lymphoma in Eμ-miR155 transgenic mice. Proc Natl Acad Sci U S A. National Academy of Sciences; 2006; 103: 7024–9. doi: 10.1073/pnas.0602266103.
210. Babar IA, Cheng CJ, Booth CJ, Liang X, Weidhaas JB, Saltzman WM, Slack FJ. Nanoparticle-based therapy in an in vivo microRNA-155 (miR-155)-dependent mouse model of lymphoma. Proc Natl Acad Sci U S A. 2012; 109: E1695-704. doi: 10.1073/pnas.1201516109.
211. Zhang Y, Roccaro AM, Rombaoa C, Flores L, Obad S, Fernandes SM, Sacco A, Liu Y, Ngo H, Quang P, Azab AK, Azab F, Maiso P, et al. LNA-mediated anti-miR-155 silencing in low-grade B-cell lymphomas. Blood. 2012; 120: 1678–86. doi: 10.1182/blood-2012-02-410647.
212. Safety, Tolerability and Pharmacokinetics of MRG-106 in Patients With Mycosis Fungoides (MF), CLL, DLBCL or ATLL - Full Text View - ClinicalTrials.gov [Internet]. Available 2020 Jul 3, from https://clinicaltrials.gov/ct2/show/NCT02580552
213. Young L, Sung J, Masters JR. Detection of mycoplasma in cell cultures. Nat Protoc. Nature Publishing Group; 2010; 5: 929–34. doi: 10.1038/nprot.2010.43.
214. Osborne CK, Hobbs K, Trent JM. Biological differences among MCF-7 human breast cancer cell lines from different laboratories. Breast Cancer Res Treat. Martinus Nijhoff/Dr. W. Junk Publishers; 1987; 9: 111–21. doi: 10.1007/BF01807363.
215. Quentmeier H, Amini RM, Berglund M, Dirks WG, Ehrentraut S, Geffers R, Macleod RAF, Nagel S, Romani J, Scherr M, Zaborski M, Drexler HG. U-2932: Two clones in one cell line, a tool for the study of clonal evolution.

Leukemia. Leukemia; 2013; 27: 1155–64. doi: 10.1038/leu.2012.358.
216. Falgreen S, Laursen MB, Bødker JS, Kjeldsen MK, Schmitz A, Nyegaard M, Johnsen HE, Dybkær K, Bøgsted M. Exposure time independent summary statistics for assessment of drug dependent cell line growth inhibition. BMC Bioinformatics. BioMed Central; 2014; 15: 168. doi: 10.1186/1471-2105-15-168.
217. Huang S, Pang L. Comparing Statistical Methods for Quantifying Drug Sensitivity Based on *In Vitro* Dose–Response Assays. Assay Drug Dev Technol. Mary Ann Liebert, Inc. 140 Huguenot Street, 3rd Floor New Rochelle, NY 10801 USA ; 2012; 10: 88–96. doi: 10.1089/adt.2011.0388.
218. Falgreen S, Dybkær K, Young KH, Xu-Monette ZY, El-Galaly TC, Laursen MB, Bødker JS, Kjeldsen MK, Schmitz A, Nyegaard M, Johnsen HE, Bøgsted M. Predicting response to multidrug regimens in cancer patients using cell line experiments and regularised regression models. BMC Cancer. 2015; 15: 235. doi: 10.1186/s12885-015-1237-6.
219. Reinholdt L, Laursen MB, Schmitz A, Bødker JS, Jakobsen LH, Bøgsted M, Johnsen HE, Dybkær K. The CXCR4 antagonist plerixafor enhances the effect of rituximab in diffuse large B-cell lymphoma cell lines. Biomark Res. 2016; 4: 12. doi: 10.1186/s40364-016-0067-2.
220. Geary N. Understanding synergy. Am J Physiol Metab. 2013; 304: E237–53. doi: 10.1152/ajpendo.00308.2012.
221. Chou TC. Drug combination studies and their synergy quantification using the chou-talalay method. Cancer Research. 2010. p. 440–6. doi: 10.1158/0008-5472.CAN-09-1947.
222. Foucquier J, Guedj M. Analysis of drug combinations: current methodological landscape. Pharmacology Research and Perspectives. Wiley-Blackwell Publishing Ltd; 2015. doi: 10.1002/prp2.149.
223. Li L, Wickham TJ, Keegan AD. Efficient transduction of murine B lymphocytes and B lymphoma lines by modified adenoviral vectors: Enhancement via targeting to FcR and heparan-containing proteins. Gene Ther. Nature Publishing Group; 2001; 8: 938–45. doi: 10.1038/sj.gt.3301487.
224. Bak RO, Hollensen AK, Primo MN, Sørensen CD, Mikkelsen JG. Potent microRNA suppression by RNA Pol II-transcribed “Tough Decoy” inhibitors. RNA. Cold Spring Harbor Laboratory Press; 2013; 19: 280–93. doi: 10.1261/rna.034850.112.
225. Isaacs A, Cox RA, Rotem Z. FOREIGN NUCLEIC ACIDS AS THE STIMULUS TO MAKE INTERFERON. Lancet. Elsevier; 1963; 282: 113–6. doi: 10.1016/S0140-6736(63)92585-6.
226. Sun L, Wu J, Du F, Chen X, Chen ZJ. Cyclic GMP-AMP synthase is a cytosolic DNA sensor that activates the type I interferon pathway. Science (80-). American Association for the Advancement of Science; 2013; 339: 786–91. doi: 10.1126/science.1232458.
227. Ranjbar B, Krogh LB, Laursen MB, Primo MN, Marques SC, Dybkær K, Mikkelsen JG. Anti-Apoptotic Effects of Lentiviral Vector Transduction

Promote Increased Rituximab Tolerance in Cancerous B-Cells. Richards KL, editor. PLoS One. 2016; 11: e0153069. doi: 10.1371/journal.pone.0153069.
228. Naldini L. In vivo gene delivery by lentiviral vectors. Thromb Haemost. 1999; 82: 552–4. Available from http://www.ncbi.nlm.nih.gov/pubmed/10605750
229. Dull T, Zufferey R, Kelly M, Mandel RJ, Nguyen M, Trono D, Naldini L. A third-generation lentivirus vector with a conditional packaging system. J Virol. 1998; 72: 8463–71.
230. Reiser J, Harmison G, Kluepfel-Stahl S, Brady RO, Karlsson S, Schubert M. Transduction of nondividing cells using pseudotyped defective high-titer HIV type 1 particles. Proc Natl Acad Sci U S A. National Academy of Sciences; 1996; 93: 15266–71. doi: 10.1073/pnas.93.26.15266.
231. Burns JC, Friedmann T, Driever W, Burrascano M, Yee JK. Vesicular stomatitis virus G glycoprotein pseudotyped retroviral vectors: Concentration to very high titer and efficient gene transfer into mammalian and nonmammalian cells. Proc Natl Acad Sci U S A. National Academy of Sciences; 1993; 90: 8033–7. doi: 10.1073/pnas.90.17.8033.
232. Jinek M, Chylinski K, Fonfara I, Hauer M, Doudna JA, Charpentier E. A programmable dual-RNA-guided DNA endonuclease in adaptive bacterial immunity. Science (80-). American Association for the Advancement of Science; 2012; 337: 816–21. doi: 10.1126/science.1225829.
233. Jinek M, East A, Cheng A, Lin S, Ma E, Doudna J. RNA-programmed genome editing in human cells. Elife. 2013; 2013. doi: 10.7554/eLife.00471.
234. Barrangou R, Fremaux C, Deveau H, Richards M, Boyaval P, Moineau S, Romero DA, Horvath P. CRISPR provides acquired resistance against viruses in prokaryotes. Science (80-). 2007; 315: 1709–12. doi: 10.1126/science.1138140.
235. Gasiunas G, Barrangou R, Horvath P, Siksnys V. Cas9-crRNA ribonucleoprotein complex mediates specific DNA cleavage for adaptive immunity in bacteria. Proc Natl Acad Sci U S A. National Academy of Sciences; 2012; 109: E2579–86. doi: 10.1073/pnas.1208507109.
236. Cong L, Ran FA, Cox D, Lin S, Barretto R, Habib N, Hsu PD, Wu X, Jiang W, Marraffini LA, Zhang F. Multiplex genome engineering using CRISPR/Cas systems. Science (80-). American Association for the Advancement of Science; 2013; 339: 819–23. doi: 10.1126/science.1231143.
237. Ran FA, Hsu PD, Wright J, Agarwala V, Scott DA, Zhang F. Genome engineering using the CRISPR-Cas9 system. Nat Protoc. Nature Publishing Group; 2013; 8: 2281–308. doi: 10.1038/nprot.2013.143.
238. Sander JD, Joung JK. CRISPR-Cas systems for editing, regulating and targeting genomes [Internet]. Nature Biotechnology. Nature Publishing Group; 2014. p. 347–50. doi: 10.1038/nbt.2842.
239. Lino CA, Harper JC, Carney JP, Timlin JA. Delivering CRISPR: a review of the challenges and approaches. Drug Deliv. Taylor and Francis Ltd; 2018; 25: 1234–57. doi: 10.1080/10717544.2018.1474964.
240. Liu B, Saber A, Haisma HJ. CRISPR/Cas9: a powerful tool for identification

of new targets for cancer treatment. Drug Discovery Today. Elsevier Ltd; 2019. p. 955–70. doi: 10.1016/j.drudis.2019.02.011.

241. Gaj T, Gersbach CA, Barbas CF. ZFN, TALEN, and CRISPR/Cas-based methods for genome engineering. Trends in Biotechnology. Elsevier Current Trends; 2013. p. 397–405. doi: 10.1016/j.tibtech.2013.04.004.
242. Kleinstiver BP, Pattanayak V, Prew MS, Tsai SQ, Nguyen NT, Zheng Z, Joung JK. High-fidelity CRISPR-Cas9 nucleases with no detectable genome-wide off-target effects. Nature. Nature Publishing Group; 2016; 529: 490–5. doi: 10.1038/nature16526.
243. Lee JK, Jeong E, Lee J, Jung M, Shin E, Kim Y hoon, Lee K, Jung I, Kim D, Kim S, Kim JS. Directed evolution of CRISPR-Cas9 to increase its specificity. Nat Commun. Nature Publishing Group; 2018; 9: 1–10. doi: 10.1038/s41467-018-05477-x.
244. Casini A, Olivieri M, Petris G, Montagna C, Reginato G, Maule G, Lorenzin F, Prandi D, Romanel A, Demichelis F, Inga A, Cereseto A. A highly specific SpCas9 variant is identified by in vivo screening in yeast. Nat Biotechnol. Nature Publishing Group; 2018; 36: 265–71. doi: 10.1038/nbt.4066.
245. Kouranova E, Forbes K, Zhao G, Warren J, Bartels A, Wu Y, Cui X. CRISPRs for optimal targeting: Delivery of CRISPR components as DNA, RNA, and protein into cultured cells and single-cell embryos. Hum Gene Ther. Mary Ann Liebert Inc.; 2016; 27: 464–75. doi: 10.1089/hum.2016.009.
246. Mout R, Ray M, Yesilbag Tonga G, Lee YW, Tay T, Sasaki K, Rotello VM. Direct Cytosolic Delivery of CRISPR/Cas9-Ribonucleoprotein for Efficient Gene Editing. ACS Nano. American Chemical Society; 2017; 11: 2452–8. doi: 10.1021/acsnano.6b07600.
247. Vakulskas CA, Dever DP, Rettig GR, Turk R, Jacobi AM, Collingwood MA, Bode NM, McNeill MS, Yan S, Camarena J, Lee CM, Park SH, Wiebking V, et al. A high-fidelity Cas9 mutant delivered as a ribonucleoprotein complex enables efficient gene editing in human hematopoietic stem and progenitor cells. Nat Med. Nature Publishing Group; 2018; 24: 1216–24. doi: 10.1038/s41591-018-0137-0.
248. Gilbert LA, Horlbeck MA, Adamson B, Villalta JE, Chen Y, Whitehead EH, Guimaraes C, Panning B, Ploegh HL, Bassik MC, Qi LS, Kampmann M, Weissman JS. Genome-Scale CRISPR-Mediated Control of Gene Repression and Activation. Cell. Cell Press; 2014; 159: 647–61. doi: 10.1016/j.cell.2014.09.029.
249. Grünewald J, Zhou R, Iyer S, Lareau CA, Garcia SP, Aryee MJ, Joung JK. CRISPR DNA base editors with reduced RNA off-target and self-editing activities. Nat Biotechnol. Nature Publishing Group; 2019; 37: 1041–8. doi: 10.1038/s41587-019-0236-6.
250. Kang JG, Park JS, Ko JH, Kim YS. Regulation of gene expression by altered promoter methylation using a CRISPR/Cas9-mediated epigenetic editing system. Sci Rep. Nature Publishing Group; 2019; 9: 1–12. doi: 10.1038/s41598-019-48130-3.

251. Shalem O, Sanjana NE, Hartenian E, Shi X, Scott DA, Mikkelsen TS, Heckl D, Ebert BL, Root DE, Doench JG, Zhang F. Genome-scale CRISPR-Cas9 knockout screening in human cells. Science (80-). American Association for the Advancement of Science; 2014; 343: 84–7. doi: 10.1126/science.1247005.
252. Southern EM, Maskos U, Elder JK. Analyzing and comparing nucleic acid sequences by hybridization to arrays of oligonucleotides: Evaluation using experimental models. Genomics. 1992; 13: 1008–17. doi: 10.1016/0888-7543(92)90014-J.
253. Holland PM, Abramson RD, Watson R, Gelfand DH. Detection of specific polymerase chain reaction product by utilizing the 5'----3' exonuclease activity of Thermus aquaticus DNA polymerase. Proc Natl Acad Sci U S A. National Academy of Sciences; 1991; 88: 7276–80.
254. Bustin SA, Benes V, Garson JA, Hellemans J, Huggett J, Kubista M, Mueller R, Nolan T, Pfaffl MW, Shipley GL, Vandesompele J, Wittwer CT. The MIQE guidelines: minimum information for publication of quantitative real-time PCR experiments. Clin Chem. 2009; 55: 611–22. doi: 10.1373/clinchem.2008.112797.
255. Hindson BJ, Ness KD, Masquelier DA, Belgrader P, Heredia NJ, Makarewicz AJ, Bright IJ, Lucero MY, Hiddessen AL, Legler TC, Kitano TK, Hodel MR, Petersen JF, et al. High-throughput droplet digital PCR system for absolute quantitation of DNA copy number. Anal Chem. American Chemical Society; 2011; 83: 8604–10. doi: 10.1021/ac202028g.
256. Due H, Schönherz AA, Ryø L, Primo MN, Jespersen DS, Thomsen EA, Roug AS, Xiao M, Tan X, Pang Y, Young KH, Bøgsted M, Mikkelsen JG, et al. MicroRNA-155 controls vincristine sensitivity and predicts superior clinical outcome in diffuse large B-cell lymphoma. Blood Adv. American Society of Hematology; 2019; 3: 1185–96. doi: 10.1182/bloodadvances.2018029660.
257. Due H, Brøndum RF, Young KH, Bøgsted M, Dybkær K. MicroRNAs associated to single drug components of R-CHOP identifies diffuse large B-cell lymphoma patients with poor outcome and adds prognostic value to the international prognostic index. BMC Cancer. BioMed Central Ltd.; 2020; 20: 237. doi: 10.1186/s12885-020-6643-8.
258. Butz H, Likó I, Czirják S, Igaz P, Khan MM, Zivkovic V, Bálint K, Korbonits M, Rácz K, Patócs A. Down-Regulation of Wee1 Kinase by a Specific Subset of microRNA in Human Sporadic Pituitary Adenomas. J Clin Endocrinol Metab. 2010; 95: E181–91. doi: 10.1210/jc.2010-0581.
259. Tili E, Michaille J-J, Wernicke D, Alder H, Costinean S, Volinia S, Croce CM. Mutator activity induced by microRNA-155 (miR-155) links inflammation and cancer. Proc Natl Acad Sci U S A. 2011; 108: 4908–13. doi: 10.1073/pnas.1101795108.
260. Moudi M, Go R, Yien CYS, Nazre M. Vinca alkaloids. International Journal of Preventive Medicine. Wolters Kluwer -- Medknow Publications; 2013. p. 1131–5. doi: 10.2165/00128415-200711380-00080.

261. Yates LR, Seoane J, Le Tourneau C, Siu LL, Marais R, Michiels S, Soria JC, Campbell P, Normanno N, Scarpa A, Reis-Filho JS, Rodon J, Swanton C, et al. The European Society for Medical Oncology (ESMO) Precision Medicine Glossary. Ann Oncol. 2018; . doi: 10.1093/annonc/mdx707.
262. Mörth C, Valachis A, Sabaa AA, Molin D, Flogegård M, Enblad G. Does the omission of vincristine in patients with diffuse large B cell lymphoma affect treatment outcome? Ann Hematol. Springer Verlag; 2018; 97: 2129–35. doi: 10.1007/s00277-018-3437-z.
263. Ceppi F, Langlois-Pelletier C, Gagné V, Rousseau J, Ciolino C, Lorenzo S De, Kevin KM, Cijov D, Sallan SE, Silverman LB, Neuberg D, Kutok JL, Sinnett D, et al. Polymorphisms of the vincristine pathway and response to treatment in children with childhood acute lymphoblastic leukemia. Pharmacogenomics. Future Medicine Ltd.; 2014; 15: 1105–16. doi: 10.2217/pgs.14.68.
264. Lopez-Lopez E, Gutierrez-Camino A, Astigarraga I, Navajas A, Echebarria-Barona A, Garcia-Miguel P, Garcia De Andoin N, Lobo C, Guerra-Merino I, Martin-Guerrero I, Garcia-Orad A. Vincristine pharmacokinetics pathway and neurotoxicity during early phases of treatment in pediatric acute lymphoblastic leukemia. Pharmacogenomics. Future Medicine Ltd.; 2016; 17: 731–41. doi: 10.2217/pgs-2016-0001.
265. Sawaki A, Miyazaki K, Takeuchi T, Kobayashi K, Imai H, Tawara I, Ono R, Nosaka T, Yamaguchi M, Katayama N. Gene Polymorphisms and Vincristine-Induced Neuropathy in Patients Who Received R-CHOP Chemotherapy. Blood. American Society of Hematology; 2019; 134: 1624–1624. doi: 10.1182/blood-2019-122796.
266. Subramanian A, Tamayo P, Mootha VK, Mukherjee S, Ebert BL, Gillette MA, Paulovich A, Pomeroy SL, Golub TR, Lander ES, Mesirov JP. Gene set enrichment analysis: a knowledge-based approach for interpreting genome-wide expression profiles. Proc Natl Acad Sci U S A. National Academy of Sciences; 2005; 102: 15545–50. doi: 10.1073/pnas.0506580102.
267. The Gene Ontology Resource: 20 years and still GOing strong. doi: 10.1093/nar/gky1055.
268. Liberzon A, Birger C, Thorvaldsdóttir H, Ghandi M, Mesirov JP, Tamayo P. The Molecular Signatures Database Hallmark Gene Set Collection. Cell Syst. Cell Press; 2015; 1: 417–25. doi: 10.1016/J.CELS.2015.12.004.
269. Gao Y, Ma X, Yao Y, Li H, Fan Y, Zhang Y, Zhao C, Wang L, Ma M, Lei Z, Zhang X. miR-155 regulates the proliferation and invasion of clear cell renal cell carcinoma cells by targeting E2F2. Oncotarget. Impact Journals LLC; 2016; 7: 20324–37. doi: 10.18632/oncotarget.7951.
270. Aprelikova O, Yu X, Palla J, Wei BR, John S, Yi M, Stephens R, Simpson RM, Risinger JI, Jazaeri A, Niederhuber J. The role of miR-31 and its target gene SATB2 in cancer-associated fibroblasts. Cell Cycle. Taylor and Francis Inc.; 2010; 9: 4387–98. doi: 10.4161/cc.9.21.13674.
271. Pang W, Su J, Wang Y, Feng H, Dai X, Yuan Y, Chen X, Yao W. Pancreatic

cancer-secreted miR-155 implicates in the conversion from normal fibroblasts to cancer-associated fibroblasts. Cancer Sci. Blackwell Publishing Ltd; 2015; 106: 1362–9. doi: 10.1111/cas.12747.

272. Tan S, Xia L, Yi P, Han Y, Tang L, Pan Q, Tian Y, Rao S, Oyang L, Liang J, Lin J, Su M, Shi Y, et al. Exosomal miRNAs in tumor microenvironment. Journal of Experimental and Clinical Cancer Research. BioMed Central Ltd.; 2020. p. 1–15. doi: 10.1186/s13046-020-01570-6.
273. Rasmussen MH, Lyskjær I, Jersie-Christensen RR, Tarpgaard LS, Primdal-Bengtson B, Nielsen MM, Pedersen JS, Hansen TP, Hansen F, Olsen JV, Pfeiffer P, Ørntoft TF, Andersen CL, et al. miR-625-3p regulates oxaliplatin resistance by targeting MAP2K6-p38 signalling in human colorectal adenocarcinoma cells. Nat Commun. Nature Publishing Group; 2016; 7: 12436. doi: 10.1038/ncomms12436.
274. Kung JTY, Colognori D, Lee JT. Long noncoding RNAs: Past, present, and future. Genetics. Genetics Society of America; 2013. p. 651–69. doi: 10.1534/genetics.112.146704.
275. Kristensen LS, Andersen MS, Stagsted LVW, Ebbesen KK, Hansen TB, Kjems J. The biogenesis, biology and characterization of circular RNAs. Nature Reviews Genetics. Nature Publishing Group; 2019. p. 675–91. doi: 10.1038/s41576-019-0158-7.
276. Cabili M, Trapnell C, Goff L, Koziol M, Tazon-Vega B, Regev A, Rinn JL. Integrative annotation of human large intergenic noncoding RNAs reveals global properties and specific subclasses. Genes Dev. Cold Spring Harbor Laboratory Press; 2011; 25: 1915–27. doi: 10.1101/gad.17446611.
277. Hansen TB, Jensen TI, Clausen BH, Bramsen JB, Finsen B, Damgaard CK, Kjems J. Natural RNA circles function as efficient microRNA sponges. Nature. Nature Publishing Group; 2013; 495: 384–8. doi: 10.1038/nature11993.
278. Wang F, Nazarali AJ, Ji S. Circular RNAs as potential biomarkers for cancer diagnosis and therapy. American Journal of Cancer Research. E-Century Publishing Corporation; 2016. p. 1167–76.
279. Strand SH, Bavafaye-Haghighi E, Kristensen H, Rasmussen AK, Hoyer S, Borre M, Mouritzen P, Besenbacher S, Orntoft TF, Sorensen KD. A novel combined miRNA and methylation marker panel (miMe) for prediction of prostate cancer outcome after radical prostatectomy. Int J Cancer. Wiley-Liss Inc.; 2019; 145: 3445–52. doi: 10.1002/ijc.32427.
280. Fredsøe J, Rasmussen AKI, Mouritzen P, Borre M, Ørntoft T, Sørensen KD. A five-microRNA model (*pCaP*) for predicting prostate cancer aggressiveness using cell-free urine. Int J Cancer. Wiley-Liss Inc.; 2019; 145: 2558–67. doi: 10.1002/ijc.32296.
281. Wilson WH. Treatment strategies for aggressive lymphomas: what works? Hematol Am Soc Hematol Educ Progr. American Society of Hematology; 2013; 2013: 584–90. doi: 10.1182/asheducation-2013.1.584.
282. Lv L, An X, Li H, Ma L. Effect of miR-155 knockdown on the reversal of

doxorubicin resistance in human lung cancer A549/dox cells. Oncol Lett. Spandidos Publications; 2016; 11: 1161–6. doi: 10.3892/ol.2015.3995.

283. Poste G. Bring on the biomarkers. Nature. 2011; 469: 156–7. doi: 10.1038/469156a.
284. Kurtz DM, Scherer F, Jin MC, Soo J, Craig AFM, Esfahani MS, Chabon JJ, Stehr H, Liu CL, Tibshirani R, Maeda LS, Gupta NK, Khodadoust MS, et al. Circulating tumor DNA measurements as early outcome predictors in diffuse large B-cell lymphoma. J Clin Oncol. American Society of Clinical Oncology; 2018; 36: 2845–53. doi: 10.1200/JCO.2018.78.5246.
285. Alcaide M, Yu S, Bushell K, Fornika D, Nielsen JS, Nelson BH, Mann KK, Assouline S, Johnson NA, Morin RD. Multiplex droplet digital PCR quantification of recurrent somatic mutations in diffuse large b-cell and follicular lymphoma. Clin Chem. American Association for Clinical Chemistry Inc.; 2016; 62: 1238–47. doi: 10.1373/clinchem.2016.255315.
286. Weiner GJ. Rituximab: Mechanism of Action. 2010; . doi: 10.1053/j.seminhematol.2010.01.011.
287. Pallasch CP, Leskov I, Braun CJ, Vorholt D, Drake A, Soto-Feliciano YM, Bent EH, Schwamb J, Iliopoulou B, Kutsch N, van Rooijen N, Frenzel LP, Wendtner CM, et al. Sensitizing Protective Tumor Microenvironments to Antibody-Mediated Therapy. Cell. Cell Press; 2014; 156: 590–602. doi: 10.1016/J.CELL.2013.12.041.
288. Connectivity Map (CMAP) | Broad Institute [Internet]. Available 2020 Aug 10, from https://www.broadinstitute.org/connectivity-map-cmap
289. How to express CRISPR in your target cells - Benchling [Internet]. Available 2020 Aug 3, from https://www.benchling.com/2016/03/24/how-to-express-crispr-in-your-target-cells/
290. Third Generation PCR | Bioradiations [Internet]. Available 2020 Aug 3, from https://www.bioradiations.com/third-generation-pcr/

APPENDIX

Appendix A. Papers

I. miR-155 as a Biomarker in B-Cell Malignancies
H. Due, P. Svendsen, J.S. Bødker, M. Bøgsted, H.E. Johnsen, T.C. Galaly, A.S. Roug, K. Dybkær.
Hindawi, BioMed**,** Research International, (2016), DOI: 10.1155/2016/9513037

II. MicroRNA-155 Controls Vincristine Sensitivity and Predicts Superior Clinical Outcome in Diffuse Large B-cell Lymphoma
H. Due, A.A. Schönherz, L. Ryø, M.N. Primo, D.S. Jespersen, E.A. Thomsen, A.S. Roug, X. Min, X. Tang, Y. Pang, K.H. Young, M. Bøgsted, J.G. Mikkelsen, K. Dybkær.
Blood Adv (2019) 3 (7): 1185–1196, DOI 10.1182/bloodadvances.2018029660

III. Aspects of vincristine-induced neuropathy in hematologic malignancies: a systematic review
M.L. Madsen, H. Due, N. Ejskjær, P. Jensen, J. Madsen, K. Dybkær.
Cancer Chemother Pharmacol 84**,** 471–485 (2019), DOI: 10.1007/s00280-019-03884-5

IV. MicroRNAs associated to single drug components of R-CHOP identifies diffuse large B-cell lymphoma patients with poor outcome and adds prognostic value to the international prognostic index
H. Due, R.F. Brøndum, K.H. Young, M. Bøgsted, K. Dybkær.
BMC Cancer **20,** 237 (2020), DOI: 10.1186/s12885-020-6643-8

Hindawi Publishing Corporation
BioMed Research International
Volume 2016, Article ID 9513037, 14 pages
http://dx.doi.org/10.1155/2016/9513037

Review Article

miR-155 as a Biomarker in B-Cell Malignancies

Hanne Due,[1,2] Pernille Svendsen,[1] Julie Støve Bødker,[1] Alexander Schmitz,[1] Martin Bøgsted,[1,3,4] Hans Erik Johnsen,[1,4,5] Tarec Christoffer El-Galaly,[1,4,5] Anne Stidsholt Roug,[2] and Karen Dybkær[1,4]

[1]Department of Haematology, Aalborg University Hospital, Hobrovej 18-22, 9100 Aalborg, Denmark
[2]Department of Haematology, Aarhus University Hospital, Tage-Hansens Gade 2, 8000 Aarhus C, Denmark
[3]Department of Mathematical Sciences, Aalborg University, Fredrik Bajers Vej 5, 9100 Aalborg, Denmark
[4]Department of Clinical Medicine, Aalborg University, Fredrik Bajers Vej 5, 9100 Aalborg, Denmark
[5]Clinical Cancer Research Center, Aalborg University Hospital, Hobrovej 18-22, 9100 Aalborg, Denmark

Correspondence should be addressed to Karen Dybkær; k.dybkaer@rn.dk

Received 23 December 2015; Accepted 3 April 2016

Academic Editor: Stefan Costinean

MicroRNAs have the potential to be useful biomarkers in the development of individualized treatment since they are easy to detect, are relatively stable during sample handling, and are important determinants of cellular processes controlling pathogenesis, progression, and response to treatment of several types of cancers including B-cell malignancies. miR-155 is an oncomiR with a crucial role in tumor initiation and development of several B-cell malignancies. The present review elucidates the potential of miR-155 as a diagnostic, prognostic, or predictive biomarker in B-cell malignancies using a systematic search strategy to identify relevant literature. miR-155 was upregulated in several malignancies compared to nonmalignant controls and overexpression of miR-155 was further associated with poor prognosis. Elevated expression of miR-155 shows potential as a diagnostic and prognostic biomarker in diffuse large B-cell lymphoma and chronic lymphocytic leukemia. Additionally, *in vitro* and *in vivo* studies suggest miR-155 as an efficient therapeutic target, supporting its oncogenic function. The use of inhibiting anti-miR structures indicates promising potential as novel anticancer therapeutics. Reports from 53 studies prove that miR-155 has the potential to be a molecular tool in personalized medicine.

1. Introduction

Personalized medicine is a new principle that aims at tailoring medical treatment of the individual patients and thereby ending the current "one-fits-all" strategy. Today's cancer diagnostics are typically based on clinical findings, morphology, histology, cytogenetic, immune-phenotyping, and molecular genetic data, but still identification of the molecular pathways driving tumorigenesis often fails [1]. Different B-cell malignancies share common molecular pathways, which is why they may benefit from the same pathway-specific targeted treatment. Additionally, tumor subtypes within one disease entity can be characterized by distinct molecular pathogenesis markers as genetic aberrations or transcription phenotypic markers but still be treated alike causing inefficient expenditure treatment regardless of potential subgroup-specific treatment efficiency. The aim of personalized medicine is to drive the development of a more accurate classification of disease, defined by molecular pathogenesis ultimately enhancing diagnosis and treatment by the use of easy detectable biomarkers [2].

Biomarkers are defined as objective indicators of biological processes, pathogenic processes, or pharmacological response to a therapeutic intervention [3]. Diagnostic biomarkers identify the presence of disease and differentiate normal from malignant or distinguish different diagnoses or progression stages. Prognostic biomarkers provide information about clinical outcome for a class of patients when given a specific treatment, whereas predictive biomarkers provide information on how patients are expected to respond to a drug or treatment regimen. Most importantly, all biomarkers should add further information to present clinical tools. In

Table 1: Cancer relevant target genes for miR-155 supported by experimental observations.

Target genes	Main effect of aberrant miR-155 expression	Reference
SHIP1	PI3K/AKT activity B-cell proliferation	[22, 23]
AID	immunoglobulin diversification/class switch	[24]
PU.1	immunoglobulin diversification/class switch	[25]
HGAL	cell motility	[26]
C/EBPβ	↑ B-cell proliferation	[23]
SMAD5	evasion of TGF-β's growth inhibitory effects	[27]
FADD	↓ apoptosis	[28]
Ripk	↓ apoptosis	[28]
SOCS1	STAT5 activation	[29]

AID, activation-induced cytidine deaminase; C/EBP , CCAAT/enhancer-binding protein ; FADD, Fas-Associated protein with Death Domain; HGAL, human germinal center-associated lymphoma; SHIP1, SH2 domain containing inositol 5′-phosphatase 1; SOCS1, suppressor of cytokine signaling protein 1.

order to ensure accurate stratification, ideal biomarkers need to be easy to detect and provide both high sensitivity and specificity [4].

MicroRNAs (miRNAs) have been demonstrated to possess biomarker potential in multiple diseases [5], both individually and when combined in signature profiles [6–9]. miRNAs are short noncoding RNAs of 20–22 nucleotides that function to regulate gene expression at the posttranscriptional level. They play fundamental roles in the regulation of cellular proliferation, differentiation, and apoptosis [10]. miRNAs are deregulated in many types of cancer, including B-cell malignancies, where they can function as oncogenes, favoring initiation and progression of cancers, or as tumor suppressors, preventing tumorigenesis [11, 12]. One of the most widely studied miRNAs in B-cell malignancies is the oncogenic miR-155, transcribed from a noncoding RNA BIC (B-cell Integration Cluster). miR-155 biogenesis is only briefly summarized since it has recently been extensive and thoroughly reviewed by others [13, 14]. At normal physiologic conditions, miR-155 is a crucial player in hematopoiesis, the immune response, and inflammation [15–18]. It has been found to be upregulated in several types of cancers [19] and has shown specific importance in the pathogenesis of B-cell malignancies. The oncogenic function of miR-155 can be explained by its target genes and the involved underlying molecular pathways presented in Table 1. Overexpression of miR-155 in mice results in development of lymphoproliferative diseases, while subsequent withdrawal leads to remission [20]. Thus, miR-155 is suggested to be a future treatment target. A high number of studies have investigated its potential as a biomarker in several B-cell malignancies, though conflicting results have been presented. To elaborate and assess the potential of miR-155 as a diagnostic, prognostic, and predictive biomarker or target of novel treatments in B-cell malignancies as a part of personalized medicine, we systematically reviewed the existing literature.

2. Materials and Methods

This review was prepared according to the Preferred Reporting for Systematic Reviews and Meta-Analyses (PRISMA) Guidelines [21].

2.1. Literature Search. PubMed and EMBASE were systematically searched for eligible articles. The search terms used in both databases are provided in Table S1 in Supplementary Material available online at http://dx.doi.org/10.1155/2016/9513037. The search was finalized on November 18, 2015. Additional studies were identified by scanning reference lists of articles. The screening process was performed by two reviewers by reading titles and abstracts, while the eligibility of full-texts was assessed in the same manner.

2.2. Inclusion and Exclusion Criteria. Studies were included in the analysis if fulfilling the following inclusion criteria: (1) concerning miR-155 expression as a biomarker or target of chemotherapeutic treatment, (2) focusing on B-cell malignancies, (3) analyzing patient samples, (4) original research articles or letters, and (5) results published in English. Articles were excluded if the present disease was reported in ≤ independent studies.

2.3. Analysis. Data concerning the specific disease, cohort size, sample type, study design of miRNA selection, analytical method, and outcome was extracted manually, and studies were grouped according to the investigated biomarker properties of miR-155 (i.e., diagnostic, prognostic, and/or predictive). Studies exploiting miR-155 as a therapeutic target were described according to their methods (e.g., *in vitro*/*in vivo*), outcomes, and impact of their findings.

3. Results

The systematic search revealed 606 articles, which were screened by reading title and abstract. A total of 126 full-texts were assessed, and 53 of these studies were included in the review, presented in Figure S1. All included articles were published in peer-reviewed scientific journals. Forty-eight of the included articles investigated the expression of miR-155 as either a diagnostic, prognostic, or predictive tool in the management of several diseases, though we excluded studies of specific diseases represented by two or less papers. Five papers exploited miR-155 as a potential target in the treatment of B-cell malignancies. As presented in Table 2, the diagnostic potential of deregulated miR-155 expression has been widely investigated in diffuse large B-cell lymphoma (DLBCL), Burkitt's lymphoma (BL), Hodgkin's lymphoma (HL), mucosa-associated lymphoid tissue lymphoma (MALT), follicular lymphoma (FL), splenic marginal zone lymphoma (SMZL), and chronic lymphatic leukemia (CLL). Additionally, the prognostic potential of miR-155 has been investigated in several studies of DLBCL and CLL, whereas the predictive potential has not been thoroughly

Table 2: miR-155 as diagnostic biomarker in B-cell malignancies.

Disease	Sample type	Cohort		Initial miRNA selection	Method	Expression	Ref
DLBCL	FFPE	90 DLBCL cases 31 controls		Previous research	RT-qPCR		[32]
DLBCL	CS	75 DLBCL cases 10 controls	T	Global screening	Microarray		[46]
	FFPE	47 DLBCL cases 15 controls	V		RT-qPCR		
DLBCL	Blood	20 DLBCL cases 20 controls	T	Previous research	RT-qPCR		[37]
		75 DLBCL cases 77 controls	V				
DLBCL	FFPE	80 DLBCL cases 12 controls		Global screening	Microarray		[33]
		80 DLBCL cases 18 FL cases				NS	
DLBCL	FFPE	11 PCNSL cases 10 nDLBCL cases		Previous research	RT-qPCR		[47]
DLBCL	CS, FFPE	35 DLBCL cases 12 controls		Global screening	RT-qPCR		[34]
		35 DLBCL cases 27 FL cases				NS	
DLBCL	CS, FFPE	18 DLBCL cases 5 controls		Previous research	RNA-ISH RT-qPCR		[48]
DLBCL	CS	29 DLBCL cases 12 BL cases	T	Global screening	Microarray		[38]
	FFPE	43 DLBCL cases 28 BL cases	V		RT-qPCR		
DLBCL	Blood	60 DLBCL cases 43 controls		Previous research	RT-qPCR		[35]
DLBCL	FFPE	19 DLBCL cases 31 exN DLBCL cases		Previous research	RT-qPCR	NS	[49]
DLBCL	CS	22 DLBCL cases 7 controls		Previous research	RT-qPCR		[50]
DLBCL	CS	79 DLBCL cases 36 BL cases		Global screening	Microarray		[39]
DLBCL	CS	23 DLBCL cases 2 controls		Previous research	RT-qPCR		[51]
DLBCL	FNAB	45 DLBCL cases 33 BL cases		Previous research	RT-qPCR		[40]
		45 DLBCL cases 19 DLBCL/BL cases					
DLBCL	FFPE	200 DLBCL cases 11 controls		Previous research	RT-qPCR		[52]
DLBCL	CS	10 DLBCL EBV− cases 11 DLBCL EBV+ cases		Global screening	Sequencing RT-qPCR	NS	[53]
DLBCL	FFPE	58 DLBCL cases 7 controls		Global screening	RT-qPCR		[36]
		58 DLBCL cases 46 FL cases				NS	
DLBCL	Ocular fluid	17 retinal DLBCL cases 12 uveitis cases		Global screening	RT-qPCR	↓	[54]
BL	CS	6 BL DLBCL (cell line)		Previous research	RT-qPCR	↓	[55]

Table 2: Continued.

Disease	Sample type	Cohort		Initial miRNA selection	Method	Expression	Ref
BL	FFPE CS	3 BL cases 2 controls		Previous research	Northern blot	↓	[56]
BL	CS	11 BL cases 11 controls		Previous research	RT-qPCR	↓	[57]
BL	CS	12 BL cases 135 other L		Global screening	Microarray	↓	[38]
HL	FFPE	42 HL cases 8 controls		Global screening	Microarray RT-qPCR	NS NS	[58]
HL	CS	25 HL cases 7 controls		Previous research	RT-qPCR		[50]
HL	CS, FFPE	5 HL cases 5 controls		Previous research	RT-qPCR	NS	[48]
MALT	CS	22 MALT cases 46 controls		Previous research	RT-qPCR		[59]
MALT	CS	4 MALT cases 4 controls*	T	Global screening	Microarray		[60]
		14 MALT cases 14 controls*	V		RT-qPCR		
MALT	CS	3 MALT cases 3 controls*	T	Global screening	Microarray		[61]
		20 MALT cases 20 controls*	V		RT-qPCR		
FL	BM	5 FL cases 3 controls		Previous research	RT-qPCR	NS	[62]
SMZL	FFPE	15 SMZL cases 11 controls		Global screening	RT-qPCR		[63]
SMZL	CS	31 SMZL cases 15 controls	T	Global screening	Microarray		[64]
	FFPE	77 SMZL cases 6 controls	V		RT-qPCR		
SMZL	CS FFPE	15 SMZL cases 9 controls		Global screening	Microarray RT-qPCR		[65]
CLL	CS	70 CLL cases 18 controls		Previous research	RT-qPCR		[66]
CLL	Blood	6 CLL cases 3 controls		Global screening	Microarray		[67]
CLL	Blood	7 CLL cases 4 controls		Previous research	Northern blot		[68]
CLL	Blood	69 CLL cases 15 controls		Global screening	Nanostring RT-qPCR		[69]
CLL	Blood	113 CLL cases 7 controls		Previous research	RT-qPCR		[70]
CLL	Blood	50 CLL cases 14 controls		Global screening	Microarray RT-qPCR		[71]
CLL	Blood	38 CLL cases 9 controls		Global screening	Microarray		[72]
CLL	Blood	56 CLL cases 7 controls		Previous research	RT-qPCR		[73]

Table 2: Continued.

Disease	Sample type	Cohort		Initial miRNA selection	Method	Expression	Ref
CLL	Blood	70 CLL cases 8 controls	T	Previous research	RT-qPCR		[74]
		23 CLL cases 12 controls	V		RT-qPCR		

Disease: DLBCL, diffuse large B-cell lymphoma; BL, Burkitt's lymphoma; HL, Hodgkin lymphoma; MALT, mucosa-associated lymphoid tissue; FL, follicular lymphoma; SMZL, splenic marginal zone lymphoma; CLL, chronic lymphocytic leukemia. *Sample type*: FFPE, formalin-fixed paraffin-embedded tissue samples; CS, clinical samples; FNABs, fine needle aspirations. *Cohort*: controls, nonmalignant tissues; PCNSL, primary CNS lymphoma; nDLBCL, nodal DLBCL; exN DLBCL, extranodal DLBCL; EBV, Epstein-Barr virus; L, lymphoma; control*, adjacent normal tissue, T; training set; V, validation set. *Method*: RT-qPCR, reverse transcription quantitative PCR; RNA-ISH, RNA *in situ* hybridization. *Expression*: ↑, increased; ↓, decreased; NS, not significant. *Ref*: reference.

studied. Hence, the following report will primarily focus on DLBCL and CLL, as the biomarker potential of miR-155 has been reported more extensively in these malignancies. Malignancies represented by few conflicting studies are not discussed further in the review.

3.1. Diffuse Large B-Cell Lymphoma. DLBCL is a highly aggressive disease representing a clinically, morphologically, and genetically heterogeneous group of non-Hodgkin lymphomas. Despite the treatment improvements by inclusion of rituximab, up to 40% of the patients eventually die from relapsing or refractory disease [30, 31]. In general, detection of precancerous lesions and early stage cancers is crucial to reducing the disease mortality. Early detection of DLBCL may likewise permit treatment of early stages, which can prevent disease-related deaths. Thus, it is necessary to identify new diagnostic biomarkers for clinical use. Through the systematic search, we found 18 studies focusing on the expression of miR-155 as a diagnostic marker in DLBCL, presented in Table 2. All studies comparing the expression level in DLBCL patients to healthy controls found a significant upregulation of miR-155 in DLBCL. The mean fold-change values span from 3 to 19 [32–36] and Fang et al. reported a cutoff value of 0.0022 and a sensitivity and specificity at 83% and 65%, respectively [37]. Distinction between non-Hodgkin lymphomas, such as DLBCL, FL, and BL, can be difficult due to great molecular and clinical heterogeneity. In addition to the need for early detection, new biomarkers should also improve the accuracy of lymphoma diagnosis and decisions of therapeutics. Three studies found miR-155 higher expressed in DLBCL compared to BL patients illustrating miR-155 as a potential diagnostic biomarker [38–40]. However, studies comparing DLBCL and FL showed no significant differential expression [33, 34, 36]. Blood samples were analyzed in two studies [35, 37] and frozen tumor tissue and FFPE tissue in the remaining.

Using gene-expression profiling, DLBCL can be divided into the two molecular subtypes: germinal center B-cell-like (GCB) and activated B-cell-like (ABC) [41, 42]. The subtypes present different clinical outcome with GCB patients having a 5-year survival rate of 60% compared to 35% for those patients with ABC DLBCL [43]. In order to simplify and make accessible in a routine clinical setting, the molecular subtype identification has been implemented in several centers by the use of immunohistochemical (IHC) analysis resulting in DLBCL subtyping into GCB/non-GCB or GCB/ABC [42, 44, 45]. In this systematic review, we identified 15 articles evaluating the prognostic impact of miR-155, of which 13 studied the correlation between miR-155 and the molecular subtypes (Table 3). miR-155 was upregulated in the ABC subtype in nine studies while the remaining three did not find significant differential expression between the subgroups. Since patients classified as ABC exhibit an adverse prognosis, miR-155 holds the potential as prognostic marker.

Conflicting results were found in studies investigating the association of miR-155 expression and clinical outcome. Zhong et al. stratified patients according to high or low expression of miR-155 with a cutoff value at 3.98 and sensitivity and specificity value at 80% and 58.5%, respectively [32]. High miR-155 expression was significantly associated with adverse prognosis, which was also reported by Iqbal et al. using similar expression level stratification [39]. Zhong et al. further demonstrated that miR-155 and the international prognostic index (IPI) were statistically significant independent prognostic factors [32]. Contradictorily, other studies found that miR-155 expression did not correlate with DLBCL outcome [36, 49, 75]. Surprisingly, Jung and Aguiar observed that high expression of miR-155 was associated with improved prognosis exclusively within the ABC subgroup [75]. Zhong et al. showed predictive potential of miR-155, where patients treated with CHOP (cyclophosphamide, doxorubicin, vincristine, and prednisone) were compared to a cohort of R-CHOP (addition of rituximab) treated patients [32]. Interestingly, high expression of miR-155 improved clinical outcome in patients treated with R-CHOP compared to CHOP. This difference was not seen in patients with low miR-155 expression, suggesting that miR-155 has the potential to guide treatment with rituximab [32]. Additionally, Iqbal et al. reported that high miR-155 expression significantly correlated with R-CHOP treatment failure, suggesting a potential role as predictive biomarker [39]. This finding was supported by *in vitro* studies showing that high miR-155 expression sensitizes cells to synthetic Akt inhibitors, suggesting a novel treatment option for resistant DLBCL patients [39].

3.2. Chronic Lymphocytic Leukemia. CLL is characterized by clonal proliferation of mature B-cells accumulating in the peripheral blood, bone marrow, lymph nodes, and spleen [76]. Despite its prevalence, no cure exists and patients are treated with various chemotherapeutic drugs at the presence of progressive or symptomatic disease [76]. Several studies investigated the expression level of miR-155 in samples from

Table 3: miR-155 as prognostic biomarker in diffuse large B-cell lymphoma (DLBCL), its expression in relation to GCB or nGCB/ABC subtyping, and direct relation to prognosis.

Cohort	Molecular subtype	Sample type	Initial miR selection	Method	Outcome			Ref
					Prognosis	Measure	Molecular subtype	
90 DLBCL (51/39)	21 GCB 69 nGCB	FFPE	Previous research	RT-qPCR	poor	RA, OR	nGCB	[32]
	20 GCB 34 nGCB	FFPE	Global screening	RT-qPCR			nGCB	[46]
	32 GCB 28 nGCB	FFPE	Global screening	Microarray			nGCB	[33]
	9 GCB 12 nGCB	FFPE	Previous research	RT-qPCR			NS	[47]
	85 GCB 34 ABC	CS	Previous research	Microarray			ABC	[89]
	17 GCB 18 ABC	CS, FFPE	Global screening	RT-qPCR			ABC	[34]
	11 GCB 7 ABC	CS, FFPE	Previous research	ISH RT-qPCR			ABC	[48]
	9 GCB 9 nGCB	FFPE	Previous research	ISH Microarray			NS	[90]
	8 GCB 15 nGCB	CS	Previous research	RT-qPCR			NS	[50]
54 DLBCL (27/27)	32 GCB 27 ABC	CS	Global screening	Microarray	poor	EFS	ABC	[39]
	4 GCB 19 ABC	CS	Previous research	RT-qPCR			ABC	[51]
129 DLBCL 24 ABC		CS	Previous research		NS improved	PFS, OS PFS, OS		[75]
53 DLBCL	25 GCB 25 nGCB	FFPE	Previous research	RT-qPCR	NS	EFS, OS	nGCB	[36]
	14 GCB 36 nGCB	FFPE	Previous research	RT-qPCR			NS	[49]
200 DLBCL (121/79)		FFPE	Previous research		NS	PFS, OS		[52]

(/) in column 1: number of patients with high and low miR-155 expression; *numbers* in column 2 indicate how many DLBCL patients included for miR-155 expression evaluation in each molecular subtype; *subtype*: GCB, germinal center B-cell-like; nGCB, non-GCB; ABC, activated B-cell-like. *Sample type*: FFPE, formalin-fixed paraffin-embedded tissue samples; CS, clinical samples. *Method*: RT-qPCR, reverse transcription quantitative PCR; ISH, *in situ* hybridization. *Prognosis*: ↑, increased expression; ↓, decreased expression; NS, not significant. *Outcome measure*: RA, response assessment; OR, overall response; EFS, event-free survival; PFS, progression-free survival; OS, overall survival. *Ref*: reference.

CLL patients as compared to healthy controls, Table 2. Interestingly, none of these studies aimed at establishing new diagnostic tools but focused on elaborating the molecular pathogenesis of the disease or use preliminary diagnostic signatures of deregulated miRNAs to single out potential prognostic biomarkers. In all studies and irrespective of the analytical technique, miR-155 was upregulated in CLL compared to healthy controls. A few studies reported a mean fold-change of miR-155 expression in the range of 2–5, while individual samples showed great varying fold-changes [67, 69–71].

The prognostic potential of miR-155 expression in CLL was studied more extensively and showed varying results, as presented in Table 3. Particularly, favorable factors showed conflicting associations with miR-155 expression. CLL is usually described by many different prognostic factors, such as clinical staging systems (Rai and Binet), somatic hypermutation of the immunoglobulin heavy chain variable region (IgHV), surface CD38 expression, expression of zeta-associated protein 70 (ZAP-70), or chromosomal abnormalities (17p, 13q, 11q, and trisomy 12) [76]. Relating miR-155 expression to the individual prognostic factors revealed no correlation. However, studies often focused on different prognostic factors, making concise comparisons and conclusions impossible. In patients with 17p deletion, the expression of miR-155 was either upregulated or nonsignificantly differentiated between groups [77, 78]. miR-155 was overexpressed in both studies investigating 11q deletions, though patients with trisomy 12 had either downregulated or unaffected expression [66, 77]. ZAP-70 expression was related to the upregulation of

miR-155 in two studies, while there was no association in four other studies [72–74, 79–81]. miR-155 was either downregulated or unaffected in patients with IgHV mutations [68, 71–74, 79–81], while 13q deletions were associated with high, low, and unaffected expression levels [66, 71, 77, 82]. Thus, the studies generally showed no specific correlation between miR-155 expression and favorable (13q deletion and IgHV mutation) or unfavorable (17p, 11q deletion, trisomy 12 and ZAP-70 expression) prognostic factors.

When the elevated expression of miR-155 was directly correlated with survival data, high expression was not consistently associated with poor prognosis. However, studies used different outcome measures, complicating the assessment of the prognostic potential of miR-155. Furthermore, studies failed to report specific treatment regimens and treatment homogeneity of their cohorts. Ferrajoli et al. investigated the survival of CLL patients stratified according to high or low plasma miR-155 expression in two different cohorts [74]. One cohort received treatment with the FCR regimen (fludarabine, cyclophosphamide, and rituximab), while the other cohort received single agent treatment with lenalidomide. High miR-155 expression was in both cohorts associated with poor treatment outcome estimated by clinical response assessment (RA) [74]. According to Lawrie et al. patients relapsing after treatment with fludarabine and rituximab either with or without alemtuzumab showed poor progression-free survival (PFS) when stratified according to high miR-155 expression [66]. It was further shown that monitoring miR-155 expression after treatment with ibrutinib could be an indicator of treatment failure. The expression of miR-155 decreased upon treatment, and patients whose expression rose above baseline during follow-up were prone to experience disease relapse [66].

Predictive biomarker potential of miR-155 has not been directly investigated, yet detection of 17p deletions by miR-155 as a surrogate marker could guide treatment decisions. Today, patients with 17p deletions are treated more aggressively due to poor prognostic results of front-line treatment with FCR [83]. As mentioned above, high miR-155 expression was associated with treatment failure in FCR and lenalidomide treated patients, suggesting potential use of miR-155 as a predictive biomarker [74].

3.3. Mucosa-Associated Lymphoid Tissue (MALT). Extranodal marginal zone lymphomas (MALT lymphomas) are rare, low-grade B-cell lymphomas of mucosa-associated lymphoid tissue. Expression of miR-155 in MALT was found elevated in three out of three eligible studies [59–61]. Thorns et al. reported a stepwise increase in miR-155 expression from benign to malignant lymphoepithelial lesions [59]. Gastric MALT can be associated with chronic inflammation triggered by infection with *Helicobacter pylori* (*H. pylori*). Antibiotic treatment leads to complete remission in 60–80% of the patients; however improved identification of nonresponsive patients is needed to guide treatment [84]. The study by Saito et al. observed that resistant patients had a higher miR-155 level than cases showing complete remission, suggesting the potential of miR-155 as a predictive indicator [61].

3.4. Splenic Marginal Zone Lymphoma (SMZL). SMZL is a rare form of small B-cell malignancy infiltrating the spleen, bone marrow, and peripheral blood. Three studies reported increased expression of miR-155 in diseased samples compared to controls [63–65]. Peveling-Oberhag et al. found a fold-change of miR-155 of 2.8 [63]. Additionally, Arribas et al. showed significantly increased miR-155 expression in SMZL spleen samples compared to nonmalignant samples from reactive spleens [64]. In contrast, the expression of miR-155 was downregulated in SMZL samples compared to spleens infiltrated by FL, CLL, and mantle cell lymphoma, though this change was not significant [64].

3.5. miR-155 as a Therapeutic Target. Due to the oncogenic function of miR-155 in especially B-cell malignancies, miR-155 holds potential as a target for future therapeutic interventions, exploited by five studies, Figure 1. Chemically modified synthetic oligonucleotides are efficient inhibitors of miRNAs *in vitro* and *in vivo*, improving systemic stability and binding affinity of the anti-miRNA [85, 86]. They bind the miRNA structure by complementary hybridization, preventing the miRNA from binding to its target mRNA. Usually, synthetic oligonucleotides such as PNA (peptide nucleic acid) and LNA (locked nucleic acid) are used. These RNA/DNA analogues are constructed by changing the nucleic acid backbone structures, and studies have proven their efficient inhibition of miR-155 *in vitro* in murine B-cells and patient-derived CLL and Waldenstrom cell lines [85, 86]. Anti-miR-155 exposure resulted in decreased cell proliferation and survival of the CLL and Waldenstrom cells [85]. Evaluation of the systemic stability and efficacy was investigated in wild type mice and Waldenstrom xenografts [85, 86]. miR-155 expression was completely inhibited in the spleen upon injection of PNA anti-miR-155 in wild type mice [86]. Zhang et al. examined the distribution and intracellular uptake of fluorescence marked LNA anti-miR-155 in hematopoietic organs in wild type mice and Waldenstrom xenografts [85]. The anti-miR-155 was successfully delivered to cells in these specific organs. Additionally, anti-miR-155 intravenous administration resulted in decreased tumor burden in the Waldenstrom xenografts [85].

Drawbacks of systemic delivery are related to biological stability in the organism and intracellular uptake of the anti-miR. Babar et al. exploited the use of a nanoparticle-based delivery system of anti-miR-155 in a transgenic mouse model overexpressing miR-155 [20]. The nanoparticle encapsulated the anti-miR-155 structure to aid its stability and delivery. Additionally, coating of the nanoparticle with cell-penetrating peptides improved the intracellular uptake of anti-miR-155 *in vivo* [20].

In order to use anti-miR-155 as therapeutics, challenges regarding nonspecific organ distribution have to be overcome. miR-155 is constitutively expressed in several tissues and has a crucial role in the function of the immune system [16, 17]. Thus, tumor specific distribution is warranted to avoid disruption of normal immunologic function, causing critical side effects. Cheng et al. showed a novel model for tumor specific distribution, utilizing tumor environment

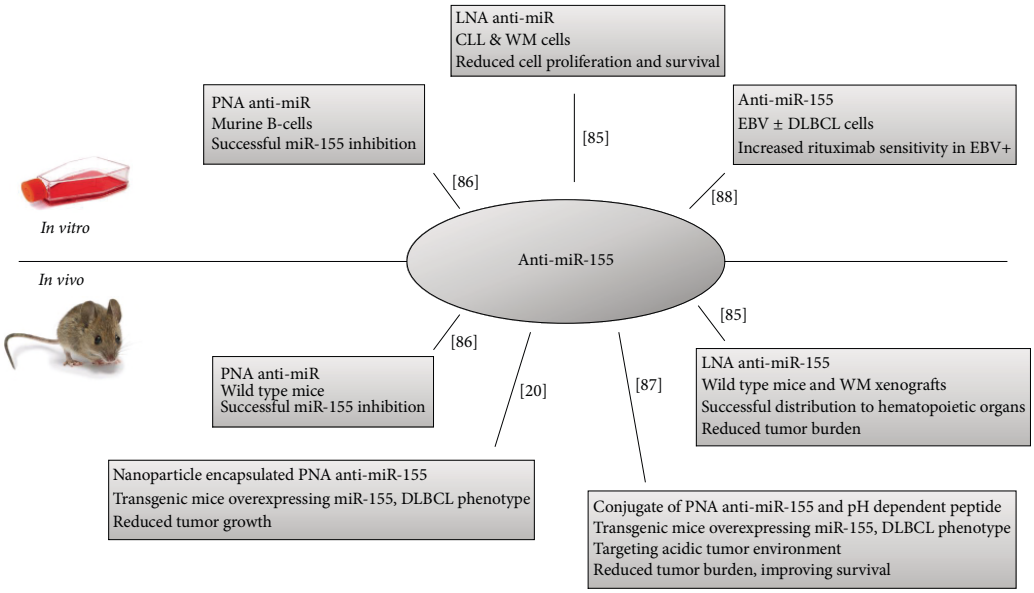

Figure 1: Studies ($n = 5$) exploiting miR-155 as a therapeutic target using anti-miR-155 structures. PNA, peptide nucleic acid; LNA, locked nucleic acid; CLL, chronic lymphocytic leukemia; WM, Waldenstrom macroglobulinemia; DLBCL, diffuse large B-cell lymphoma; EBV+, Epstein-Barr virus positive; EBV−, Epstein-Barr virus negative.

acidity, a hallmark of cancer [87]. They developed a conjugate of the anti-miR-155 structure and a pH-induced transmembrane structure peptide. The peptide has the ability to localize the acidic tumor microenvironment and at low pH, the peptide forms an inducible transmembrane helix promoting translocation of impermeable molecules across the cell membrane. Hereby the anti-miR-155 is efficiently delivered into the tumor cells causing reduced cell viability. Using the same miR-155 overexpressing transgene mice as Babar et al., the mice spontaneously developed lymphoma progressing from follicular hyperplasia to DLBCL. Administration of the anti-miR-155 conjugate at the time of tumor manifestation resulted in reduced tumor volume, suppressed metastatic spread of neoplastic cells, and improved survival compared to controls. High-dose administration to healthy mice showed absence of systemic toxicity, including maintenance of normal liver and kidney function [87]. Thus, this study introduces a novel model for using anti-miR as anticancer drug, having great impact on both targeted drug delivery and personalized medicine, since individual miR-155 expression levels are easily measured.

As mentioned, resistance to therapy is observed in 40% of patients with DLBCL and consequently, novel treatment options for resistant patients are needed [31]. Iqbal et al. reported treatment failure of R-CHOP in patients with high miR-155 expression and suggested Akt inhibitors as alternative therapeutics, since miR-155 activates this specific pathway [39]. The effect of Akt inhibitors was investigated in Epstein-Barr virus positive (EBV+) cell lines by Kim et al. [88]. Initially they found EBV+ cell lines to be resistant toward rituximab, having a phosphorylated Akt pathway, and simultaneous overexpression of miR-155. Akt inhibitors restored the sensitivity toward rituximab, and anti-miR-155 significantly reduced the cell survival upon rituximab exposure [88]. Thus, both Akt inhibitors and anti-miR-155 hold potential as add-on drugs to increase the response of DLBCL patients treated with R-CHOP.

3.6. Targets of miR-155. To understand how miR-155 act and identify the underlying molecular mechanisms driving tumorigenesis, many studies have investigated the target genes, of which some are listed in Table 1. Identification of targets and the involved pathways is important since it puts the biomarker into molecular perspective and additionally is crucial to understanding of the underlying molecular effects of using anti-miR-155 as an antineoplastic drug.

miR-155 was reported to target *SHIP1* and *C/EBPβ*, which are two important inhibitors of the IL-6 signaling pathway. Downregulation of these genes blocks B-cell differentiation and causes an improved cell survival due to activation of PI3K/Akt and MAPK pathway [22, 23]. Additionally, by targeting *HGAL*, a lymphocyte motility inhibitor, miR-155 promotes cell migration, which could contribute to a more aggressive disease [26]. Overexpression of miR-155 also leads to downregulation of *SMAD5*, a modulator of TGF-β signaling. miR-155 overexpression renders DLBCL cells resistant to growth inhibitory effects of TGF-β and BMP via defective p21 induction and impaired cell cycle arrest [27].

Table 4: miR-155 as prognostic biomarker in CLL, its expression in relation to established prognostic factors, and direct relation to prognosis.

Cohort CLL		Sample type	Initial miR selection	Method	Outcome*				Ref
					Unfavorable factors	Favorable factors	Prognosis	Measure	
70		CS	Previous research	RT-qPCR					[66]
109 (56/53)		CS	Previous research	nCounter	↑	↓	↑ poor	OS PFS	[79]
9 (4/5)		Blood					poor	Relapse	
8 (4/4)		Blood	Previous research	Northern blot		NS			[68]
43 (18/25)		Blood	Previous research	RT-qPCR	NS	NS			[70]
70	T	Blood	Global screening	Microarray					[91]
24	V			RT-qPCR					
70 (33/37)		FFPE Blood	Previous research	RT-qPCR	NS	NS			[80]
50		Blood	Global screening	Microarray	NS	NS			[71]
143		Blood	Previous research	RT-qPCR	NS	NS	poor	RA OS	[74]
85 (31/45)							poor	RA	
86 (55/31)	T	Blood	Previous research	RT-qPCR	↑	↓	↑ poor	TFS	[81]
181 (95/86)	V			Microarray	↑	↓	↑ poor	TFS	
94	T	CS	Global screening	Microarray			poor	TIT	[92]
50	V								
61	T	CS	Global screening	Microarray	↑	↓			[77]
29	V			RT-qPCR	↑	↓			
104 (64/40)		Blood	Previous research	RT-qPCR			NS	OS PFS	[78]
56		Blood	Previous research	RT-qPCR	NS	NS			[73]
28		Blood	Global screening	Microarray	NS	NS	NS	TIT	[72]

Cohort: T, training set; V, validation set. *Sample type*: CS, clinical sample; FFPE, formalin-fixed paraffin-embedded tissue samples. *Method*: RT-qPCR, reverse transcription quantitative PCR. *Outcome*: * unfavorable factors: 17p deletion, 11q deletion, trisomy 12, $CD38^+$ cells, ZAP-70 expression > 20%, and/or advanced disease stage determined by either Rai or Binet. Favorable factors: normal karyotype, IgHV mutations, and/or 13q deletion [76]; ↑, increased expression; ↓, decreased expression; NS, not significant. *Outcome measure*: OS, overall survival; PFS, progression-free survival; RA, response assessment; TFS, treatment-free survival; TI, time to initial treatment. *Ref*: reference.

The two death domain containing genes *FADD* and *Ripk1* are also identified as target genes of miR-155. It is thus reasonable to assume that miR-155 targeting of these transcripts could lead to antiapoptotic effects [28].

4. Discussion

This review identified a total of 53 studies addressing the potential of miR-155 as putative biomarker or as a therapeutic target in B-cell malignancies. The results, presented in Tables 2, 3, and 4, display that miR-155 expression may function as a valuable tool in both diagnosis and prognostic evaluation of DLBCL patients and having prognostic impact in CLL as the results showed consistency across multiple studies. Few studies reported diagnostic potential of miR-155 expression in MALT, SMZL, FL, and HL. However, based on the limited number of studies and samples included in those, the significance needs reconfirmation in independent studies using larger cohorts.

The results of miR-155 as diagnostic marker of DLBCL were very consistent and independent of sample type, cohort size, and methodology. High expression of miR-155 enables stratification of DLBCL patients from healthy controls and BL patients, supporting its potential as a diagnostic tool. In contrast, lack of accuracy in differentiating DLBCL from FL patients was observed. This systematic review also presents evidence that miR-155 expression is associated with DLBCL molecular subtypes, even though some studies did not find

a significant differential expression [47, 49, 50, 90]. Cohort sizes varied considerably across studies and generally the larger the cohort, the more valid the result. Studies reporting nonsignificant results stand out with small cohorts exemplified by Fischer et al. having 21 patients included compared to the cohort of 90 in the study by Zhong et al. [32, 47]. Another important matter that makes the studies less comparable is the fact that the subtype classification of the DLBCL patients into GCB and non-GCB/ABC is performed by IHC analysis using different staining strategies and interpretation algorithms. Additionally, IHC is difficult to standardize due to variation between laboratories, such as sample handling, antibodies utilized, and observers.

The most surprising observation was made by Jung and Aguiar, finding miR-155 overexpression association with improved outcome in ABC DLBCL [75]. The reason for this association is not immediately clear; however, they suggest that action of target genes contributes to the findings. Noteworthily, only 24 ABC patients are stratified into low or high miR-155 expression illustrating the need to expand and validate the data in order to trust the information [75].

miR-155 was significantly upregulated in all studies comparing CLL cases to healthy controls, indicating diagnostic potential. However, CLL is easily diagnosed in clinical cases from blood analysis, arguing against the need of a novel diagnostic biomarker for this disease [83]. miR-155 as prognostic marker in CLL is not unambitious. However, an association of miR-155 expression and favorable prognostic factors differed greatly between studies. This could be due to the individual different factors investigated such as specific deletions and mutations. Noteworthily, studies failed to report the specific treatment regimens giving potential bias because the prognosis is dependent on the effectiveness of the treatment. In addition, if patients did not receive the same treatment, the studies are less comparable. In general, high miR-155 expression was often associated with more aggressive disease and poor prognosis, though not significant across all studies. Ultimately, miR-155 expression was not consistently sufficient in stratifying CLL patients according to individual prognostic factors. In contrast, elevated miR-155 expression as an independent factor was associated with poor clinical outcome across studies, suggesting its potential as a direct prognostic biomarker in CLL.

Considering the fact that miR-155 is an oncomiR [11], the findings of high expression in the poor prognostic ABC subtype and the adverse prognostic impact of miR-155 expression on survival in DLBCL are consistent and in accordance with the observed association of high expression and more aggressive disease in CLL.

When analyzing the findings, it is also important to consider differences in methodology. Initial global microarray screenings were performed in several studies; however, they were not based on the same microarray models giving variations in the miRNA covering probes. The other widely used method is RT-qPCR which is based on another technique and relies on probes other than those used in microarray detection. The fold-change and accuracy of the studies therefore cannot be directly compared across studies but concordance of upregulated miR-155 and pure outcome independent of platform supports the robustness of the association. In several studies, a training cohort is utilized to identify miR-155 as potential diagnostic or prognostic tool and subsequently a validation cohort is analyzed to test and validate the result, increasing the significance of the findings. Others exploit the same cohort but validate the result using a different detection technique. Both approaches strengthen the observations and make the findings more valid.

Different sample types have potential to cause conflicting results. Studies regarding diagnostic evaluation of miR-155 in DLBCL analyze blood samples, formalin-fixed/paraffin-embedded tissues, and frozen tissues; however, no inconsistency is observed, indicating stable expression and robust detection of miR-155 despite sample types, preparation, and storage. Each sample type has different advantages. FFPE tissue samples are the most abundant available archival material and miRNA can successfully be isolated from processed formalin-fixed material, due to miRNAs relative resistance toward RNase degradation. Using RT-qPCR and microarray analysis, similar results of miRNA expression are found in FFPE and frozen material [93]. Lawrie et al. and Fang et al. studied miR-155 expression in blood samples to investigate the potential as noninvasive biomarker [35, 37]. Search for noninvasive biomarkers for diagnosis, prognosis, and monitoring of cancers has long been the goal of clinical research.

A guideline for Strengthening the Reporting of Observational studies in Epidemiology-Molecular Epidemiology (STROBE-ME) has been proposed, though several studies included in this review failed to report their investigations thoroughly (e.g., sample types, storage, and handling). Additionally, the studies included in this review differed in their aims, outcomes measures, and methods, complicating the general comparison of the studies and rendering a statistical meta-analysis impossible. The validity of this systematic review is improved by the fact that PRISMA guidelines are met and that the search strategy encompassed MESH/ENTRY terms and free text words.

Introducing new potential biomarkers into the clinic holds great difficulties and challenges. Therefore, the Early Detection Research Network (EDRN) has suggested a systematic approach guiding the process of biomarker development similar to the clinical stages of drug development [94]. Phase 1 includes preclinical investigations, where tumor tissue is compared to healthy controls in order to identify differential characteristics. A clinical biomarker assay is developed and tested in phase 2, including evaluation of the biomarkers ability to distinguish subjects with cancer from those without cancer. Phase 3 is a retrospective investigation of the biomarkers ability to detect presence of disease before it is clinically diagnosed, whereas phase 4 evaluates biomarker properties in a prospective follow-up study. Finally, phase 5 evaluates whether the biomarker and early diagnosis improved the overall benefit for the screened population. Although the guideline focuses on developing diagnostic biomarkers, the structure is potentially valuable for prognostic and predictive biomarkers as well. All included diagnostic studies of CLL were consistent with phase 1 investigations, though as mentioned before a new diagnostic

biomarker of CLL would hold limited clinical use. In addition, prognostic investigations of miR-155 in CLL could be described as phase 1 investigations, where a biomarker assay and assessment are still missing. Studies reporting miR-155 as potential diagnostic biomarker of DLBCL are all on the early phases of diagnostic biomarker development as well, which is why clinical implementation will require further studies at higher developmental phases. Only Fang et al. reported evaluation of miR-155's ability to distinguish DLBCL patients from healthy controls [37]. Thus, miR-155 cannot be considered as a diagnostic biomarker in clinical use at short term.

In order to implement the concept of personalized medicine, new molecular biomarkers need to be established to improve early diagnosis, patient stratification according to high-risk patients, and predictions of treatment response. According to the present assessment, miR-155 could hold potential as a novel diagnostic biomarker in several B-cell malignancies, including DLBCL and CLL. However, miR-155 still needs to move through the remaining biomarker developmental steps and evaluations before its potential use can be fully exploited. However, one important disadvantage of miR-155 as a diagnostic biomarker is that it is overexpressed not only in one specific malignancy but also in several, complicating diagnostic discriminations of the different malignancies. Noteworthily, an important advantage is the validated target genes of miR-155, which puts the biomarker into perspectives of molecular pathways.

Elevated miR-155 expression was generally associated with poor survival in both CLL and DLBCL, showing independent prognostic impact, though as a marker for the present prognostic tools (e.g., chromosomal subtyping and ABC/GCB) it did not add further information. In general, prognostic biomarkers only hold beneficial information, if nonresponsive patients can be treated differently. The biomarker then moves from prognostic to predictive, where it can be used to guide treatment choices. No thorough investigations have been reported of miR-155 as a predictive biomarker, though its prognostic observations could imply the need for new treatment options for patients with a high expression level. Akt inhibitors (currently in clinical trials [95]) have been suggested as efficient therapeutics for the treatment of patients with high miR-155 expression, since miR-155 activates this pathway. Logically, other novel treatments could evidently be anti-miRNAs suppressing the miR-155 expression and its oncogenic function. Their effect has been proved both *in vitro* and *in vivo*, and a targeted distribution model strengthens the potential as a novel therapeutic. At the present time, new clinical phase I trial of cutaneous T cell lymphoma (CTCL) investigates the safety and tolerability of anti-miR-155 (MRG-106) [96]. Presumably, this treatment might show interesting potential in DLBCL and CLL patients as well. Noteworthily, miravirsen, anti-miR-122, was the first microRNA targeted drug ever to reach clinical trials in 2009, for the management of hepatitis C viral infection [97]. Interestingly, miR-122 was later shown to be overexpressed in CTCL, suggesting that inhibition of miR-122 might also be a promising strategy in improving treatment outcome in these patients [98].

5. Conclusion

In summary, the expression of miR-155 shows potential as a diagnostic and prognostic biomarker, though further studies are warranted to assess its use in treatment prediction. Interestingly elevated expression was generally associated with poor treatment response, which is why it has been investigated and evidenced as an efficient therapeutic target. These properties prove that miR-155 has the potential to be a molecular tool in personalized medicine, bringing us one step closer to improvements of diagnosis and treatment.

Disclosure

Hanne Due and Pernille Svendsen shared first authorship.

Competing Interests

The authors declare that they have no competing interests.

Authors' Contributions

Hanne Due and Pernille Svendsen contributed equally to this paper.

Acknowledgments

The authors would like to extend their gratitude to the Medical Library at Aalborg University Hospital, Denmark, for assistance in the search process, and the Medical Specialist, Heinrich Kopp's Grant, who provided funding for the project.

References

[1] E. Campo, S. H. Swerdlow, N. L. Harris, S. Pileri, H. Stein, and E. S. Jaffe, "The 2008 WHO classification of lymphoid neoplasms and beyond: evolving concepts and practical applications," *Blood*, vol. 117, no. 19, pp. 5019–5032, 2011.

[2] National Research Council (US) Committee on a Framework for Developing a New Taxonomy of Disease, *Toward Precision Medicine: Building a Knowledge Network for Biomedical Research and a New Taxonomy of Disease*, National Academies Press (US), Washington, DC, USA, 2011.

[3] Biomarkers Definitions Working Group, "Biomarkers and surrogate endpoints: preferred definitions and conceptual framework," *Clinical Pharmacology & Therapeutics*, vol. 69, no. 3, pp. 89–95, 2001.

[4] M. S. Pepe, H. Janes, G. Longton, W. Leisenring, and P. Newcomb, "Limitations of the odds ratio in gauging the performance of a diagnostic, prognostic, or screening marker," *American Journal of Epidemiology*, vol. 159, no. 9, pp. 882–890, 2004.

[5] H. Lan, H. Lu, X. Wang, and H. Jin, "MicroRNAs as potential biomarkers in cancer: opportunities and challenges," *BioMed Research International*, vol. 2015, Article ID 125094, 17 pages, 2015.

[6] J. Xu, Z. Cao, W. Liu et al., "Plasma miRNAs effectively distinguish patients with pancreatic cancer from controls: a multicenter study," *Annals of Surgery*, 2015.

[7] H. Ding, Z. Huang, M. Chen et al., "Identification of a panel of five serum miRNAs as a biomarker for Parkinson's disease," *Parkinsonism & Related Disorders*, vol. 22, pp. 68–73, 2015.

[8] S. C. Marques, M. B. Laursen, J. S. Bødker et al., "MicroRNAs in B-cells: from normal differentiation to treatment of malignancies," *Oncotarget*, vol. 6, no. 1, pp. 7–25, 2015.

[9] L. K. Jørgensen, M. Ø. Poulsen, M. B. Laursen et al., "MicroRNAs as novel biomarkers in diffuse large B-Cell lymphoma—a systematic review," *Danish Medical Journal*, vol. 62, no. 5, Article ID A5048, 2015.

[10] M. D. Jansson and A. H. Lund, "MicroRNA and cancer," *Molecular Oncology*, vol. 6, no. 6, pp. 590–610, 2012.

[11] H. Xue, L.-M. Hua, M. Guo, and J.-M. Luo, "SHIP1 is targeted by miR-155 in acute myeloid leukemia," *Oncology Reports*, vol. 32, no. 5, pp. 2253–2259, 2014.

[12] L. Huang, J. Luo, Q. Cai et al., "MicroRNA-125b suppresses the development of bladder cancer by targeting E2F3," *International Journal of Cancer*, vol. 128, no. 8, pp. 1758–1769, 2011.

[13] R. Mashima, "Physiological roles of miR-155," *Immunology*, vol. 145, no. 3, pp. 323–333, 2015.

[14] K. Musilova and M. Mraz, "MicroRNAs in B-cell lymphomas: how a complex biology gets more complex," *Leukemia*, vol. 29, no. 5, pp. 1004–1017, 2015.

[15] R. W. Georgantas III, R. Hildreth, S. Morisot et al., "CD34+ hematopoietic stem-progenitor cell microRNA expression and function: a circuit diagram of differentiation control," *Proceedings of the National Academy of Sciences of the United States of America*, vol. 104, no. 8, pp. 2750–2755, 2007.

[16] R. M. O'Connell, K. D. Taganov, M. P. Boldin, G. Cheng, and D. Baltimore, "MicroRNA-155 is induced during the macrophage inflammatory response," *Proceedings of the National Academy of Sciences of the United States of America*, vol. 104, no. 5, pp. 1604–1609, 2007.

[17] M. Ceppi, A. M. Pereira, I. Dunand-Sauthier et al., "MicroRNA-155 modulates the interleukin-1 signaling pathway in activated human monocyte-derived dendritic cells," *Proceedings of the National Academy of Sciences of the United States of America*, vol. 106, no. 8, pp. 2735–2740, 2009.

[18] T.-H. Thai, D. P. Calado, S. Casola et al., "Regulation of the germinal center response by MicroRNA-155," *Science*, vol. 316, no. 5824, pp. 604–608, 2007.

[19] W. Zhang, J. He, F. Zhang et al., "Prognostic role of microRNA-155 in various carcinomas: results from a meta-analysis," *Disease Markers*, vol. 34, no. 6, pp. 379–386, 2013.

[20] I. A. Babar, C. J. Cheng, C. J. Booth et al., "Nanoparticle-based therapy in an in vivo microRNA-155 (miR-155)-dependent mouse model of lymphoma," *Proceedings of the National Academy of Sciences of the United States of America*, vol. 109, no. 26, pp. E1695–E1704, 2012.

[21] A. Liberati, D. G. Altman, J. Tetzlaff et al., "The PRISMA statement for reporting systematic reviews and meta-analyses of studies that evaluate health care interventions: explanation and elaboration," *PLoS Medicine*, vol. 6, no. 7, Article ID e1000100, 2009.

[22] R. M. O'Connell, A. A. Chaudhuri, D. S. Rao, and D. Baltimore, "Inositol phosphatase SHIP1 is a primary target of miR-155," *Proceedings of the National Academy of Sciences of the United States of America*, vol. 106, no. 17, pp. 7113–7118, 2009.

[23] S. Costinean, S. K. Sandhu, I. M. Pedersen et al., "Src homology 2 domain-containing inositol-5-phosphatase and CCAAT enhancer-binding protein β are targeted by miR-155 in B cells of Eμ-*MiR*-155 transgenic mice," *Blood*, vol. 114, no. 7, pp. 1374–1382, 2009.

[24] G. Teng, P. Hakimpour, P. Landgraf et al., "MicroRNA-155 is a negative regulator of activation-induced cytidine deaminase," *Immunity*, vol. 28, no. 5, pp. 621–629, 2008.

[25] E. Vigorito, K. L. Perks, C. Abreu-Goodger et al., "microRNA-155 regulates the generation of immunoglobulin class-switched plasma cells," *Immunity*, vol. 27, no. 6, pp. 847–859, 2007.

[26] L. N. Dagan, X. Jiang, S. Bhatt, E. Cubedo, K. Rajewsky, and I. S. Lossos, "miR-155 regulates HGAL expression and increases lymphoma cell motility," *Blood*, vol. 119, no. 2, pp. 513–520, 2012.

[27] D. Rai, S.-W. Kim, M. R. McKeller, P. L. M. Dahia, and R. C. T. Aguiar, "Targeting of SMAD5 links microRNA-155 to the TGF-β pathway and lymphomagenesis," *Proceedings of the National Academy of Sciences of the United States of America*, vol. 107, no. 7, pp. 3111–3116, 2010.

[28] E. Tili, J.-J. Michaille, A. Cimino et al., "Modulation of miR-155 and miR-125b levels following lipopolysaccharide/TNF-α stimulation and their possible roles in regulating the response to endotoxin shock," *The Journal of Immunology*, vol. 179, no. 8, pp. 5082–5089, 2007.

[29] L.-F. Lu, T.-H. Thai, D. P. Calado et al., "Foxp3-dependent microRNA155 confers competitive fitness to regulatory T cells by targeting SOCS1 protein," *Immunity*, vol. 30, no. 1, pp. 80–91, 2009.

[30] L. H. Sehn, J. Donaldson, M. Chhanabhai et al., "Introduction of combined CHOP plus rituximab therapy dramatically improved outcome of diffuse large B-cell lymphoma in British Columbia," *Journal of Clinical Oncology*, vol. 23, no. 22, pp. 5027–5033, 2005.

[31] R. Vaidya and T. E. Witzig, "Prognostic factors for diffuse large B-cell lymphoma in the R(X)CHOP era," *Annals of Oncology*, vol. 25, no. 11, pp. 2124–2133, 2014.

[32] H. Zhong, L. Xu, J.-H. Zhong et al., "Clinical and prognostic significance of miR-155 and miR-146a expression levels in formalin-fixed/paraffin-embedded tissue of patients with diffuse large B-cell lymphoma," *Experimental and Therapeutic Medicine*, vol. 3, no. 5, pp. 763–770, 2012.

[33] C. H. Lawrie, J. Chi, S. Taylor et al., "Expression of microRNAs in diffuse large B cell lymphoma is associated with immunophenotype, survival and transformation from follicular lymphoma," *Journal of Cellular and Molecular Medicine*, vol. 13, no. 7, pp. 1248–1260, 2009.

[34] C. H. Lawrie, S. Soneji, T. Marafioti et al., "MicroRNA expression distinguishes between germinal center B cell-like and activated B cell-like subtypes of diffuse large B cell lymphoma," *International Journal of Cancer*, vol. 121, no. 5, pp. 1156–1161, 2007.

[35] C. H. Lawrie, S. Gal, H. M. Dunlop et al., "Detection of elevated levels of tumour-associated microRNAs in serum of patients with diffuse large B-cell lymphoma," *British Journal of Haematology*, vol. 141, no. 5, pp. 672–675, 2008.

[36] A. Roehle, K. P. Hoefig, D. Repsilber et al., "MicroRNA signatures characterize diffuse large B-cell lymphomas and follicular lymphomas," *British Journal of Haematology*, vol. 142, no. 5, pp. 732–744, 2008.

[37] C. Fang, D.-X. Zhu, H.-J. Dong et al., "Serum microRNAs are promising novel biomarkers for diffuse large B cell lymphoma," *Annals of Hematology*, vol. 91, no. 4, pp. 553–559, 2012.

[38] L. Di Lisio, M. Sánchez-Beato, G. Gómez-López et al., "MicroRNA signatures in B-cell lymphomas," *Blood Cancer Journal*, vol. 2, no. 2, article e57, 2012.

[39] J. Iqbal, Y. Shen, X. Huang et al., "Global microRNA expression profiling uncovers molecular markers for classification and prognosis in aggressive B-cell lymphoma," *Blood*, vol. 125, no. 7, pp. 1137–1145, 2015.

[40] M. Zajdel, G. Rymkiewicz, M. Chechlinska et al., "miR expression in MYC-negative DLBCL/BL with partial trisomy 11 is similar to classical Burkitt lymphoma and different from diffuse large B-cell lymphoma," *Tumor Biology*, vol. 36, no. 7, pp. 5377–5388, 2015.

[41] A. A. Alizadeh, M. B. Elsen, R. E. Davis et al., "Distinct types of diffuse large B-cell lymphoma identified by gene expression profiling," *Nature*, vol. 403, no. 6769, pp. 503–511, 2000.

[42] C. P. Hans, D. D. Weisenburger, T. C. Greiner et al., "Confirmation of the molecular classification of diffuse large B-cell lymphoma by immunohistochemistry using a tissue microarray," *Blood*, vol. 103, no. 1, pp. 275–282, 2004.

[43] A. Rosenwald, G. Wright, W. C. Chan et al., "The use of molecular profiling to predict survival after chemotherapy for diffuse large-B-cell lymphoma," *The New England Journal of Medicine*, vol. 346, no. 25, pp. 1937–1947, 2002.

[44] W. W. L. Choi, D. D. Weisenburger, T. C. Greiner et al., "A new immunostain algorithm classifies diffuse large B-cell lymphoma into molecular subtypes with high accuracy," *Clinical Cancer Research*, vol. 15, no. 17, pp. 5494–5502, 2009.

[45] J. A. Read, J. L. Koff, L. J. Nastoupil, J. N. Williams, J. B. Cohen, and C. R. Flowers, "Evaluating cell-of-origin subtype methods for predicting diffuse large B-cell lymphoma survival: a meta-analysis of gene expression profiling and immunohistochemistry algorithms," *Clinical Lymphoma, Myeloma and Leukemia*, vol. 14, no. 6, pp. 460.e2–467.e2, 2014.

[46] S. Caramuta, L. Lee, D. M. Özata et al., "Role of microRNAs and microRNA machinery in the pathogenesis of diffuse large B-cell lymphoma," *Blood Cancer Journal*, vol. 3, no. 10, article e152, 2013.

[47] L. Fischer, M. Hummel, A. Korfel, D. Lenze, K. Joehrens, and E. Thiel, "Differential micro-RNA expression in primary CNS and nodal diffuse large B-cell lymphomas," *Neuro-Oncology*, vol. 13, no. 10, pp. 1090–1098, 2011.

[48] J. Kluiver, S. Poppema, D. de Jong et al., "BIC and miR-155 are highly expressed in Hodgkin, primary mediastinal and diffuse large B cell lymphomas," *The Journal of Pathology*, vol. 207, no. 2, pp. 243–249, 2005.

[49] J.-L. Robertus, G. Harms, T. Blokzijl et al., "Specific expression of miR-17-5p and miR-127 in testicular and central nervous system diffuse large B-cell lymphoma," *Modern Pathology*, vol. 22, no. 4, pp. 547–555, 2009.

[50] H. Huskova, K. Korecka, J. Karban et al., "Oncogenic microRNA-155 and its target PU.1: an integrative gene expression study in six of the most prevalent lymphomas," *International Journal of Hematology*, vol. 102, no. 4, pp. 441–450, 2015.

[51] P. S. Eis, W. Tam, L. Sun et al., "Accumulation of miR-155 and BIC RNA in human B cell lymphomas," *Proceedings of the National Academy of Sciences of the United States of America*, vol. 102, no. 10, pp. 3627–3632, 2005.

[52] H. Go, J.-Y. Jang, P.-J. Kim et al., "MicroRNA-21 plays an oncogenic role by targeting FOXO1 and activating the PI3K/AKT pathway in diffuse large B-cell lymphoma," *Oncotarget*, vol. 6, no. 17, pp. 15035–15049, 2015.

[53] J. Imig, N. Motsch, J. Y. Zhu et al., "microRNA profiling in Epstein-Barr virus-associated B-cell lymphoma," *Nucleic Acids Research*, vol. 39, no. 5, pp. 1880–1893, 2011.

[54] J. Tuo, D. Shen, H. H. Yang, and C.-C. Chan, "Distinct MicroRNA-155 expression in the vitreous of patients with primary vitreoretinal lymphoma and uveitis," *American Journal of Ophthalmology*, vol. 157, no. 3, pp. 728–734, 2014.

[55] T. Zhang, K. Nie, and W. Tam, "BIC is processed efficiently to microRNA-155 in Burkitt lymphoma cells," *Leukemia*, vol. 22, no. 9, pp. 1795–1797, 2008.

[56] J. Kluiver, E. Haralambieva, D. De Jong et al., "Lack of BIC and microRNA miR-155 expression in primary cases of Burkitt lymphoma," *Genes Chromosomes and Cancer*, vol. 45, no. 2, pp. 147–153, 2006.

[57] M. Metzler, M. Wilda, K. Busch, S. Viehmann, and A. Borkhardt, "High expression of precursor MicroRNA-155/BIC RNA in children with burkitt lymphoma," *Genes Chromosomes and Cancer*, vol. 39, no. 2, pp. 167–169, 2004.

[58] K. Jones, J. P. Nourse, C. Keane, A. Bhatnagar, and M. K. Gandhi, "Plasma microRNA are disease response biomarkers in classical hodgkin lymphoma," *Clinical Cancer Research*, vol. 20, no. 1, pp. 253–264, 2014.

[59] C. Thorns, J. Kuba, V. Bernard et al., "Deregulation of a distinct set of microRNAs is associated with transformation of gastritis into MALT lymphoma," *Virchows Archiv*, vol. 460, no. 4, pp. 371–377, 2012.

[60] J. Cai, X. Liu, J. Cheng et al., "MicroRNA-200 is commonly repressed in conjunctival MALT lymphoma, and targets cyclin E2," *Graefe's Archive for Clinical and Experimental Ophthalmology*, vol. 250, no. 4, pp. 523–531, 2012.

[61] Y. Saito, H. Suzuki, H. Tsugawa et al., "Overexpression of miR-142-5p and miR-155 in gastric mucosa-associated lymphoid tissue (MALT) lymphoma resistant to *Helicobacter pylori* eradication," *PLoS ONE*, vol. 7, no. 11, Article ID e47396, 2012.

[62] Y. Takei, N. Ohnishi, M. Kisaka, and K. Mihara, "Determination of abnormally expressed microRNAs in bone marrow smears from patients with follicular lymphomas," *SpringerPlus*, vol. 3, article 288, 2014.

[63] J. Peveling-Oberhag, G. Crisman, A. Schmidt et al., "Dysregulation of global microRNA expression in splenic marginal zone lymphoma and influence of chronic hepatitis C virus infection," *Leukemia*, vol. 26, no. 7, pp. 1654–1662, 2012.

[64] A. J. Arribas, C. Gómez-Abad, M. Sánchez-Beato et al., "Splenic marginal zone lymphoma: comprehensive analysis of gene expression and miRNA profiling," *Modern Pathology*, vol. 26, no. 7, pp. 889–901, 2013.

[65] M. Bouteloup, A. Verney, N. Rachinel et al., "MicroRNA expression profile in splenic marginal zone lymphoma," *British Journal of Haematology*, vol. 156, no. 2, pp. 279–281, 2012.

[66] C. H. Lawrie, E. Ballabio, O.-J. Dyar et al., "MicroRNA expression in chronic lymphocytic leukaemia," *British Journal of Haematology*, vol. 147, no. 3, pp. 398–402, 2009.

[67] D.-X. Zhu, W. Zhu, C. Fang et al., "MiR-181a/b significantly enhances drug sensitivity in chronic lymphocytic leukemia cells via targeting multiple anti-apoptosis genes," *Carcinogenesis*, vol. 33, no. 7, pp. 1294–1301, 2012.

[68] S. Marton, M. R. Garcia, C. Robello et al., "Small RNAs analysis in CLL reveals a deregulation of miRNA expression and novel miRNA candidates of putative relevance in CLL pathogenesis," *Leukemia*, vol. 22, no. 2, pp. 330–338, 2008.

[69] Y. Y. Yeh, H. G. Ozer, A. M. Lehman et al., "Characterization of CLL exosomes reveals a distinct microRNA signature and enhanced secretion by activation of BCR signaling," *Blood*, vol. 125, no. 21, pp. 3297–3305, 2015.

[70] K. Vargova, N. Curik, P. Burda et al., "MYB transcriptionally regulates the miR-155 host gene in chronic lymphocytic leukemia," *Blood*, vol. 117, no. 14, pp. 3816–3825, 2011.

[71] C. P. Pallasch, M. Patz, Y. Jung Park et al., "miRNA deregulation by epigenetic silencing disrupts suppression of the oncogene PLAG1 in chronic lymphocytic leukemia," *Blood*, vol. 114, no. 15, pp. 3255–3264, 2009.

[72] S. Li, H. F. Moffett, J. Lu et al., "Microrna expression profiling identifies activated B cell status in chronic lymphocytic leukemia cells," *PLoS ONE*, vol. 6, no. 3, Article ID e16956, 2011.

[73] V. Fulci, S. Chiaretti, M. Goldoni et al., "Quantitative technologies establish a novel microRNA profile of chronic lymphocytic leukemia," *Blood*, vol. 109, no. 11, pp. 4944–4951, 2007.

[74] A. Ferrajoli, T. D. Shanafelt, C. Ivan et al., "Prognostic value of miR-155 in individuals with monoclonal B-cell lymphocytosis and patients with B chronic lymphocytic leukemia," *Blood*, vol. 122, no. 11, pp. 1891–1899, 2013.

[75] I. Jung and R. C. T. Aguiar, "MicroRNA-155 expression and outcome in diffuse large B-cell lymphoma," *British Journal of Haematology*, vol. 144, no. 1, pp. 138–140, 2009.

[76] T. L. Parker and M. P. Strout, "Chronic lymphocytic leukemia: prognostic factors and impact on treatment," *Discovery Medicine*, vol. 11, no. 57, pp. 115–123, 2011.

[77] R. Visone, L. Z. Rassenti, A. Veronese et al., "Karyotype-specific microRNA signature in chronic lymphocytic leukemia," *Blood*, vol. 114, no. 18, pp. 3872–3879, 2009.

[78] S. Rossi, M. Shimizu, E. Barbarotto et al., "MicroRNA fingerprinting of CLL patients with chromosome 17p deletion identify a miR-21 score that stratifies early survival," *Blood*, vol. 116, no. 6, pp. 945–952, 2010.

[79] D. Guinn, A. S. Ruppert, K. Maddocks et al., "miR-155 expression is associated with chemoimmunotherapy outcome and is modulated by Bruton's tyrosine kinase inhibition with Ibrutinib," *Leukemia*, vol. 29, no. 5, pp. 1210–1213, 2015.

[80] M. Wang, L. P. Tan, M. K. Dijkstra et al., "miRNA analysis in B-cell chronic lymphocytic leukaemia: proliferation centres characterized by low miR-150 and high BIC/miR-155 expression," *The Journal of Pathology*, vol. 215, no. 1, pp. 13–20, 2008.

[81] B. Cui, L. Chen, S. Zhang et al., "Micro RNA-155 influences B-cell receptor signaling and associates with aggressive disease in chronic lymphocytic leukemia," *Blood*, vol. 124, no. 4, pp. 546–554, 2014.

[82] A. E. Rodriguez, J. A. Hernandez, M. Hernandez et al., "Chronic lymphocytic leukemia (CLL) with a high number of losses in 13Q is associated with different biological features," *Laboratory Investigation*, vol. 93, article 358A, 2013.

[83] B. Eichhorst, T. Robak, E. Montserrat et al., "Chronic lymphocytic leukaemia: ESMO Clinical Practice Guidelines for diagnosis, treatment and follow-up," *Annals of Oncology*, vol. 26, supplement 5, Article ID mdv303, pp. v50–v54, 2015.

[84] A. Ruskoné-Fourmestraux, A. Lavergne, P. H. Aegerter et al., "Predictive factors for regression of gastric MALT lymphoma after anti-Helicobacter pylori treatment," *Gut*, vol. 48, no. 3, pp. 297–303, 2001.

[85] Y. Zhang, A. M. Roccaro, C. Rombaoa et al., "LNA-mediated anti-miR-155 silencing in low-grade B-cell lymphomas," *Blood*, vol. 120, no. 8, pp. 1678–1686, 2012.

[86] M. M. Fabani, C. Abreu-Goodger, D. Williams et al., "Efficient inhibition of miR-155 function in vivo by peptide nucleic acids," *Nucleic Acids Research*, vol. 38, no. 13, pp. 4466–4475, 2010.

[87] C. J. Cheng, R. Bahal, I. A. Babar et al., "MicroRNA silencing for cancer therapy targeted to the tumour microenvironment," *Nature*, vol. 518, no. 7537, pp. 107–110, 2015.

[88] J. H. Kim, W. S. Kim, and C. Park, "Epstein-Barr virus latent membrane protein-1 protects B-cell lymphoma from rituximab-induced apoptosis through miR-155-mediated Akt activation and up-regulation of Mcl-1," *Leukemia and Lymphoma*, vol. 53, no. 8, pp. 1586–1591, 2012.

[89] D. Rai, S. Karanti, I. Jung, P. L. M. Dahia, and R. C. T. Aguiar, "Coordinated expression of microRNA-155 and predicted target genes in diffuse large B-cell lymphoma," *Cancer Genetics and Cytogenetics*, vol. 181, no. 1, pp. 8–15, 2008.

[90] H. D. Munch-Petersen, U. Ralfkiaer, L. D. Sjö et al., "Differential expression of miR-155 and miR-21 in tumor and stroma cells in diffuse large B-Cell lymphoma," *Applied Immunohistochemistry and Molecular Morphology*, vol. 23, no. 3, pp. 188–195, 2015.

[91] A. E. Rodríguez, J. Á. Hernández, R. Benito et al., "Molecular characterization of chronic lymphocytic leukemia patients with a high number of losses in 13q14," *PLoS ONE*, vol. 7, no. 11, Article ID e48485, 2012.

[92] G. A. Calin, M. Ferracin, A. Cimmino et al., "A microRNA signature associated with prognosis and progression in chronic lymphocytic leukemia," *The New England Journal of Medicine*, vol. 353, no. 17, pp. 1793–1801, 2005.

[93] J. Li, P. Smyth, R. Flavin et al., "Comparison of miRNA expression patterns using total RNA extracted from matched samples of formalin-fixed paraffin-embedded (FFPE) cells and snap frozen cells," *BMC Biotechnology*, vol. 7, article 36, 2007.

[94] M. S. Pepe, R. Etzioni, Z. Feng et al., "Phases of biomarker development for early detection of cancer," *Journal of the National Cancer Institute*, vol. 93, no. 14, pp. 1054–1061, 2001.

[95] National Library of Medicine (US), "Trametinib and Akt inhibitor GSK2141795 in treating patients with acute myeloid leukemia," ClinicalTrials.gov, National Library of Medicine (US), Bethesda, Md, USA, 2015.

[96] miRagen Therapeutics, "Safety, tolerability and pharmacokinetic study of MRG-106 in patients with cutaneous T cell lymphoma (CTCL), MF subtype," in *ClinicalTrials.gov*, National Library of Medicine (US), Bethesda, Md, USA, 2015.

[97] E. S. Hildebrandt-Eriksen, Y. Z. Bagger, T. B. Knudsen et al., "A unique therapy for HCV inhibits microRNA-122 in humans and results in HCV RNA suppression in chronically infected chimpanzees: results from primate and first-in-human studies," *Hepatology*, vol. 50, no. 6, p. LB19, 2009.

[98] V. Manfè, E. Biskup, A. Rosbjerg et al., "MiR-122 regulates p53/Akt signalling and the chemotherapy-induced apoptosis in cutaneous T-cell lymphoma," *PLoS ONE*, vol. 7, no. 1, Article ID e29541, 2012.

Supplementary

Table S1. Search strategy in PubMed and EMBASE

Database	PubMed	EMBASE
Search Terms	#1: "Lymphoma"[Mesh] #2: lymphoma* #3: "b-lymphocytes"[MeSH Terms] OR "b-lymphocytes" OR "B-cell" #4: "Lymphoma, B-Cell"[Mesh] #5: burkitt[tw] #6: #1 OR #2 OR #3 OR #4 OR #5 #7: rno-miR-155 OR rno miR 155 OR rno-miR 155 5p OR rno-miR-155-5p #8: mmu-mir-155 OR mmu mir 155 OR Mir155 #9: miR 155 OR miRNA 155 OR hsa mir 155 OR microRNA 155 #10: miR-155 OR miRNA 155 OR hsa-mir-155 OR microRNA-155 #11: "MIRN155 microRNA, human"[Supplementary Concept] OR "MIRN155 microRNA, rat"[Supplementary Concept] OR "Mirn155 microRNA, mouse"[Supplementary Concept] #12: #7 OR #8 OR #9 OR #10 OR #11 #13: #6 OR #12 No filters	#1: microRNA 155/ #2: (rno-miR-155 or rno miR 155 or rno-miR 155 5p or rno-miR-155-5p or mmu-mir-155 or mmu mir 155 or Mir155 or miR 155 or miRNA 155 or hsa mir 155 or microRNA 155 or miR-155 or miRNA 155 or hsa-mir-155 or microRNA-155).mp. #3: #1 or #2 #4: exp B lymphocyte/ #5: B-cell lymphoma/ #6: (b-lymphocytes or B-cell).mp. #7: exp lymphoma/ #8: lymphoma*.mp. #9: or/#4-8 #10: #3 and #9 No filters

Figure S1. Flow diagram of study selection

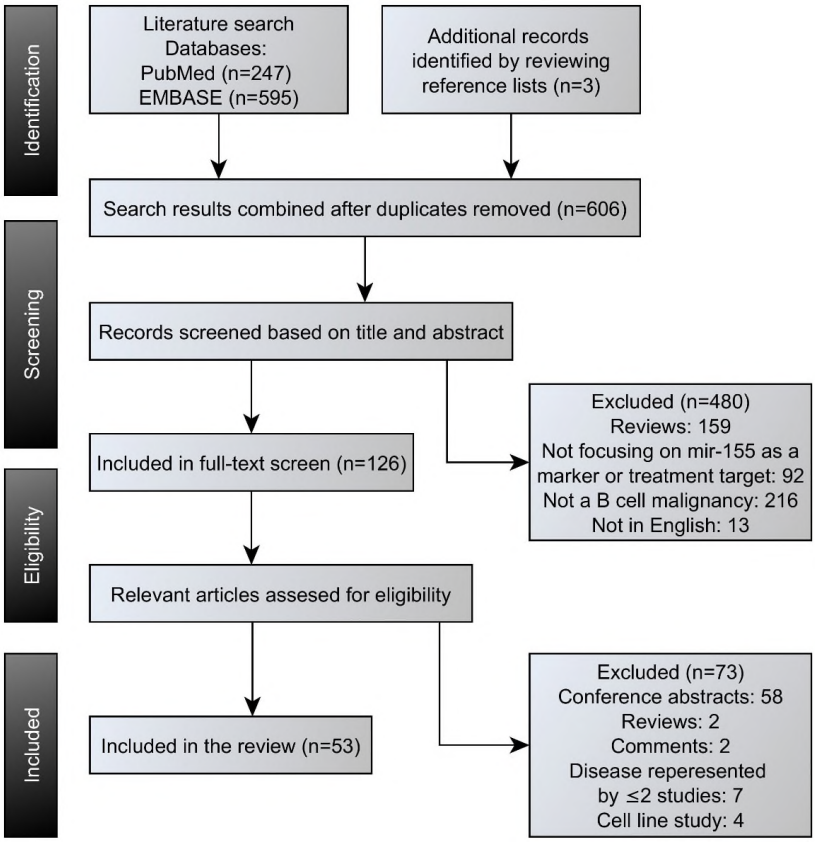

REGULAR ARTICLE

blood advances

MicroRNA-155 controls vincristine sensitivity and predicts superior clinical outcome in diffuse large B-cell lymphoma

Hanne Due,[1] Anna Amanda Schönherz,[1,2] Laura Ryø,[1,3] Maria Nascimento Primo,[3] Ditte Starberg Jespersen,[1] Emil Aagaard Thomsen,[3] Anne Stidholt Roug,[1] Min Xiao,[4] Xiaohong Tan,[4] Yuyang Pang,[4] Ken H. Young,[4] Martin Bøgsted,[1,5,6] Jacob Giehm Mikkelsen,[3] and Karen Dybkær[1,5,6]

[1]Department of Hematology, Aalborg University Hospital, Aalborg, Denmark; [2]Center for Quantitative Genetics and Genomics, Department of Molecular Biology and Genetics, and [3]Department of Biomedicine, Aarhus University, Aarhus, Denmark; [4]The University of Texas MD Anderson Cancer Center, Houston, TX; [5]Clinical Cancer Research Center, Aalborg University Hospital, Aalborg, Denmark; and [6]Department of Clinical Medicine, Aalborg University, Aalborg, Denmark.

Key Points

- Induced miR-155 expression promotes vincristine sensitivity in DLBCL cell lines.
- High miR-155 expression is associated with superior clinical outcome in patients with DLBCL of the GCB subclass.

A major clinical challenge of diffuse large B-cell lymphoma (DLBCL) is that up to 40% of patients have refractory disease or relapse after initial response to therapy as a result of drug-specific molecular resistance. The purpose of the present study was to investigate microRNA (miRNA) involvement in vincristine resistance in DLBCL, which was pursued by functional in vitro analysis in DLBCL cell lines and by outcome analysis of patients with DLBCL treated with rituximab, cyclophosphamide, doxorubicin, vincristine, and prednisone (R-CHOP). Differential miRNA expression analysis identified miR-155 as highly expressed in vincristine-sensitive DLBCL cell lines compared with resistant ones. Ectopic upregulation of miR-155 sensitized germinal-center B-cell-like (GCB)–DLBCL cell lines to vincristine, and consistently, reduction and knockout of miR-155 induced vincristine resistance, documenting that miR-155 functionally induces vincristine sensitivity. Target gene analysis identified miR-155 as inversely correlated with Wee1, supporting Wee1 as a target of miR-155 in DLBCL. Chemical inhibition of Wee1 sensitized GCB cells to vincristine, suggesting that miR-155 controls vincristine response through Wee1. Outcome analysis in clinical cohorts of DLBCL revealed that high miR-155 expression level was significantly associated with superior survival for R-CHOP-treated patients of the GCB subclass, independent of international prognostic index, challenging the commonly accepted perception of miR-155 as an oncomiR. However, miR-155 did not provide prognostic information when analyzing the entire DLBCL cohort or activated B-cell–like classified patients. In conclusion, we experimentally confirmed a direct link between high miR-155 expression and vincristine sensitivity in DLBCL and documented an improved clinical outcome of GCB-classified patients with high miR-155 expression level.

Introduction

Diffuse large B-cell lymphoma (DLBCL) is the most frequent type of non-Hodgkin's lymphoma, characterized by great heterogeneity regarding clinical presentation, tumor biology, and prognosis.[1] Gene expression profiling (GEP) defines cell-of-origin subtypes reflecting normal B-cell differentiation stages and permits classification of DLBCL into activated B-cell-like (ABC) and germinal-center B-cell–like (GCB), which differ in pathogenic activation mechanisms, genetic aberrations, and clinical outcome.[2,3] Although this classification has expanded our biological understanding of DLBCL, molecular mechanisms related to treatment response and resistance are still not fully understood.

Submitted 10 December 2018; accepted 4 March 2019. DOI 10.1182/bloodadvances.2018029660.

The full-text version of this article contains a data supplement.

The addition of rituximab (R) to the multiagent chemotherapy regimen cyclophosphamide, doxorubicin, vincristine, and prednisolone (CHOP) has increased DLBCL survival substantially; however, 30% to 40% of patients ultimately die of relapse or refractory disease because of treatment resistance.[4-6] As a consequence, novel treatments and predictive biomarkers are urgently warranted, and equally important, improved biological understanding is required for mechanisms leading to resistance. Several clinical trials have aimed at improving the R-CHOP regimen by dose adjustments, cycles, or add-on drugs, but with limited benefit, emphasizing that increased knowledge of R-CHOP resistance is still highly relevant.[7-9] The antimitotic drug vincristine has been used as anticancer therapy for more than 40 years and is a cornerstone for efficacy of R-CHOP because of its broad cytotoxic effect, limited bone marrow suppression, and high tolerability.[10,11] Despite wide use of vincristine, little is known about determinants of vincristine resistance in treatment of DLBCL, a caveat when attempting to improve clinical outcome.

Recent studies demonstrate that noncoding RNAs, and in particular microRNAs (miRNAs), play important roles in the pathogenesis of DLBCL.[12-14] miRNAs regulate gene expression by targeting mRNA for translational repression or degradation and are involved in cardinal physiologic and pathologic processes.[15] Aberrant miRNA expression is a common feature of malignancies and has been linked to chemotherapy resistance.[16-18] One of the most extensively studied miRNAs in normal B-cell differentiation and hematological cancers is miR-155,[19,20] which acts as an oncomiR in the pathogenesis and aggressiveness of DLBCL.[21] In line, miR-155 levels in patients with ABC are significantly higher compared with those detected in patients classified as having GCB,[19] and transgenic mice overexpressing miR-155 spontaneously develop DLBCL,[22] emphasizing its importance in lymphomagenesis.

Early detection of drug-specific resistance is of pivotal importance to successful cancer therapy, and defining miRNA involvement could provide information on resistance mechanisms of the drug and make miRNAs themselves biomarkers and treatment targets. Because vincristine is a cornerstone in the treatment of DLBCL, we studied the involvement of miRNAs in the response to this antimitotic drug. To pinpoint miRNAs controlling vincristine response, 13 DLBCL cell lines were subjected to systematic dose-response experiments and grouped as resistant, intermediate, or sensitive.[23] Global miRNA expression profiling of these cell lines in untreated condition was performed and miRNAs differentially expressed between vincristine sensitive and resistant cell lines were identified, showing miR-155 to be highly expressed in vincristine-sensitive cells. Hence, experimental manipulations of miR-155 expression using lentiviral gene delivery in DLBCL cells were performed to determine the functional effect of miR-155 in vincristine response, and subsequently a prognostic value of miR-155 was documented in 2 independent R-CHOP-treated DLBCL cohorts.

Materials and methods

Cell lines

DLBCL cell lines (supplemental Table 1) were cultured at 37°C in a humidified atmosphere of 95% air and 5% CO_2 with RPMI1640 medium, 10% fetal bovine serum, and 1% penicillin/streptomycin. HEK293T cells were maintained in Dulbecco's modified Eagle medium containing 5% fetal bovine serum and 1% penicillin/streptomycin. All cell lines were authenticated by DNA barcoding[23] and examined for mycoplasma infection.

Clinical samples

Diagnostic biopsies from 73 patients with DLBCL (supplemental Table 2) were collected in agreement with the RetroGen research protocol and reviewed and approved by the health ethic committee of the North Denmark Region (approval jr. no. N-20140099), allowing exemption from the Declaration of Helsinki requirement of informed consent according to sections 3 to 5 in the Danish Act on Research Ethics Review of Health Research Projects. Informed consent was waived, as this notifiable database research project did not involve any health risks and, under the given conditions, could not otherwise put a strain on the trial subject. In addition, it would be impossible or disproportionately difficult to obtain informed consent or proxy consent, respectively, because of the use of archival samples and because several patients have died since collection. Of the 73 patients with DLBCL, 69 were treated with standard R-CHOP. In addition, we used Gene Expression Omnibus data (GSE10846[24] and GSE31312[3]).

Dose-response assays

Vincristine dose-response screens were performed on DLBCL cell lines, as previously described.[23,25] Each cell line was subjected to 18 increasing concentrations for 48 hours, and dose-responses were evaluated using a 3-(4,5 dimethylthiazol-2-yl)-5-(3-carboxymethoxyphenyl-2-(4-sulfophenyl)-2H-tetrazolium assay.

RNA extraction

RNA was extracted using a protocol combining TRIzol (Invitrogen) and mirVana miRNA Isolation Kit (Ambion/ThermoFisher Scientific)[26] or a RNAqueous Micro scale RNA Isolation kit (<500 000 cells; ThermoFisher Scientific). RNA integrity and concentration were determined using an Agilent 2100 Bioanalyzer and NanoDrop ND-1000 spectrophotometer, respectively.

Microarray profiling

miRNA expression profiling was performed using GeneChip miRNA 1.0.2 arrays (Affymetrix), as previously described,[17] and CEL files are deposited at Gene Expression Omnibus (GSE72648). GEP of clinical samples and transduced SU-DHL-5 cells was performed using Affymetrix GeneChip HG-U133 Plus2.0 arrays. CEL files were generated using the Affymetrix Gene-Chip Command Console Software and deposited at Gene Expression Omnibus (GSE109027). Data comply with Minimum Information About a Microarray Experiment requirements.

Reverse transcription quantitative polymerase chain reaction

miR-155 expression was determined by TaqMan miRNA reverse transcription quantitative polymerase chain reaction (RT-qPCR; Thermo Fisher Scientific). Two independent cDNA syntheses were conducted and pooled before amplification qPCR analysis (hsa-miR-155 [002623], RNU6B [001093], RNU24 [001001]). Each sample was analyzed in triplicate, using Mx3000P (Stratagene/Agilent Technologies). miRNA expression was normalized to RNU6B and RNU24 and $\log_2$ transformed.

Plasmid construction

A lentiviral vector containing multiple cloning sites for insertion of PCR-amplified miRNA sequences was generated.[27,28] The sequence

encoding pri-miR-155 was amplified from HeLa cells, using primers 5′-AAAGCGGCCGCCATCTTTTAATTGCCAATTTCTCTACC-3′ and 5′-AAAGCGGCCGCGTTTAAGGTTGAACATCCCAGTGACC-3′. Fragments were *NotI*-digested and inserted into *Bsp120I* digested plasmid from corynebacterium callunae (pCCL) with a multiple cloning site (MCS) immediately downstream of the H1 promoter (H1) and phosphoglycerate kinase promotor (PGK) controlling enhanced green fluorescent protein (eGFP) (pCCL/H1-MCS-PGK-eGFP). For miR-155 inhibition, a Tough Decoy (TuD)–expressing construct with high miRNA-suppressive capacity was generated by a 2-step cloning strategy.[29,30] DNA sequences containing inhibitor sequence flanked by *NheI*/*AscI* sites were synthesized and cloned into pUC57 by GeneScript. Inhibitor sequences were cleaved from pUC57 and cloned into *AvrII*/*AscI*-digested pCCL/PGK-eGFP,H1-MCS. Sequences including TuD were PCR-amplified from lentiviral vectors encoding H1 driven inhibitor, using 5′-AAAAGGTACCGTATGAGACCACCCTAGCCC-3′ and 5′-AAAAGGTACCCAGAGAGACCCAGTACAAGC-3′. *KpnI*-digested PCR products were cloned into *KpnI*-digested pCCL/PGK-eGFP.

To test functionality, sense and antisense oligonucleotides harboring miR-155 target sequence were annealed and cloned into *NotI*/*XhoI*-digested psiCHECK-2 vector (Promega).[29] Co-transfections of HEK293T cells were performed with 7 ng pCCL/U1-miRNA. PGK-eGFP, 14ng psiCHECK-miRtarget ,and 80 ng pCCL/PGK-eGFP-TuD, using X-tremeGENE 9 (Roche). Renilla and Firefly luciferase expression levels were measured 48 hours posttransfection, using Dual-Glo Luciferase Reporter Assay System (Promega). Renilla luciferase activity was normalized to Firefly and presented relative to negative control (pCCL/PGK-eGFP).

All plasmids were verified by sequencing (GATC; Konstanz, Germany).

Lentivirus production and transduction

To generate lentiviral vectors, 1×10^7 HEK293T cells were seeded in 25 mL Dulbecco's modified Eagle medium. Twenty-four hours after seeding, cells were transfected with 9.07 μg pMD.2G, 7.26 μg pRSV-Rev, 31.46 μg pMDlg/*p*-RRE, and 31.46 μg lentiviral transfer vector. Both 48 and 72 hours posttransfection, viral supernatant was harvested, filtered (0.45 μm), and ultracentrifuged. Virus yield was determined by measurements of p24 capsid protein, using p24 Antigen ELISA Kit (XpressBio). DLBCL cells were seeded at 300 000 cells/mL in 1 mL standard RPMI and transduced with virus corresponding to 85 ng p24. DLBCL cell lines SU-DHL-5, OCI-Ly7, NU-DHL-1, and RIVA were selected on the basis of ABC/GCB classification, resistance/sensitivity to vincristine, and lentiviral transducibility.[27] RT-qPCR was used to confirm changes in miR-155 expression.

CRISPR-Cas9 knockout

Single guide RNA (sgRNA) was designed to target the functional part of *MIR155HG* (supplemental Figure 1). Sense and antisense oligonucleotides encoding the sgRNA were annealed and cloned into pLV/CRISRP-v2, using *BsmbI* site.[31] OCI-Ly7 was transduced with LV/CRISPR-sgRNA-miR-155 or LV/CRISPR-sgRNA-control, the latter without target in the human genome (5′-ACGGAGGCTAAGCGTCGCAA-3′) and subjected to puromycin selection (0.5 μg/mL). After 2 weeks, gDNA was extracted using standard NaCl/EtOH precipitation protocol, and gDNA encompassing the Cas9 cut sites was amplified using 5′-AACTCCGAAGAGCGGTT-3′ and 5′-GGTTGAACATCCCAGTGACC-3′. Indel frequencies were determined by sequence-based Tracking of Indels by Decomposition analysis.[32] miR-155 knockout clones from single-cell expansion were generated by seeding 96-well plates at concentrations of 0.5 cell/well in 50 μL standard RPMI, 100 μL conditioned medium, and 50 μL RPMI containing 55% fetal bovine serum and 3% penicillin/streptomycin. Tracking of Indels by Decomposition analysis and RT-qPCR was performed in individual clones.

Dose-response screen of transduced cells

Transduced cells and miR-155 knockout clones were seeded at 3×10^5 cells/mL in 1 mL standard RPMI. Cells were exposed to vincristine for 48 hours, and viable cells were counted using trypan blue exclusion. Transduced cells were treated with 2 concentrations of vincristine (0.0005-0.001 μg/mL), whereas miR-155 knockout cells were exposed to 0.0005, 0.001, and 0.0015 μg/mL. Transductions and functional assays were performed in triplicate in 2 independent assays.

Western blot

Cell lysates were prepared using RIPA Lysis Buffer supplemented with complete miniprotease inhibitors, and protein concentration was determined using BCA Pierce (Thermo Fisher Scientific). Western blotting analysis was performed following standard Bio-Rad procedures loading 20 μg total protein. Antibodies used were β-actin (1:10 000, Abcam, ab6276), Wee1 (1:1,000, Santa Cruz Biotechnology, sc-5285), Ship-1 (1:1000, Santa Cruz Biotechnology, sc-8425), and rabbit-anti-mouse IgG (1:10 000, Abcam, ab6728).

Double drug analysis

Wee1 inhibitor MK-1775 (Selleck chemical) was dissolved in dimethyl sulfoxide. OCI-Ly7 cells were seeded in 96-well plates at a density of 0.25×10^6 cells/mL, 24 hours before drug was added. Cells were exposed to 0.0015 μg/mL vincristine, 400 nM MK-1775, or 0.0015 μg/mL vincristine and 400 nM MK-1775 for 48 hours, and metabolically active cells were determined by 3-(4,5 dimethylthiazol-2-yl)-5-(3-carboxymethoxyphenyl-2-(4-sulfophenyl)-2H-tetrazolium-containing CellTiter 96 Reagent at a concentration of 20% of pre-additional well content. Absorbance was measured at 492 nm (BMG, LABTECH).

Statistical analysis

Statistical analyses were performed with R (v.3.3.3).[33] Array-based miRNA and gene expression data were cohort-wise background corrected and normalized at the probe and gene level, applying a Robust Multichip Average approach,[34] respectively.

Differential miRNA expression analysis was performed using the *limma* Bioconductor package (v.3.26.9),[35] setting $P < .05$ and $FC > |2|$ as the significance threshold.

To increase statistical power, external R-CHOP restricted cohorts[3,24] were combined into a meta-cohort. The meta-cohort was batch corrected using ComBat implemented in the *sva* Bioconductor package (v.3.18.0),[36,37] and miR-155 expression was quantified through the *MIR155HG* probe set 229437_at included in HG-U133 Plus2.0 GeneChip. Validity of array-based quantification was confirmed through correlation analysis, with RT-qPCR quantified miR-155 expression in the in-house cohort.

Confounding effects of ABC/GCB subclasses and Cheson response evaluation on miR-155 expression were investigated through simple

linear regression analysis. Survival analyses were performed using Kaplan-Meier and log-rank test statistics for progression-free survival (PFS) and overall survival (OS). Furthermore, simple and multiple Cox proportional hazards regression analyses were conducted using an additive model with international prognostic index, ABC/GCB, and miR-155 expression (dichotomized by median split into low and high or as a continuous variable) as independent confounders. Linear regression and survival analyses were conducted for all patients with DLBCL and restricted to ABC and GCB classified patients, respectively.

Gene set enrichment analysis (GSEA) was performed for transduced cells (miR-155 vs control and TuD-155 vs control), using the GSEA desktop application (v.3.0)[38] with preranked gene lists, 2000 permutations of gene set randomization, and default settings otherwise. GSEA was restricted to gene sets included in the *Hallmark* collection from the Molecular Signatures Database (v.6.0),[38,39] excluding sets with fewer than 15 or more than 500 genes. Gene sets with normalized $P \leq .05$ and FDR $q \leq 0.25$ were considered significantly enriched.

If not mentioned otherwise, 2-sided Student *t* tests were performed to evaluate statistical significance, and significance thresholds were set to 0.05.

Results

Identification of vincristine response-specific miRNAs

DLBCL cell lines subjected to vincristine dose-response screens were ranked according to their sensitivity, using area under the dose-response curve, and trichotomized into groups of sensitive, intermediate, and resistant cells (supplemental Table 1).[23,25] To identify miRNAs associated with vincristine response, global miRNA profiling was conducted for each cell line in untreated condition, and subsequent differential miRNA expression analysis between vincristine-sensitive and vincristine-resistant cell lines identified 15 differentially expressed miRNAs (supplemental Table 3). Low miR-155 expression displayed the strongest association to vincristine resistance and was selected for further analyses (supplemental Figure 2). Of notice, miR-155 was the top candidate irrespective of split strategy used to categorize cell lines as sensitive and resistant (4 sensitive, 5 intermediate, and 4 resistant; 6 sensitive and 7 resistant; data not shown).

Downregulation of miR-155 promotes vincristine resistance

To substantiate involvement of miR-155 in vincristine response, lentiviral vectors encoding pri-miR-155 or TuD-155 for stable up- and downregulation, respectively, were designed (Figure 1A).

Two GCB-DLBCL cell lines, SU-DHL-5 and OCI-Ly7, that are intrinsically sensitive and resistant, respectively, to vincristine with high and low levels of endogenous miR-155 (supplemental Table 1) were transduced. Forty-eight hours posttransduction, the expression level of miR-155 was significantly increased by lentiviral vectors encoding pri-miR-155 and reduced by TuD-155 (Figure 1BI-EI). Ectopic expression of miR-155 did not have toxic effects because total cell number was unchanged (supplemental Figure 3). Moreover, GSEA conducted for transcriptional profiles of transduced SU-DHL-5 cells revealed that top enriched gene sets detected in miR-155 overexpressing cells compared with controls were associated with G2/M checkpoints and mitotic spindle assembly. Consistently, those gene sets were enriched in control samples when compared with cells with miR-155 knock-down (supplemental Tables 4 and 5; supplemental Figure 4). Based on the antimitotic effect of vincristine, those results suggest that miR-155 and vincristine affect comparable biological processes.

Induction of miR-155 significantly increased vincristine sensitivity in both GCB cell lines, and decreased miR-155 expression consistently caused vincristine resistance in intrinsic vincristine-sensitive SU-DHL-5 cells, whereas no change in response was observed in the vincristine-resistant cell line OCI-Ly7 (Figure 1Bii-Eii). Because downregulation of miR-155 did not affect vincristine response in OCI-Ly7, 2 miR-155 knockout clones were generated (supplemental Figure 5; Figure 2B). As a result of miR-155 depletion, cell viability decreased, whereas no difference between vector control and the parental wild-type counterpart was observed (Figure 2A). Furthermore, miR-155 knockout increased vincristine resistance over a range of concentrations (Figure 2C), indicating that miR-155 functionally affected vincristine response in DLBCL cells of the GCB subclass.

In addition, ABC cell lines RIVA and NU-DHL-1, characterized by intrinsically intermediate response to vincristine and comparably high endogenous expression of miR-155 (supplemental Table 1), were similarly analyzed. Applying the TuD model system decreased miR-155 expression in RIVA cells; however, it did not cause unambiguous effect on vincristine sensitivity (supplemental Figure 6BI-BII). Although functionality of the model systems was confirmed (supplemental Figure 7),[28] transduction with LV/miR-155 in RIVA and LV/TuD-155 in NU-DHL-1 did not generate significant changes in intracellular levels of miR-155, and consequently, vincristine dose-response analysis was not performed (supplemental Figure 6AI,DI). Overexpression of miR-155 in NU-DHL-1 cells did not affect vincristine response either (supplemental Figure 6CI-CII), indicating that miR-155 does not play a pivotal role in vincristine response in ABC cells as opposed to GCB cells.

The cell-cycle checkpoint gene *WEE1* is a direct target of miR-155

To identify target genes of miR-155 with an effect on vincristine response, transcriptional profiles of ectopic miR-155 expressing SU-DHL-5 cells were analyzed. On the basis of the antimitotic effect of vincristine, resistance mechanisms could be related to cell cycle processes, and thus negatively correlated genes associated with gene ontologies of cell cycle processes were selected ($n = 64$; supplemental Table 6).

To investigate whether selected genes were potential miR-155 targets, miR-155-mRNA interaction was investigated using well-documented miRNA prediction algorithms (TargetScan, miRDB, microT-CDC, and microRNA.org) and TarBase, a database of experimentally validated miRNA-mRNA interactions. Only 1 gene, *WEE1*, was predicted as a putative miR-155 target by all algorithms, and was found as experimentally verified in TarBase. Notably, the miR-155 binding site of *WEE1* is actively recognized by miR-155 in luciferase-based reporter assays,[40,41] and in agreement, induced protein level of Wee1 was observed in miR-155 knockout clones (Figure 2D-E). *WEE1* encodes a kinase controlling G2/M phase by inhibitory phosphorylation of Cdk1, through which Wee1 also affects sensitivity to antimicrotubule drugs.[42] In accordance,

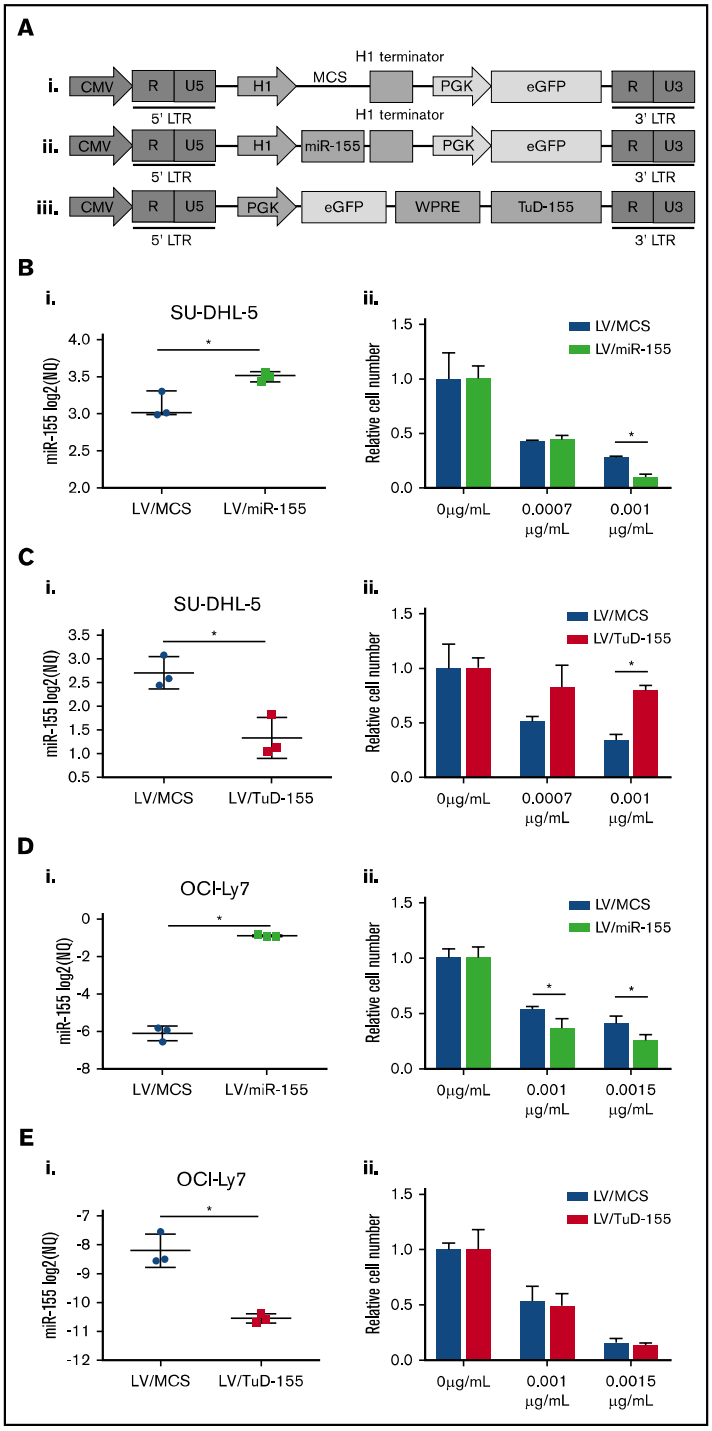

Figure 1. Changes in miR-155 expression in GCB-DLBCL cell lines affect vincristine response. (A) Schematic overview of lentiviral vector plasmids used as control (i), for expression of miR-155 (ii) and TuD-155 (iii) inhibitor in fusion with eGFP. (B-E) Up- and downregulation of miR-155 was detected by RT-qPCR in (Bi,Ci) SU-DHL-5 and (Di,Ei) OCI-Ly7 cells and followed by vincristine dose-response analysis. (Bii,Cii,Dii,Eii) Drug response is illustrated as percentage of living cells related to the no-drug treated condition. CMV, cytomegalovirus promoter; LTR, long terminal repeat; NQ, normalized quantity; PGK, phosphoglycerate kinase promoter; WPRE, woodchuck hepatitis virus posttranscriptional regulatory element.

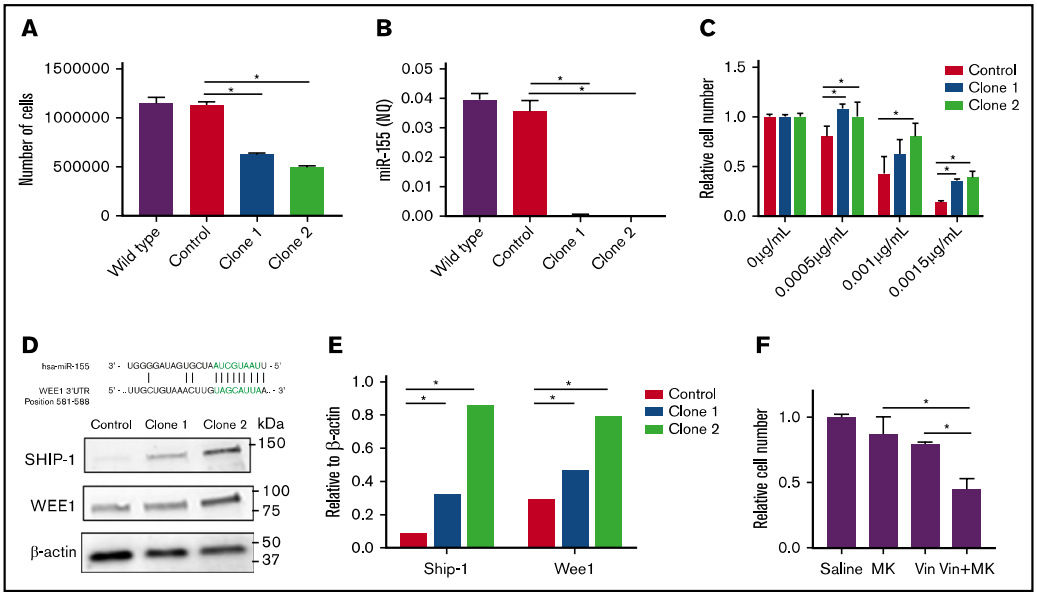

Figure 2. miR-155 knockout experiments. Two independent miR-155 knockout clones were generated in OCI-Ly7 cells by the CRISPR-Cas9 technology. Wild-type accounts for untransduced OCI-Ly7 cells, whereas control is an OCI-Ly7 population subjected to a sgRNA not targeting the human genome. (A) Cell proliferation was determined by the trypan blue exclusion method after 48 hours of growth in wild-type, control cells, and miR-155 knockout clones. (B) miR-155 expression detected by RT-qPCR. (C) Vincristine dose-response analysis using 0.0005 µg/mL, 0.001 µg/mL, and 0.0015 µg/mL. Drug response is illustrated as percentage of living cells related to the no-drug condition. (D) Detection of Wee1 protein by western blotting. β-actin was used as loading control and Ship-1, a validated target of miR-155,[53] as positive control. (E) Quantification of western blot bands. Ship-1 and Wee1 levels are depicted as relative to β-actin levels. (F) Chemical inhibition of Wee1 by MK-1775. Wild-type OCI-Ly7 cells were exposed to saline, 400 nM MK-1775, 0.0015 µg/mL vincristine or 400 nM MK-1175 and 0.0015 µg/mL vincristine for 48 hours, and the number of metabolically cells were determined by 3-(4,5 dimethylthiazol-2-yl)-5-(3-carboxymethoxyphenyl-2-(4-sulfophenyl)-2H-tetrazolium assay. Drug response is presented as the number of cells relative to the no-drug condition. MK, MK-1775; Vin, vincristine.

chemical inhibition of Wee1 in wild-type OCI-Ly7 cells decreased the number of living cells and enhanced killing when given in combination with vincristine (Figure 2F).

Prognostic effect of miR-155 expression in GCB-DLBCL

The relationship between miR-155 expression and ABC/GCB subclasses was examined in the in-house cohort, for which miR-155 expression was assayed by RT-qPCR. Higher expression of miR-155 was observed in the ABC subclass (supplemental Figure 8), in accordance with previous observations.[19]

To investigate the prognostic value of miR-155, dichotomized miR-155 expression was analyzed for association with OS and PFS in R-CHOP-treated patients. Because miR-155 is differentially expressed between patients with ABC and GCB-DLBCL, which display different pathogenesis and prognosis, survival analysis was performed both overall and according to ABC and GCB subclasses. A tendency for association between miR-155 and OS and PFS was observed in the entire DLBCL cohort and for GCB-classified patients, with low miR-155 expression characterizing poor outcome (Figure 3; supplemental Figure 9).

To verify this trend, we investigated the prognostic value in an independent meta-cohort of 701 patients with DLBCL, in which miR-155 expression was quantified through the precursor *MIR155HG*. In the in-house cohort, mature miR-155 expression measured by RT-qPCR was highly correlated to its precursor measured by microarray (supplemental Figure 10), supporting array-based miR-155 expression assessment. Analysis of these data revealed differential expression of miR-155 between ABC and GCB-DLBCL (supplemental Figure 8), consistent with the in-house cohort.

When evaluating the prognostic effect of miR-155 expression, prognostic stratification was confirmed within the GCB subclass, with significantly shorter OS and PFS of patients with low levels of miR-155 (Figure 4). However, miR-155 expression did not provide prognostic information within the ABC subclass or the entire cohort. These observations were supported by simple Cox proportional hazards regression analysis (Table 1), and are in accordance with the in-house cohort.

In addition, multiple Cox proportional hazards regression analysis was conducted to test the prognostic value of miR-155 when combined with other prognostic tools of DLBCL. For multiple Cox regression analysis, independent variables were only included in the model if significant results were obtained when performing simple Cox regression analyses. The analysis revealed that the prognostic value of miR-155 was independent of the well-established international prognostic index in the GCB subclass, irrespective of

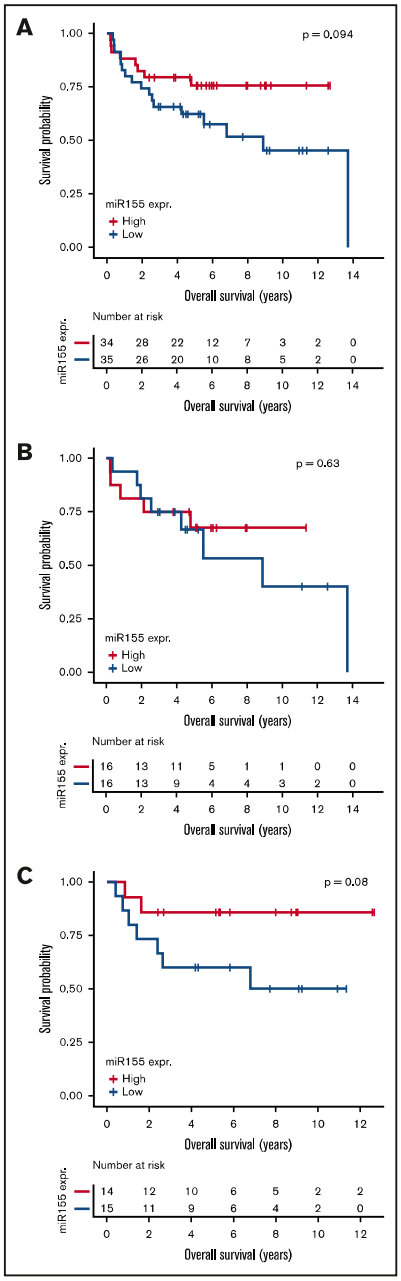

Figure 3. Analysis of prognostic effect of miR-155 expression. Kaplan-Meier plots depicting OS of R-CHOP-treated patients with DLBCL in the in-house cohort. The analysis was conducted for all patients with DLBCL (A), ABC-classified patients (B), and GCB-classified patients (C). For each cohort, patients were dichotomized by median split of miR-155 expression.

dichotomized or continuous miR-155 expression (Table 1; supplemental Table 7). Thus, miR-155 identifies a subgroup with inferior prognosis among GCB-classified patients. In accordance, patients with stable or progressive disease at time of response evaluation[43] display lower levels of miR-155 than patients in complete remission (supplemental Figure 11), supporting the association between low miR-155 expression and vincristine resistance.

Discussion

In a 2-step strategy, we defined miRNA involvement in vincristine resistance in DLBCL, first by elucidating the biological role of miRNAs in vincristine response by functional analysis and second by evaluating the biomarker potential in 2 independent R-CHOP-treated DLBCL cohorts. Identification of vincristine response-specific miRNAs documented miR-155 as highly expressed in vincristine-sensitive DLBCL cell lines, and functional validation confirmed a direct link between miR-155 expression and vincristine response in DLBCL cells. To compensate for cell line-specific biological effects, analyses were performed in 2 ABC and GCB-DLBCL cell lines, strengthening the biological interpretation. Induction of miR-155 increased vincristine sensitivity in GCB cells, with the strongest phenotype obtained in vincristine-resistant OCI-Ly7. The endogenous level of miR-155 is relatively low in OCI-Ly7, supporting significantly increased effect on vincristine response on induction. Only a complete knockout generated by indel introduction induced clear cellular resistance in OCI-Ly7, showing that TuD-155-directed reduction of already low miR-155 levels was not sufficient to cause phenotypic alterations. When applying similar approaches in ABC cells, no unambiguous association between miR-155 and vincristine response was observed. However, as a result of high endogenous miR-155 expression in ABC cells, it may be challenging to further increase miR-155 levels. In GCB cells, in contrast, lentiviral intervention altered the intracellular level of miR-155 independent of endogenous levels, suggesting a more stringent and complex regulation of miR-155 in ABC-DLBCL. Of notice, miR-155 is regulated by a feedback loop through NF-κB signaling, a pathway reported to be constitutively active in ABC-DLBCL.[44,45]

GSEA revealed that ectopic expression of miR-155 affected G2/M checkpoints and genes involved in mitotic spindle assembly. In accordance, the cell-cycle checkpoint gene *WEE1* was inversely correlated with miR-155 in exogenously modified GCB-DLBCL cells, and in addition, induced levels of Wee1 protein were observed in miR-155 knockout clones. Although Wee1 is an experimentally verified target of miR-155,[41] it has not previously been validated in DLBCL cells, which is of great importance, as affected targets vary depending on the cell type in which the miRNA is expressed.[46]

A study by Visconti et al.[42] reported that the Fcp1-Wee1-Cdk1 axis controls spindle assembly checkpoints (SAC), which ensures proper chromosome segregation by delaying mitosis exit until mitotic spindle assembly.[47] Antimicrotubule drugs, including vincristine, impede mitotic spindle assembly by targeting microtubules, leading to the activation of SAC and extension of mitosis, which promotes apoptosis.[47,48] Resistance to these types of drugs has been related to the ability of cancer cells to slip through the SAC and exit mitosis prematurely, and thereby resist killing.[48,49] Activation of Wee1 stimulates SAC slippage,[42] suggesting that increased vincristine resistance mediated by

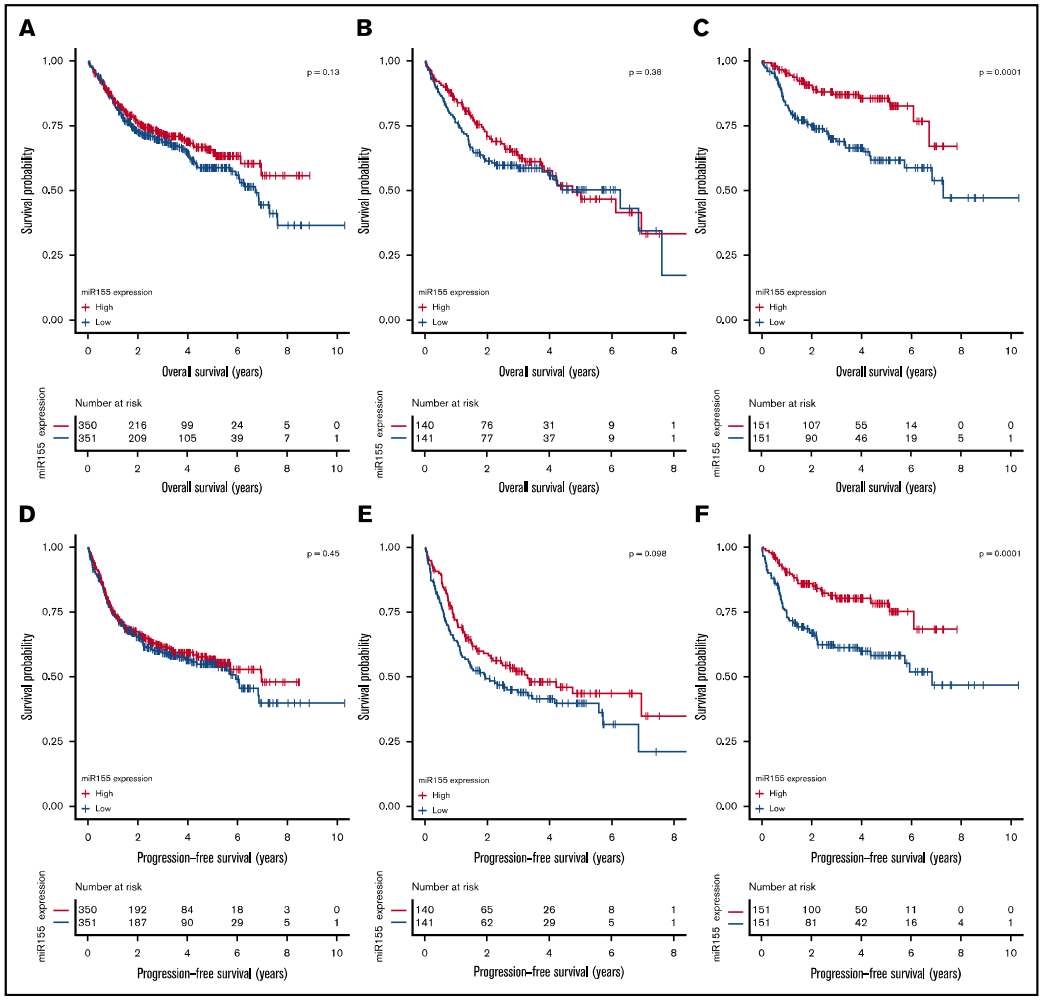

Figure 4. Analysis of association between OS and PFS and miR-155 expression. Kaplan-Meier plot depicting OS (A-C) and PFS (D-F) of R-CHOP-treated patients with DLBCL in the meta-cohort, consisting of R-CHOP–restricted Lymphoma/Leukemia Molecular Profiling Project and International DLBCL Rituximab-CHOP Consortium MD Anderson Project data. Before analysis, data were ComBat normalized to compensate for study-wise batch effect. Analyses were conducted for all patients with DLBCL (A,D), ABC-classified patients (B,E), and GCB-classified patients (C,F). For each cohort, patients were dichotomized by median split of *MIR155HG* expression.

miR-155 knockout could occur through upregulation of Wee1 and increased Wee1 signaling. However, it is important to emphasize that this study only addresses miR-155 signaling through Wee1. miR-155 could mediate vincristine resistance by regulating other targets as well, yet comprehensive target gene analysis was not the focus in this study.

Genetic and chemical inhibition of Wee1 strengthens the SAC, prolongs mitosis, and enhances killing of vincristine-treated acute lymphoblastic leukemia cells.[42,50] In agreement, MK-1775, a chemical inhibitor of Wee1, boosted the effect of vincristine in GCB-DLBCL cells in this study. Interestingly, MK-1775 potentiated the cytotoxic effect of doxorubicin, another vital component of R-CHOP,[51] supporting combination therapy of R-CHOP and MK-1775 in relapsed or refractory DLBCL.

miR-155 is involved in numerous processes that could affect drug response, including MAPK, PI3K/AKT, and RhoA signaling.[52-55] In line, decreased miR-155 expression in epidermoid carcinoma cells increased cisplatin resistance by increasing the amount of Wee1 protein,[56] similar to the mechanism of miR-155-induced vincristine resistance reported in this study. Furthermore, suppression of miR-155 was found to reverse doxorubicin resistance in lung cancer cells, whereas it did not affect the response in DLBCL cells, highlighting

Table 1. *MIR155HG* expression is an IPI-independent prognostic marker for R-CHOP-treated patients with GCB-DLBCL

			Simple			Multiple		
	n	no.	HR	95% CI	*P*	HR	95% CI	*P*
All DLBCL								
miR-155								
Low	293	90	1			—		
High	293	107	1.17	0.88-1.54	.28	—	—	—
IPI								
0-1	71	6	1			1		
2-3	314	84	3.76	1.64-8.61	.0017	3.42	1.49-7.84	.0038
4-5	201	106	9.61	4.22-21.88	7.19e-08	8.29	3.62-18.98	5.73e-07
Subclass								
ABC	242	105	1			1		
GCB	248	58	0.45	0.33-0.62	1.09e-06	0.55	0.40-0.76	.00032
UC	96	34	0.73	0.50-1.08	.11	0.71	0.48-1.05	.089
ABC-DLBCL								
miR-155								
Low	121	57	1			—		
High	121	48	0.78	0.53-1.14	.20	—	—	—
IPI								
0-1	15	2	1			—		
2-3	125	38	3.57	0.86-14.89	.080	—	—	—
4-5	102	65	10.37	2.51-42.87	.0012	—	—	—
GCB-DLBCL								
miR-155								
Low	124	41	1			1		
High	124	17	0.40	0.23-0.71	.0017	0.46	0.26-0.81	.0071
IPI								
0-1	48	2	1			1		
2-3	140	32	6.22	1.49-25.97	.012	5.91	1.42-24.69	.015
4-5	60	24	12.53	2.96-53.06	.0006	11.10	2.61-47.15	.0011

Array-based miR-155 expression and outcome were analyzed by simple and multiple Cox proportional hazards regression analyses for OS. IPI (international prognostic index) score information was not available for all patients, thus cohort sizes are reduced in this setting (115 samples were removed). *MIR155HG* expression was dichotomized by median split in each of the individual cohorts: all DLBCL patients, ABC-classified patients, and GCB-classified patients.

—, value not available because variables were only included in multiple Cox proportional hazards regression analysis if significant results were obtained in simple Cox proportional hazards regression analysis; CI, 95% lower and upper confidence intervals; HR, hazard ratio; n, number of samples; no., number of events.

the tissue-specific effect of a particular miRNA.[13,57] Whether miR-155 has an effect on other compounds of R-CHOP is unknown. However, rituximab exerts its action through CD20, whereas cyclophosphamide has alkylating properties and furthermore induces cytokine release, leading to antibody-mediated elimination,[58] all of which are mechanisms differing from those of vincristine. Thus, miR-155 does most likely not affect rituximab and cyclophosphamide response through Wee1, but has the potential through other targets.

To evaluate the prognostic effect of miR-155, expression levels were analyzed for association with clinical outcome. It is noteworthy that the clinical outcome is a result of the entire R-CHOP regimen, and therefore, we investigated the prognostic potential of miR-155 regardless of its association to vincristine response. Investigation of the meta-cohort demonstrated decreased OS and PFS for patients with GCB-DLBCL with low *MIR155HG* expression. Notably, miR-155 identifies a subgroup of GCB-DLBCL with inferior clinical outcome comparable to ABC-classified patients. The beneficial effect of miR-155 on clinical outcome was a surprising observation when considering the commonly accepted perception of miR-155 as an oncomiR, yet documenting that the effect of a particular miRNA is dependent on the cell type in which it is expressed.

When examining the association between miR-155 and the ABC/GCB subclasses, it was confirmed that miR-155 is more expressed in ABC-DLBCL,[19] which is in accordance with the role of miR-155 as an oncomiR, as ABC-classified patients have a dismal prognosis. Furthermore, clinical analysis revealed that miR-155 only displayed prognostic value within the GCB subclass, highlighting the molecular heterogeneity between the 2 molecular subclasses of DLBCL. These findings, in combination with the different functional effect of miR-155 on vincristine response in ABC and

GCB cells, suggest that miR-155 affects different targets, depending on the cell of origin.

Contradictory to the beneficial effect of miR-155 observed in this study, Iqbal et al[13] reported high miR-155 expression to be associated with R-CHOP treatment failure in DLBCL. However, unlike the current study, patients with DLBCL were divided according to survival risk and not miR-155 expression, and furthermore, without subtype-specific focus. In addition, by dichotomizing patients with DLBCL on miR-155 expression, Zhong et al[59] documented inferior prognosis of patients with DLBCL with high miR-155 levels, whereas no prognostic stratification was observed in the study of Go et al.[60] Yet, to the best of our knowledge, this is the first prognostic evaluation of miR-155 with a DLBCL subtype-specific focus, thereby taking the different pathogenesis of the molecular subclasses into consideration.

In conclusion, experimentally, we confirm a direct functional link between miR-155 expression and vincristine response in DLBCL. This role is supported by prognostic evaluation in 2 independent DLBCL cohorts treated with R-CHOP, documenting a significantly improved clinical outcome of GCB-classified patients with high miR-155 expression. The data suggest that the role of miR-155 on vincristine response is important enough to affect OS and PFS of patients with GCB-DLBCL treated with R-CHOP.

Acknowledgments

The authors greatly appreciate the technical assistance from Louise Hvilshøj Madsen and Helle Høholt, Department of Hematology, Aalborg University Hospital, Aalborg, Denmark.

This study was supported by grants from The Danish Cancer Society and The North Region Research Foundation, Denmark.

Authorship

Contribution: H.D., A.S.R., and K.D. designed the research; H.D., M.X., X.T., Y.P., K.E.Y., and K.D. collected the data; H.D., L.R., M.N.P., D.S.J., and E.A.T. performed experiments; H.D., J.G.M., and K.D. optimized the experimental setup; H.D., A.A.S., and M.B. performed statistical analysis and generated the figures; H.D. wrote the paper; and all authors contributed to data interpretation and critically revised and approved the final manuscript.

Conflict-of-interest disclosure: The authors declare no competing financial interests.

Correspondence: Karen Dybkær, Department of Clinical Medicine/Aalborg University and Department of Hematology, Aalborg University Hospital, Sdr Skovvej 15, 9000 Aalborg, Denmark; e-mail: k.dybkaer@rn.dk.

References

1. Nogai H, Dörken B, Lenz G. Pathogenesis of non-Hodgkin's lymphoma. *J Clin Oncol*. 2011;29(14):1803-1811.
2. Alizadeh AA, Eisen MB, Davis RE, et al. Distinct types of diffuse large B-cell lymphoma identified by gene expression profiling. *Nature*. 2000;403(6769):503-511.
3. Visco C, Li Y, Xu-Monette ZY, et al. Comprehensive gene expression profiling and immunohistochemical studies support application of immunophenotypic algorithm for molecular subtype classification in diffuse large B-cell lymphoma: a report from the International DLBCL Rituximab-CHOP Consortium Program Study. *Leukemia*. 2012;26(9):2103-2113.
4. Coiffier B, Lepage E, Briere J, et al. CHOP chemotherapy plus rituximab compared with CHOP alone in elderly patients with diffuse large-B-cell lymphoma. *N Engl J Med*. 2002;346(4):235-242.
5. Sehn LH, Donaldson J, Chhanabhai M, et al. Introduction of combined CHOP plus rituximab therapy dramatically improved outcome of diffuse large B-cell lymphoma in British Columbia. *J Clin Oncol*. 2005;23(22):5027-5033.
6. Vaidya R, Witzig TE. Prognostic factors for diffuse large B-cell lymphoma in the R(X)CHOP era. *Ann Oncol*. 2014;25(11):2124-2133.
7. Jaeger U, Trneny M, Melzer H, et al; AGMT-NHL13 Investigators. Rituximab maintenance for patients with aggressive B-cell lymphoma in first remission: results of the randomized NHL13 trial. *Haematologica*. 2015;100(7):955-963.
8. Seymour JF, Pfreundschuh M, Trněný M, et al; MAIN Study Investigators. R-CHOP with or without bevacizumab in patients with previously untreated diffuse large B-cell lymphoma: final MAIN study outcomes. *Haematologica*. 2014;99(8):1343-1349.
9. Leonard JP, Kolibaba KS, Reeves JA, et al. Randomized phase II study of R-CHOP with or without bortezomib in previously untreated patients with non-germinal center B-cell-like diffuse large B-cell lymphoma. *J Clin Oncol*. 2017;35(31):3538-3546.
10. Gidding CE, Kellie SJ, Kamps WA, de Graaf SS. Vincristine revisited. *Crit Rev Oncol Hematol*. 1999;29(3):267-287.
11. Wilson WH. Treatment strategies for aggressive lymphomas: what works? *Hematology (Am Soc Hematol Educ Program)*. 2013;2013(1):584-590.
12. Verma A, Jiang Y, Du W, Fairchild L, Melnick A, Elemento O. Transcriptome sequencing reveals thousands of novel long non-coding RNAs in B cell lymphoma. *Genome Med*. 2015;7(1):110.
13. Iqbal J, Shen Y, Huang X, et al. Global microRNA expression profiling uncovers molecular markers for classification and prognosis in aggressive B-cell lymphoma. *Blood*. 2015;125(7):1137-1145.
14. Musilova K, Mraz M. MicroRNAs in B-cell lymphomas: how a complex biology gets more complex. *Leukemia*. 2015;29(5):1004-1017.
15. Bartel DP. MicroRNAs: genomics, biogenesis, mechanism, and function. *Cell*. 2004;116(2):281-297.
16. Blower PE, Chung J-H, Verducci JS, et al. MicroRNAs modulate the chemosensitivity of tumor cells. *Mol Cancer Ther*. 2008;7(1):1-9.
17. Marques SC, Ranjbar B, Laursen MB, et al. High miR-34a expression improves response to doxorubicin in diffuse large B-cell lymphoma. *Exp Hematol*. 2016;44(4):238-246.
18. Rasmussen MH, Lyskjær I, Jersie-Christensen RR, et al. miR-625-3p regulates oxaliplatin resistance by targeting MAP2K6-p38 signalling in human colorectal adenocarcinoma cells. *Nat Commun*. 2016;7(1):12436.

19. Due H, Svendsen P, Bødker JS, et al. miR-155 as a biomarker in B-Cell malignancies. *BioMed Res Int*. 2016;2016:9513037.

20. Kluiver J, Kroesen B-J, Poppema S, van den Berg A. The role of microRNAs in normal hematopoiesis and hematopoietic malignancies. *Leukemia*. 2006; 20(11):1931-1936.

21. Jardin F, Figeac M. MicroRNAs in lymphoma, from diagnosis to targeted therapy. *Curr Opin Oncol*. 2013;25(5):480-486.

22. Babar IA, Cheng CJ, Booth CJ, et al. Nanoparticle-based therapy in an in vivo microRNA-155 (miR-155)-dependent mouse model of lymphoma. *Proc Natl Acad Sci USA*. 2012;109(26):E1695-E1704.

23. Falgreen S, Dybkær K, Young KH, et al. Predicting response to multidrug regimens in cancer patients using cell line experiments and regularised regression models. *BMC Cancer*. 2015;15(1):235.

24. Lenz G, Wright G, Dave SS, et al; Lymphoma/Leukemia Molecular Profiling Project. Stromal gene signatures in large-B-cell lymphomas. *N Engl J Med*. 2008;359(22):2313-2323.

25. Falgreen S, Laursen MB, Bødker JS, et al. Exposure time independent summary statistics for assessment of drug dependent cell line growth inhibition. *BMC Bioinformatics*. 2014;15(1):168.

26. Dybkær K, Bøgsted M, Falgreen S, et al. Diffuse large B-cell lymphoma classification system that associates normal B-cell subset phenotypes with prognosis. *J Clin Oncol*. 2015;33(12):1379-1388.

27. Ranjbar B, Krogh LB, Laursen MB, et al. Anti-apoptotic effects of lentiviral vector transduction promote increased rituximab tolerance in cancerous B-cells. *PLoS One*. 2016;11(4):e0153069.

28. Rasmussen TK, Andersen T, Bak RO, et al. Overexpression of microRNA-155 increases IL-21 mediated STAT3 signaling and IL-21 production in systemic lupus erythematosus. *Arthritis Res Ther*. 2015;17(1):154.

29. Bak RO, Hollensen AK, Primo MN, Sørensen CD, Mikkelsen JG. Potent microRNA suppression by RNA Pol II-transcribed 'Tough Decoy' inhibitors. *RNA*. 2013;19(2):280-293.

30. Hollensen AK, Thomsen R, Bak RO, et al. Improved microRNA suppression by WPRE-linked tough decoy microRNA sponges. *RNA*. 2017;23(8): 1247-1258.

31. Sanjana NE, Shalem O, Zhang F. Improved vectors and genome-wide libraries for CRISPR screening. *Nat Methods*. 2014;11(8):783-784.

32. Brinkman EK, Chen T, Amendola M, van Steensel B. Easy quantitative assessment of genome editing by sequence trace decomposition. *Nucleic Acids Res*. 2014;42(22):e168.

33. R Core Team. R: A Language and Environment for Statistical Computing. Vienna, Austria: R Foundation for Statistical Computing; 2017.

34. Irizarry RA, Hobbs B, Collin F, et al. Exploration, normalization, and summaries of high density oligonucleotide array probe level data. *Biostatistics*. 2003; 4(2):249-264.

35. Ritchie ME, Phipson B, Wu D, et al. limma powers differential expression analyses for RNA-sequencing and microarray studies. *Nucleic Acids Res*. 2015; 43(7):e47.

36. Johnson WE, Li C, Rabinovic A. Adjusting batch effects in microarray expression data using empirical Bayes methods. *Biostatistics*. 2007;8(1):118-127.

37. Leek JT, Johnson WE, Parker HS, Jaffe AE, Storey JD. The sva package for removing batch effects and other unwanted variation in high-throughput experiments. *Bioinformatics*. 2012;28(6):882-883.

38. Subramanian A, Tamayo P, Mootha VK, et al. Gene set enrichment analysis: a knowledge-based approach for interpreting genome-wide expression profiles. *Proc Natl Acad Sci USA*. 2005;102(43):15545-15550.

39. Liberzon A, Birger C, Thorvaldsdóttir H, Ghandi M, Mesirov JP, Tamayo P. The Molecular Signatures Database (MSigDB) hallmark gene set collection. *Cell Syst*. 2015;1(6):417-425.

40. Butz H, Likó I, Czirják S, et al. Down-regulation of Wee1 kinase by a specific subset of microRNA in human sporadic pituitary adenomas. *J Clin Endocrinol Metab*. 2010;95(10):E181-E191.

41. Tili E, Michaille J-J, Wernicke D, et al. Mutator activity induced by microRNA-155 (miR-155) links inflammation and cancer. *Proc Natl Acad Sci USA*. 2011;108(12):4908-4913.

42. Visconti R, Della Monica R, Palazzo L, et al. The Fcp1-Wee1-Cdk1 axis affects spindle assembly checkpoint robustness and sensitivity to antimicrotubule cancer drugs. *Cell Death Differ*. 2015;22(9):1551-1560.

43. Cheson BD, Pfistner B, Juweid ME, et al; International Harmonization Project on Lymphoma. Revised response criteria for malignant lymphoma. *J Clin Oncol*. 2007;25(5):579-586.

44. Ma X, Becker Buscaglia LE, Barker JR, Li Y. MicroRNAs in NF-kappaB signaling. *J Mol Cell Biol*. 2011;3(3):159-166.

45. Davis RE, Brown KD, Siebenlist U, Staudt LM. Constitutive nuclear factor kappaB activity is required for survival of activated B cell-like diffuse large B cell lymphoma cells. *J Exp Med*. 2001;194(12):1861-1874.

46. Clark PM, Loher P, Quann K, Brody J, Londin ER, Rigoutsos I. Argonaute CLIP-Seq reveals miRNA targetome diversity across tissue types. *Sci Rep*. 2014;4(1):5947.

47. Musacchio A, Salmon ED. The spindle-assembly checkpoint in space and time. *Nat Rev Mol Cell Biol*. 2007;8(5):379-393.

48. Gascoigne KE, Taylor SS. Cancer cells display profound intra- and interline variation following prolonged exposure to antimitotic drugs. *Cancer Cell*. 2008;14(2):111-122.

49. Rieder CL, Maiato H. Stuck in division or passing through: what happens when cells cannot satisfy the spindle assembly checkpoint. *Dev Cell*. 2004;7(5): 637-651.

50. Ghelli Luserna Di Rora A, Iacobucci I, Beeharry N, et al. The Wee1 inhibitor, MK-1775, sensitizes leukemic cells to different antineoplastic drugs interfering with DNA damage response pathway. *Blood*. 2015;126(23):1276.

51. Hirai H, Arai T, Okada M, et al. MK-1775, a small molecule Wee1 inhibitor, enhances anti-tumor efficacy of various DNA-damaging agents, including 5-fluorouracil. *Cancer Biol Ther*. 2010;9(7):514-522.

52. Huang X, Shen Y, Liu M, et al. Quantitative proteomics reveals that miR-155 regulates the PI3K-AKT pathway in diffuse large B-cell lymphoma. *Am J Pathol*. 2012;181(1):26-33.

53. Costinean S, Sandhu SK, Pedersen IM, et al. Src homology 2 domain-containing inositol-5-phosphatase and CCAAT enhancer-binding protein beta are targeted by miR-155 in B cells of Emicro-MiR-155 transgenic mice. *Blood*. 2009;114(7):1374-1382.

54. Lee E-R, Kim J-Y, Kang Y-J, et al. Interplay between PI3K/Akt and MAPK signaling pathways in DNA-damaging drug-induced apoptosis. *Biochim Biophys Acta*. 2006;1763(9):958-968.

55. Doublier S, Riganti C, Voena C, et al. RhoA silencing reverts the resistance to doxorubicin in human colon cancer cells. *Mol Cancer Res*. 2008;6(10):1607-1620.

56. Pouliot LM, Chen Y-C, Bai J, et al. Cisplatin sensitivity mediated by WEE1 and CHK1 is mediated by miR-155 and the miR-15 family. *Cancer Res*. 2012;72(22):5945-5955.

57. Lv L, An X, Li H, Ma L. Effect of miR-155 knockdown on the reversal of doxorubicin resistance in human lung cancer A549/dox cells. *Oncol Lett*. 2016;11(2):1161-1166.

58. Pallasch CP, Leskov I, Braun CJ, et al. Sensitizing protective tumor microenvironments to antibody-mediated therapy. *Cell*. 2014;156(3):590-602.

59. Zhong H, Xu L, Zhong J-H, et al. Clinical and prognostic significance of miR-155 and miR-146a expression levels in formalin-fixed/paraffin-embedded tissue of patients with diffuse large B-cell lymphoma. *Exp Ther Med*. 2012;3(5):763-770.

60. Go H, Jang J-Y, Kim P-J, et al. MicroRNA-21 plays an oncogenic role by targeting FOXO1 and activating the PI3K/AKT pathway in diffuse large B-cell lymphoma. *Oncotarget*. 2015;6(17):15035-15049.

Supplementary material for:

MicroRNA-155 Controls Vincristine Sensitivity and Predicts Superior Clinical Outcome in Diffuse Large B-cell Lymphoma

Hanne Due, Anna Amanda Schönherz, Laura Ryø, Maria Nascimento Primo, Ditte Starberg Jespersen, Emil Aagaard Thomsen, Anne Stidsholdt Roug, Min Xiao, Xiaohong Tan, Yuyang Pang, Ken H Young, Martin Bøgsted, Jacob Giehm Mikkelsen, and Karen Dybkær.

Supplementary Tables

Supplementary Table 1. Cell line specifications.

Cell line	AUC	Vincristine class	ABC/GCB	Endogenous miR-155
OCI-Ly19	53.99	Sensitive	UC	11.79
FARAGE	56.11	Sensitive	GCB	13.01
SU-DHL-5	57.86	Sensitive	GCB	11.20
MC-116	61.97	Intermediate	GCB	12.48
NU-DHL-1	70.72	Intermediate	ABC	10.40
OCI-Ly3	74.83	Intermediate	ABC	14.18
HBL-1	84.53	Intermediate	ABC	13.65
U2932	85.34	Intermediate	GCB	12.70
NU-DUL-1	90.25	Intermediate	UC	11.02
RIVA	108.99	Intermediate	ABC	12.32
OCI-Ly7	114.49	Resistant	GCB	6.66
SU-DHL-8	126.06	Resistant	GCB	8.14
DB	130.75	Resistant	GCB	8.10

DLBCL cell lines DB, NU-DHL-1, NU-DUL-1, MC-116, and SU-DHL-5 were purchased from DSMZ (German Collection of Microorganisms and Cell Cultures), while FARAGE, HBL-1, OCI-Ly3, OCI-Ly7, OCI-Ly19, RIVA, SU-DHL-8, and U2932 were kindly provided by Dr. Jose A. Martinez-Climent (Molecular Oncology Laboratory, University of Navarra, Pamplona, Spain). The cell lines are ranked according to vincristine sensitivity based on area under dose-response curve (AUC).[1] Division into tertiles defines 3 sensitive, 7 intermediate, and 3 resistant cell lines. Based on GEP, DLBCL cell lines were classified into ABC/GCB subclasses by Wright classification using published algorithms at hemaClass.org.[2] Endogenous miR-155 expression levels are measured by GeneChip miRNA 1.0.2 arrays. Data is RMA normalized, thus the specified values are in log2

scale. For technical validation of miRNA array data, the expression levels of miR-155 were determined by RT-qPCR (data not shown).

Supplementary Table 2. Patient characteristics.

Characteristic	In-house cohort	Meta-cohort
No. of patients	73	701
Sex		
Female	30 (41%)	297 (42%)
Male	43 (59%)	404 (58%)
Age at diagnosis		
Median	64	62
Range	20-87	17-82
IPI score		
0-1	21 (29%)	71 (10%)
2-3	36 (49%)	314 (45%)
4-5	12 (16%)	201 (29%)
NA	4 (6%)	115 (16%)
ABC/GCB		
ABC	32 (44%)	302 (43%)
GCB	32 (44%)	281 (40%)
UC	9 (12%)	118 (17%)

IPI, International prognostic index; NA, not available; UC, unclassified.

Supplementary Table 3. Vincristine response specific miRNAs.

miRNA	P-value	Log2(Fold change)	Fold change	Fold change description
hsa-miR-155	0.0008	4.37	20.67	Resistant down vs. sensitive
hsa-miR-148a	0.03	3.14	8.82	Resistant down vs. sensitive
hsa-miR-21	0.01	2.79	6.90	Resistant down vs. sensitive
hsa-let7b	0.02	2.75	6.75	Resistant down vs. sensitive
hsa-miR-21-star	0.006	2.29	4.90	Resistant down vs. sensitive
hsa-miR-23a	0.03	2.07	4.21	Resistant down vs. sensitive
hsa-miR-501-3p	0.04	1.99	3.98	Resistant down vs. sensitive
hsa-miR-24	0.02	1.89	3.71	Resistant down vs. sensitive
hsa-let7c	0.01	1.45	2.73	Resistant down vs. sensitive
hsa-miR-550	0.02	1.32	2.50	Resistant down vs. sensitive
hsa-miR-378-star	0.006	1.20	2.29	Resistant down vs. sensitive
hsa-miR-658	0.04	1.19	2.28	Resistant down vs. sensitive
hsa-miR-675	0.01	1.09	2.13	Resistant down vs. sensitive
hsa-miR-484	0.05	1.14	2.20	Resistant up vs. sensitive
hsa-miR-223	0.009	1.27	2.41	Resistant up vs. sensitive

Differentially expressed miRNAs detected comparing global miRNA expression profiles of vincristine sensitive and resistant DLBCL cell lines (p-values ≤ 0.05 and FC >|2|).

Supplementary Table 4. Enriched gene sets identified through GSEA analysis conducted for miR-155 vs. control

Gene sets enriched in miR-155	Total size	ES	NES	NOM p-val	FDR q-val	Enrichment Rank (ES)
E2F_TARGETS	188	0.8	2.83	0	0	2223
MYC_TARGETS_V1	171	0.78	2.74	0	0	2596
G2M_CHECKPOINT	189	0.74	2.63	0	0	2223
MYC_TARGETS_V2	55	0.84	2.5	0	0	1574
MTORC1_SIGNALING	185	0.53	1.91	0	0	2326
HYPOXIA	189	0.52	1.83	0	0	1880
GLYCOLYSIS	191	0.51	1.82	0	0	2538
SPERMATOGENESIS	128	0.53	1.81	0	0	2125
DNA_REPAIR	133	0.52	1.79	0	0	2328
MITOTIC_SPINDLE	195	0.47	1.7	0	0.001	1714
OXIDATIVE_PHOSPHORYLATION	175	0.46	1.62	0	0.003	3042
ESTROGEN_RESPONSE_LATE	194	0.38	1.38	0.004	0.039	3332
UV_RESPONSE_UP	153	0.39	1.36	0.012	0.044	2845
Gene sets enriched in control	**Total size**	**ES**	**NES**	**NOM p-val**	**FDR q-val**	**Enrichment Rank (ES)**
MYOGENESIS	193	-0.35	-1.23	0.052	0.117	3423
IL2_STAT5_SIGNALING	189	-0.35	-1.26	0.032	0.154	1693
APICAL_JUNCTION	194	-0.36	-1.26	0.041	0.166	2391
KRAS_SIGNALING_DN	186	-0.36	-1.29	0.029	0.171	3077
APOPTOSIS	146	-0.39	-1.35	0.017	0.108	1833
P53_PATHWAY	192	-0.38	-1.36	0.013	0.108	2756
PI3K_AKT_MTOR_SIGNALING	99	-0.43	-1.41	0.023	0.082	1345
IL6_JAK_STAT3_SIGNALING	83	-0.52	-1.68	0.002	0.004	2056
ALLOGRAFT_REJECTION	183	-0.52	-1.85	0	0	2002
INTERFERON_GAMMA_RESPONSE	180	-0.55	-1.93	0	0	1983
INTERREFON_ALPHA_RESPONSE	86	-0.67	-2.16	0	0	1982

Gene set enrichment analysis (GSEA) was conducted for transcriptional profiles of SU-DHL-5 cells transduced with LV/miR-155 and LV/MCS, respectively. GSEA was restricted to genes sets included in the *Hallmark* collection (50 gene sets) from the Molecular Signature Database. Gene sets with normalized p-value≤0.05 and FDR q-value≤0.25 were considered significantly enriched. Only significant gene sets were shown in the table. Abbreviations: Total size, number of genes included in the gene set; ES, enrichment score; NES, normalized enrichment score; NOM p-val, multiple test corrected p-value for gene set size normalized ES; FDR q-val, false discovery rate of normalized ES.

Supplementary Table 5. Enriched gene sets identified through GSEA analysis conducted for TuD-155 vs. control

Gene sets enriched in TuD	Total size	ES	NES	NOM p-val	FDR q-Val	Enrichment Rank (ES)
n.d.	n.d.	n.d.	n.d.	n.d.	n.d.	n.d.
Gene sets enriched in control	**Total size**	**ES**	**NES**	**NOM.p.val**	**FDR.q.Val**	**Enrichment Rank**
XENOBIOTIC_METABOLISM	191	-0.33	-1.28	0.043	0.139	2335
MITOTIC_SPINDLE	195	-0.33	-1.29	0.033	0.134	3184
UV_RESPONSE_UP	153	-0.36	-1.37	0.015	0.068	3270
P53_PATHWAY	192	-0.37	-1.42	0.007	0.045	3051
ADIPOGENESIS	187	-0.39	-1.53	0.001	0.014	4682
MYC_TARGETS_V2	55	-0.53	-1.73	0	0.001	3681
FATTY_ACID_METABOLISM	144	-0.46	-1.74	0	0.001	3457
DNA_REPAIR	133	-0.47	-1.74	0	0.001	4388
MTORC1_SIGNALING	185	-0.45	-1.76	0	0.001	3914
OXIDATIVE_PHOSPHORYLATION	175	-0.48	-1.84	0	0	5592
HYPOXIA	189	-0.49	-1.9	0	0	2180
GLYCOLYSIS	191	-0.49	-1.92	0	0	2787
G2M_CHECKPOINT	189	-0.54	-2.1	0	0	2787
MYC_TARGETS_V1	171	-0.59	-2.29	0	0	3600
E2F_TARGETS	188	-0.65	-2.51	0	0	3463

Gene set enrichment analysis (GSEA) was conducted for transcriptional profiles of SU-DHL-5 cells transduced with LV/TuD-155 and LV/MCS, respectively. GSEA was restricted to genes sets included in the *Hallmark* collection (50 gene sets) from the Molecular Signature Database. Gene sets with normalized p-value≤0.05 and FDR q-value≤0.25 were considered significantly enriched. Only significant gene sets were shown in the table. Abbreviations: Total size, number of genes included in the gene set; ES, enrichment score; NES, normalized enrichment score; NOM p-val, multiple test corrected p-value for gene set size normalized ES; FDR q-val, false discovery rate of normalized ES; n.d., not detected.

Supplementary Table 6. Negatively correlated genes associated with cell cycle processes.

		Prediction algorithms				
Gene Symbol	Gene Ontology Biological Process	TagetScan	miRDB	mircroRNA .org	MicroT-DCD	TarBase
WEE1	G2/M transition	+	+	+	+	IP, RA
CAB39 *RPS6KB1*	Cell cycle arrest G1/S transition	+	+	+	+	-
GSK3B	Re-entry into mitosis	+	-	+	+	PR
PARD3B *TFDP2*	Mitotic cell cycle	+	-	-	+	-
C7orf25 *PAK2* *RBBP4*	G1/S transition Mitotic cell cycle G2/M transition	-	-	-	+	-
38961, APPL1 CABLEES1, CCPG1, HAPECAM2, MAPRE2, PVRIG, RABGAP1, RASSF2, SGSM3,	Cell cycle	-	-	-	-	-
CSNK2A1, FAM89B, GARASP1, HISTH14, MAU2, MCPH1, NEK6, NUP188, NUP214, POLD4	Mitotic cell cycle	-	-	-	-	-
CLIP1, KIF2B	Mitotic cell cycle Microtubule	-	-	-	-	-
CAMK2D, CRLF3, CUL3, EIF4E, ITGB1, MARK4, PIM2, PPP3CA, PPP6C, PSMB9, PSMD9, SPDYA, UBA52, VIL1	G1/S transition	-	-	-	-	-
ANAPC10, CDK5RAP, CSNK1D, DCTN2, DYNC1|2, ENSA, EP300, FBXL15, PCM1, PPM1D, PPP1R12A, PPP2R2A, SDCCAG8, STK16, TUBG2, TUBGCP6	G2/M transition	-	-	-	-	-
CCNG2	Cell cycle checkpoint	-	-	-	-	-
CAB39L, SESN2	Cell cycle arrest	-	-	-	-	-

GEP of SU-DHL-5 cells transduced with LV/miR-155, LV/TuD-155, and the comparable negative control LV/MCS were investigated for identifying negatively correlated gene expressions. The 64 genes related to cell cycle processes were investigated as potential miR-155 targets using four well-documented miRNA-mRNA prediction algorithms: TargetScan v7.1, miRDB, microRNA.org, and MicroT-CDC.[3–6] Published experimental

validated miRNA-mRNA interactions were identified from TarBase v7.0.[7] IP, immunoprecipitation; PR, proteomics; RA, reporter assay; - not identified; + identified. If more than one gene is noted in the Gene Symbol Column, +/- symbol is related to all the genes.

Supplementary Table 7. Simple and multiple Cox regression analyses conducted for: (A) all DLBCL patients, (B) ABC classified patients, and (C) GCB classified patients included in the R-CHOP restricted meta-cohort.

		n	no.	Simple			Multiple		
				HR	95% CI	*P*	HR	95% CI	*P*
A.									
All DLBCL	IPI								
	0-1	71	6	1			1		
	2-3	314	84	3.76	1.64-8.61	0.0017	3.29	1.43-7.56	0.0050
	4-5	201	106	9.61	4.22-21.88	7.19e-08	8.09	3.53-18.54	7.78e-07
	Subclass								
	ABC	242	105	1			1		
	GCB	248	58	0.45	0.33-0.62	1.09e-06	0.41	0.28-0.59	1.37e-06
	UC	96	34	0.73	0.50-1.08	0.11	0.52	0.34-0.81	0.0032
	miR-155								
	Continuous	586	197	0.95	0.86-1.04	0.28	-	-	-
B.									
ABC-DLBCL	IPI								
	0-1	15	2	1					
	2-3	125	38	3.57	0.86-14.89	0.080	-	-	-
	4-5	102	65	10.37	2.51-42.87	0.0012	-	-	-
	miR-155								
	Continuous	242	105	0.85	0.71-1.00	0.052	-	-	-
C.									
GCB-DLBCL	IPI								
	0-1	48	2	1			1		
	2-3	140	32	6.22	1.49-25.97	0.012	5.95	1.43-24.86	0.014
	4-5	60	24	12.53	2.96-53.06	0.0006	11.37	2.68-48.26	0.00098
	miR-155								
	Continuous	248	58	0.72	0.60-0.86	0.00044	0.74	0.62-0.89	0.0016

Array-based miR-155 expression (continuous) and outcome were analyzed by simple and multiple Cox proportional hazards regression analyses for overall survival. IPI score information was not available for all patients, thus cohort sizes are reduced in this setting (115 samples were removed). The multiple Cox proportional regression analysis was performed using an additive model with IPI (trichotomized; IPI 0-1, IPI 2-3, IPI 4-5), ABC/GCB (ABC, GCB, UC), and miR-155 expression (continuous) as independent confounders. Abbreviations: CI, 95% lower and upper confidence intervals; HR, hazard ratio; n, number of samples; no., number of events; - value not available since variables were only included in multiple Cox proportional hazards regression analysis if significant results were obtained in simple Cox proportional hazards regression analysis.

Supplementary Figures

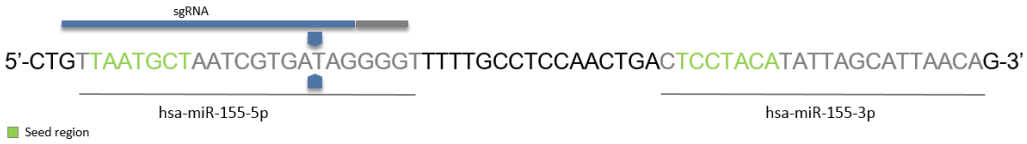

Supplementary Figure 1. Schematic presentation of sgRNA for miR-155 knock-out by the CRISPR-Cas9 technology. The single guide RNA (sgRNA) targets the functional part of miR-155-5p of the miR-155 encoding gene *MIR155HG*.[8] The expected Cas9 cut site is marked by ■ . The sequences encoding miR-155-5p and miR-155-3p (miR-155-star) are marked in grey and seed regions are marked in green.

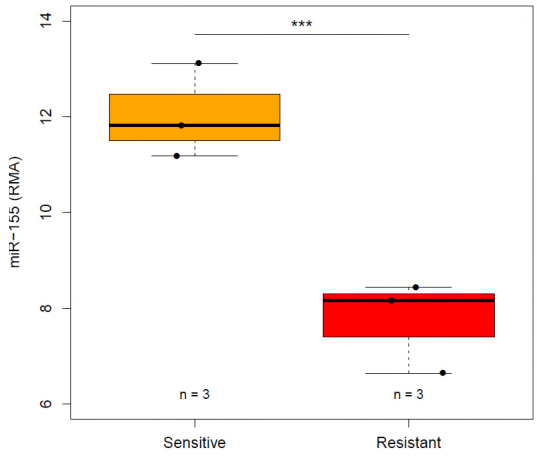

Supplementary Figure 2. miR-155 expression in DLBCL cell lines. Expression levels of miR-155 in vincristine sensitive (OCI-Ly19, FARAGE, SU-DHL-5) and resistant DLBCL cell lines (OCI-Ly7, SU-DHL-8, DB) determined by GeneChip miRNA 1.0.2 microarrays. *** $p<0.001$

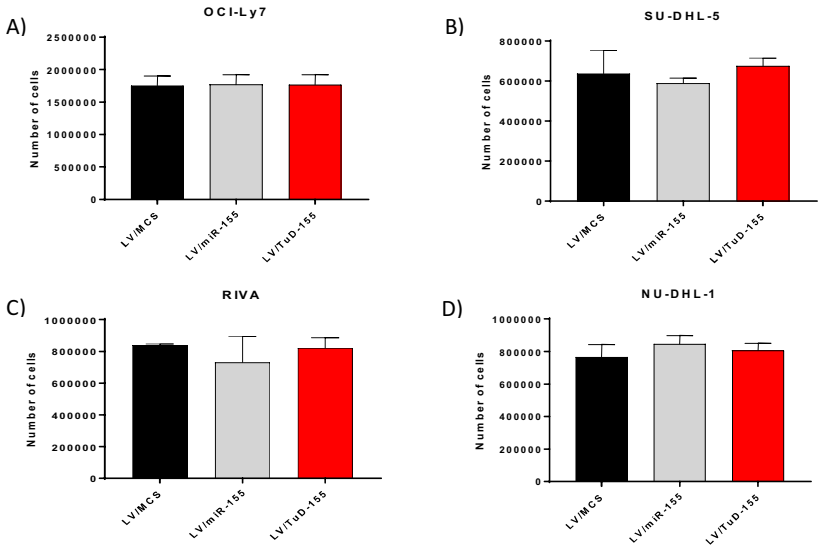

Supplementary Figure 3. Cell growth post-transduction. Cell proliferation was determined by the trypan blue exclusion method after 48 hours of growth in (A) OCI-Ly7, (B) SU-DHL-5, (C) RIVA, and (D) NU-DHL-1 cells transduced with LV/miR-155, LV/TuD-155, and LV/MCS. These cell lines were chosen for *in vitro* studies based on ABC/GCB classification, resistance/sensitivity to vincristine, and lentiviral transducibility.[9] The latter is of great importance, since B-cells generally are difficult to transduce.

A)

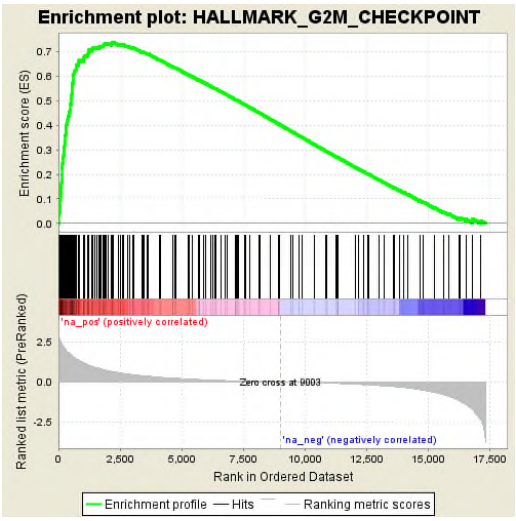

B)

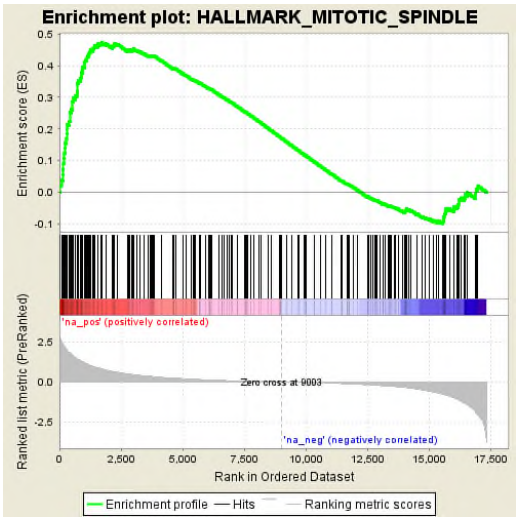

C)

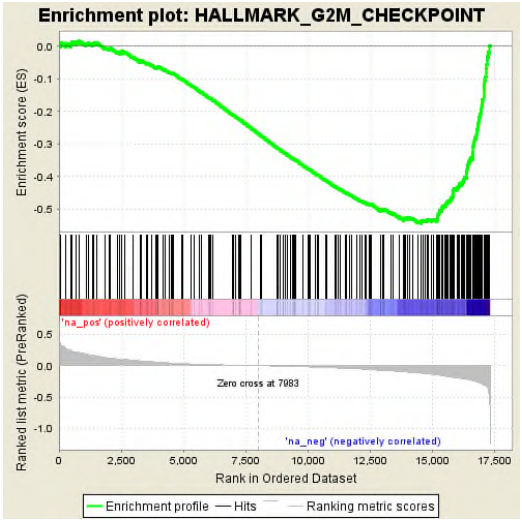

D)

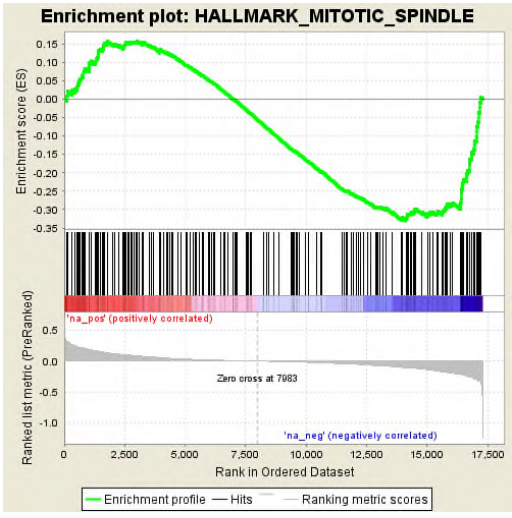

Supplementary Figure 4. Enrichment plots generated by GSEA analysis for (A+B) miR-155 vs. control and (C+D) TuD-155 vs. control. GSEA was conducted for transcriptional profiles of SU-DHL-5 cells transduced with LV/miR-155, LV/TuD-155 and LV/MCS (control), respectively. GSEA was restricted to genes sets included in the *Hallmark* collection (50 gene sets) from the Molecular Signature Database. Gene sets with normalized p-value≤0.05 and FDR q-value≤0.25 were considered significantly enriched. Significance of each enrichment score was calculated by 2000 permutation tests. Since vincristine functions as an antimitotic drug, only

significantly enriched gene sets associated with G2/M checkpoints and mitotic spindle assembly were depicted. The green line represents the running-sum statistic used to calculate the enrichment score (ES) of the gene set. The ES is represented as maximum deviation from zero encountered in the running-sum statistic. The vertical black bars beneath the enrichment score curve indicate the positions of gene set members and their expression profile (red, upregulated; blue, downregulated).

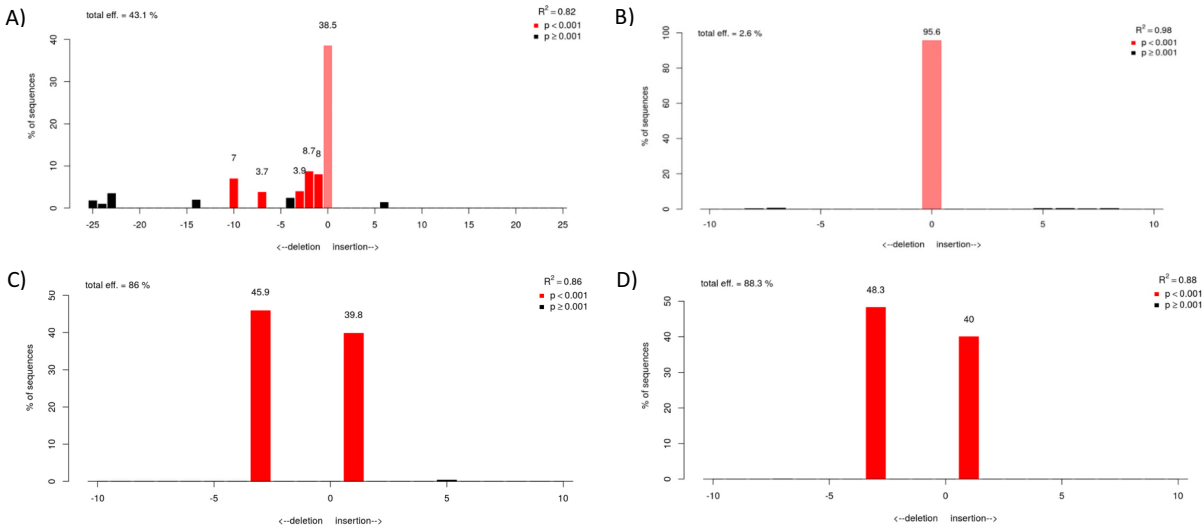

Supplementary Figure 5. Indel frequencies. Indel frequencies determined by TIDE analysis in: (A) OCI-Ly7 cells transduced with LV/CRISPR-sgRNA-miR-155. (B) OCI-Ly7 cells transduced with LV/CRISPR-sgRNA-control. (C+D) miR-155 knock-out clone 1 and 2, respectively, which are characterized by a single nucleotide insertion on one allele and a 3 nucleotide deletion on the other.

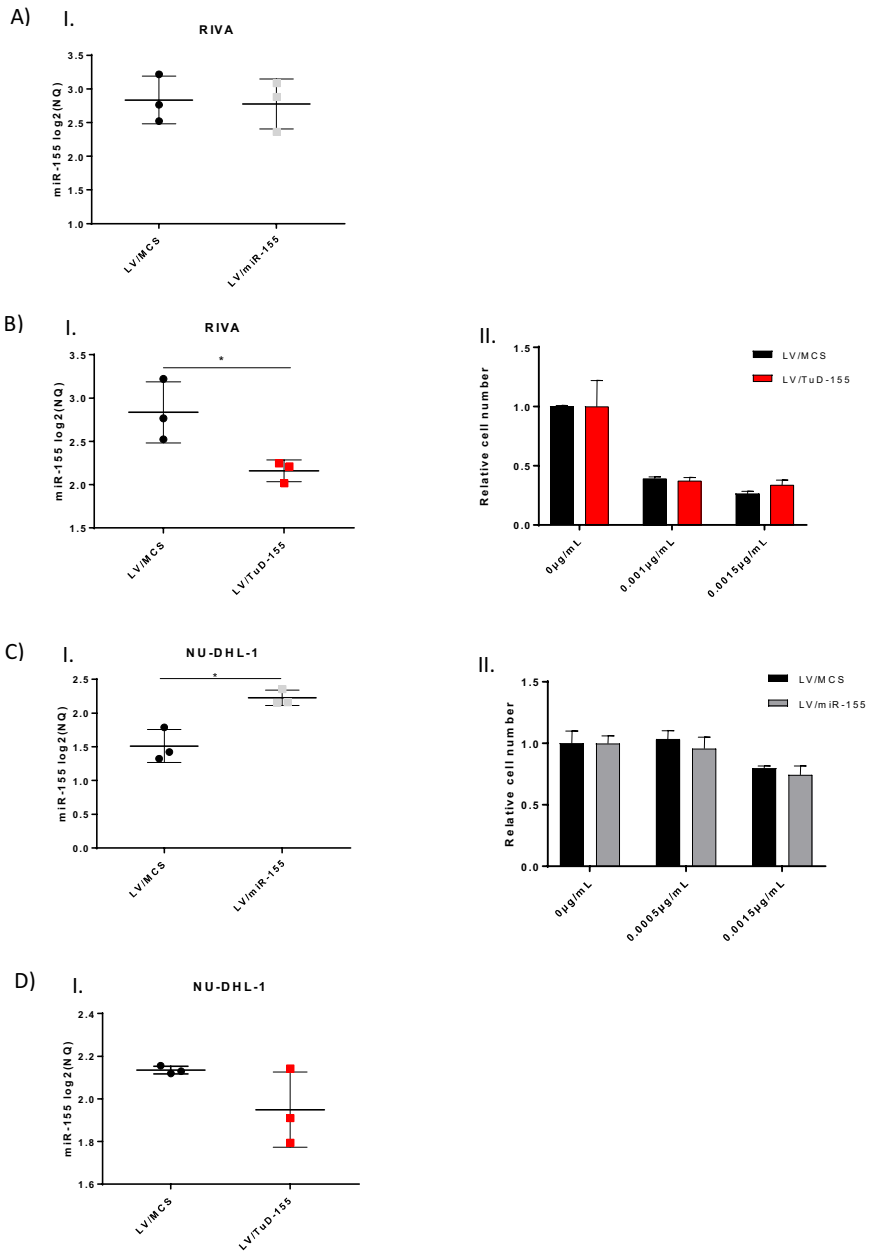

Supplementary Figure 6. Manipulation of miR-155 expression in ABC-DLBCL cell lines do not affect vincristine response. (AI+BI) Expression levels of miR-155 were determined upon lentiviral transductions of

RIVA cells. (BII) Vincristine dose-response analysis was performed for TuD-155 transduced cells, since miR-155 was significantly down-regulated. (CI+DI) Similarly, NU-DHL-1 cells were transduced and miR-155 expression was measured and (CII) vincristine response was investigated in miR-155 over-expressing cells (LV/miR-155). Vincristine response is shown as number of cells relative to the no-drug condition. NQ, normalized quantity.

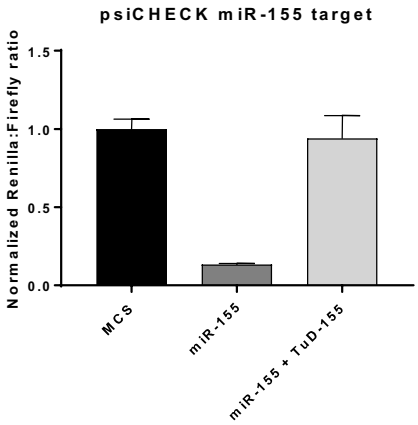

Supplementary Figure 7. Suppression of miR-155 by TuD-155. Dual luciferase reporter assays were performed in HEK293 cells co-transfected with psiCHECK-miRtarget, pCCL/U1-miRNA.PGK-eGFP and pCCL/PGK-eGFP-TuD.

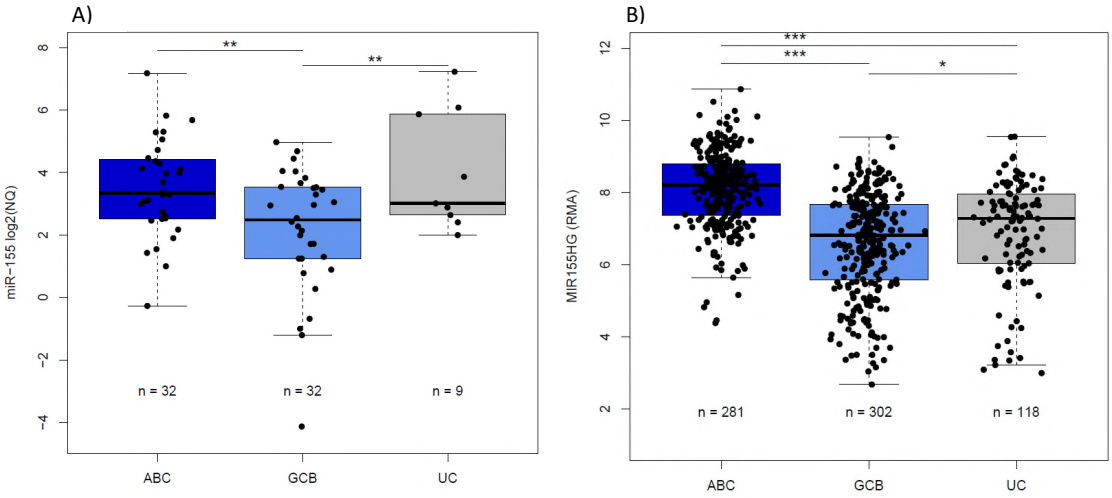

Supplementary Figure 8. miR-155 expression in ABC/GCB subclasses of DLBCL. (A) Expression levels of miR-155 in the ABC/GCB subclasses of the in-house cohort measured by RT-qPCR. (B) Expression levels of *MIR155HG* determined by microarray (Human Genome U133 Plus 2.0) in the meta-cohort. Significance levels: * p<0.05, ** p<0.01, ***p<0.001. NQ, normalized quantity; RMA, Robust Multichip Average normalized.

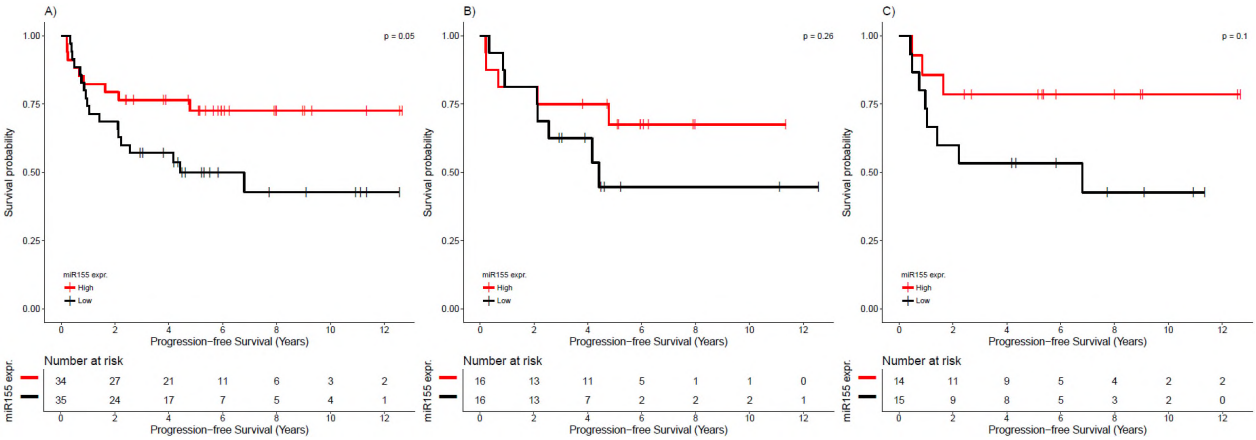

Supplementary Figure 9. Analysis of association between progression-free survival and miR-155 expression. Kaplan-Meier plots depicting progression-free survival of R-CHOP treated DLBCL patients in the in-house cohort. The analysis was conducted for (A) all DLBCL patients, (B) ABC classified patients, and (C) GCB classified patients. For each cohort, patients were dichotomized by median split of miR-155 expression.

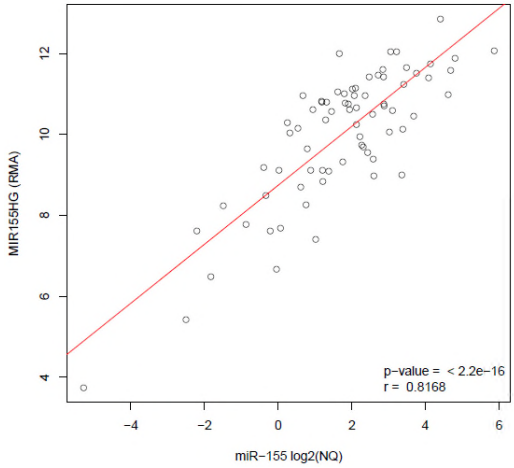

Supplementary Figure 10. Correlation analysis between *MIR155HG* and miR-155 expression. In the in-house cohort of 73 samples, the mature miR-155 expression measured by RT-qPCR was well correlated to its precursor *MIR155HG* measured by microarray (HG-U133; 229437_at) (r=0.8, p<2.2e-16). NQ, normalized quantity; RMA, Robust Multichip Analysis normalized.

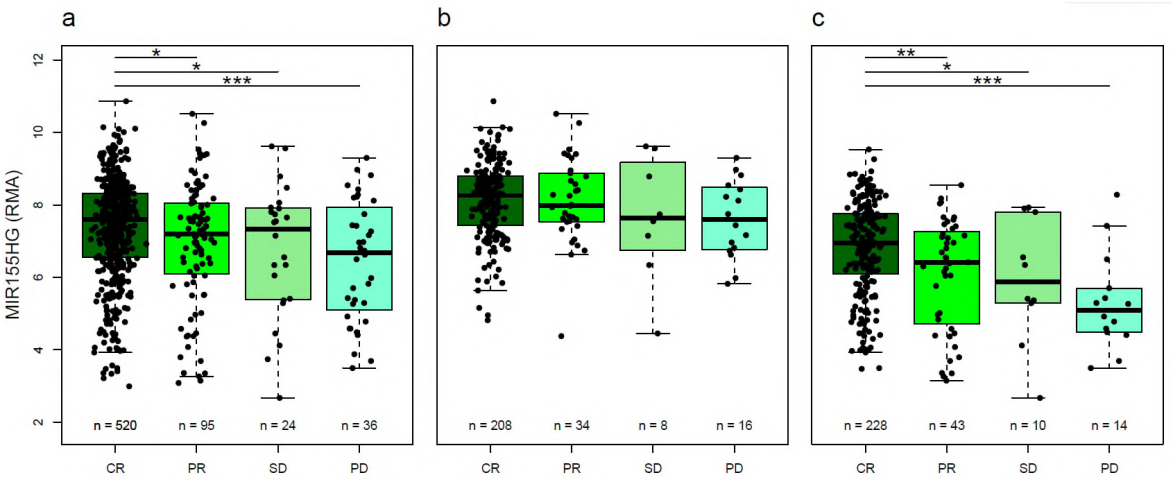

Supplementary Figure 11. MIR155HG expression levels in Cheson response evaluation classes. Response evaluations of patients in the validation cohort were extracted and investigated for association to MIR155HG expression. The analysis was performed for (A) all DLBCL patients, (B) ABC classified patients, and (C) for GCB classified patients. Significance levels: * p<0.05, ** p<0.01, ***p<0.001. CR, complete remission; PD, progressive disease; PR, partial remission; RMA, Robust Multichip Average normalized; SD, stable disease.

Supplementary References

1. Falgreen S, Dybkær K, Young KH, et al. Predicting response to multidrug regimens in cancer patients using cell line experiments and regularised regression models. *BMC Cancer*. 2015;15(1):235.

2. Falgreen S, Ellern Bilgrau A, Brøndum RF, et al. hemaClass.org: Online One-By-One Microarray Normalization and Classification of Hematological Cancers for Precision Medicine. *PLoS One*. 2016;11(10):e0163711.

3. TargetScanHuman 7.1.

4. Wong N, Wang X. miRDB: an online resource for microRNA target prediction and functional annotations. *Nucleic Acids Res.* 2015;43(D1):D146–D152.

5. Betel D, Wilson M, Gabow A, Marks DS, Sander C. The microRNA.org resource: targets and expression. *Nucleic Acids Res.* 2007;36(Database):D149–D153.

6. Paraskevopoulou MD, Georgakilas G, Kostoulas N, et al. DIANA-microT web server v5.0: service integration into miRNA functional analysis workflows. *Nucleic Acids Res.* 2013;41(W1):W169–W173.

7. Vlachos IS, Paraskevopoulou MD, Karagkouni D, et al. DIANA-TarBase v7.0: indexing more than half a million experimentally supported miRNA:mRNA interactions. *Nucleic Acids Res.* 2015;43(D1):D153–D159.

8. sgRNA Designer: CRISPRko.

9. Ranjbar B, Krogh LB, Laursen MB, et al. Anti-Apoptotic Effects of Lentiviral Vector Transduction Promote Increased Rituximab Tolerance in Cancerous B-Cells. *PLoS One*. 2016;11(4):e0153069.

Cancer Chemotherapy and Pharmacology (2019) 84:471–485
https://doi.org/10.1007/s00280-019-03884-5

REVIEW ARTICLE

Aspects of vincristine-induced neuropathy in hematologic malignancies: a systematic review

Marie Lindhard Madsen[1] · Hanne Due[1,2] · Niels Ejskjær[2,3] · Paw Jensen[1,4] · Jakob Madsen[1] · Karen Dybkær[1,2,4]

Received: 29 January 2019 / Accepted: 4 June 2019 / Published online: 18 June 2019

Abstract

Purpose Vincristine is widely used as anticancer therapy for a variety of hematological malignancies. The treatment is limited by progressive vincristine-induced neuropathy, possibly including both peripheral sensory and motor nerves, autonomic nervous functions, and the central nervous system. This dose-limiting side-effect can diminish quality of life and, furthermore, cause discontinuation of vincristine treatment. The present review elucidates the current knowledge regarding vincristine-induced neuropathy in hematologic malignancies, focusing on neuropathy assessment, clinical and molecular predictive markers, drug–drug interference, prevention, and treatment.

Methods This review is conducted by a systematic search strategy for the identification of relevant literature in the PubMed and Embase databases.

Results No clinical parameters displayed convincing potential as predictors of vincristine-induced neuropathy; however, preexisting neuropathy was consistently reported to be associated with an increased risk of neurotoxicity. In contrast, molecular markers, including polymorphisms in genes involved in the pharmacodynamics and pharmacokinetics of vincristine, displayed great potential as predictive markers of neuropathy incidence and severity. Furthermore, antifungal drugs, such as itraconazole and voriconazole, decrease the metabolism of vincristine and consequently lead to severe neuropathy when co-administered with vincristine, underscoring why fluconazole should be the antifungal drug of choice.

Conclusion Reports from the 71 included studies clearly emphasize the lack of consistency in neuropathy assessment, grading systems, and reporting, making it difficult to interpret results between studies. Thus, truer clinical and molecular markers could emerge if the consistency of neuropathy detection and reporting increases by the use of conventional standardized neuropathy assessment tools and grading scales.

Keywords Vincristine · Vincristine-induced neuropathy · Neurotoxicity · Hematologic malignancies · Biomarkers

Introduction

Vincristine is a chemotherapy drug belonging to the group of vinka alkaloids, which also includes vinblastine and vindesine, which has been widely used since its approval in 1963 [1]. The antimitotic drug is used in the treatment of several solid tumors and hematologic malignancies, including breast cancer, non-Hodgkin's lymphomas (NHL), and leukemia [2]. Vincristine exerts its anti-neoplastic effect by inhibiting polymerization of tubulin and incorporation into microtubules, which prevents mitotic spindle assembly, leading to extension of mitosis and thereby apoptosis [3, 4].

The dose-limiting side effect of vincristine is neurotoxicity, which may lead to severe peripheral sensory and motor neuropathies affecting quality of life (QOL), treatment delay, and vincristine substitution or discontinuation. The impact

Marie Lindhard Madsen and Hanne Due Shared first authorship.

Electronic supplementary material The online version of this article (https://doi.org/10.1007/s00280-019-03884-5) contains supplementary material, which is available to authorized users.

✉ Karen Dybkær
k.dybkaer@rn.dk

[1] Department of Hematology, Aalborg University Hospital, Sdr. Skovvej 15, 9000 Aalborg, Denmark

[2] Department of Clinical Medicine, Aalborg University, Sdr. Skovvej 15, 9000 Aalborg, Denmark

[3] Steno Diabetes Center North Denmark, Aalborg University Hospital, 9000 Aalborg, Denmark

[4] Clinical Cancer Research Center, Aalborg University Hospital, Sdr. Skovvej 15, 9000 Aalborg, Denmark

of adapted use of vincristine on outcome is debatable [5–7]. Vincristine interferes with microtubules, which are critical components of nerve axons functioning as tracks for vesicle-mediated transport, and leads to axonopathy that manifests slowly and progressively [8]. Vincristine-induced neuropathy (VIN) spans a broad spectrum of dysfunctions that fall into three categories: sensory, motor, and autonomic neuropathy (Table 1). The most common is peripheral sensory and motor nerve neuropathy characterized by numbness, paresthesia, impaired balance, weakened tendon reflexes, and altered gait [9]. Autonomic dysfunctions includes constipation, paralytic ileus, urinary retention and orthostatic hypotension [10, 11]. Furthermore, several cranial nerve palsies and some central nerve system (CNS) toxicities have been reported (Table 1) [12–27], even though vincristine poorly penetrates the blood–brain barrier [28]. Although neurotoxicity is widely recognized as a common side-effect of vincristine treatment in hematologic neoplasms, little is known about the true incidence, short- and long-term manifestations and severity due to lack of consistency in detection, definition, and reporting.

Overall survival for adult hematologic cancer patients has improved during the past decades due to new treatment options, and more than 80% of children with acute lymphoblastic leukemia (ALL) are now long-term survivors [29]. This therapeutic success, however, comes with the cost of more people experiencing early- and late-onset adverse effects, consequently affecting the recovering patient's QOL, which is especially important in children with a long expected lifespan after treatment. Although the intensity of the symptoms may not be extensive, the inconvenience is not correlated, and QOL can be greatly impaired [30]. Given the increasing numbers of cancer survivors, the clinical significance of chemotherapy-induced neuropathy is increasing; consequently, clinical and molecular risk predictors, prevention and treatment options, and measuring methods are urgently warranted. In this paper, we systematically review parameters related to vincristine-induced neurotoxicity in hematologic patients, and we discuss their importance.

Methods

This review was completed according to the Preferred Reporting for Systematic Reviews and Meta-analyses (PRISMA) Guidelines [31].

Search strategy and study selection

PubMed and Embase databases were systematically searched for current literature on VIN in patients with hematologic malignancies. Supplementary Table 1 outlines the search strategy. The search was performed on 16 July 2018 and identified 1949 articles after removal of duplicates, which subsequently were manually screened based on title and abstract by two independent individuals. Articles not focusing on hematologic malignancies or vincristine-induced neuropathy were excluded as were reviews, conference abstracts, nonhuman studies, and data not published in English. The remaining articles were assessed for eligibility by full-text screening, and 71 articles were included in this systematic review after applying the same exclusion parameters (Supplementary Fig. 1).

Table 1 Types of vincristine-induced neuropathy

Type	Definition	Symptoms	References
Sensory neuropathy	Sensory nerve damage	Paresthesia in form of numbness, tingling and pricking. Pain, impaired vibration/touch sensitivity/temperature recognition	[9, 92]
Motor neuropathy	Motor nerve damage	Motor weakness, walking difficulties, muscle cramps, weakened tendon reflexes and fine motor skills	[92]
Autonomic neuropathy	Autonomic nerve damage	Constipation, ileus, urinary retention, incontinence, hypotension	[11, 92]
Optic neuropathy	Cranial nerve II damage	Blurred vision, color vision deficiency, transient/permanent blindness	[12, 13]
Oculomotor nerve palsy	Cranial nerve III damage	Ptosis, ophthalmoplegia	[14–16]
Abducens nerve palsy	Cranial nerve VI damage	Ptosis, strabismus, ocular muscle paresis, diplopia	[17, 18]
Facial nerve palsy	Cranial nerve VII damage	Limited movement of facial muscles and jaw	[19]
Acoustic nerve palsy	Cranial nerve VIII damage	Hearing loss	[20]
Ototoxicity	Cochlear damage	Decrease in frequencies, decrease of contralateral suppression amplitudes	[21]
Hypoglossal nerve palsy	Cranial nerve XII damage	Loss of tongue movement	[19]
Vocal cord palsy	Laryngeal nerve damage	Stridor, respiratory distress, persistent cough	[22, 23]
Encephalopathy/PRES	Cerebral dysfunction	Disorientation, hemiplegia, global aphasia, seizures	[24, 25]
SIADH	Cerebral axonal swelling	Hyponatremia, seizures, mental changes	[26, 27]

PRES posterior reversible encephalopathy syndrome, *SIADH* syndrome of inappropriate antidiuretic hormone secretion

Results

A total of 71 articles were included in this systematic review (Supplementary Fig. 1). Of these articles, 13 investigated VIN measuring methods [9, 32–43], while 11 records investigated clinical risk predictors for VIN development [44–54]. Fifteen records studied molecular risk parameters [5, 55–68]. In addition 12 records described interactions between vincristine and other drugs, mainly antifungal triazoles [1, 69–79], while 8 records addressed prevention and treatment options [10, 19, 80–85]. The remaining 12 records were of mixed character and included long-term effects, assessment of QOL, and dose-dependent VIN studies [30, 86–96].

The 71 articles include studies of VIN in both pediatric and adult hematologic malignancies, including ALL, diffuse large B cell lymphoma, follicular lymphoma, multiple myeloma, Burkitt lymphoma, anaplastic large-cell lymphoma, and Hodgkin's lymphoma. The reported frequency of vincristine-induced neurotoxicity in these studies varies tremendously from approximately 100% [34] to 10% [48] depending on patient exclusion criteria, vincristine doses and number of treatment cycles, and the methods of obtaining neuropathy information.

Methods for VIN measuring

Numerous methods for assessment of neuropathy are used in different studies. There is no gold standard, making it difficult to compare studies. This lack of a standard is most likely the reason why the reported incidence of neuropathy in patients treated with vincristine varies so significantly. In 1981, the World Health Organization (WHO) initiated a set of recommendations on standardized approaches to recording baseline data, reporting of treatment, reporting of response, and grading of acute and subacute toxicity to assess the problem that it is difficult for investigators to compare their results with those of others [97]. WHO's peripheral neuropathy score comprises 5 grades (0–4); noteworthy, only two of the included studies applied WHO's neurotoxicity score [5, 65].

In 2003, the National Cancer Institute of the National Institutes of Health released the Common Terminology Criteria for Adverse Events (CTCAE), which was revised from a widely used neuropathy grading scale, named the Common Toxicity Criteria, that was developed in 1984 [98]. CTCAE is still occasionally used today [67]. However, as it was shown to underestimate both incidence and severity of neuropathy, several scores have been made to overcome this problem, including the Total Neuropathy Score (TNS) [34, 99]. TNS consists of ten items that are both subjective and objective; however, the TNS was found to be too burdensome and time-consuming for application in everyday clinical practice and consequently reduced into a clinical version (TNSc), a reduced version (TNSr), and a neuropathy score that quite often used in pediatric patients, called the Pediatric modified Total Neuropathy Score (Ped-mTNS) [32]. The Ped-mTNS consists of the first seven items of TNS and was shown to be a reliable and valid measure of VIN in school-aged children [33]. Compared with Ped-mTNS, CTCAE version 3.0 failed to identify sensory neuropathy in 40% of subjects and significant motor neuropathy in 15% when applied on children treated for ALL, lymphoma or non-CNS solid tumors [34]. Thus, the detection method itself greatly influences the result, illustrating the need to introduce and unify detection and quantification of VIN.

A study examined the validity, reliability and clinical feasibility of several VIN measures in ALL children [35]. The study mostly concentrated on a variation of TNS, referred to as Total Neuropathy Score-Pediatric Vincristine (TNS-PV), which was found useful for measuring VIN in children over the age of 5 years; additionally, some of the items were responsive to change over time. Furthermore, they tested CTCAE version 4.0 and the Balis grading scale, which both presented a risk of underestimating VIN. The FACES pain scale was feasible for pain severity quantification in children of all ages. In addition to the previously established measurements, they developed a simple test V-Rex consisting of the two most responsive items, vibration and reflex, which is better than standard grading scale methods according the study [35].

Symptoms of VIN are mostly subjective; thus, self-reported data could be preferable in VIN assessment. The European Organization for Research and Treatment of Cancer (EORTC) developed a questionnaire intended to supplement the core quality of life questionnaire to assess chemotherapy-induced neuropathy (QLQ-CIPN20) [42]. The 20-item questionnaire includes information on symptoms and functional limitations, and comparison to CTCAE in two large datasets revealed a strong correlation between patients with high CTCAE grade and QLQ-CIPN20 score, documenting the validity of self-reported data in terms of chemotherapy-induced neuropathy [43].

Interestingly, studies have shown a difference between children and adults in the type of nerves that are the most affected with a predominance of sensory neuropathy in adults [90, 100, 101]. Electrodiagnostic examinations, including nerve conduction of different nerves, T-reflex measurement and needle electromyography, showed a electrophysiological and clinical motor predominance in children aged 1–17 years [39], which is consistent with other studies using nerve conduction and somatosensory evoked potentials [9, 38, 41, 86]. Furthermore, a study demonstrated

that measurements of compound muscle action potential amplitude on the median and/or peroneal nerve could objectively grade VIN in children [9]. In addition to sensory and motor, the third neuropathy modality is autonomic. Heart rate variability, reflecting a vagal nerve lesion, is useful to detect and quantify autonomic cardioneuropathy in children diagnosed with ALL [36]. Furthermore, a study used The Michigan Autonomic Symptoms Survey, but interestingly no abnormalities in autonomic functions were found [40].

Many new neurotoxicity scores have continuously been developed. Of these scores, some focus on objective findings, while others are of more subjective character. Although CTCAE still develops new versions, it seems to have been outdated by newer approaches. Despite findings suggesting motor predominance in children and sensory predominance in adults, no consensus exists on the best methods of obtaining VIN information in hematological patients of different age.

Clinical predictors

Although occurrence of neurotoxicity is high, little is known about risk factors for developing neuropathy during vincristine treatment. A consensus about possible risk factors is lacking, and numerous parameters are only studied and reported in a limited number of studies with relatively small study populations. The dose-limitation of vincristine is 1.4 mg/m^2 in each cycle with a maximum of 2 mg per cycle, and higher doses exert greater toxicity and questionably result in better treatment outcome [91, 92, 102]. The most consistent observation is that the severity of neuropathy increases with accumulated vincristine dose [49, 92, 103]. Furthermore, several studies report advanced age in pediatric patients as a clinical risk factor [61, 69, 73]. However, some studies do not find this correlation in pediatric or adult patients [44, 49] and others even suggest the opposite for both groups [54, 88, 95].

It has been suggested that neuropathy incidence could be disease dependent given that a significantly higher incidence in patients suffering from lymphoma is observed compared with nonlymphoid cancer patients (e.g., leukemia, breast cancer, malignant melanoma) [88]. Fourteen out of 23 patients with lymphoma and 5/37 patients without lymphoma developed neuropathy despite comparable dosage [88], and concordant observations were made by others [46]. A higher percentage of lymphoma patients have elevated levels of serum alkaline phosphatase, which significantly prolongs elimination of vincristine and results in longer vincristine exposure and associated toxicities [46]. Furthermore, the results from this study indicate that area under the vincristine plasma concentration time curve and elevated serum alkaline phosphatase are predictors of VIN [46]; however, the latter observation is contradicted in a study of 26 patients reporting that serum alkaline phosphatase is not important [92].

Several factors have been suggested as possible predictors for VIN. A study from 2010 aimed to identify predictors for chemotherapy-induced peripheral neuropathy, including vincristine, in 52 patients [49]. It was discovered that the number of chemotherapy cycles was a predictor of VIN, whereas age and coadministration with nonsteroidal anti-inflammatory drugs did not correlate with neuropathy incidence and severity. Consistently, Anghelescu et al. observed no difference in age between ALL patients with or without neuropathy development [44]. No differences in sex, BMI group, initial leukocyte count, ALL immunophenotype, DNA index, or different genetic translocations were noted. The only significant clinical predictive variable observed was white non-Hispanic race [44].

Another study focused on the potential effect of micronutrient deficiency on VIN by measurement of serum vitamin E, vitamin B_{12} and folate together with nerve conduction studies at a mean 20 months after the last vincristine injection; however, no significant association was observed [45]. Furthermore, the impact of liver dysfunction was examined in two independent studies, where one recommended reduced vincristine dosage [46] whereas the other did not [88].

Despite the fact that some records mention diabetes mellitus as a risk factor for developing VIN [103–105], thorough studies are lacking. Patients with diabetes are at risk of diabetic neuropathy; therefore, it could be logical to assume that diabetic patients are at higher risk for VIN. Noteworthy, diabetic neuropathy is a long-term risk of diabetes; therefore, it is important to be aware of the difference between diabetes as a risk factor and diabetic neuropathy as a secondary risk factor.

Hyperglycemia is a common side-effect of corticosteroid therapy that is often noted with vincristine treatment and potentially leads to diabetes [106]. The effect of hyperglycemia was studied in 278 patients with ALL during induction chemotherapy regimens including vincristine [48]. Hyperglycemia was defined as glucose level ≥ 200 mg/dL on ≥ 2 determinations, and the study included 20 patients (7%) previously diagnosed with diabetes. Statistically significant differences in peripheral neuropathy were not noted between 103 patients with hyperglycemia and the 175 patients without; furthermore, a subanalysis of patients with previously diagnosed diabetes or elevated baseline blood glucose did not reveal any differences. Consistently, no difference in neuropathy incidence was found when comparing diabetic patients requiring diabetic medications with nondiabetic patients [54].

Furthermore, the consequences of hyperglycemia in elderly patients were examined and included 162 patients with NHL treated with vincristine among other

chemotherapeutic drugs [47]. The authors found that baseline hyperglycemia, stage, creatinine clearance and hyperglycemia during chemotherapy was associated with grade 3–4 toxicity of 18 symptoms, including neuropathy, diarrhea, fatigue and pneumonia, without separate and focused analysis of the individual symptoms.

The risk of severe neurotoxicity due to other forms of pre-existing diseases than diabetes is more substantiated. Care should be taken when administrating vincristine to Charcot-Marie-Tooth disease (CMT) patients, the most common hereditary neuropathic disease. A clinical challenge is undiagnosed cases of CMT, and seeking information about family history of CMT before initiating chemotherapy with vincristine could possibly prevent patients from severe neuropathy given that pediatric ALL often is diagnosed before the age of 10 and CMT after the age of 10 [51]. Pediatric and adult cancer patients are at risk of undiagnosed CMT [50]. Even small doses of vincristine that are normally not associated with neuropathy can cause exaggerated and irreversible neuropathy in these patients [50]. Another form of neuropathy presenting clinical problems is the autoimmune Guillain–Barré syndrome (GBS). Acute onset GBS can be difficult to differentiate from VIN, and this differential diagnoses is important to have in mind as GBS can be treated with immunoglobulins. Uncertainty still remains whether GBS and VIN can exaggerate one another [52, 53].

This section clearly emphasizes the inconsistency between studies; however, clinical parameters, including white non-Hispanic race and preexisting neuropathy, such as CMT, are consistently reported in more than one study to predict increased risk of VIN. When assessing the currently available literature, preexisting diabetes does not increase the risk of VIN. Hyperglycemia presenting during induction chemotherapy or later in the course of chemotherapy also does not increase the risk of VIN.

Molecular predictors

The hepatic cytochrome P450 3A (CYP3A) enzyme subfamily is the most important system for drug metabolism. Vincristine is primarily metabolized by CYP3A4 and CYP3A5, of which the latter is considerably more effective [107]. Given that 60% of African–Americans express the CYP3A5 enzyme compare with 33% of Caucasians [108], several studies have investigated race-specific genotypes and tested whether African–Americans metabolize vincristine more effectively, resulting in lower vincristine exposure and associated toxicities (Table 2). A retrospective study analyzed 92 Caucasian and 21 African–American pediatric ALL patients and identified VIN symptoms in 35% of Caucasians compared with 5% of African–Americans [57]. Additionally, Caucasians experienced more severe vincristine-associated neuropathy and had more reductions in total doses. However, it is important to highlight that race is used as a surrogate for the *CYP3A5* genotype, and no genotyping was conducted.

The most common genetic germline polymorphisms are *CYP3A4*1B*, *CYP3A5*3*, and *CYP3A5*6*, of which the latter two variants induce splice variants and protein truncation leading to substantially decreased expression of CYP3A5 in the liver [108]. Increased incidence of VIN has been observed in patients who expressed *CYP3A5*3*; although the percentage of African–Americans expressing *CYP3A5*3* was greater than Caucasians, the difference did not reach statistical significance potentially due to the small sample size [64]. Furthermore, a higher incidence of neuropathy was detected in Caucasians (81%) than African–Americans (77%); however, substantially higher frequencies were noted for both ethnicities compared with the study by Renbarger et al. [57] (Table 2).

CYP3A variants were determined by others without focusing on ethnicity [55, 56, 59, 66, 67] (Table 2). The CYP3A5 genotype was studied in 78 Kenyan children with different cancer diagnoses [67]. Seventy-one of the 78 subjects (91%) were homo- or heterozygous for the *CYP3A5*1* allele, which are phenotypic identical and lead to high expression of CYP3A5. Children with genotypes causing low CYP3A5 expression had significantly higher detectable vincristine levels in plasma compared with high expressers. Regardless of several neuropathy assessment tools, minimal neuropathy was detected, and no difference in neuropathy incidence or severity was observed despite differences in vincristine plasma concentrations. Noteworthy, Kenyan children experienced negligible VIN compared with US children despite receiving at least 33% more vincristine at baseline due to protocol-specific dosing [67], indirectly supporting the observations of race and CYP3A genotype.

Genotyping of 105 Caucasian children with ALL revealed that 82% of the patient are low CYP3A5 expressers (*CYP3A5*3* genotype) with a higher incidence and severity of vincristine-induced side effects and more reductions of vincristine compared with CYP3A5 expressers [59]. Thus, the *CYP3A5*3* genotype causes increased vincristine exposure, leading to higher neuropathy incidence and severity grade; however, information on clinical impact was not reported.

Studies to date have focused on genetic variants of genes involved in the pharmacokinetics of vincristine. Other biological processes can also affect VIN; hence, polymorphisms in microRNAs regulating vincristine-related genes have been examined [5]. A mutation in the seed region of miR-3117 was detected that could affect binding to the drug transporter genes ABCC1 and RALB1, which are predicted to be targets of miR-3117 in at least six prediction databases and consequently affect the regulation and expression of the targets. In addition, they identified a mutation causing alteration of

Table 2 Molecular predictors of vincristine-induced neuropathy

Polymorphism	Outcome	Race	No. of patients	Genotyping	Neuropathy assessment	References
Race used as surrogate for CYP3A5	VIN in 35% of Caucasians and 5% of African–Americans ↑ VIN severity in Caucasians Dose reduction in 4% of Caucasians and 0.1% of African–Americans	92 Caucasians 21 African–Americans	113 children (ALL)	Not performed	Not reported	[57]
CYP3A5*3	82% of non-African–Americans 25% of African–Americans	31 African–Americans 502 Other	533 children (ALL)	Pyro-sequencing	CCG toxicity criteria	[55]
CYP3A4*1B CYP3A5*3	NS					
CYP3A5*6	NS					
	VIN in 81% of Caucasians and 77% Africans–Americans	37 Caucasians 17 African–Americans	54 children (ALL)	RT-qPCR	Balis Pediatric Scale	[64]
CYP3A5*3	67% of the patients: 27 Caucasians, VIN in 82% 8 African–Americans, VIN in 75%					
CYP3A*1/*1 CYP3A*1 CYP3A5*3	91% of patients CYP3A5 high expressers CYP3A5 low expressers Higher vincristine plasma dose No difference in VIN	Kenyan	78 children (Leukemia/ Lymphoma: 44 solid tumors: 34)	OpenArray RT-qPCR	NCI-CTCAE, Balis Pediatric Scale, Faces Pain Scale, Pediatric Neuropathic Pain Scale, TNS	[67]
CYP3A1*/*1 CYP3A5*1/*3 CYP3A5*3/3* CYP3A5*6 CYP3A*7	1% of patients 15% of patients VIN in 18% 84% of patients VIN in 22% 0% of patients	Turkish	115 children (ALL: 72 solid tumors: 43)	RFLP	NCI-CTCAE	[66]
CYP3A5*3/*3 CYP3A5*1/*3	82% of patients (CYP3A5 low expressers) ↑ VIN incidence + severity ↑ dose reductions 18% of patient (CYP3A5 expressers) ↓ VIN incidence + severity	105 Caucasians 1 African–American 1 Asian	107 children (preB ALL)	RT-qPCR	NCI-CTCAE	[59]
CYP3A5*3	↑ Risk of VIN	44 black, 167 white, 1 Asian, 28 other	240 children (ALL)	Not specified	NCI-CTCAE	[56]

Table 2 (continued)

Polymorphism	Outcome	Race	No. of patients	Genotyping	Neuropathy assessment	References
miR-3117*	↓ Risk of VIN Potentially affects regulation of drug transporters ABCC1 and RALBP1	Spanish	175 children (preB ALL)	GoldenGate Genotype Assay	WHO Peripheral Nervous System toxicity Criteria	[5]
miR4481*	↑ Risk of VIN Involved in peripheral nerve regeneration					
	VIN in 27% of patients	209 European 43 African 2 Asian 44 Hispanic 23 Other	321 children (ALL)	GeneChip 500 K array or SNP 6.0 array	NCI-CTCAE	[61]
CEP72*	16% of patients VIN in 56%, ↑ risk and severity					
CEP72*	31% of cases and 10% of controls. CEP72* cases: ↑ VIN	Cases: 3 Hispanic, 38 Non-Hispanic, 7 unknown. Control: 4 Hispanic, 41 Non-Hispanic, 3 Unknown	48 adults with VIN (Cases) 48 adults without VIN (Controls) (ALL)	RT-qPCR	NCI-CTCAE	[62]
	25.4% VIN in early phase 4.2% VIN in late phase	Spanish	142 children (B-ALL)	PCR	NCI-CTCAE	[63]
CEP72*	No association to neurotoxicity during the early phase of treatment					
CEP72*	↑ Incidence of VIN Detected in 16% of VIN cases and in 5% without VIN	78% European	224 children (ALL)	RT-qPCR	NCI-CTCAE	[68]
ABCC1* SLC5A7*	↑ VIN severity ↑ VIN severity			Custom Infinium Panel		
ACTG1*	↑ VIN severity grade	Caucasian	339 children (ALL)	Sequenom Genotyping	NCI-CTCAE	[60]
CAPG*	↑ VIN severity grade					
ABCB1*	↓ Risk of VIN					
ABCC2*	↑ VIN severity grade	Spanish	152 children (B-ALL)	GoldenGate Genotyping Assay	WHO Peripheral Nervous System toxicity Criteria	[65]
GLI1*	Early-onset VIN in 4% ↑ VIN	Not specified	250 adults (MM)	Custom-build targeted genotyping (3404 SNPs)	NCI-CTCAE	[58]
ABCC1*	Late-onset VIN in 7% ↑ VIN					

ALL acute lymphoblastic leukemia, *NCI-CTCAE* National Center Institute Common Terminology Criteria for Adverse Events, *NS* no significance, *MM* multiple myeloma, *RFLP* PCR-Restriction Fragment Length Polymorphism, *TNS* total neuropathy score

the secondary structure of miR-4481a mutation, which is potentially involved in peripheral nerve generation. Consistently, polymorphisms in ABCC1 and ABCB1 drug transporters correlate with neurotoxicity, which also applies to ACTG1 and CAPG1 polymorphisms that are targeted upon vincristine treatment [60, 68]. By dividing VIN into early- and late-onset, it was observed that early-onset neurotoxicity was associated with upregulation of genes and SNPs in genes involved in cell cycle and proliferation, whereas late-onset neurotoxicity was characterized by polymorphisms in genes involved in absorption, distribution, metabolism and excretion [58].

A study was conducted for the identification of genetic germline variants associated with the occurrence and severity of VIN in 321 pediatric ALL patients using Affymetrix GeneChip 500 K or SNP 6.0 array [61]. They identified a SNP in the promoter region of CEP72 that encodes a centrosomal protein essential for microtubule formation, which is directly involved in the mechanism of action of vincristine. This mutation introduces a binding site for transcriptional repression leading to lower expression of CEP72, which causes microtubule instability and increased vincristine sensitivity [61]. The CEP72 variant was observed in 50 of 321 pediatric ALL patients, which had a significantly higher incidence and severity grade of neurotoxicity that was consistent with findings of others [68]. Furthermore, they examined the variant in adult ALL patients using a case–control setup with 48 patients who developed VIN and 48 who did not, which confirmed the high incidence of neurotoxicity in CEP72 variant patients [62]. Consistent with these findings, the potential of the CEP72 variant as a marker of VIN was investigated in Spanish ALL-diagnosed children; however, no association was found [63]. The inconsistency between studies could be due to population differences and the fact that the studies by Diouf et al. [61] focused on neuropathy in the later phase of treatment compared with the early phase in the study by Gutierrez-Camino et al. [63]. As no association was found, they conducted another study analyzing SNPs in 8 genes and 13 miRNAs involved in vincristine pharmacokinetics, which revealed strong association between neurotoxicity and polymorphisms in ABCC2 [65].

Several genes involved in the pharmacokinetics and pharmacodynamics of vincristine display potential as predictive markers of VIN risk. Thus, genotyping can be useful to guide individualized treatment to maximize the therapeutic benefit and avoid unnecessary toxicity even if the role of race and early/late VIN remains incompletely characterized.

Drug–drug interference

Concomitant administration of drugs always carries the risk of drug–drug interaction. This effect can delay, decrease or enhance the absorption or metabolism of either drug, consequently affect the drug action and cause adverse effects. A major cause of morbidity and mortality in patients with hematological malignancies treated with immunosuppressive protocols are invasive fungal infections [70]. Antifungal triazole drugs, such as fluconazole, itraconazole and voriconazole, are the main agents for prophylaxis and treatment [1], and itraconazole is preferred given its broader spectrum of activity, especially against *Aspergillus* infections [75]. Unfortunately, the combination of vincristine and itraconazole has proven unfortunate (Table 3).

Several case reports and retrospective studies describe the outcome of VIN when antifungal triazoles are co-administered [1, 69–76]. This interaction is mostly described in pediatric ALL patients but is also seen in adults (Table 3). Especially during chemotherapy induction, children are at increased risk of fungal infections due to neutropenia and corticosteroid administration; therefore, antifungal prophylaxis could be worth considering [69]. This interaction was first described in 1995 where 4 out of 14 adults experienced severe neurotoxicity during vincristine induction therapy and antifungal prophylaxis with itraconazole [72]. The prescribed itraconazole dose in this report was 400 mg/day; however, the same outcome has been observed and reported in several other cases treated with lower doses (Table 3). The study compared neurotoxic complications with a previous series of 460 ALL patients treated with an identical cytostatic regimen and found that the incidence of VIN enlarged and the symptoms were more severe. This severely aggravated neurotoxicity is also described by others [70, 75]; in addition, CNS toxicity has been recorded in 30% of the patients receiving itraconazole [76].

As mentioned, vincristine is metabolized by CYP3A. Fluconazole and itraconazole inhibit the action of CYP3A, and the former is far less potent than itraconazole [109]. Furthermore, itraconazole inhibits the P-glycoprotein efflux pump, a vincristine transporter, resulting in higher intracellular vincristine concentrations [110]. Thus, coadministration of vincristine and itraconazole decreases the metabolism of vincristine to a greater extent than coadministration with fluconazole, causing notably enhanced neurotoxicity. Consistently, three studies did not observe significant differences in neuropathy upon fluconazole treatment [69, 71, 73], whereas six independent studies report higher incidence and severe neuropathy upon itraconazole treatment [1, 70, 72, 74–76] (Table 3).

A study by Yang et al. found that coadministration of vincristine with itraconazole or voriconazole resulted in a significantly higher incidence of vincristine-associated adverse effects than in patients treated with fluconazole and control patients only treated with vincristine [1]. Additionally, they found that the incidence of VIN was significantly higher in itraconazole-treated patients compared with patients treated with voriconazole.

Table 3 Drug–drug interactions with antifungal drugs

Drug	Dose	Diagnosis	No. of patients	Neurotoxic outcome	References
Fluconazole	4 mg/kg/day max 200 mg/day 5 patients: 300–400 mg/day	ALL	197 children	NS	[69]
Fluconazole	4 mg/kg/day	ALL	31 children	NS	[73]
Fluconazole Voriconazole Fluconazole and voriconazole	Not stated	ALL ($n=114$) HL ($n=16$)	130 patients < 22 y/o	NS	[71]
Fluconazole	8 mg/kg/day iv ($n=42$)	ALL	136 cases	NS	[1]
Itraconazole	5 mg/kg/day os ($n=44$)			VIN, CNS, autonomic	
Voriconazole	8 mg/kg/day capsules ($n=6$)			VIN severity: Itraconazole > voriconazole	
Fluconazole	5 mg/kg/day ($n=1$)	ALL	20 children	NS	[76]
Itraconazole	5 mg/kg/day ($n=16$)			VIN, CNS, SIADH, ileus	
Voriconazole	14 mg/kg/day iv ($n=3$)			VIN	
Itraconazole	400 mg/day capsules	ALL	14 patients 16–29 y/o	Severe VIN, ileus	[72]
Itraconazole	5 mg/kg/day capsules	ALL ($n=7$) B-cell NHL ($n=1$) T cell NHL ($n=1$)	9 children	VIN, autonomic, seizures, SIADH	[75]
Itraconazole	200 mg/day capsules	ALL	2 patients 19 and 55 y/o	Autonomic, SIADH	[74]
Itraconazole	200 mg/day os	ALCL ($n=1$) DLBCL ($n=3$) FL ($n=1$) unspecified lymphoma ($n=2$)	7 adults	Severe VIN, ileus	[70]

ALCL anaplastic large cell lymphoma, *ALL* acute lymphoblastic leukemia, *DLBCL* diffuse large B-cell lymphoma, *FL* follicular lymphoma, *HL* Hodgkin's lymphoma, *iv* intravenous, *NHL* non-Hodgkin's lymphoma, *NS* no significance, *os* oral solution, *SIADH* syndrome of inappropriate antidiuretic hormone secretion, *y/o* years old

Numerous drugs are capable of CYP3A inhibition/induction and consequently have the potential to interfere with vincristine. Protease inhibitor-based antiretroviral therapy, such as ritonavir, causes excessive neurotoxicity when co-administered with vinblastine, another vinka alkaloid, due to CYP3A4 inhibition [77, 78]. Furthermore, a study from a 1996 report on drug–drug interactions between colony-stimulating factors and vincristine indicated that the underlying mechanisms for the observed induced neuropathy is not thoroughly studied; to our knowledge, the mechanism not been reported to date [79].

Drug interactions should always be kept in mind when administering more than one drug but especially when administering toxic drugs, such as chemotherapy. When using vincristine, which is almost completely metabolized by the liver, it is important to be aware of concomitant use of a drug that is also metabolized by CYP3A. Fluconazole should be preferred over both voriconazole and itraconazole for antifungal prophylaxis or treatment given that itraconazole especially has the potential to cause severe neurotoxicity.

Prevention and treatment

Vincristine-induced neuropathy can be momentary and reversible; however, it is occasionally irreversible [87, 89]. Regardless, neuropathy may consequently necessitate dose-reduction or cessation, thus reducing the treatment efficacy and potentially shortening the overall survival time. Another perspective is that neuropathy can significantly impact the QOL [94], and neuropathy severity does not necessarily correlate with how much it affects the patient [30]. These problems can potentially be overcome by identifying substances with the ability to prevent and/or treat neuropathy.

Several agents have been suggested and tested for prevention and treatment of VIN; however, the results have not been promising. Currently, convincing evidence of useful pharmacologic interventions is lacking.

A study provides information on the beneficial effects from bracing and physical therapy to prevent fixed contractures/surgery when suffering from peroneal nerve palsy [80]. An older study from 1992 proposed Org 2766, a corticotropin (4–9) analogue, as a means to ameliorating vincristine neuropathy

and additionally observed higher neurotoxicity in the placebo group [81]. Another study did not find Org 2766 to be neuroprotective [85].

Gabapentin has been tested both as prophylaxis and treatment in pediatric ALL; however, no conclusions could be made other than gabapentin did not prevent the recurrence of neuropathic pain [44]. Moreover, analgesic adjuvants given to reduce neuropathy symptoms did not show adequate prophylactic efficacy [49].

Pyridoxine (vitamin B6) and pyridostigmine (acetylcholinesterase inhibitor) have been used in the treatment of different types of VIN. Treatment of 4 ALL patients with pyridoxine and pyridostigmine for sensorimotor polyneuropathy resulted in full recovery 1–2 weeks after treatment initiation [82]. In agreement, a case study presented an ALL patient who on day 61 was diagnosed with bilateral cranial nerve VII and XII palsy and subsequently treated with intravenous pyridoxine, and complete recovery of symptoms was achieved after 2 weeks of treatment [19]. In both reports, uncertainty remained regarding whether pyridoxine/pyridostigmine was responsible for the resolution as it could have been a consequence of vincristine discontinuation.

To evaluate potential preventive effects of glutamic acid, a randomized study was conducted on 94 children diagnosed with hematological malignancies and 12 with Wilms tumor who received either glutamic acid (1.5 g/day divided into 3 doses) or placebo [10]. They found a statistically significant difference between the two groups when assessing paresthesia, patellar/Achilles reflexes, and frequency of constipation but not until the third and fourth visit, suggesting that glutamic acid may improve tolerance of vincristine. In contrast, a larger randomized study in which 200 children with ALL or NHL and 50 children with Wilms tumor or rhabdomyosarcoma received either preventive glutamic acid (250 mg capsules 3 times a day, body surface area $<1\ m^2 = 1$ capsule, $>1\ m^2 = 2$ capsules) or placebo did not find a statistically significant difference in any parameters [83]. Another similar amino acid, glutamine, has shown possible beneficial effects on sensory neuropathy and self-reported QOL [84]. The study included 31 children with hematological malignancies and 18 children with nonhematological malignancies, which were only analyzed as one group.

Due to the high prevalence of VIN, it would be of great significance to find possible prevention or treatment measures. Unfortunately, it has not been possible to find a substance with this property in current studies. Many of the substances are only tested a few times and in small studies, but glutamine could display potential if further studied.

Discussion

This systematic review identified a total of 71 studies addressing the circumstances concerning VIN in hematological patients. Although this subject obviously contains many aspects, almost none of the findings are clear-cut. In general, more research is needed given that VIN can necessitate treatment alterations and possibly last for a long period of time, significantly impacting QOL.

In addition to a cumulative dose, this systematic review did not find consistency for any clinical predictors potentially due to differences in cohort sizes, vincristine doses and cycles, and neuropathy assessment tools. In addition, several studies include patients with different cancer diagnoses, which potentially could introduce a bias given that vincristine interacts differently with cancers [46, 88]. Consequently, further studies in larger settings are urgently warranted to fully elaborate the impact of these clinical parameters.

Caution is important with patients already suffering from CMT; however, the rareness and common time of diagnosis of this condition make it troublesome. A simple self-reporting checklist, which is not expensive or time-consuming for hospital staff, could be helpful to identify undiagnosed CMT patients before administrating vincristine [50].

With the greater attention towards molecular importance, the existence of molecular predictors present promise. Studies of molecular predictors differed in genotype detection technique and neuropathy detection method and grading, which complicated the general cross-comparison of the studies. Despite these differences, variants in the vincristine metabolizer *CYP3A5* leading to reduced CYP3A5 expression were consistently reported as a risk factor for VIN (Table 2). Noteworthy, the frequency of *CYP3A5* variants varies between ethnicities; consequently, the reported incidence of VIN is higher in Caucasians than African–Americans. Thus, ethnicity could be used as a risk factor for VIN; however, it is important to emphasize that it is only a surrogate for CYP3A5 and that individual genotype assessment is preferable. In addition to vincristine metabolizers, genetic alterations in genes involved in vincristine pharmacodynamics were associated with VIN. A SNP in CEP72 showed great promise as predictor of VIN in two independent ALL cohorts [62, 68] but failed stratification in a Spanish ALL cohort [63]. Molecular risk factors clearly contribute to a better understanding of vincristine neurotoxicity and are potentially useful in the identification of individuals at higher risk, which could optimize and personalize vincristine dosing, leading to maximum response while minimizing the risk of long-term neuropathy.

The results of drug–drug interference as a cause of increased risk of VIN were very consistent and

independent of cohort size, diagnosis and methodology. Coadministration with itraconazole and to lesser extent voriconazole is an important aspect of VIN cause and worsening (Table 3). Based on the findings included in this review, fluconazole appears safer when concomitantly used with vincristine and should be preferred as antifungal prophylaxis and treatment. Given that the mechanism of this interaction involves inhibition of CYP3A in the liver, it could be advisable to be aware of other strong CYP3A inhibitors or inducers.

Unfortunately, neither substances for preventing VIN nor treatment options have been discovered to date, resulting in substitution, reduction or discontinuation as the only method of handling neurotoxicity. Glutamic acid potentially prevents or at least improves tolerance of vincristine in one study.

In general, various neuropathy detection methods and grading systems are used for all aspects of neuropathy examined in this review, making it very difficult to compare studies and interpret the results between studies. Although the WHO had great intentions to create a standardized tool of assessing information about neuropathy, it obviously did not succeed or persist as a useful rating scale since only two of the 71 included studies used this tool. Nerve conduction studies are thought to be the most accurate method of quantifying VIN but are time consuming, costly and discomforting to be a standard VIN measurement in clinical practice. In contrast, subjective measures introduce the risk of inter-observational variability. With the many new neurotoxicity scores used today, it is yet again of importance to agree on but not necessarily standardize which score fits which situation best and thereby makes it possible to compare studies.

Conclusion

In conclusion, clinical parameters did not show convincing potential as predictors of VIN. In contrast, molecular markers, including polymorphisms in the hepatic vincristine metabolizer CYP3A5, displayed great promise in predicting increased incidence and severity of neuropathy; however, further studies are warranted to assess its use in treatment prediction. Consistently, antifungal drugs, such as itraconazole and voriconazole, inhibit the action of CYP3A5; consequently, coadministration of vincristine and these drugs decreases vincristine metabolism, leading to enhanced neuropathy side effects. More true markers of both clinical and molecular origin may emerge if consistency in VIN detection and reporting increases through the use of standardized neuropathy assessment tools and grading scales.

Acknowledgements The authors would like to extend their gratitude to Conni Skrubbeltrang, Medical Library, Aalborg University Hospital, Denmark for assistance in the systematic literature search process.

Authors' contribution MLM and HD contributed equally to this paper. MLM and HD performed the literature search, screened the articles, and wrote the paper. All authors designed the study and critically revised and approved the final manuscript.

Compliance with ethical standards

Conflict of interest Author M.L.M declares that she has no conflict of interest. Author H.D declares that she has no conflict of interest. Author N.E declares that he has no conflict of interest. Author P.J declares that he has no conflict of interest. Author J.M declares that he has no conflict of interest. Author K.D declares that she has no conflict of interest.

References

1. Yang L, Yu L, Chen X, Hu Y, Wang B (2015) Clinical analysis of adverse drug reactions between vincristine and triazoles in children with acute lymphoblastic leukemia. Med Sci Monit 21:1656–1661. https://doi.org/10.12659/MSM.893142
2. Gidding CE, Kellie SJ, Kamps WA, de Graaf SS (1999) Vincristine revisited. Crit Rev Oncol Hematol 29(3):267–287
3. Correia JJ (1991) Effects of antimitotic agents on tubulin–nucleotide interactions. Pharmacol Ther 52(2):127–147
4. Gascoigne KE, Taylor SS (2008) Cancer cells display profound intra- and interline variation following prolonged exposure to antimitotic drugs. Cancer Cell 14(2):111–122. https://doi.org/10.1016/j.ccr.2008.07.002
5. Gutierrez-Camino A, Umerez M, Martin-Guerrero I, Garcia de Andoin N, Santos B, Sastre A, Echebarria-Barona A, Astigarraga I, Navajas A, Garcia-Orad A (2017) Mir-pharmacogenetics of vincristine and peripheral neurotoxicity in childhood B-cell acute lymphoblastic leukemia. Pharmacogenom J. https://doi.org/10.1038/s41397-017-0003-3
6. Utsu Y, Takaishi K, Inagaki S, Arai H, Yuasa H, Masuda S, Matsuura Y, Aotsuka N, Wakita H (2016) Influence of dose reduction of vincristine in R-CHOP on outcomes of diffuse large B cell lymphoma. Ann Hematol 95(1):41–47. https://doi.org/10.1007/s00277-015-2514-9
7. Morth C, Valachis A, Sabaa AA, Molin D, Flogegard M, Enblad G (2018) Does the omission of vincristine in patients with diffuse large B cell lymphoma affect treatment outcome? Ann Hematol 97(11):2129–2135. https://doi.org/10.1007/s00277-018-3437-z
8. Chan SY, Worth R, Ochs S (1980) Block of axoplasmic transport in vitro by vinca alkaloids. J Neurobiol 11(3):251–264. https://doi.org/10.1002/neu.480110304
9. Kavcic M, Koritnik B, Krzan M, Velikonja O, Prelog T, Stefanovic M, Debeljak M, Jazbec J (2017) Electrophysiological studies to detect peripheral neuropathy in children treated with vincristine. J Pediatr Hematol Oncol 39(4):266–271. https://doi.org/10.1097/MPH.0000000000000825
10. Mokhtar GM, Shaaban SY, Elbarbary NS, Fayed WA (2010) A trial to assess the efficacy of glutamic acid in prevention of vincristine-induced neurotoxicity in pediatric malignancies: a

pilot study. J Pediatr Hematol Oncol 32(8):594–600. https://doi.org/10.1097/MPH.0b013e3181e9038d
11. El Hayek M, Trad O, Jamil A (2005) Vincristine-induced urinary bladder paralysis. J Pediatr Hematol Oncol 27(5):286–287. https://doi.org/10.1097/01.mph.0000165130.21539.a3
12. Adhikari S, Dongol RM, Hewett Y, Shah BK (2014) Vincristine-induced blindness: a case report and review of literature. Anticancer Res 34(11):6731–6733
13. Sanderson PA, Kuwabara T, Cogan DG (1976) Optic neuropathy presumably caused by vincristine therapy. Am J Ophthalmol 81(2):146–150
14. Palkar AH, Nair AG, Desai RJ, Potdar NA, Shinde CA (2015) Vincristine-induced neuropathy presenting as ptosis and ophthalmoplegia in a 2-year-old boy. J Pediatr Ophthalmol Strabismus 52:34–37. https://doi.org/10.3928/01913913-20150629-01
15. Bay A, Yilmaz C, Yilmaz N, Oner AF (2006) Vincristine induced cranial polyneuropathy. Indian J Pediatr 73(6):531–533. https://doi.org/10.1007/bf02759902
16. Soysal T, Ferhanoglu B, Bilir M, Akman N (1993) Oculomotor nerve palsy associated with vincristine treatment. Acta Haematol 90(4):209–210
17. Lash SC, Williams CPR, Marsh CS, Crithchley C, Hodgkins PR, MacKie EJ (2004) Acute sixth-nerve palsy after vincristine therapy. J AAPOS 8(1):67–68. https://doi.org/10.1016/j.jaapos.2003.07.010
18. Toker E, Yenice O, Ogut MS (2004) Isolated abducens nerve palsy induced by vincristine therapy. J AAPOS 8(1):69–71. https://doi.org/10.1016/s1091853103003239
19. Ngamphaiboon N, Sweeney R, Wetzler M, Wang ES (2010) Pyridoxine treatment of vincristine-induced cranial polyneuropathy in an adult patient with acute lymphocytic leukemia: case report and review of the literature. Leuk Res 34(8):e194–e196. https://doi.org/10.1016/j.leukres.2010.01.026
20. Mahajan SL, Ikeda Y, Myers TJ, Baldini MG (1981) Acute acoustic nerve palsy associated with vincristine therapy. Cancer 47(10):2404–2406
21. Riga M, Psarommatis I, Korres S, Varvutsi M, Giotakis I, Apostolopoulos N, Ferekidis E (2007) Neurotoxicity of vincristine on the medial olivocochlear bundle. Int J Pediatr Otorhinolaryngol 71(1):63–69. https://doi.org/10.1016/j.ijporl.2006.09.001
22. Latiff ZA, Kamal NA, Jahendran J, Alias H, Goh BS, Syed Zakaria SZ, Jamal R (2010) Vincristine-induced vocal cord palsy: case report and review of the literature. J Pediatr Hematol Oncol 32(5):407–410. https://doi.org/10.1097/MPH.0b013e3181e01584
23. Whittaker JA, Griffith IP (1977) Recurrent laryngeal nerve paralysis in patients receiving vincristine and vinblastine. BMJ 1(6071):1251–1252
24. Scheithauer W, Ludwig H, Maida E (1985) Acute encephalopathy associated with continuous vincristine sulfate combination therapy: case report. Invest New Drugs 3(3):315–318
25. How J, Blattner M, Fowler S, Wang-Gillam A, Schindler SE (2016) Chemotherapy-associated posterior reversible encephalopathy syndrome: a case report and review of the literature. Neurologist 21(6):112–117. https://doi.org/10.1097/nrl.0000000000000105
26. Tomiwa K, Mikawa H, Hazama F, Yazawa K, Hosoya R, Ohya T, Nishimura K (1983) Syndrome of inappropriate secretion of antidiuretic hormone caused by vincristine therapy: a case report of the neuropathology. J Neurol 229(4):267–272
27. Robertson GL, Bhoopalam N, Zelkowitz LJ (1973) Vincristine neurotoxicity and abnormal secretion of antidiuretic hormone. Arch Intern Med 132(5):717–720
28. Kellie SJ, Barbaric D, Koopmans P, Earl J, Carr DJ, de Graaf SS (2002) Cerebrospinal fluid concentrations of vincristine after bolus intravenous dosing: a surrogate marker of brain penetration. Cancer 94(6):1815–1820
29. Moghrabi A, Levy DE, Asselin B, Barr R, Clavell L, Hurwitz C, Samson Y, Schorin M, Dalton VK, Lipshultz SE, Neuberg DS, Gelber RD, Cohen HJ, Sallan SE, Silverman LB (2007) Results of the Dana-Farber Cancer Institute ALL Consortium Protocol 95-01 for children with acute lymphoblastic leukemia. Blood 109(3):896–904. https://doi.org/10.1182/blood-2006-06-027714
30. Kautio AL, Haanpää M, Kautiainen H, Kalso E, Saarto T (2011) Burden of chemotherapy-induced neuropathy-a cross-sectional study. Support Care Cancer 19(12):1991–1996. https://doi.org/10.1007/s00520-010-1043-2
31. Moher D, Liberati A, Tetzlaff J, Altman DG (2009) Preferred reporting items for systematic reviews and meta-analyses: the prisma statement. Ann Intern Med 151(4):264–269. https://doi.org/10.7326/0003-4819-151-4-200908180-00135
32. Lieber S, Blankenburg M, Apel K, Hirschfeld G, Hernaiz Driever P, Reindl T (2018) Small-fiber neuropathy and pain sensitization in survivors of pediatric acute lymphoblastic leukemia. Eur J Paediatr Neurol EJPN 22(3):457–469. https://doi.org/10.1016/j.ejpn.2017.12.019
33. Gilchrist LS, Tanner L (2013) The pediatric-modified total neuropathy score: a reliable and valid measure of chemotherapy-induced peripheral neuropathy in children with non-CNS cancers. Support Care Cancer 21(3):847–856. https://doi.org/10.1007/s00520-012-1591-8
34. Gilchrist LS, Marais L, Tanner L (2014) Comparison of two chemotherapy-induced peripheral neuropathy measurement approaches in children. Support Care Cancer 22(2):359–366. https://doi.org/10.1007/s00520-013-1981-6
35. Lavoie Smith EM, Li L, Hutchinson RJ, Ho R, Burnette WB, Wells E, Bridges C, Renbarger J (2013) Measuring vincristine-induced peripheral neuropathy in children with acute lymphoblastic leukemia. Cancer Nurs 36(5):E49–E60. https://doi.org/10.1097/NCC.0b013e318299ad23
36. Hirvonen HE, Salmi TT, Heinonen E, Antila KJ, Valimaki IA (1989) Vincristine treatment of acute lymphoblastic leukemia induces transient autonomic cardioneuropathy. Cancer 64(4):801–805
37. Guiheneuc P, Ginet J, Groleau JY, Rojouan J (1980) Early phase of vincristine neuropathy in man. Electrophysiological evidence for a dying-back phenomenon, with transitory enhancement of spinal transmission of the monosynaptic reflex. J Neurol Sci 45(2–3):355–366
38. Toopchizadeh V, Barzegar M, Rezamand A, Feiz AH (2009) Electrophysiological consequences of vincristine contained chemotherapy in children: a cohort study. J Pediatr Neurol 7(4):351–356. https://doi.org/10.3233/JPN-2009-0333
39. Courtemanche H, Magot A, Ollivier Y, Rialland F, Leclair-Visonneau L, Fayet G, Camdessanche JP, Pereon Y (2015) Vincristine-induced neuropathy: atypical electrophysiological patterns in children. Muscle Nerve 52(6):981–985. https://doi.org/10.1002/mus.24647
40. Ramchandren S, Leonard M, Mody RJ, Donohue JE, Moyer J, Hutchinson R, Gurney JG (2009) Peripheral neuropathy in survivors of childhood acute lymphoblastic leukemia. J Periph Nerv Syst JPNS 14(3):184–189. https://doi.org/10.1111/j.1529-8027.2009.00230.x
41. Kava M, Walsh P, SrinivasJois R, Cole C, Lewis B, Nagarajan L (2017) Clinical and electrophysiological characteristics of vincristine induced peripheral neuropathy in children during cancer chemotherapy: does vitamin E have a role. JICNA 17 (75)
42. Postma TJ, Aaronson NK, Heimans JJ, Muller MJ, Hildebrand JG, Delattre JY, Hoang-Xuan K, Lanteri-Minet M, Grant R, Huddart R, Moynihan C, Maher J, Lucey R (2005) The development of an EORTC quality of life questionnaire to assess

chemotherapy-induced peripheral neuropathy: the QLQ-CIPN20. Eur J Cancer (Oxford, England: 1990) 41(8):1135–1139. https://doi.org/10.1016/j.ejca.2005.02.012
43. Le-Rademacher J, Kanwar R, Seisler D, Pachman DR, Qin R, Abyzov A, Ruddy KJ, Banck MS, Lavoie Smith EM, Dorsey SG, Aaronson NK, Sloan J, Loprinzi CL, Beutler AS (2017) Patient-reported (EORTC QLQ-CIPN20) versus physician-reported (CTCAE) quantification of oxaliplatin- and paclitaxel/carboplatin-induced peripheral neuropathy in NCCTG/Alliance clinical trials. Supportive Care Cancer 25(11):3537–3544. https://doi.org/10.1007/s00520-017-3780-y
44. Anghelescu DL, Faughnan LG, Jeha S, Relling MV, Hinds PS, Sandlund JT, Cheng C, Pei D, Hankins G, Pauley JL, Pui CH (2011) Neuropathic pain during treatment for childhood acute lymphoblastic leukemia. Pediatr Blood Cancer 57(7):1147–1153. https://doi.org/10.1002/pbc.23039
45. Jain P, Gulati S, Toteja GS, Bakhshi S, Seth R, Pandey RM (2015) Serum alpha tocopherol, vitamin B12, and folate levels in childhood acute lymphoblastic leukemia survivors with and without neuropathy. J Child Neurol 30(6):786–788. https://doi.org/10.1177/0883073814535495
46. Desai ZR, Van den Berg HW, Bridges JM, Shanks RG (1982) Can severe vincristine neurotoxicity be prevented? Cancer Chemother Pharmacol 8(2):211–214
47. Brunello A, Kapoor R, Extermann M (2011) Hyperglycemia during chemotherapy for hematologic and solid tumors is correlated with increased toxicity. Am J Clin Oncol 34(3):292–296. https://doi.org/10.1097/COC.0b013e3181e1d0c0
48. Weiser MA, Cabanillas ME, Konopleva M, Thomas DA, Pierce SA, Escalante CP, Kantarjian HM, O'Brien SM (2004) Relation between the duration of remission and hyperglycemia during induction chemotherapy for acute lymphocytic leukemia with a hyperfractionated cyclophosphamide, vincristine, doxorubicin, and dexamethasone/methotrexate-cytarabine regimen. Cancer 100(6):1179–1185. https://doi.org/10.1002/cncr.20071
49. Kanbayashi Y, Hosokawa T, Okamoto K, Konishi H, Otsuji E, Yoshikawa T, Takagi T, Taniwaki M (2010) Statistical identification of predictors for peripheral neuropathy associated with administration of bortezomib, taxanes, oxaliplatin or vincristine using ordered logistic regression analysis. Anticancer Drugs 21(9):877–881. https://doi.org/10.1097/CAD.0b013e32833db89d
50. Ibañez-Juliá MJ, Berzero G, Reyes-Botero G, Maisonobe T, Lenglet T, Slim M, Louis S, Balaguer A, Sanson M, Le Guern E, Latour P, Ricard D, Stojkovic T, Psimaras D (2018) Antineoplastic agents exacerbating Charcot Marie Tooth disease: red flags to avoid permanent disability. Acta Oncol 57(3):403–411. https://doi.org/10.1080/0284186X.2017.1415462
51. Chauvenet AR, Shashi V, Selsky C, Morgan E, Kurtzberg J, Bell B (2003) Vincristine-induced neuropathy as the initial presentation of Charcot–Marie–Tooth disease in acute lymphoblastic leukemia: a Pediatric Oncology Group study. J Pediatr Hematol Oncol 25(4):316–320. https://doi.org/10.1097/00043426-200304000-00010
52. Re D, Schwenk A, Hegener P, Bamborschke S, Diehl V, Tesch H (2000) Guillain-Barre syndrome in a patient with non-Hodgkin's lymphoma. Ann Oncol 11(2):217–220
53. Bhushan B, Bhargava A, Kasundra GM, Shubhakaran K, Sood I (2015) Guillain-Barre syndrome in acute lymphoblastic leukemia: causal or coincidental. J Pediatr Neurosci 10(1):64–66. https://doi.org/10.4103/1817-1745.154358
54. Okada N, Hanafusa T, Sakurada T, Teraoka K, Kujime T, Abe M, Shinohara Y, Kawazoe K, Minakuchi K (2014) Risk factors for early-onset peripheral neuropathy caused by vincristine in patients with a first administration of R-CHOP or R-CHOP-like chemotherapy. J Clin Med Res 6(4):252–260. https://doi.org/10.14740/jocmr1856w
55. Aplenc R, Glatfelter W, Han P, Rappaport E, La M, Cnaan A, Blackwood MA, Lange B, Rebbeck T (2003) CYP3A genotypes and treatment response in paediatric acute lymphoblastic leukaemia. Br J Haematol 122(2):240–244. https://doi.org/10.1046/j.1365-2141.2003.04430.x
56. Kishi S, Cheng C, French D, Pei D, Das S, Cook EH, Hijiya N, Rizzari C, Rosner GL, Frudakis T, Pui CH, Evans WE, Relling MV (2007) Ancestry and pharmacogenetics of antileukemic drug toxicity. Blood 109(10):4151–4157. https://doi.org/10.1182/blood-2006-10-054528
57. Renbarger JL, McCammack KC, Rouse CE, Hall SD (2008) Effect of race on vincristine-associated neurotoxicity in pediatric acute lymphoblastic leukemia patients. Pediatr Blood Cancer 50(4):769–771. https://doi.org/10.1002/pbc.21435
58. Broyl A, Corthals SL, Jongen JL, van der Holt B, Kuiper R, de Knegt Y, van Duin M, el Jarari L, Bertsch U, Lokhorst HM, Durie BG, Goldschmidt H, Sonneveld P (2010) Mechanisms of peripheral neuropathy associated with bortezomib and vincristine in patients with newly diagnosed multiple myeloma: a prospective analysis of data from the HOVON-65/GMMG-HD4 trial. Lancet Oncol 11(11):1057–1065. https://doi.org/10.1016/s1470-2045(10)70206-0
59. Egbelakin A, Ferguson MJ, MacGill EA, Lehmann AS, Topletz AR, Quinney SK, Li L, McCammack KC, Hall SD, Renbarger JL (2011) Increased risk of vincristine neurotoxicity associated with low CYP3A5 expression genotype in children with acute lymphoblastic leukemia. Pediatr Blood Cancer 56(3):361–367. https://doi.org/10.1002/pbc.22845
60. Ceppi F, Langlois-Pelletier C, Gagne V, Rousseau J, Ciolino C, De Lorenzo S, Kevin KM, Cijov D, Sallan SE, Silverman LB, Neuberg D, Kutok JL, Sinnett D, Laverdiere C, Krajinovic M (2014) Polymorphisms of the vincristine pathway and response to treatment in children with childhood acute lymphoblastic leukemia. Pharmacogenomics 15(8):1105–1116. https://doi.org/10.2217/pgs.14.68
61. Diouf B, Crews KR, Lew G, Pei D, Cheng C, Bao J, Zheng JJ, Yang W, Fan Y, Wheeler HE, Wing C, Delaney SM, Komatsu M, Paugh SW, McCorkle JR, Lu X, Winick NJ, Carroll WL, Loh ML, Hunger SP, Devidas M, Pui CH, Dolan ME, Relling MV, Evans WE (2015) Association of an inherited genetic variant with vincristine-related peripheral neuropathy in children with acute lymphoblastic leukemia. JAMA 313(8):815–823. https://doi.org/10.1001/jama.2015.0894
62. Stock W, Diouf B, Crews KR, Pei D, Cheng C, Laumann K, Mandrekar SJ, Luger S, Advani A, Stone RM, Larson RA, Evans WE (2017) An inherited genetic variant in CEP72 promoter predisposes to vincristine-induced peripheral neuropathy in adults with acute lymphoblastic leukemia. Clin Pharmacol Ther 101(3):391–395. https://doi.org/10.1002/cpt.506
63. Gutierrez-Camino A, Martin-Guerrero I, Lopez-Lopez E, Echebarria-Barona A, Zabalza I, Ruiz I, Guerra-Merino I, Garcia-Orad A (2016) Lack of association of the CEP72 RS924607 TT genotype with vincristine-related peripheral neuropathy during the early phase of pediatric acute lymphoblastic leukemia treatment in a Spanish population. Pharmacogenet Genom 26(2):100–102. https://doi.org/10.1097/FPC.0000000000000191
64. Sims RP (2016) The effect of race on the CYP3A-mediated metabolism of vincristine in pediatric patients with acute lymphoblastic leukemia. J Oncol Pharm Pract 22(1):76–81. https://doi.org/10.1177/1078155214553143
65. Lopez-Lopez E, Gutierrez-Camino A, Astigarraga I, Navajas A, Echebarria-Barona A, Garcia-Miguel P, Garcia de Andoin N, Lobo C, Guerra-Merino I, Martin-Guerrero I, Garcia-Orad A

(2016) Vincristine pharmacokinetics pathway and neurotoxicity during early phases of treatment in pediatric acute lymphoblastic leukemia. Pharmacogenomics 17(7):731–741. https://doi.org/10.2217/pgs-2016-0001
66. Kayilioglu H, Kocak U, Kan Karaer D, Percin EF, Sal E, Tekkesin F, Isik M, Oner N, Belen FB, Yilmaz Keskin E, Okur A, Albayrak M, Kaya Z, Pinarli FG, Yenicesu I, Karadeniz C, Oguz A, Gursel T (2017) Association of CYP3A5 expression and vincristine neurotoxicity in pediatric malignancies in Turkish population. J Pediatr Hematol Oncol 39(6):458–462. https://doi.org/10.1097/mph.0000000000000910
67. Skiles JL, Chiang C, Li CH, Martin S, Smith EL, Olbara G, Jones DR, Vik TA, Mostert S, Abbink F, Kaspers GJ, Li L, Njuguna F, Sajdyk TJ, Renbarger JL (2018) CYP3A5 genotype and its impact on vincristine pharmacokinetics and development of neuropathy in Kenyan children with cancer. Pediatr Blood Cancer. https://doi.org/10.1002/pbc.26854
68. Wright GEB, Amstutz U, Drogemoller BI, Shih J, Rassekh SR, Hayden MR, Carleton BC, Ross CJD (2018) Pharmacogenomics of vincristine-induced peripheral neuropathy implicates pharmacokinetic and inherited neuropathy genes. Clin Pharmacol Ther. https://doi.org/10.1002/cpt.1179
69. Smitherman AB, Faircloth CB, Deal A, Troy M, Gold SH (2017) Vincristine toxicity with co-administration of fluconazole during induction therapy for pediatric acute lymphoblastic leukemia. Pediatr Blood Cancer. https://doi.org/10.1002/pbc.26525
70. Takahashi N, Kameoka Y, Yamanaka Y, Ubukawa K, Saito K, Fujishima M, Fujishima N, Saito H, Hirokawa M, Scott SA, Sawada K (2008) Itraconazole oral solution enhanced vincristine neurotoxicity in five patients with malignant lymphoma. Intern Med (Tokyo, Japan) 47(7):651–653
71. Nikanjam M, Sun A, Albers M, Mangalindin K, Song E, Vempaty H, Sam D, Capparelli EV (2018) Vincristine-associated neuropathy with antifungal usage: a kaiser northern California experience. J Pediatr Hematol Oncol 40(5):e273–e277. https://doi.org/10.1097/MPH.0000000000001220
72. Bohme A, Ganser A, Hoelzer D (1995) Aggravation of vincristine-induced neurotoxicity by itraconazole in the treatment of adult ALL. Ann Hematol 71(6):311–312
73. Teusink AC, Ragucci D, Shatat IF, Kalpatthi R (2012) Potentiation of vincristine toxicity with concomitant fluconazole prophylaxis in children with acute lymphoblastic leukemia. Pediatr Hematol Oncol 29(1):62–67. https://doi.org/10.3109/08880018.2011.624163
74. Gillies J, Hung KA, Fitzsimons E, Soutar R (1998) Severe vincristine toxicity in combination with itraconazole. Clin Lab Haematol 20(2):123–124
75. Kamaluddin M, McNally P, Breatnach F, O'Marcaigh A, Webb D, O'Dell E, Scanlon P, Butler K, O'Meara A (2001) Potentiation of vincristine toxicity by itraconazole in children with lymphoid malignancies. Acta Paediatr 90(10):1204–1207
76. van Schie RM, Bruggemann RJ, Hoogerbrugge PM, te Loo DM (2011) Effect of azole antifungal therapy on vincristine toxicity in childhood acute lymphoblastic leukaemia. J Antimicrob Chemother 66(8):1853–1856. https://doi.org/10.1093/jac/dkr223
77. Cheung MC, Hicks LK, Leitch HA (2010) Excessive neurotoxicity with ABVD when combined with protease inhibitor-based antiretroviral therapy in the treatment of AIDS-related Hodgkin lymphoma. Clin Lymphoma Myeloma Leukemia 10(2):E22–E25. https://doi.org/10.3816/CLML.2010.n.025
78. Ezzat HM, Cheung MC, Hicks LK, Boro J, Montaner JS, Lima VD, Harris M, Leitch HA (2012) Incidence, predictors and significance of severe toxicity in patients with human immunodeficiency virus-associated Hodgkin lymphoma. Leukemia Lymphoma 53(12):2390–2396. https://doi.org/10.3109/10428194.2012.697560
79. Weintraub M, Adde MA, Venzon DJ, Shad AT, Horak ID, Neely JE, Seibel NL, Gootenberg J, Arndt C, Nieder ML, Magrath IT (1996) Severe atypical neuropathy associated with administration of hematopoietic colony-stimulating factors and vincristine. J Clin Oncol 14(3):935–940. https://doi.org/10.1200/jco.1996.14.3.935
80. Ryan JR, Emami A (1983) Vincristine neurotoxicity with residual equinocavus deformity in children with acute leukemia. Cancer 51(3):423–425
81. van Kooten B, van Diemen HA, Groenhout KM, Huijgens PC, Ossenkoppele GJ, Nauta JJ, Heimans JJ (1992) A pilot study on the influence of a corticotropin (4–9) analogue on Vinca alkaloid-induced neuropathy. Arch Neurol 49(10):1027–1031
82. Akbayram S, Akgun C, Dogan M, Sayin R, Caksen H, Oner AF (2010) Use of pyridoxine and pyridostigmine in children with vincristine-induced neuropathy. Indian J Pediatr 77(6):681–683. https://doi.org/10.1007/s12098-010-0096-z
83. Bradfield SM, Sandler E, Geller T, Tamura RN, Krischer JP (2015) Glutamic acid not beneficial for the prevention of vincristine neurotoxicity in children with cancer. Pediatr Blood Cancer 62(6):1004–1010. https://doi.org/10.1002/pbc.25384
84. Sands S, Ladas EJ, Kelly KM, Weiner M, Lin M, Ndao DH, Dave A, Vahdat LT, Bender JG (2017) Glutamine for the treatment of vincristine-induced neuropathy in children and adolescents with cancer. Support Care Cancer 25(3):701–708. https://doi.org/10.1007/s00520-016-3441-6
85. Koeppen S, Verstappen CC, Korte R, Scheulen ME, Strumberg D, Postma TJ, Heimans JJ, Huijgens PC, Kiburg B, Renzing-Kohler K, Diener HC (2004) Lack of neuroprotection by an ACTH (4–9) analogue. A randomized trial in patients treated with vincristine for Hodgkin's or non-Hodgkin's lymphoma. J Cancer Res Clin Oncol 130(3):153–160. https://doi.org/10.1007/s00432-003-0524-9
86. Jain P, Gulati S, Seth R, Bakhshi S, Toteja GS, Pandey RM (2014) Vincristine-induced neuropathy in childhood all (acute lymphoblastic leukemia) survivors: prevalence and electrophysiological characteristics. J Child Neurol 29(7):932–937. https://doi.org/10.1177/0883073813491829
87. Harila-Saari AH, Vainionpää LK, Kovala TT, Tolonen EU, Lanning BM (1998) Nerve lesions after therapy for childhood acute lymphoblastic leukemia. Cancer 82(1):200–207. https://doi.org/10.1002/(SICI)1097-0142(19980101)82:1%3c200:AID-CNCR87%3e3.0.CO;2-5
88. Watkins SM, Griffin JP (1978) High incidence of vincristine-induced neuropathy in lymphomas. BMJ 1(6113):610–612
89. Tay CG, Lee VWM, Ong LC, Goh KJ, Ariffin H, Fong CY (2017) Vincristine-induced peripheral neuropathy in survivors of childhood acute lymphoblastic leukaemia. Pediatric Blood Cancer. https://doi.org/10.1002/pbc.26471
90. Postma TJ, Benard BA, Huijgens PC, Ossenkoppele GJ, Heimans JJ (1993) Long-term effects of vincristine on the peripheral nervous system. J Neurooncol 15(1):23–27
91. Verstappen CC, Koeppen S, Heimans JJ, Huijgens PC, Scheulen ME, Strumberg D, Kiburg B, Postma TJ (2005) Dose-related vincristine-induced peripheral neuropathy with unexpected off-therapy worsening. Neurology 64(6):1076–1077. https://doi.org/10.1212/01.wnl.0000154642.45474.28
92. Haim N, Epelbaum R, Ben-Shahar M, Yarnitsky D, Simri W, Robinson E (1994) Full dose vincristine (without 2-mg dose limit) in the treatment of lymphomas. Cancer 73(10):2515–2519
93. Lavoie Smith EM, Li L, Chiang C, Thomas K, Hutchinson RJ, Wells EM, Ho RH, Skiles J, Chakraborty A, Bridges CM, Renbarger J (2015) Patterns and severity of vincristine-induced peripheral neuropathy in children with acute lymphoblastic leukemia. J Periph Nerv Syst 20(1):37–46. https://doi.org/10.1111/jns.12114

94. Kim BJ, Park HR, Roh HJ, Jeong DS, Kim BS, Park KW, Cho SC, So YT, Oh SY, Kim SJ (2010) Chemotherapy-related polyneuropathy may deteriorate quality of life in patients with B-cell lymphoma. Q Life Res 19(8):1097–1103. https://doi.org/10.1007/s11136-010-9670-0
95. Vainionpaa L (1993) Clinical neurological findings of children with acute lymphoblastic leukaemia at diagnosis and during treatment. Eur J Pediatr 152(2):115–119. https://doi.org/10.1007/BF02072486
96. Gilchrist LS, Tanner LR, Ness KK (2017) Short-term recovery of chemotherapy-induced peripheral neuropathy after treatment for pediatric non-CNS cancer. Pediatr Blood Cancer 64(1):180–187. https://doi.org/10.1002/pbc.26204
97. Miller AB, Hoogstraten B, Staquet M, Winkler A (1981) Reporting results of cancer treatment. Cancer 47(1):207–214
98. Trotti A, Colevas AD, Setser A, Basch E (2007) Patient-reported outcomes and the evolution of adverse event reporting in oncology. J Clin Oncol 25(32):5121–5127. https://doi.org/10.1200/jco.2007.12.4784
99. Cavaletti G, Frigeni B, Lanzani F, Piatti M, Rota S, Briani C, Zara G, Plasmati R, Pastorelli F, Caraceni A, Pace A, Manicone M, Lissoni A, Colombo N, Bianchi G, Zanna C (2007) The Total Neuropathy Score as an assessment tool for grading the course of chemotherapy-induced peripheral neurotoxicity: comparison with the National Cancer Institute-Common Toxicity Scale. J Periph Nerv Syst JPNS 12(3):210–215. https://doi.org/10.1111/j.1529-8027.2007.00141.x
100. Gilchrist L (2012) Chemotherapy-induced peripheral neuropathy in pediatric cancer patients. Semin Pediatr Neurol 19(1):9–17. https://doi.org/10.1016/j.spen.2012.02.011
101. Bakogeorgos M, Georgoulias V (2017) Risk-reduction and treatment of chemotherapy-induced peripheral neuropathy. Expert Rev Anticancer Ther 17(11):1045–1060. https://doi.org/10.1080/14737140.2017.1374856
102. Hussain M, Wozniak AJ, Edelstein MB (1993) Neurotoxicity of antineoplastic agents. Crit Rev Oncol Hematol 14(1):61–75
103. Wolf S, Barton D, Kottschade L, Grothey A, Loprinzi C (2008) Chemotherapy-induced peripheral neuropathy: prevention and treatment strategies. Eur J Cancer 44(11):1507–1515. https://doi.org/10.1016/j.ejca.2008.04.018
104. Quasthoff S, Hartung HP (2002) Chemotherapy-induced peripheral neuropathy. J Neurol 249(1):9–17
105. Grisold W, Cavaletti G, Windebank AJ (2012) Peripheral neuropathies from chemotherapeutics and targeted agents: diagnosis, treatment, and prevention. Neuro-oncology 14(Suppl. 4):45–54. https://doi.org/10.1093/neuonc/nos203
106. Gulliford MC, Charlton J, Latinovic R (2006) Risk of diabetes associated with prescribed glucocorticoids in a large population. Diabetes Care 29(12):2728–2729. https://doi.org/10.2337/dc06-1499
107. Dennison JB, Kulanthaivel P, Barbuch RJ, Renbarger JL, Ehlhardt WJ, Hall SD (2006) Selective metabolism of vincristine in vitro by CYP3A5. Drug Metab Dispos 34(8):1317–1327. https://doi.org/10.1124/dmd.106.009902
108. Kuehl P, Zhang J, Lin Y, Lamba J, Assem M, Schuetz J, Watkins PB, Daly A, Wrighton SA, Hall SD, Maurel P, Relling M, Brimer C, Yasuda K, Venkataramanan R, Strom S, Thummel K, Boguski MS, Schuetz E (2001) Sequence diversity in CYP3A promoters and characterization of the genetic basis of polymorphic CYP3A5 expression. Nat Genet 27(4):383–391. https://doi.org/10.1038/86882
109. Venkatakrishnan K, von Moltke LL, Greenblatt DJ (2000) Effects of the antifungal agents on oxidative drug metabolism: clinical relevance. Clin Pharmacokinet 38(2):111–180. https://doi.org/10.2165/00003088-200038020-00002
110. Wang E-j, Lew K, Casciano CN, Clement RP, Johnson WW (2002) Interaction of common azole antifungals with P glycoprotein. Antimicrob Agents Chemother 46(1):160–165. https://doi.org/10.1128/AAC.46.1.160-165.2002

Supplementary Table 1. Search strategy in PubMed and Embase

Database	PubMed	Embase
Search terms	#1: "Vincristine" [Mesh] #2: Vincristine* #3: Oncovin* #4: "Vinblastine" [Mesh] #5: Vinblastin* #6: #1 OR #2 OR #3 OR #4 OR #5 #7: neuropath* #8: "Neurotoxicity Syndromes" [Mesh:noexp] #9: neurotoxicit* #10: sensory impairment* #11: #7 OR #8 OR #9 OR #10 #12: "Hematologic Neoplasms" [Mesh] #13: "Lymphoma" [Mesh] #14: "Leukemia" [Mesh] #15: hematolog* OR haematolog* #16: leukemia OR lymphoma* #17: "Hematologic Diseases" [Mesh] #18: "Multiple Myeloma" [Mesh] #19: myeloma* #20: #12 OR #13 OR #14 OR #15 OR #16 OR #17 OR #18 OR #19 #21: #6 AND #11 AND #20 No filters	#1: 'vincristine'/exp #2: vincristin*:ti,ab,kw #3: 'vincristine sulfate'/exp #4: oncovin*:ti,ab,kw #5: 'vinblastine'/exp #6: vinblastin*:ti,ab,kw #7: #1 OR #2 OR #3 OR #4 OR #5 OR #6 #8: 'peripheral neuropathy'/exp #9: (peripheral NEAR/2 (neuropath* OR toxicit*)):ti,ab,kw #10: #8 OR #9 #11: leukemia:ti,ab,kw OR lymphoma*:ti,ab,kw OR myeloma:ti,ab,kw #12: 'hematologic malignancy'/exp #13: #11 OR #12 #14: #7 AND #10 AND #13 Filters: NOT 'conference abstract'/lt NOT 'nonhuman'/de

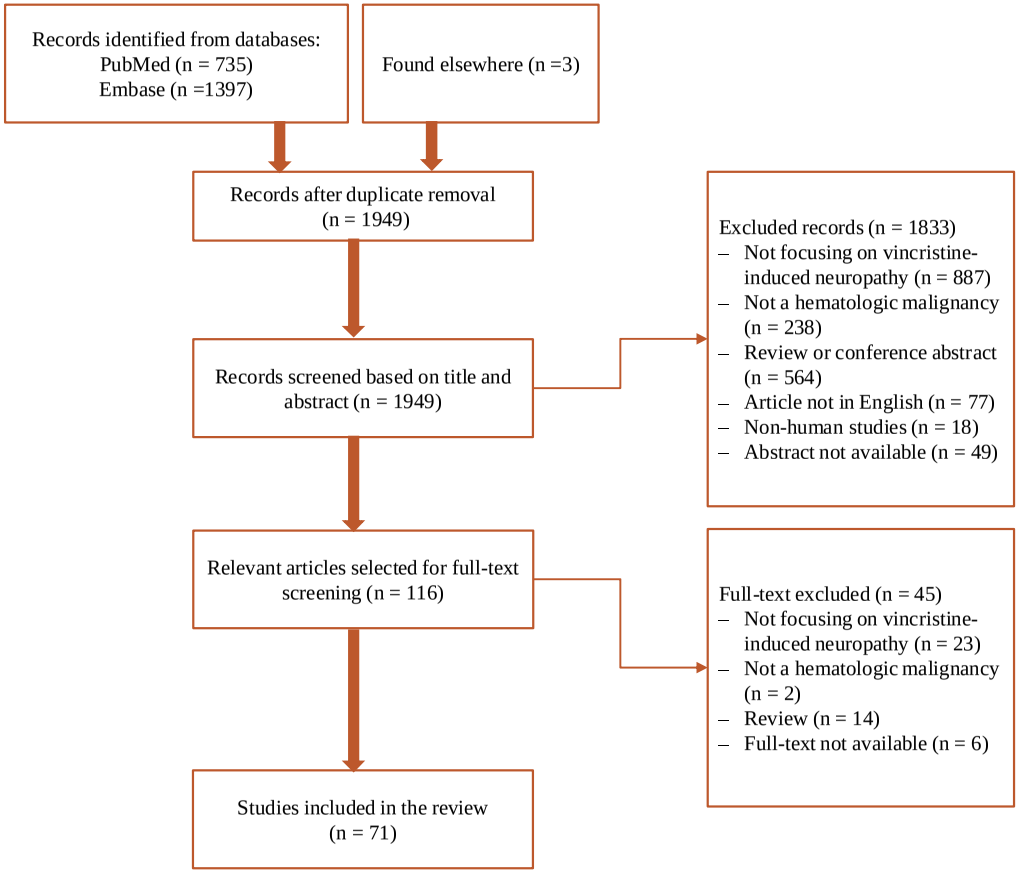
Records identified from databases:
PubMed (n = 735)
Embase (n =1397)
Found elsewhere (n =3)
Records after duplicate removal
(n = 1949)
Records screened based on title and abstract (n = 1949)
Excluded records (n = 1833)
– Not focusing on vincristine-induced neuropathy (n = 887)
– Not a hematologic malignancy (n = 238)
– Review or conference abstract (n = 564)
– Article not in English (n = 77)
– Non-human studies (n = 18)
– Abstract not available (n = 49)
Relevant articles selected for full-text screening (n = 116)
Full-text excluded (n = 45)
– Not focusing on vincristine-induced neuropathy (n = 23)
– Not a hematologic malignancy (n = 2)
– Review (n = 14)
– Full-text not available (n = 6)
Studies included in the review
(n = 71)

Due et al. BMC Cancer (2020) 20:237
https://doi.org/10.1186/s12885-020-6643-8

BMC Cancer

RESEARCH ARTICLE Open Access

MicroRNAs associated to single drug components of R-CHOP identifies diffuse large B-cell lymphoma patients with poor outcome and adds prognostic value to the international prognostic index

Hanne Due[1,2†], Rasmus Froberg Brøndum[1,3†], Ken H. Young[4], Martin Bøgsted[1,2,3] and Karen Dybkær[1,2,3*]

Abstract

Background: Treatment resistance is a major clinical challenge of diffuse large B-cell lymphoma (DLBCL) where approximately 40% of the patients have refractory disease or relapse. Since DLBCL is characterized by great clinical and molecular heterogeneity, the purpose of the present study was to investigate whether miRNAs associated to single drug components of R-CHOP can improve robustness of individual markers and serve as a prognostic classifier.

Methods: Fifteen DLBCL cell lines were tested for sensitivity towards single drug compounds of the standard treatment R-CHOP: rituximab (R), cyclophosphamide (C), doxorubicin (H), and vincristine (O). For each drug, cell lines were ranked using the area under the dose-response curve and grouped as either sensitive, intermediate or resistant. Baseline miRNA expression data were obtained for each cell line in untreated condition, and differential miRNA expression analysis between sensitive and resistant cell lines identified 43 miRNAs associated to growth response after exposure towards single drugs of R-CHOP. Using the Affymetrix HG-U133 platform, expression levels of miRNA precursors were assessed in 701 diagnostic DLBCL biopsies, and miRNA-panel classifiers predicting disease progression were build using multiple Cox regression or random survival forest. Classifiers were validated and ranked by repeated cross-validation.

Results: Prognostic accuracies were assessed by Brier Scores and time-varying area under the ROC curves, which revealed better performance of multivariate Cox models compared to random survival forest models. The Cox model including miR-146a, miR-155, miR-21, miR-34a, and miR-23a~miR-27a~miR-24-2 cluster performed the best and successfully stratified GCB-DLBCL patients into high- and low-risk of disease progression. In addition, combination of the Cox miRNA-panel and IPI substantially increased prognostic performance in GCB classified patients.

Conclusion: As a proof of concept, we found that expression data of drug associated miRNAs display prognostic utility and adding these to IPI improves prognostic stratification of GCB-DLBCL patients treated with R-CHOP.

Keywords: Diffuse large B-cell lymphoma (DLBCL), Drug response, miRNA, Prognosis, Classification

* Correspondence: k.dybkaer@rn.dk
†Hanne Due and Rasmus Froberg Brøndum contributed equally to this work.
[1]Department of Hematology, Aalborg University Hospital, Sdr. Skovvej 15, DK-9000 Aalborg, Denmark
[2]Department of Clinical Medicine, Aalborg University, Aalborg, Denmark
Full list of author information is available at the end of the article

Background

Diffuse large B-cell lymphoma (DLBCL) is the most common type of malignant lymphoma, accounting for 30–40% of all newly diagnosed non-Hodgkin lymphomas. It is a highly aggressive and heterogeneous disease with respect to clinical presentation, tumor biology, and prognosis [1]. Gene expression profiling (GEP) enables cell-of-origin classification of DLBCL into two histologically indistinguishable molecular subclasses: the activated B-cell-like (ABC) and the germinal center B-cell-like (GCB), which reflect a subset of the normal B-cell differentiation stages. These subclasses differ in pathogenesis, genetic aberrations, and survival outcome [2, 3] and have entered clinical prognostic evaluation, complementing the international prognostic index (IPI), which has been the gold standard for decades [3, 4].

First-line treatment for newly diagnosed DLBCL patients is a multi-agent regimen combining the anti-CD20 monoclonal antibody rituximab with the three chemotherapeutics cyclophosphamide, doxorubicin, and vincristine, and the corticosteroid prednisone (R-CHOP). Although addition of rituximab to the regimen has improved treatment outcome of DLBCL substantially, up to 40% of patients have refractory disease or relapse after initial response to therapy due to drug-specific molecular resistance [5–7]. Study of the pharmacological principles underlying the R-CHOP regimen revealed no synergistic interaction but very low cross-resistance, showing a strong combination of independently effective drugs without overlapping mechanisms of resistance [8]. Thus, identification of biomarkers predictive for single drug components of R-CHOP is of great importance when attempting to improve clinical outcome.

microRNAs (miRNAs) are endogenous, small non-coding RNA molecules regulating gene expression at the post-transcriptional level [9]. Compelling evidence has demonstrated that miRNA expression is dysregulated in human cancers, with several miRNAs functioning as oncogenes or tumor suppressors [10]. Deregulation of miRNAs occurs early and consistently in tumor development and progression, and thus constitutes a promising source for discovery of novel biomarkers. Indeed, specific miRNAs and global miRNA expression profiles have shown significant potential as diagnostic as well as prognostic biomarkers for DLBCL [11–13], and several studies support their role in chemotherapy resistance [14–16]. Since DLBCL is a highly heterogeneous disease at the molecular level, we hypothesized that a panel of miRNAs associated to individual components of R-CHOP can improve robustness of individual markers and serve as a prognostic classifier predicting disease progression in DLBCL patients.

To test this hypothesis, we determined the global miRNA transcriptome and performed systematic dose-response drug screens in a DLBCL-specific cell line panel to identify single drug associated miRNAs. Applying multivariate Cox regression and random survival forest techniques, prognostic miRNA-panel classifiers were developed and the predictive accuracies were subsequently evaluated by Brier scores and time varying area under the ROC curves.

Methods

Cell lines

Fifteen human DLBCL-derived cell lines DB, NU-DHL-1, NU-DUL-1, MC-116, SU-DHL-4, SU-DHL-5 (DSMZ, German Collection of Microorganisms and Cell Cultures) and FARAGE, HBL-1, OCI-Ly3, OCI-Ly7, OCI-Ly8, OCI-Ly19, RIVA, SU-DHL-8, and U2932 (Provided by Dr. Jose A. Martinez-Climent, Molecular Oncology Laboratory, University of Navarra, Pamplona, Spain) were included (Table 1). The cell lines were cultured under standard conditions at 37 °C in humidified atmosphere of 95% air and 5% CO_2 with RPMI1640 medium containing 10% fetal bovine serum (FBS) and 1% penicillin/streptomycin (P/S) for no longer than 20 passages. All cell lines were authenticated by DNA barcoding as previously described [18] and examined for mycoplasma infection when terminating their culturing period.

Clinical cohorts

The study was conducted in accordance with the Declaration of Helsinki and tumor biopsies from 73 primary DLBCL patients were collected at time of diagnosis in accordance with the RetroGen research protocol, approved by the Health Ethic Committee of North Denmark Region (Approval jr. no. N-20140099). All patients were treated with R-CHOP according to standard protocols. This retrospective cohort is referred to as the AAU dataset. In addition, we used the following data sets from the National Center for Biotechnology Information Gene Expression Omnibus (GEO) repository: Lymphoma/Leukemia Molecular Profiling Project R-CHOP (LLMPP R-CHOP) (GSE10846) [19] and International DLBCL Rituximab-CHOP Consortium MD Anderson Project (IDRC) (GSE31312) [20]. All patients were classified into the molecular ABC/GCB subclasses using GEP (Table 2).

Dose-response experiments

Dose-response screens with rituximab, cyclophosphamide, doxorubicin, and vincristine, respectively, were performed as described previously [18, 21]. Since cyclophosphamide is a prodrug that requires hepatic activation to produce its active metabolite, the synthetic oxazaphophorine derivate mafosfamide was used in the

Table 1 Cell line specifications

Cell line	Seeding concentration	Rituximab		Cyclophosphamide		Doxorubicin		Vincristine		ABC/GCB
	cells/mL	AUC		AUC		AUC		AUC		
DB	0.125×10^6	318.1	Int	345.6	Res	275.5	Res	130.7	Res	GCB
FARAGE	0.25×10^6	344.1	Int	311.0	Res	179.6	Sen	56.1	Sen	GCB
HBL-1	0.25×10^6	421.9	Res	226.0	Int	272.2	Int	84.5	Int	ABC
MC-116	0.25×10^6	NA	NA	NA	NA	271.8	Int	62.0	NA*	GCB
NU-DHL-1	0.125×10^6	316.6	Int	171.7	Sen	200.6	Sen	NA	NA	ABC
NU-DUL-1	0.25×10^6	236.4	Sen	214.1	Sen	223.9	Int	90.3	Int	UC
OCI-Ly3	0.125×10^6	407.6	Res	261.7	Int	253.4	Int	74.8	Int	ABC
OCI-Ly7	0.125×10^6	218.3	Res	257.9	Sen	324.9	Res	114.5	Int	GCB
OCI-Ly8	0.25×10^6	406.6	Res	NA	NA	NA	NA	NA	NA	UC
OCI-Ly19	0.25×10^6	400.4	Res	202.1	Sen	166.9	Sen	54.0	Sen	UC
RIVA	0.25×10^6	275.8	Res	296.0	Int	326.7	Res	109.0	Res	ABC
SU-DHL-4	0.25×10^6	150.4	Sen	NA	NA	288.8	Res	NA	NA	GCB
SU-DHL-5	0.25×10^6	251.2	Sen	164.5	Sen	201.5	Sen	57.9	Sen	GCB
SU-DHL-8	0.5×10^6	425.0	Res	270.6	Int	222.0	Sen	126.1	Res	GCB
U2932	0.4×10^6	354.1	Int	329.8	Res	294.8	Res	85.3	Int	GCB

For each drug, DLBCL cell lines were ranked according to sensitivity based on area under the dose-response curve (AUC) for rituximab, cyclophosphamide, doxorubicin, and vincristine. Division into tertiles defines: Rituximab, 4 sensitive, 5 intermediate, 5 resistant; Cyclophosphamide, 4 sensitive, 4 intermediate, 4 resistant; Doxorubicin, 5 sensitive, 4 intermediate, 5 resistant; Vincristine, 4 sensitive, 4 intermediate, 4 resistant. Based on GEP, DLBCL cell lines were classified into ABC/GCB subclasses by Wright classification using published algorithms at hemaClass.org [17]. ABC, activated B-cell like; GCB, germinal center B-cell like; Int, intermediate; NA, not available; Res, resistant; Sen, sensitive; * excluded due to large variation between replicates

dose-response assays. As the pharmacological effect of R-CHOP has limited cross-resistance rather than synergism [8], single drug screens were used instead of combinations in order to identify miRNAs that were specifically associated to response for the individual components of the treatment regimen. The cells were seeded 24 h prior to addition of the drug using cell line specific seeding concentrations to ensure exponential growth for 48 h (Table 1). For rituximab dose-response screens, each cell line was subjected to 16 concentrations in serial 2-fold dilutions ranging from 133.3 μg/mL to 407×10^{-5}μg/mL and 30 min after rituximab addition, normal pooled human AB serum (INR IPLA-SERAB, Novakemi AB, Sweden) was added to a final concentration of 20%. For cyclophosphamide, doxorubicin, and vincristine, the cell lines were exposed to 18 drug-specific concentrations in 2-fold dilutions starting from 80, 10, and 20 μg/mL, respectively [21]. The number of metabolic active cells was evaluated after 48 h of drug exposure using MTS assay (CellTiter 96 Aqueous One Solution Reagent, Promega, Madison, WI). Absorbance was measured at 492 nm using an Optima Fluorostar plate reader (BMG LAB-TECH, Ortenberg, Germany). All border wells were omitted from data analysis in order to avoid border effect. All drug screens were conducted with 3 replicates of each drug dose and with 3 biological replicates for each cell line. Since a fixed time of drug exposure were used, fast proliferating cells will appear more sensitive compared to slow proliferating ones. Therefore, area under the dose-response curve were used as summary statistic of the drug screens, making the results independent of cell line doubling time as it takes growth kinetic into account [21].

Global miRNA and mRNA expression profiling

Total RNA was extracted using a modified protocol combining TRIzol Reagent (Invitrogen, Paisley, UK) and mirVana miRNA Isolation Kit (Ambion/ThermoFisher Scientific, Grand Island, NY) as previously described [22]. RNA quality and concentration was determined by Agilent 2100 Bioanalyzer analysis (Agilent Technologies, Santa Clara, CA) and NanoDrop ND-1000 spectrophotometer (ThermoFisher Scientific), respectively. miRNA expression profiling was performed using GeneChip miRNA 1.0.2 arrays (Affymetrix, Santa Clara, CA) according to the manufacturer's protocol. The cell lines DB, FARAGE, OCI-Ly3, OCI-Ly7, OCI-Ly8, OCI-Ly19, NU-DHL-1, RIVA, and U2932 were prepared for hybridization using Flashtag HSR kit from Genesphere (Genesphere, Hatfield, PA) whereas HBL-1, MC-116, NU-DUL-1, SU-DHL-4, SU-DHL-5, and SU-DHL-8 were prepared using Fashtag Biotin HSR RNA labeling kit (Affymetrix) [14]. For GEP, RNA was labeled and hybridized to Affymetrix GeneChip Human Genome U133 (HG-U133) Plus 2.0 arrays, as described by the manufacturer. Generated miRNA and HG-U133 CEL files are

deposited at NCBI GEO repository GSE72648 and GSE109027, respectively. The data comply with MIAME requirements [23].

Experimental validation of miRNA expression in cell lines by digital droplet polymerase chain reaction

Two independent cDNA syntheses were conducted and pooled before amplification in digital droplet polymerase chain reaction (ddPCR) analysis. Each sample was analyzed in duplicate/triplicate using ddPCR assays and correlated to probes on U133 + 2; hsa-miR-146a (000468), hsa-miR-155 (002623), hsa-miR-21 (000397), hsa-miR-27a (000408) and hsa-miR-34a (000426). miRNA expression was normalized to RNU6B (001093) and RNU24 (001001) and log2 transformed prior to correlation to miRNA specific probes on U133 + 2 (232504_at for miR-146a, 22937_at for miR-155, 220990_s_at for miR-21, 1555847_a_at for miR-23a –miR-27a-miR-24-2, and 235571_at for miR-34a). Correlation coefficients shown in Supplementary Figure 5.

Statistical analysis

All statistical analyses were performed with R version 3.5.1; an accompanying knitR document with detailed information on the analysis and package versions is supplied in Supplementary Document S2. Prior to statistical analysis, the array data were cohort-wise background corrected and normalized at probe level by robust multi-chip average (RMA) [24] implemented in the Bioconductor package *affy* v1.58 [25].

Differentially expressed miRNAs between DLBCL cells lines classified as sensitive and resistant for rituximab, cyclophosphamide, doxorubicin, and vincristine, respectively, were identified using the empirical Bayes method [26] implemented in the R package *limma* v3.36.3 [27]. Since cell lines were prepared for hybridization to the miRNA 1.0.2 microarray platform with different labeling kits [14], differential miRNA expression analyses were adjusted for possible confounding with a kit effect by including it as a covariate in the model. MiRNAs with absolute log-fold changes greater than two ($|FC| > 2$) were considered as differentially expressed and were included in the list of candidate miRNAs subjected for further analysis. The set of candidate miRNAs for development of the prognostic classifier was chosen by filtering the set of differentially expressed miRNAs against those detected by HG-U133 probe sets. For each candidate probe set, correlation analysis between miRNA 1.0.2 array and HG-U133 array was conducted to validate HG-U133 array-based miRNA expression assessment.

Three clinical data sets (Table 2) were combined into a meta-cohort for training and validation of the prognostic classifiers. Validation was performed by repeated cross-validation with 10 folds and 10 repeats rather than using an independent validation set, since only two large clinical cohorts were available and we wanted to investigate the potential of a model trained on a combined dataset. By repeating the cross-validation we were able to investigate the variation in prediction accuracy resulting from the randomization in the cross-validation folds.

Table 2 Patient characteristics

	IDRC	LLMPP R-CHOP	AAU
n	468	233	73
Gender			
Female	198 (42%)	99 (42%)	30 (41%)
Male	270 (58%)	134 (58%)	43 (59%)
Age			
Median	63	61	66
Range	18–92	17–92	20–87
IPI			
0–1	254 (54%)	94 (40%)	48 (66%)
2–5	168 (36%)	70 (30%)	21 (29%)
NA	46 (10%)	69 (30%)	4 (5%)
ABC / GCB			
ABC	199 (43%)	93 (40%)	32 (44%)
GCB	225 (48%)	107 (46%)	32 (44%)
UC	44 (9%)	33 (14%)	9 (12%)

Number of patients and percentage within cohort / variable. *ABC* activated B-cell-like, *GCB* germinal center B-cell-like, *IPI* International prognostic index, *NA* not available, *n* number of patients, *UC* unclassified

To compensate for cohort-wise technical batch effects, the ComBat function implemented in the R-package *sva* [28] was applied. Training of prognostic classifiers were performed for all DLBCL patients and for subsets of ABC and GCB classified patients, respectively. Progression-free survival (PFS) was chosen as the outcome, since it is a treatment evaluation parameter as closely as possible to the time of drug exposure and the tested miRNAs were all associated directly to drug specific response. Furthermore, overall survival (OS) was used for verification of findings.

The prognostic miRNA-panel models were identified and trained by both multivariate Cox regression or random survival forest with 1000 trees using either drug-specific probes alone or in combination with a dichotomized IPI score (IPI "0–1" and "2–5" for low and high risk, respectively). The random survival forest implementation from the R-package *randomForestSRC* v2.7.0 was used [29–31]. For Cox regression models, variable selection was performed by preselecting probes that had a statistically significant effect in univariate Cox regressions adjusted for study effects ($p < 0.05$). The preselection of probes was performed for each cross-validation

fold and repetition to avoid sharing information between training and validation sets. Additionally, univariate Cox regression models using either IPI or age as input features were trained and used as a baseline comparison for the models including miRNA probes. The prognostic accuracies of the classifiers were validated by performing 10-fold cross-validation using either all DLBCL patients in the combined dataset, or the respective subsets of ABC or GCB classified patients. The models were ranked by the Brier score and time varying area under the ROC curves by comparing the predicted survival probability for each individual in the combined validation set from the cross-validations to the observed PFS and OS every half year from zero to five years.

The linear predictions from the Cox models in the cross-validation were used to get a score for each individual, by averaging across the scores from the 10 repeats of the cross-validation. By splitting these scores into tertiles Kaplan-Meier plots for low, intermediate, and high risk patients were generated within the respective cohorts and with significance evaluated by log-rank tests. Since more than 90% of events for both PFS and OS happened within the first 5 years Kaplan-Meier plots were restricted to this period. For all Kaplan-Meier analyses, significance threshold were set to 0.05.

Results

Identification of miRNAs associated with drug-specific response

Triplicate dose-response experiments were analyzed using area under the dose-response curve for rituximab, cyclophosphamide, doxorubicin, and vincristine, respectively, taking the individual cell line doubling time into account [21]. For each drug, the cell lines were ranked according to their sensitivity, grouped into tertiles and categorized as sensitive, intermediate responsive, or resistant (Table 1). Global miRNA expression screens were conducted on untreated cell lines for optimal candidate selection and subsequent differential miRNA expression analysis between sensitive and resistant cell lines identified 43 miRNAs to be associated with compounds of the R-CHOP regimen (Supplementary Tables 1, 2, 3, and 4). The majority of miRNAs associated with vincristine and doxorubicin were downregulated in resistant DLBCL cells, whereas rituximab resistance was primarily associated with upregulated miRNAs (Supplementary Tables 1, 3, and 4). Conversely, differentially expressed miRNAs for cyclophosphamide were equally distributed between up- and downregulation (Supplementary Table 2). Several miRNAs were associated with more than one drug (Fig. 1); of notice, 6 out of 13 miRNAs were shared between vincristine and doxorubicin. Additionally, miR-146a, miR-148a, miR-155, miR-221, and

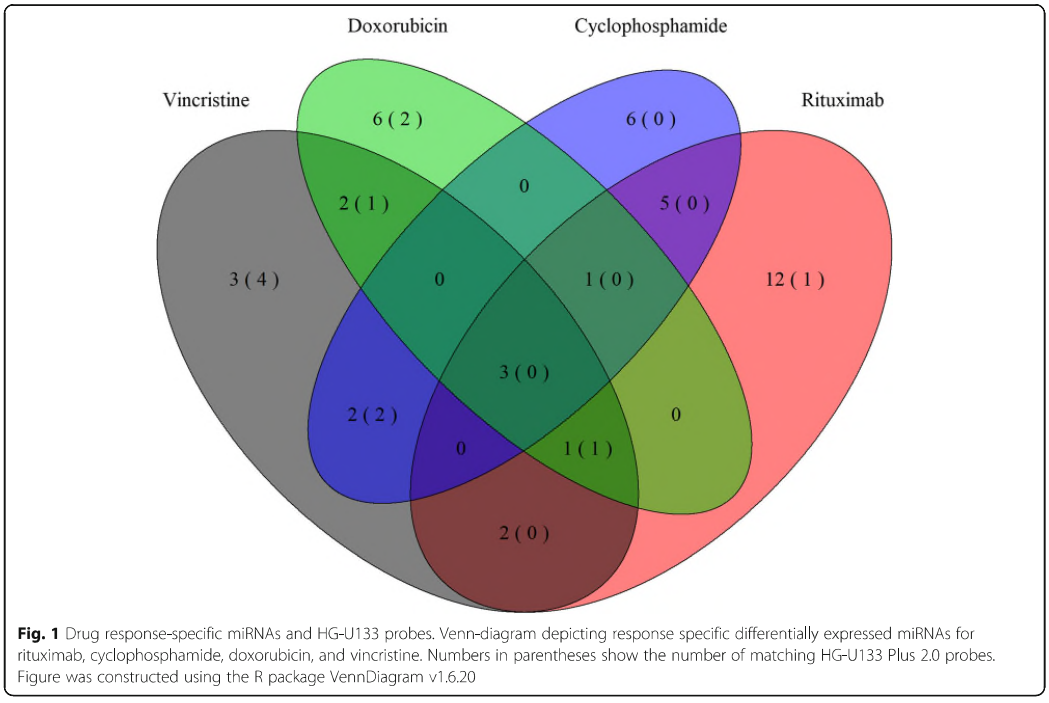

Fig. 1 Drug response-specific miRNAs and HG-U133 probes. Venn-diagram depicting response specific differentially expressed miRNAs for rituximab, cyclophosphamide, doxorubicin, and vincristine. Numbers in parentheses show the number of matching HG-U133 Plus 2.0 probes. Figure was constructed using the R package VennDiagram v1.6.20

miR-222 displayed ambiguous association to responses of different compounds of the regimen.

Since the miRNA microarray platform is not used in clinical context, miRNAs were matched to HG-U133 microarray probe sets detecting miRNA encoding genes, which reduced the candidate list to 11 probe sets detecting the following 9 miRNAs: miR-146a, miR-155, miR-21, miR-23a~27a~ 24–2 cluster, miR-34a, miR-503, and let-7b, which cover drug specific miRNAs for all four drugs (Fig. 1, Table 3).

miRNA-panel prognostic classifier

Based on the identified drug-specific miRNAs, multiple Cox regression and random survival forest models were used to build classifiers predicting disease progression in patients with DLBCL to test both parametric and non-parametric ensemble based survival models. Since ABC and GCB-classified patients display different miRNA expression patterns, pathogenesis and clinical outcome [2, 3, 11], the training and validation of prognostic models were conducted for all DLBCL patients and for ABC and GCB classified patients, respectively. Additionally, since IPI is well-established in the clinical setting, it was essential to evaluate if the prognostic miRNA classifiers added to the prognostic performance of IPI.

Prognostic accuracies of the generated miRNA-panel classifiers were assessed by Brier scores, which revealed better performance of the multivariate Cox models compared to the random survival forest models that had the largest prediction error regardless of input features (Fig. 2a-c). In contrast, evaluations of predictive performances by time varying area under the ROC curves were not as unambiguous, however, the highest predictive accuracy was still observed for multivariate Cox models (Fig. 2d-e). Comparison of analyses conducted for the respective cohorts (All DLBCL, ABC, and GCB patients) showed the lowest prediction errors for all models within the GCB subclass (Fig. 2a-c), with a multivariate Cox miRNA-panel model displaying prognostic utility comparable to IPI (Fig. 2f). In addition, combination of the miRNA-panel and IPI substantially increased prognostic performance in GCB classified patients (Fig. 2f), indicating a prognostic signal from the response-specific miRNAs independent of IPI. Furthermore, the Cox model combining IPI and the miRNA probe sets within the GCB subclass had the highest prognostic utility for all cross-validation repetitions showing a robust improvement.

In the ABC subclass, the developed miRNA-panel classifier did not provide additional prognostic information to IPI, either alone or in combination with IPI (Fig. 2b and e), suggesting little utility of the drug-specific miRNAs in this subclass. In agreement, similar results for ABC and GCB classified patients were observed when comparing the predicted PFS to the observed OS (Supplementary Figure 1). Consequently, the analyses were focused on the GCB subclass of DLBCL, which accounts for 46% of all cases (Table 2).

A linear prediction score was obtained for each individual in the combined GCB dataset by averaging the scores from the validation sets across the 10 repetitions of cross-validation for the multivariate Cox models using miRNA probe sets alone or in combination with IPI. These scores were used to rank the individual risk for all GCB classified patients, and by splitting the scores into tertiles, all GCB DLBCL patients were classified in

Table 3 Candidate miRNAs

Probe ID (HG-U133)	miRNA	Drug sensitivity	Annotation grade
232504_at	miR-146a	↓ Cyc, ↑ Vin	A
238225_at	miR-146a	↓ Cyc, ↑ Vin	B
229437_at	miR-155	↓ Rtx, ↑ Dox, ↑Vin	A
220990_s_at	miR-21	↑ Vin	A
229417_at	miR-21	↑ Vin	E
235317_at	miR-23a~miR-27a~miR-24-2	↑ Dox, ↑ Vin	B
1555847_a_at	miR-23a~miR-27a~miR-24-2	↑ Dox, ↑ Vin	A
235571_at	miR-34a	↑ Dox, ↑ Vin	A
1557342_a_at	let-7b	↑ Vin	A
241464_s_at	let-7b	↑ Vin	B
227488_at	miR-503	↓ Rtx	B

Differentially expressed miRNAs detected by HG-U133 Plus 2.0 probes were selected as candidate miRNAs. The list consisted of 11 probe sets detecting 9 miRNAs. The annotation grade was assessed by NetAffx (Affymetrix) a transcript assignment pipeline creating a relationship between GeneChip probe sets and current transcript record. The transcript assignment grades fall into five categories A-E that describe the quality of the direct evidence. Grade A is a matching probe set having nine or more probes matching transcript mRNA. Grade B transcript assignments have partial overlap between transcripts and target sequence. Grade E is given when no transcript is found. Abbreviations: ↑ and ↓ defines up- and downregulation, respectively, in drug sensitive cell lines. Cyc, cyclophosphamide; Dox, doxorubicin; Rtx, rituximab; Vin, vincristine

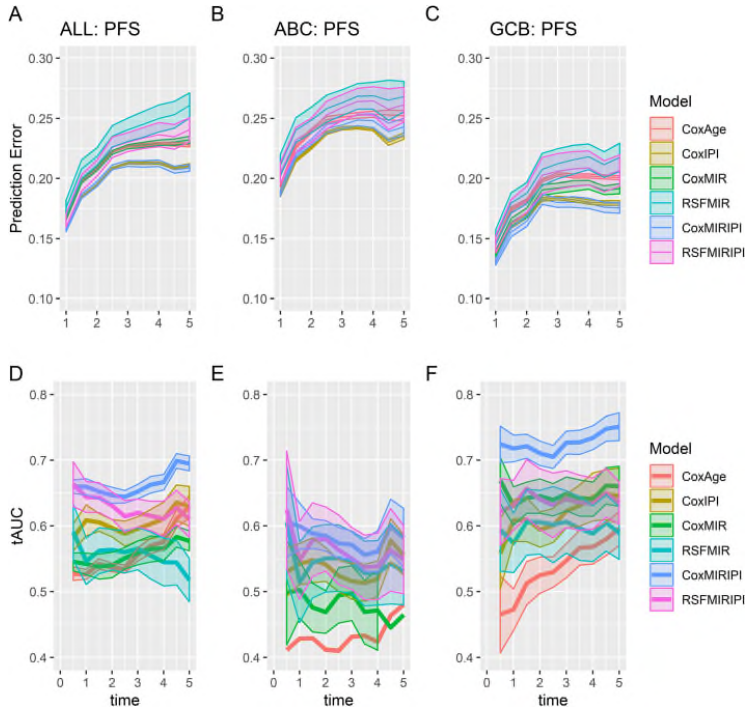

Fig. 2 Evaluation of prognostic accuracy. Predicted survival from various prognostic classifiers vs observed progression free survival with the Brier score (top row, **a-c**) or tAUC (bottom row, **d-f**). Figures display means + − 2SD evaluated across the 10 cross-validation repetitions. The prognostic classifiers include: multivariate Cox regression models using either age (CoxAge), IPI (CoxIPI), miRNA expression (CoxMIR), or miRNA expression combined with IPI score (CoxMIRIPI), and random survival forest models using miRNA expression (RSFMIR) or miRNA expression in combination with IPI (RSFMIRIPI). Time in years. Figure was constructed using the R packages *ggplot2* v3.2.1 and *gridExtra* v2.3. ABC, activated B-cell-like; GCB, germinal center B-cell-like; IPI, international prognostic index; MIR, microRNA panel; PFS, progression-free survival; RSF, random survival forest; tAUC, time-varying are under the ROC curve

defined groups of low, intermediate, and high-risk, the latter with significantly inferior prognosis as shown in the Kaplan-Meier plots for PFS and OS (Fig. 3, Supplementary Figure 2). The low and intermediate-risk group are not very distinct for the model including only miRNA probe sets, addition of IPI, however, clearly separates the patients into the distinct risk groups. The prognostic potential of the miRNA-panel was tested in each individual dataset validating the findings of inferior survival of patients with high-risk score (Supplementary Figure 3a-d).

In accordance, GCB DLBCL patients with stable or progressive disease at time of response evaluation [32] display higher risk scores (Fig. 4), with the biggest difference in mean risk scores for the model including IPI. In addition, the multivariate Cox regression model combining IPI and probe sets detecting drug-specific miRNAs (miR-146a, miR-155, miR-21, miR-34a, and the miR-23a~miR-27a~miR-24-2 cluster) displayed the strongest prognostic performance (Fig. 2c and f) and was selected as the best model. Selected features and coefficients of the developed prognostic classifier are presented in Table 4, showing that most of the prognostic signal is carried by IPI, and that some of the probes have insignificant signal, although they were significant in the univariate analysis (Supplementary Table 5). Six of the candidate probe sets were not included in the final model, as they did not display significant effect in univariate Cox regression analysis (Supplementary Table 5).

Expression levels of the probe sets included in the final prognostic model (Table 4) were highly correlated to the mature miRNA measured by miRNA array (Supplementary Figure 4), supporting HG-U133 array-based miRNA expression assessment. Of notice, expression of the six miRNAs without significant effect were not correlated to the mature miRNA

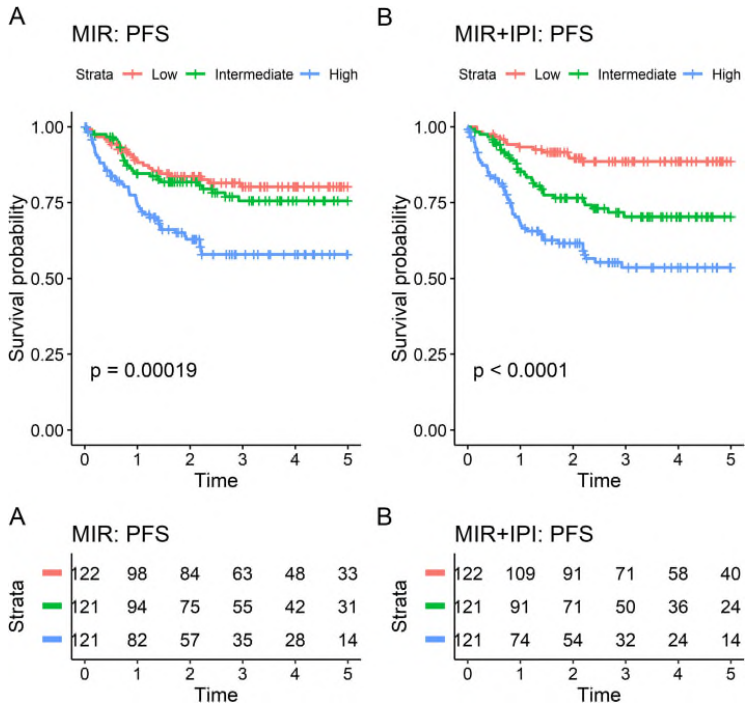

Fig. 3 Predicted risk group vs 5-year progression free survival in the combined GCB dataset. Risk groups were obtained by taking the average predicted risk score across validation folds for the repeated cross-validation for the multivariate Cox models using (**a**) miRNA probes either alone or (**b**) in combination with IPI and splitting these into tertiles. Figure was constructed using the R package *survminer* v0.4.6

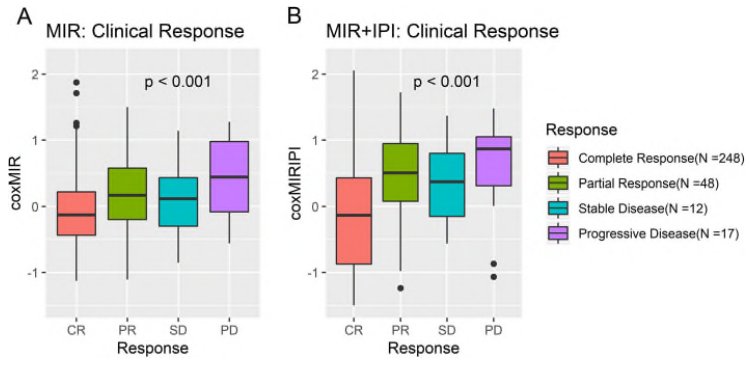

Fig. 4 Risk scores in Cheson response evaluation classes. Response evaluations of GCB classified patients were investigated for association to predicted risk scores. CR, complete remission; PD, progressive disease; PR, partial response; SD, stable disease. Risk scores were obtained by taking the average predicted risk score across validation folds for the repeated cross-validation for the multivariate Cox models using miRNA probes either alone or in combination with IPI. Figure was constructed using the R packages *ggplot2* v3.2.1 and *gridExtra* v2.3

Table 4 Selected features and corresponding coefficients for the final multivariate Cox model

Feature	miRNA	Hazard Ratio
IPI2–5		3.335
232504_at	miR-146a	0.857
229437_at	miR-155	0.868
220990_s_at	miR-21	0.995
1555847_a_at	miR-23a~miR-27a~miR-24-2	0.958
235571_at	miR-34a	0.776

The model was trained within the GCB subset of patients. MiRNA probes were pre-filtered to only include those significant in univariate Cox regression

(Supplementary Figure 4), most likely due to low probe set specificity (Annotation Grade B and E, Table 3). For all drug-specific miRNAs a hazard ratio below 1 is observed (Table 4), indicating that higher expression is associated with better prognosis corresponding to the original observation of down-regulation being associated to resistance in vitro (Table 3). Additionally, it is evident that vincristine and doxorubicin are the main contributors to the prognostic miRNA signature as most of the miRNAs in the final classifier were initially included due to significant effect on doxorubicin and vincristine resistance.

Discussion

Here, we combined global miRNA expression profiles and systematic dose-response screens to identify miRNAs associated to growth responses towards single drug components of the R-CHOP regimen. MiRNA-panel classifiers that assign individual DLBCL patients into low- and high-risk patients were generated utilizing two different approaches, multivariate Cox regression and random survival forest.

Several of the identified drug-specific miRNAs displayed ambiguous association to compounds of the R-CHOP regimen. Thus, high expression of miR-155 was associated with sensitivity to both doxorubicin and vincristine and with resistance to rituximab, most likely due to different drug mechanisms of actions and affected target genes. Noteworthy, doxorubicin and vincristine had 46% of the response specific miRNAs in common (miR-23a~miR-27a~miR-24, miR-34a, miR-155, and miR-222), indicating resistance mechanisms affecting the same molecular pathways. Consistently, ectopic induction of miR-34a have been shown to sensitize Ewing's sarcoma cells to doxorubicin and vincristine [33].

Anti-tumor drugs often have several mechanisms of actions. Cyclophosphamide has, beside the function as an alkylating agent, been shown to induce cytokine release from the cancer cells, thereby attracting macrophages and facilitating antibody-mediated elimination [34]. Our in vitro drug screen system lacks stromal cells and the tumor microenvironment, thus, it is important to emphasize that the identified cyclophosphamide-specific miRNAs is restricted to the DNA crosslinking mechanism of action. Furthermore, prednisone is a synthetic corticosteroid drug suppressing the immune system without cytotoxic effects and consequently, not included in this study. The majority of the miRNAs included in the final prognostic miRNA signature are associated with doxorubicin and vincristine, which consistently, are the two major cornerstones for efficacy of R-CHOP [35].

Evaluation of prognostic impact in this study is based on retrospective clinical cohorts where treatment conditions are not strictly unified regarding number of cycles, dosing [19, 20] and individual dose reductions due to side-effects like neuropathy [36]. Taking this and the pharmacological information on no synergistic effect of R-CHOP into account [8], single drug screens were used rather than combinational assays to identify candidate miRNAs to be assessed in non-weighted models using either multivariate Cox regression or random survival forest models. The candidate miRNA originating from single drug screens are thus tested and evaluated for prognostic impacts in DLBCL patients receiving the full R-CHOP regimen, ensuring that only miRNAs with enough statistical power alone in univariate Cox-regression analysis and in modelled combinations are included in the final miRNA signature/panel.

The gene expression-based ABC/GCB subclasses of DLBCL rely on distinct oncogenic mechanisms [37, 38] and since affected miRNA targets vary depending upon the cell type and differentiation stage in which the miRNA is expressed [39], prognostic classifiers were generated separately in ABC and GCB subclasses. The drug-response specific miRNA-panel demonstrated a significant prognostic association with PFS and OS in GCB classified DLBCL patients treated with R-CHOP. Consistently, the complete response rate after R-CHOP was significantly higher for low-risk patients than high-risk, documenting association between miRNA expression and response to R-CHOP.

Of the seven miRNAs significant in univariate Cox regression, expression levels of miR-21, miR-146a, and miR-155 have been confirmed to differentiate the ABC/GCB subclasses in ≥4 studies [11, 12, 40–46], emphasizing the molecular heterogeneity between the two molecular subclasses of DLBCL. This difference in expression levels as well as the cell type specific effect of a particular miRNA, could be the reason why only little prognostic utility of the miRNA-panel was observed for ABC classified patients in contrast to GCB patients. Additionally, IPI displayed lower prognostic accuracy in these patients compared to GCB classified patients,

indicating that new prognostic tools for ABC-DLBCL are needed.

The prognostic gold standard IPI is based solely on clinical parameters [4] and does not provide insight into the molecular pathways driving tumorigenesis and treatment resistance. Thus, molecular markers could potentially improve the prognostic accuracy of IPI and simultaneously provide information about the underlying molecular mechanisms. In line, combination of IPI with drug-specific miRNAs increased the prognostic accuracy in GCB-DLBCL. miRNAs display potential as a promising source of biomarkers as they, due to their small size, are relatively resistant to RNase degradation and are well-preserved in FFPE tissue [47]. Additionally, miRNAs can be detected in plasma and serum, thus, holding potential as liquid biomarkers [45, 48]. However, this study is proof of concept that addition of single drug-specific miRNAs to IPI improves prognostic stratification.

The prognostic utility of the miRNA probe sets was tested by training models using both the widely used semi-parametric multivariate Cox model, and the non-parametric ensemble based random survival forest. The Cox models relies on an assumption of proportional hazards and has a straightforward interpretation of parameters, whereas the random forest model makes no such assumptions and is able to fit more complex interactions among variables in the training data, but is more difficult to interpret. However, in our data we found no benefit of the random survival model compared to the Cox model. This might be caused by the limited number of variables which means that the individual survival trees are of limited depth, leading to too much bias in the predictions. Experimental validation of miRNA expression levels in cell lines are performed by ddPCR prior to correlation to miRNA specific probes on U133 + 2 (Supplementary Figure 4) generating coefficients of correlations ranging between 0.65 and 0.94 (Supplementary document S2, Table 5) supporting the usability of miRNAs in prognostic models with IPI.

A possible drawback of the current study is the lack of an independent external validation set, since the prediction accuracies from the cross-validation might be overestimated. The focus of the current study is, however, not the absolute but the relative prediction accuracy and thus ranking of different models. The ranking of the models could be affected by the randomization into cross-validation folds, results however showed that the multivariate cox model including both miRNA probe sets and IPI had superior prognostic signal within the GCB subgroup, regardless of cross-validation randomization, strengthening the hypothesis that miRNAs carry independent prognostic signal from IPI. However, further studies including an external validation set are needed before making recommendations on clinical application.

The miRNAs included in the final model are well studied miRNAs with known functions in normal B-cell differentiation and tumorigenesis [13, 49, 50]. miR-21 and miR-155 has been reported to be upregulated and to possess oncogenic properties in numerous cancers including breast cancer, glioblastoma, and DLBCL [51–55]. In addition, they have shown specific importance in the pathogenesis of DLBCL, highlighted by the fact that transgenic mice overexpressing miR-21 or miR-155 spontaneously develop lymphoma [56, 57]. In line, high expression of miR-21 is associated with inferior prognosis in DLBCL patients [55], and functional studies document a direct link between high miR-21 expression and CHOP resistance through regulation of PTEN [58]. miR-155 has been shown to control vincristine sensitivity in DLBCL cells through downregulation of Wee1 and clinical outcome analysis documented a significantly prolonged survival of GCB-classified DLBCL patient with high miR-155 expression [16].

Conclusions

In conclusion, we found as proof of concept that adding gene expression data detecting drug-specific miRNAs to the clinically established IPI improved the prognostic stratification of GCB-DLBCL patients treated with R-CHOP.

Supplementary information

Supplementary information accompanies this paper at https://doi.org/10.1186/s12885-020-6643-8.

Additional file 1: Table 1. Rituximab response-specific miRNAs. **Table 2.** Cyclophosphamide response-specific miRNAs. **Table 3.** Doxorubicin response-specific miRNAs. **Table 4.** Vincristine response-specific miRNAs. **Table 5.** Uni and multivariate cox regression analysis. **Figure 1.** Predicted survival from various prognostic classifiers vs observed overall survival with the brier score (top row) or time varying AUC (bottom row). **Figure 2.** Predicted risk group vs 5-year overall survival in the combined GCB dataset. **Figure 3.** Predicted risk group vs 5-year overall survival in GCB classified patients within each dataset: IDRC, LLMPPR-CHOP, and AAU. **Figure 4.** Correlation analysis between mature miRNA and miRNA encoding gene. **Figrue 5.** Correlation analysis between mature miRNA and miRNA encoding gene.

Additional file 2. MicroRNA associated to single drug components of R-CHOP identifies diffuse large B-cell lymphoma patients with poor outcome and adds prognostic value to the international prognostic index.

Abbreviations

ABC: Activated B-cell-like; ddPCR: Digital droplet polymerase chain reaction; DLBCL: Diffuse large B-cell lymphoma; GCB: The germinal center B-cell-like; GEO: Gene Expression Omnibus; GEP: Gene expression profiling; IDRC: International DLBCL Rituximab-CHOP Consortium MD Anderson Project; IPI: International prognostic index; LLMPP R-CHOP: Lymphoma/Leukemia Molecular Profiling Project R-CHOP; miRNA: MicroRNA; OS: Overall survival; PFS: Progression-free survival; R-CHOP: Rituximab, cyclophosphamide, doxorubicin, vincristine, prednisone; RMA: Robust multichip average; tAUC: Time varying area under the ROC curves

Acknowledgments
This work was presented at the 61st ASH Annual Meeting & Exposition, Orlando, December 2019 [59]. We greatly appreciate the technical assistance from Louise Hvilshøj Madsen and Helle Høholt, Department of Haematology, Aalborg University Hospital, Denmark.

Authors' contributions
H.D, R.F.B, M.B, and K.D designed the research; H.D, R.F.B, K.H.Y, M.B, and K.D collected the data; H.D and R.F.B performed experiments and statistical modelling, H.D and R.F.B. wrote the paper. All authors contributed to data interpretation and critically revised and approved the final manuscript.

Funding
This work was supported by grants from The Danish Cancer Society and The North Region Research Foundation, Denmark. The role of this grant was to financially support a PhD study of chemotherapy resistance in DLBCL. The funding bodies had no implications on the study design, collections, analysis, and interpretation of data or writing the manuscript.

Availability of data and materials
The datasets supporting the conclusions of this article are available in the National Center for Biotechnology Information Gene Expression Omnibus (GEO) repository, GSE72648 (https://www.ncbi.nlm.nih.gov/geo/query/acc.cgi?acc=GSE72648) and GSE109027 (https://www.ncbi.nlm.nih.gov/geo/query/acc.cgi?acc=GSE109027). In addition, we used the following online available data sets: Lymphoma/Leukemia Molecular Profiling Project R-CHOP (GSE10846) and International DLBCL Rituximab-CHOP Consortium MD Anderson Project (GSE31312).

Ethics approval and consent to participate
Tumor biopsies were collected in accordance with the RetroGen research protocol, reviewed approved by the Health Ethic Committee of North Denmark Region (Approval jr. no. N-20140099) allowing exemption from the requirement of informed consent according to Sections 3 to 5 in Danish Act on Research Ethics Review of Health Research Projects. Informed consent was waived since this notifiable database research project did not involve any health risks and under the given conditions could not otherwise put a strain on the trial subject.

Consent for publication
Not applicable.

Competing interests
The authors declare that they have no competing interests.

Author details
[1]Department of Hematology, Aalborg University Hospital, Sdr. Skovvej 15, DK-9000 Aalborg, Denmark. [2]Department of Clinical Medicine, Aalborg University, Aalborg, Denmark. [3]Clinical Cancer Research Center, Aalborg University Hospital, Aalborg, Denmark. [4]Duke University Medical Center, Division of Hematopathology and Department of Pathology, Durham, NC, USA.

Received: 25 September 2019 Accepted: 17 February 2020
Published online: 20 March 2020

References

1. Nogai H, Dörken B, Lenz G. Pathogenesis of non-Hodgkin's lymphoma. J Clin Oncol. 2011;29:1803–11. https://doi.org/10.1200/JCO.2010.33.3252.
2. Alizadeh AA, Eisen MB, Davis RE, Ma C, Lossos IS, Rosenwald A, et al. Distinct types of diffuse large B-cell lymphoma identified by gene expression profiling. Nature. 2000;403:503–11. https://doi.org/10.1038/35000501.
3. Swerdlow SH, Campo E, Pileri SA, Harris NL, Stein H, Siebert R, et al. The 2016 revision of the World Health Organization classification of lymphoid neoplasms. Blood. 2016;127:2375–90.
4. Project TIN-HLPF. A predictive model for aggressive non-Hodgkin's lymphoma. N Engl J Med. 1993;329:987–94. https://doi.org/10.1056/NEJM199309303291402.
5. Coiffier B, Lepage E, Briere J, Herbrecht R, Tilly H, Bouabdallah R, et al. CHOP chemotherapy plus rituximab compared with CHOP alone in elderly patients with diffuse large-B-cell lymphoma. N Engl J Med. 2002;346:235–42. https://doi.org/10.1056/NEJMoa011795.
6. Sehn LH, Donaldson J, Chhanabhai M, Fitzgerald C, Gill K, Klasa R, et al. Introduction of combined CHOP plus rituximab therapy dramatically improved outcome of diffuse large B-cell lymphoma in British Columbia. J Clin Oncol. 2005;23:5027–33. https://doi.org/10.1200/JCO.2005.09.137.
7. Friedberg JW. Relapsed/refractory diffuse large B-cell lymphoma. Hematol Am Soc Hematol Educ Progr. 2011;2011:498–505. https://doi.org/10.1182/asheducation-2011.1.498.
8. Palmer AC, Chidley C, Sorger PK. A curative combination cancer therapy achieves high fractional cell killing through low cross-resistance and drug additivity. Elife. 2019;8:e50036. https://doi.org/10.7554/eLife.50036.
9. Bartel DP. MicroRNAs: genomics, biogenesis, mechanism, and function. Cell. 2004;116:281–97. https://doi.org/10.1016/S0092-8674(04)00045-5.
10. Zhang B, Pan X, Cobb GP, Anderson TA. microRNAs as oncogenes and tumor suppressors. Dev Biol. 2007;302:1–12. https://doi.org/10.1016/J.YDBIO.2006.08.028.
11. Iqbal J, Shen Y, Huang X, Liu Y, Wake L, Liu C, et al. Global microRNA expression profiling uncovers molecular markers for classification and prognosis in aggressive B-cell lymphoma. Blood. 2015;125:1137–45. https://doi.org/10.1182/blood-2014-04-566778.
12. Due H, Svendsen P, Bødker JS, Schmitz A, Bøgsted M, Johnsen HE, et al. miR-155 as a Biomarker in B-Cell Malignancies. Biomed Res Int. 2016;2016:1–14. doi:https://doi.org/10.1155/2016/9513037.
13. Marques SC, Laursen MB, Bødker JS, Kjeldsen MK, Falgreen S, Schmitz A, et al. MicroRNAs in B-cells: from normal differentiation to treatment of malignancies. Oncotarget. 2015;6:7–25. https://doi.org/10.18632/oncotarget.3057.
14. Marques SC, Ranjbar B, Laursen MB, Falgreen S, Bilgrau AE, Bødker JS, et al. High miR-34a expression improves response to doxorubicin in diffuse large B-cell lymphoma. Exp Hematol. 2016;44:238–246.e2.
15. Rasmussen MH, Lyskjær I, Jersie-Christensen RR, Tarpgaard LS, Primdal-Bengtson B, Nielsen MM, et al. miR-625-3p regulates oxaliplatin resistance by targeting MAP2K6-p38 signalling in human colorectal adenocarcinoma cells. Nat Commun. 2016;7:12436. https://doi.org/10.1038/ncomms12436.
16. Due H, Schönherz AA, Ryø L, Primo MN, Jespersen DS, Thomsen EA, et al. MicroRNA-155 controls vincristine sensitivity and predicts superior clinical outcome in diffuse large B-cell lymphoma. Blood Adv. 2019;3:1185–96.
17. Falgreen S, et al. hemaClass. org: online one-by-one microarray normalization and classification of hematological cancers for precision medicine. PLoS One. 2016;11(10).
18. Falgreen S, Dybkær K, Young KH, Xu-Monette ZY, El-Galaly TC, Laursen MB, et al. Predicting response to multidrug regimens in cancer patients using cell line experiments and regularised regression models. BMC Cancer. 2015;15:235. https://doi.org/10.1186/s12885-015-1237-6.
19. Lenz G, Wright G, Dave SS, Xiao W, Powell J, Zhao H, et al. Stromal gene signatures in large-B-cell lymphomas. N Engl J Med. 2008;359:2313–23. https://doi.org/10.1056/NEJMoa0802885.
20. Visco C, Li Y, Xu-Monette ZY, Miranda RN, Green TM, Li Y, et al. Comprehensive gene expression profiling and immunohistochemical studies support application of immunophenotypic algorithm for molecular subtype classification in diffuse large B-cell lymphoma: a report from the international DLBCL rituximab-CHOP Consortiu. Leukemia. 2012;26:2103–13.
21. Falgreen S, Laursen M, Bødker J, Kjeldsen M, Schmitz A, Nyegaard M, et al. Exposure time independent summary statistics for assessment of drug dependent cell line growth inhibition. BMC Bioinformatics. 2014;15:168. https://doi.org/10.1186/1471-2105-15-168.
22. Dybkær K, Bøgsted M, Falgreen S, Bødker JS, Kjeldsen MK, Schmitz A, et al. Diffuse large B-cell lymphoma classification system that associates normal B-cell subset phenotypes with prognosis. J Clin Oncol. 2015;33:1379–88. https://doi.org/10.1200/JCO.2014.57.7080.
23. Brazma A, Hingamp P, Quackenbush J, Sherlock G, Spellman P, Stoeckert C, et al. Minimum information about a microarray experiment (MIAME)—toward standards for microarray data. Nat Genet. 2001;29:365–71. https://doi.org/10.1038/ng1201-365.
24. Irizarry RA, Hobbs B, Collin F, Beazer-Barclay YD, Antonellis KJ, Scherf U, et al. Exploration, normalization, and summaries of high density oligonucleotide array probe level data. Biostatistics. 2003;4:249–64. https://doi.org/10.1093/biostatistics/4.2.249.
25. Gautier L, Cope L, Bolstad BM, Irizarry RA. Affy—analysis of Affymetrix GeneChip data at the probe level. Bioinformatics. 2004;20:307–15. https://doi.org/10.1093/bioinformatics/btg405.

26. Phipson B, Lee S, Majewski IJ, Alexander WS, Smyth GK. Robust hyperparameter estimation protects against hypervariable genes and improves power to detect differential expression. Ann Appl Stat. 2016;10:946–63.
27. Ritchie ME, Phipson B, Wu D, Hu Y, Law CW, Shi W, et al. Limma powers differential expression analyses for RNA-sequencing and microarray studies. Nucleic Acids Res. 2015;43:e47. https://doi.org/10.1093/nar/gkv007.
28. Leek JT, Johnson WE, Parker HS, Fertig EJ, Jaffe AE, Storey JD, Zhang Y TL. sva: Surrogate Variable Analysis. R package version 3.28.0. 2018.
29. Ishwaran H, Kogalur UB, Blackstone EH, Lauer MS. Random survival forests. Ann Appl Stat. 2008;2:841–60 http://arxiv.org/abs/0811.1645v1.
30. Ishwaran H, Kogalur UB. Random survival forests for R. R News. 2007;7:25–31 https://cran.r-project.org/doc/Rnews/.
31. Ishwaran H, Kogalur UB. Fast unified random forests for survival, regression, and classification (RF-SRC). 2019. https://cran.r-project.org/package=randomForestSRC.
32. Cheson BD, Pfistner B, Juweid ME, Gascoyne RD, Specht L, Horning SJ, et al. Revised response criteria for malignant lymphoma. J Clin Oncol. 2007;25:579–86. https://doi.org/10.1200/JCO.2006.09.2403.
33. Nakatani F, Ferracin M, Manara MC, Ventura S, Del Monaco V, Ferrari S, et al. miR-34a predicts survival of Ewing's sarcoma patients and directly influences cell chemo-sensitivity and malignancy. J Pathol J Pathol. 2012;226:796–805. https://doi.org/10.1002/path.3007.
34. Pallasch CP, Leskov I, Braun CJ, Vorholt D, Drake A, Soto-Feliciano YM, et al. Sensitizing protective tumor microenvironments to antibody-mediated therapy. Cell. 2014;156:590–602. https://doi.org/10.1016/J.CELL.2013.12.041.
35. Wilson WH. Treatment strategies for aggressive lymphomas: what works? Hematol Am Soc Hematol Educ Progr. 2013;2013:584–90. https://doi.org/10.1182/asheducation-2013.1.584.
36. Madsen ML, Due H, Ejskjær N, Jensen P, Madsen J, Dybkær K. Aspects of vincristine-induced neuropathy in hematologic malignancies: a systematic review. Cancer Chemother Pharmacol. 2019;84(3):471–85. https://doi.org/10.1007/s00280-019-03884-5.
37. Lenz G, Wright GW, Tolga Emre NC, Kohlhammer H, Dave SS, Davis RE, et al. Molecular subtypes of diffuse large B-cell lymphoma arise by distinct genetic pathways. 2008. www.pnas.org/cgi/content/full/.
38. Pasqualucci L, Trifonov V, Fabbri G, Ma J, Rossi D, Chiarenza A, et al. Analysis of the coding genome of diffuse large B-cell lymphoma. Nat Genet. 2011;43:830–7. https://doi.org/10.1038/ng.892.
39. Clark PM, Loher P, Quann K, Brody J, Londin ER, Rigoutsos I. Argonaute CLIP-Seq reveals miRNA targetome diversity across tissue types. Sci Rep. 2015;4:5947. https://doi.org/10.1038/srep05947.
40. Caramuta S, Lee L, Özata DM, Akçakaya P, Georgii-Hemming P, Xie H, et al. Role of microRNAs and microRNA machinery in the pathogenesis of diffuse large B-cell lymphoma. Blood Cancer J. 2013;3:e152. https://doi.org/10.1038/bcj.2013.49.
41. Lawrie CH, Saunders NJ, Soneji S, Palazzo S, Dunlop HM, Cooper CDO, et al. MicroRNA expression in lymphocyte development and malignancy. Leukemia. 2008;22:1440–6. https://doi.org/10.1038/sj.leu.2405083.
42. Lawrie CH, Chi J, Taylor S, Tramonti D, Ballabio E, Palazzo S, et al. Expression of microRNAs in diffuse large B cell lymphoma is associated with immunophenotype, survival and transformation from follicular lymphoma. J Cell Mol Med. 2009;13:1248–60. https://doi.org/10.1111/j.1582-4934.2008.00628.x.
43. Malumbres R, Sarosiek KA, Cubedo E, Ruiz JW, Jiang X, Gascoyne RD, et al. Differentiation stage-specific expression of microRNAs in B lymphocytes and diffuse large B-cell lymphomas. Blood. 2009;113:3754–64. https://doi.org/10.1182/blood-2008-10-184077.
44. Lawrie CH, Soneji S, Marafioti T, Cooper CDO, Palazzo S, Paterson JC, et al. Microrna expression distinguishes between germinal center B cell-like and activated B cell-like subtypes of diffuse large B cell lymphoma. Int J Cancer. 2007;121:1156–61. https://doi.org/10.1002/ijc.22800.
45. Chen W, Wang H, Chen H, Liu S, Lu H, Kong D, et al. Clinical significance and detection of microRNA-21 in serum of patients with diffuse large B-cell lymphoma in Chinese population. Eur J Haematol. 2014;92:407–12. https://doi.org/10.1111/ejh.12263.
46. Zhong H, Xu L, Zhong J-H, Xiao F, Liu Q, Huang H-H, et al. Clinical and prognostic significance of miR-155 and miR-146a expression levels in formalin-fixed/paraffin-embedded tissue of patients with diffuse large B-cell lymphoma. Exp Ther Med. 2012;3:763–70. https://doi.org/10.3892/etm.2012.502.
47. Li J, Smyth P, Flavin R, Cahill S, Denning K, Aherne S, et al. Comparison of miRNA expression patterns using total RNA extracted from matched samples of formalin-fixed paraffin-embedded (FFPE) cells and snap frozen cells. BMC Biotechnol. 2007;7:36. https://doi.org/10.1186/1472-6750-7-36.
48. Jones K, Nourse JP, Keane C, Bhatnagar A, Gandhi MK. Plasma microRNA are disease response biomarkers in classical Hodgkin lymphoma. Clin Cancer Res. 2014;20:253–64. https://doi.org/10.1158/1078-0432.CCR-13-1024.
49. Kurkewich JL, Hansen J, Klopfenstein N, Zhang H, Wood C, Boucher A, et al. The miR-23a~27a~24-2 microRNA cluster buffers transcription and signaling pathways during hematopoiesis. PLoS Genet. 2017;13:e1006887. https://doi.org/10.1371/journal.pgen.1006887.
50. Thai T-H, Calado DP, Casola S, Ansel KM, Xiao C, Xue Y, et al. Regulation of the germinal center response by microRNA-155. Science. 2007;316:604–8. https://doi.org/10.1126/science.1141229.
51. Qian B, Katsaros D, Lu L, Preti M, Durando A, Arisio R, et al. High miR-21 expression in breast cancer associated with poor disease-free survival in early stage disease and high TGF-β1. Breast Cancer Res Treat. 2009;117:131–40. https://doi.org/10.1007/s10549-008-0219-7.
52. Jiang S, Zhang H-W, Lu M-H, He X-H, Li Y, Gu H, et al. MicroRNA-155 functions as an OncomiR in breast cancer by targeting the suppressor of cytokine signaling 1 gene. Cancer Res. 2010;70:3119–27. https://doi.org/10.1158/0008-5472.CAN-09-4250.
53. Yang CH, Yue J, Pfeffer SR, Fan M, Paulus E, Hosni-Ahmed A, et al. MicroRNA-21 promotes glioblastoma tumorigenesis by down-regulating insulin-like growth factor-binding protein-3 (IGFBP3). J Biol Chem. 2014;289:25079–87. https://doi.org/10.1074/jbc.M114.593863.
54. Marsigliante S, D'Urso OF, Storelli C, Mallardo M, Gianfreda CD, Montinaro A, et al. miR-155 is up-regulated in primary and secondary glioblastoma and promotes tumour growth by inhibiting GABA receptors. Int J Oncol. 2012;41:228–34. https://doi.org/10.3892/ijo.2012.1420.
55. Go H, Jang J-Y, Kim P-J, Kim Y-G, Nam SJ, Paik JH, et al. MicroRNA-21 plays an oncogenic role by targeting FOXO1 and activating the PI3K/AKT pathway in diffuse large B-cell lymphoma. Oncotarget. 2015;6:15035–49. https://doi.org/10.18632/oncotarget.3729.
56. Babar IA, Cheng CJ, Booth CJ, Liang X, Weidhaas JB, Saltzman WM, et al. Nanoparticle-based therapy in an in vivo microRNA-155 (miR-155)-dependent mouse model of lymphoma. Proc Natl Acad Sci U S A. 2012;109:E1695–704. https://doi.org/10.1073/pnas.1201516109.
57. Medina PP, Nolde M, Slack FJ. OncomiR addiction in an in vivo model of microRNA-21-induced pre-B-cell lymphoma. Nature. 2010;467:86–90. https://doi.org/10.1038/nature09284.
58. Bai H, Wei J, Deng C, Yang X, Wang C, Xu R. MicroRNA-21 regulates the sensitivity of diffuse large B-cell lymphoma cells to the CHOP chemotherapy regimen. Int J Hematol. 2013;97:223–31. https://doi.org/10.1007/s12185-012-1256-x.
59. Dybkær K, Due H, Brøndum RF, Young KH, Bøgsted M. Addition of Drug-Response Specific Micro-RNAs to the International Prognostic Index Improves Prognostic Stratification of GCB-DLBCL Patients Treated with R-CHOP. Blood. 2019;134(Supplement_1):1623.

Publisher's Note

Supplementary document S1

MicroRNAs associated to single drug components of R-CHOP identifies diffuse large B-cell lymphoma patients with poor outcome and adds prognostic value to the international prognostic index

Hanne Due, Rasmus Froberg Brøndum, Ken H. Young, Martin Bøgsted, and Karen Dybkær

Supplementary Tables

Supplementary Table 1. Rituximab response-specific miRNAs.

	logFC	AveExpr	t	P.Value	adj.P.Val	B
hsa-miR-222_st	6,127705	6,746617	2,335574	0,046563	0,99527	-4,46427
hsa-miR-221_st	5,053428	6,674317	1,886941	0,094462	0,99527	-4,50909
hsa-miR-155_st	3,043049	10,72422	1,965219	0,083584	0,99527	-4,50105
hsa-miR-345_st	2,866339	4,783869	1,723372	0,121665	0,99527	-4,52602
hsa-miR-30a_st	2,786987	4,874182	2,433865	0,039838	0,99527	-4,45496
hsa-miR-125b_st	2,598253	4,129437	1,049439	0,323503	0,99527	-4,59299
hsa-miR-183_st	2,526305	5,650952	3,008412	0,016116	0,99527	-4,40543
hsa-miR-503_st	2,517528	3,58562	2,299829	0,04928	0,99527	-4,4677
hsa-miR-9-star_st	2,441592	2,589669	3,016243	0,015921	0,99527	-4,40481
hsa-miR-551b_st	2,399113	2,331537	1,782125	0,111144	0,99527	-4,51992
hsa-miR-27b_st	2,294824	5,77071	2,15522	0,061967	0,99527	-4,48188
hsa-miR-424-star_st	2,293201	3,463778	1,858482	0,098741	0,99527	-4,51202
hsa-miR-99a_st	2,121462	3,714087	0,905464	0,390688	0,997061	-4,60535
hsa-miR-708_st	2,108274	4,108474	1,155873	0,279847	0,99527	-4,58322
hsa-miR-886-5p_st	2,069917	4,041259	0,988245	0,3509	0,997061	-4,59838
hsa-miR-886-3p_st	2,059803	3,926248	1,353949	0,211383	0,99527	-4,56395
hsa-miR-30a-star_st	2,039417	1,706873	1,795034	0,108949	0,99527	-4,51859
hsa-miR-629-star_st	-2,25157	3,931262	-2,16803	0,060724	0,99527	-4,48061
hsa-miR-151-3p_st	-2,46828	6,287612	-2,63478	0,028975	0,99527	-4,43666
hsa-miR-1303_st	-2,53781	2,774613	-2,41659	0,040945	0,99527	-4,45658
hsa-miR-151-5p_st	-2,73673	9,110051	-3,10579	0,013857	0,99527	-4,39791
hsa-miR-193b-star_st	-3,76472	4,193284	-3,83514	0,004628	0,99527	-4,34937
hsa-miR-193b_st	-4,03679	7,623577	-3,91546	0,004119	0,99527	-4,3448
hsa-miR-138_st	-4,16554	6,175924	-3,0731	0,014576	0,99527	-4,4004

Differentially expressed miRNAs detected comparing global miRNA expression profiles of rituximab sensitive and resistant DLBCL cell lines.

Supplementary Table 2. Cyclophosphamide response-specific miRNAs.

	logFC	AveExpr	t	P.Value	adj.P.Val	B
hsa-miR-146a_st	4,703233	9,474632	1,863339	0,103797	0,957447	-4,41698
hsa-miR-148a_st	2,945592	5,477236	1,728867	0,126546	0,957447	-4,58636
hsa-miR-193b-star_st	2,551795	4,381195	1,831364	0,108821	0,957447	-4,45761
hsa-miR-30a_st	2,492496	3,816329	2,71736	0,029269	0,918181	-3,29987
hsa-miR-99b_st	2,396544	2,20903	2,000733	0,084656	0,957447	-4,24042
hsa-miR-551b_st	2,350764	2,459864	1,485161	0,180185	0,971399	-4,88087
hsa-miR-148a-star_st	2,321438	2,687642	1,890166	0,099756	0,957447	-4,38275
hsa-miR-664-star_st	2,152382	3,391757	2,159586	0,066825	0,957447	-4,03327
hsa-miR-152_st	2,023634	4,542684	2,094523	0,073626	0,957447	-4,11841
hsa-miR-151-3p_st	-2,23555	5,757154	-2,31506	0,053015	0,957447	-3,8288
hsa-miR-486-3p_st	-2,30555	2,473152	-7,08054	0,000178	0,075391	0,853311
hsa-miR-151-5p_st	-2,71017	7,972961	-1,35084	0,21792	0,984429	-5,03406
hsa-miR-138_st	-3,66317	6,355507	-1,66731	0,138474	0,957447	-4,66244
hsa-miR-486-5p_st	-4,4186	4,465431	-7,28733	0,000148	0,075391	0,976114
hsa-miR-221_st	-5,31488	7,620498	-1,82912	0,109182	0,957447	-4,46044
hsa-miR-222_st	-5,98562	7,443487	-1,72428	0,1274	0,957447	-4,59206
hsa-miR-708_st	-6,07315	4,649318	-6,33909	0,000356	0,100596	0,367718

Differentially expressed miRNAs detected comparing global miRNA expression profiles of cyclophosphamide sensitive and resistant DLBCL cell lines.

Supplementary Table 3. Doxorubicin response-specific miRNAs.

	logFC	AveExpr	t	P.Value	adj.P.Val	B
hsa-miR-222_st	-6,37335	6,110226	-2,86841	0,01821	0,955019	-4,35893
hsa-miR-221_st	-5,51097	6,38203	-2,95342	0,015839	0,955019	-4,34936
hsa-miR-34a_st	-3,28063	3,920212	-2,12977	0,06153	0,955019	-4,45114
hsa-miR-27a_st	-2,84788	6,522453	-3,52912	0,006252	0,955019	-4,29097
hsa-miR-708_st	-2,7983	4,150388	-1,92045	0,08644	0,955019	-4,47946
hsa-miR-200c_st	-2,62599	5,556842	-1,63585	0,135722	0,955019	-4,51833
hsa-miR-23a_st	-2,60387	9,104988	-3,11672	0,012131	0,955019	-4,33167
hsa-miR-155_st	-2,1725	10,32635	-1,5163	0,16318	0,955019	-4,53447
hsa-miR-129-5p_st	2,009089	2,5239	2,751015	0,022094	0,955019	-4,37252
hsa-miR-193b-star_st	2,192303	4,765981	1,659642	0,130781	0,955019	-4,5151
hsa-miR-1295_st	2,240827	2,366998	2,595591	0,028558	0,955019	-4,39119
hsa-miR-181a-2-star_st	2,466703	4,281511	1,525795	0,16083	0,955019	-4,5332
hsa-miR-125a-5p_st	2,477203	3,493375	2,06706	0,068163	0,955019	-4,45957

Differentially expressed miRNAs detected comparing global miRNA expression profiles of doxorubicin sensitive and resistant DLBCL cell lines.

Supplementary Table 4. Vincristine response-specific miRNAs.

	logFC	AveExpr	t	P.Value	adj.P.Val	B
hsa-miR-886-5p_st	-2,03165	4,060709	-1,62739	0,155239	0,94908	-4,54467
hsa-miR-27a_st	-2,08251	6,60642	-1,83862	0,116057	0,94908	-4,52719
hsa-miR-708_st	-2,09384	4,1347	-0,97634	0,36694	0,94908	-4,59881
hsa-miR-146a_st	-2,10943	9,790432	-1,1267	0,303288	0,94908	-4,58685
hsa-miR-21-star_st	-2,28182	4,20414	-3,37078	0,015242	0,94908	-4,43104
hsa-miR-886-3p_st	-2,32203	3,868368	-2,28088	0,063129	0,94908	-4,49342
hsa-let-7b_st	-2,34635	9,877806	-1,59086	0,163205	0,94908	-4,54775
hsa-miR-148a_st	-2,60258	4,725986	-1,55092	0,172358	0,94908	-4,55113
hsa-miR-221_st	-2,81947	5,78796	-1,0042	0,354391	0,94908	-4,59665
hsa-miR-34a_st	-3,14712	3,557925	-1,65758	0,14894	0,94908	-4,54214
hsa-miR-21_st	-3,21691	4,197068	-3,41433	0,014451	0,94908	-4,42913
hsa-miR-222_st	-3,85905	5,283139	-1,20921	0,272469	0,94908	-4,58005
hsa-miR-155_st	-3,95284	10,24486	-2,566	0,042918	0,94908	-4,47421

Differentially expressed miRNAs detected comparing global miRNA expression profiles of vincristine sensitive and resistant DLBCL cell lines.

Supplementary Table 5. Uni and multivariate cox regression analysis

	miRNA	uni.HR	uni.conf	uni.p	multi.HR	multi.conf	multi.p
238225_at	miR-146a	0.92	(0.49;1.71)	0.792	(0.61;2.14)	(0.61;2.14)	0.669
232504_at	miR-146a	0.69	(0.58;0.81)	0.000	(0.65;1)	(0.65;1)	0.047
229437_at	miR-155	0.75	(0.66;0.85)	0.000	(0.73;1.04)	(0.73;1.04)	0.120
220990_s_at	miR-21	0.74	(0.62;0.88)	0.001	(0.79;1.39)	(0.79;1.39)	0.760
229417_at	miR-21	0.90	(0.55;1.46)	0.666	(0.54;1.42)	(0.54;1.42)	0.591
235317_at	miR-23a	0.98	(0.64;1.5)	0.932	(0.8;2.29)	(0.8;2.29)	0.257
1555847_a_at	miR-23a	0.76	(0.59;0.97)	0.025	(0.61;1.23)	(0.61;1.23)	0.418
235571_at	miR-34a	0.54	(0.38;0.77)	0.001	(0.44;1.02)	(0.44;1.02)	0.064
1557342_a_at	hsa-let-7b	1.02	(0.57;1.84)	0.945	(0.46;1.51)	(0.46;1.51)	0.549
241464_s_at	hsa-let-7b	0.73	(0.33;1.58)	0.422	(0.35;1.62)	(0.35;1.62)	0.464
227488_at	miR-503	1.11	(0.62;1.98)	0.726	(0.57;1.93)	(0.57;1.93)	0.875

Hazard ratio (HR), 95% confidence interval and p-value for uni- and multivariate Cox regression.

Supplementary Figures

Supplementary figure 1:

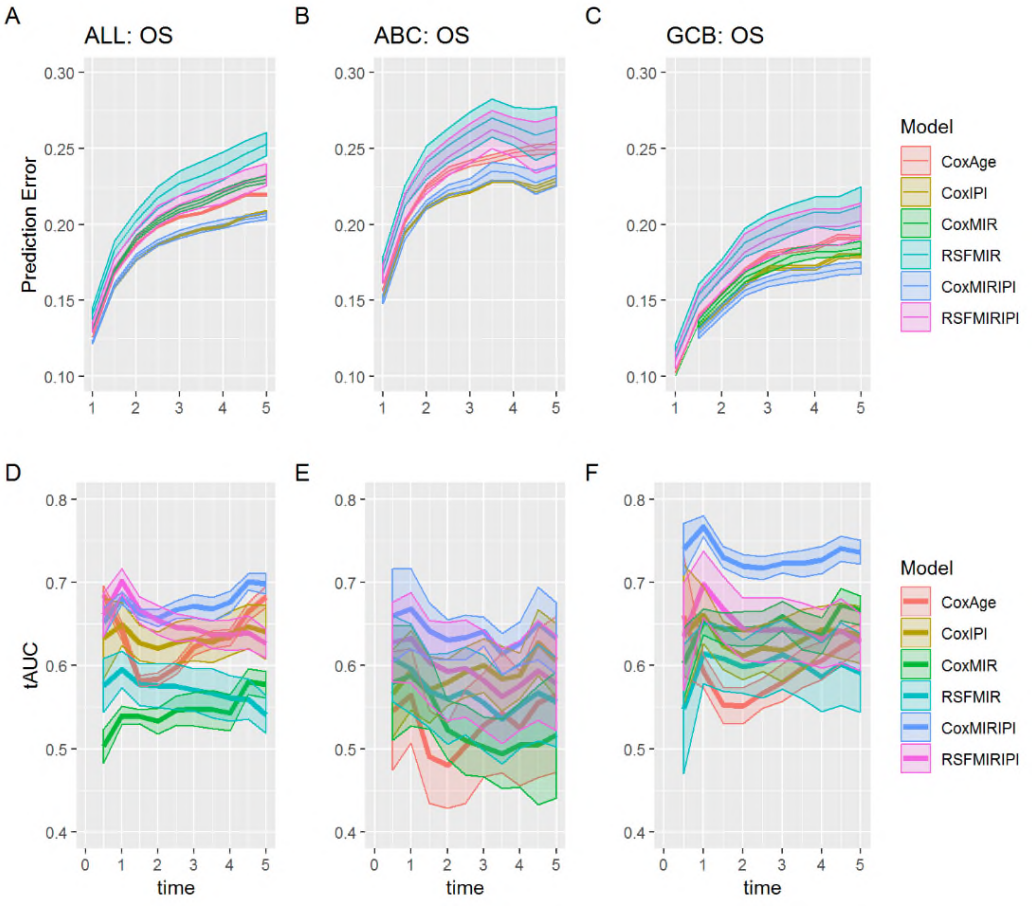

Predicted survival from various prognostic classifiers vs observed overall survival with the brier score (top row) or time varying AUC (bottom row). Figures display means +- 2SD evaluated across the 10 cross-validation repetitions. The prognostic classifiers include: multivariate Cox regression models using either age (CoxAge), IPI (CoxIPI), miRNA expression (CoxMIR), or miRNA expression combined with IPI score (CoxMIRIPI), and random survival forest models using miRNA expression (RSFMIR) or miRNA expression in combination with

IPI (RSFMIRIPI). ABC, activated B-cell-like; GCB, germinal center B-cell-like; IPI, international prognostic index; MIR, microRNA panel; PFS, progression-free survival; RSF, random survival forest. Time in years.

Supplementary figure 2:

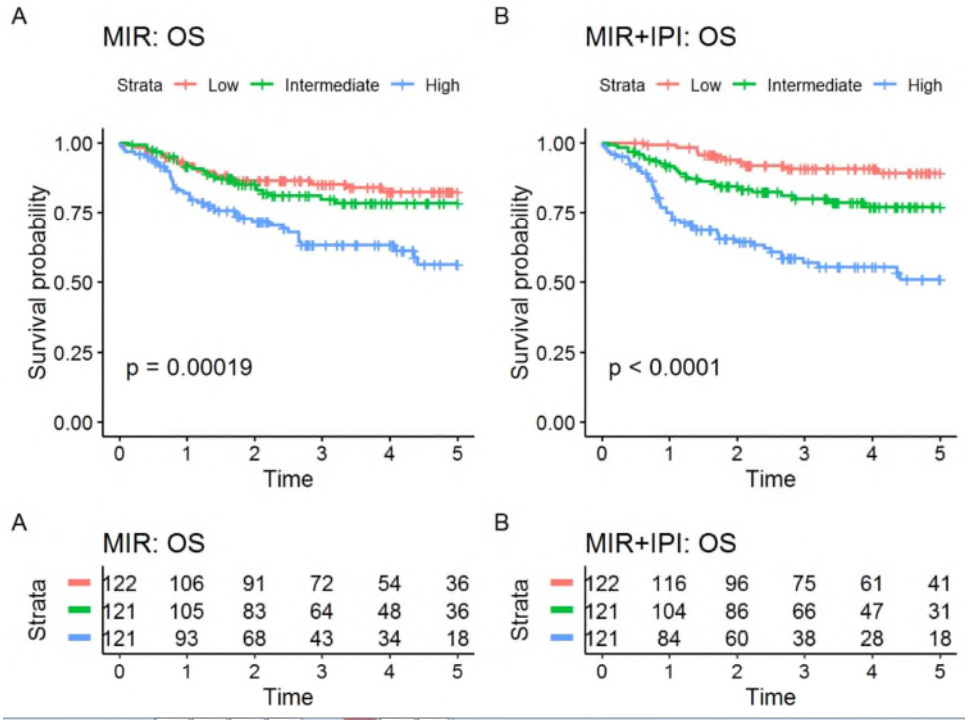

Predicted risk group vs 5-year overall survival in the combined GCB dataset. Risk scores were obtained by taking the average predicted risk score across validation folds for the repeated cross-validation and diving these into tertiles.

Supplementary figure 3:

A

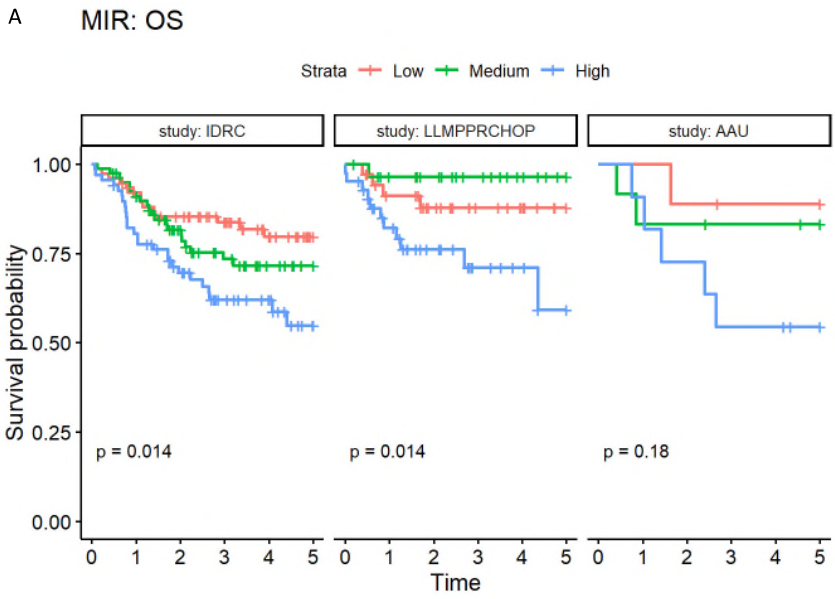

B

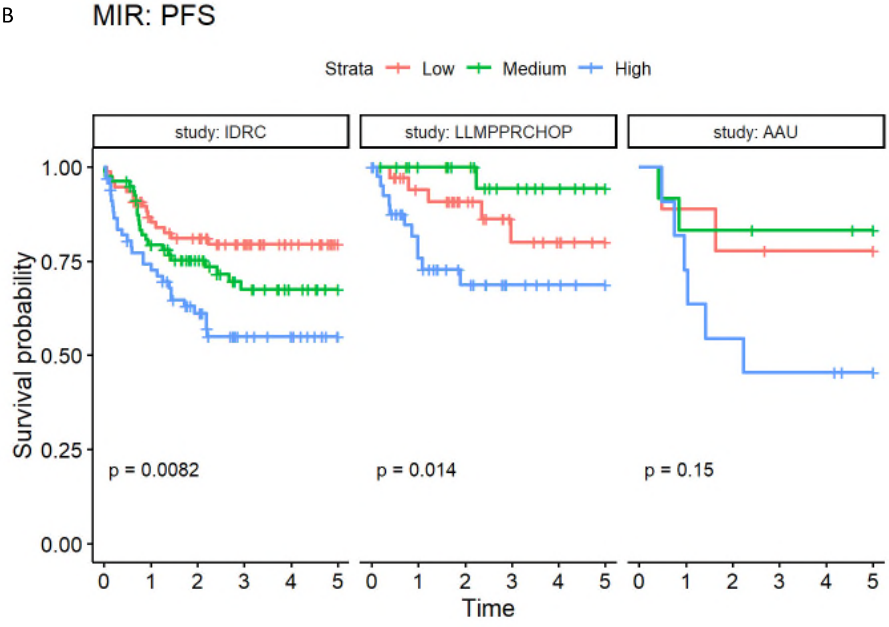

C

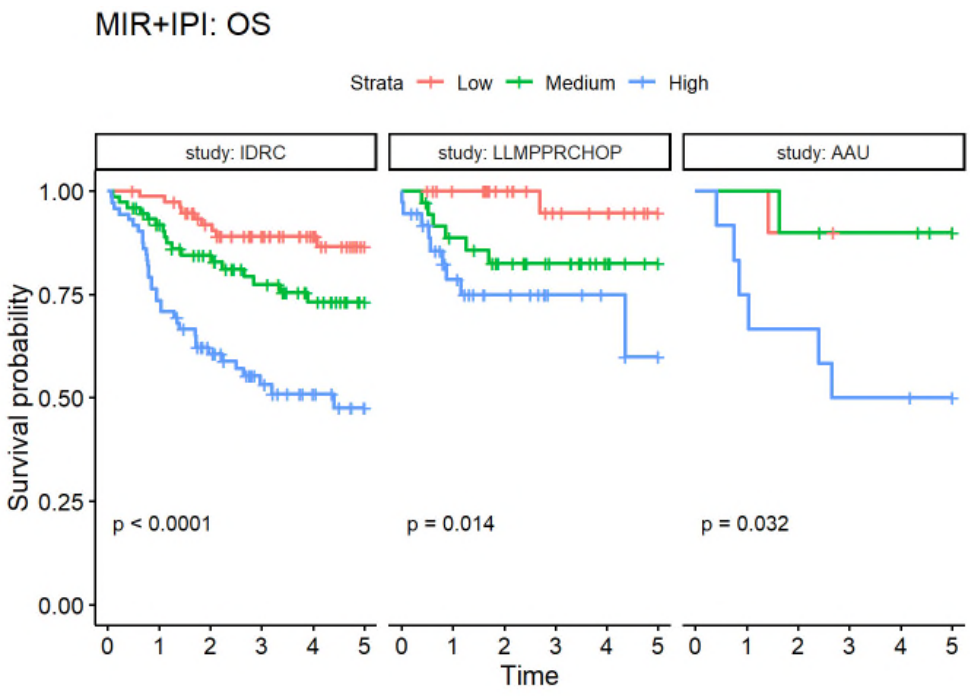
MIR+IPI: OS
Strata Low Medium High
study: IDRC
study: LLMPPRCHOP
study: AAU
Survival probability
1.00
0.75
0.50
0.25
0.00
p < 0.0001
p = 0.014
p = 0.032
0 1 2 3 4 5
Time

D

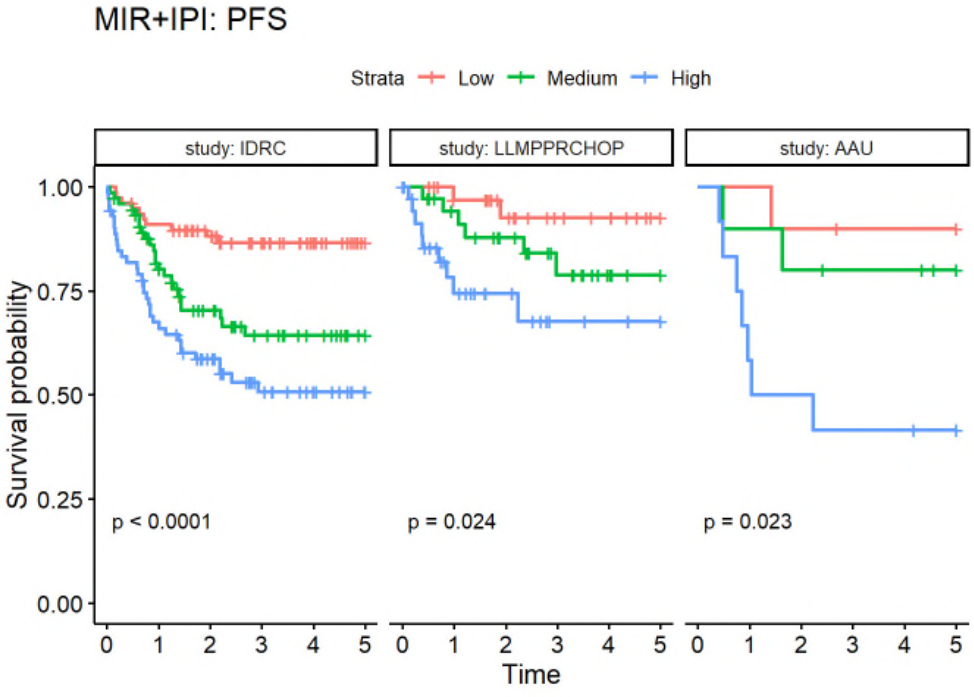
MIR+IPI: PFS
Strata Low Medium High
study: IDRC
study: LLMPPRCHOP
study: AAU
Survival probability
1.00
0.75
0.50
0.25
0.00
p < 0.0001
p = 0.024
p = 0.023
0 1 2 3 4 5
Time

Predicted risk group vs 5-year overall survival in GCB classified patients within each dataset: IDRC, LLMPPR-CHOP, and AAU. Risk scores were obtained by taking the average predicted risk score across validation folds for the repeated cross-validation and diving these into tertiles.

Supplementary figure 4:

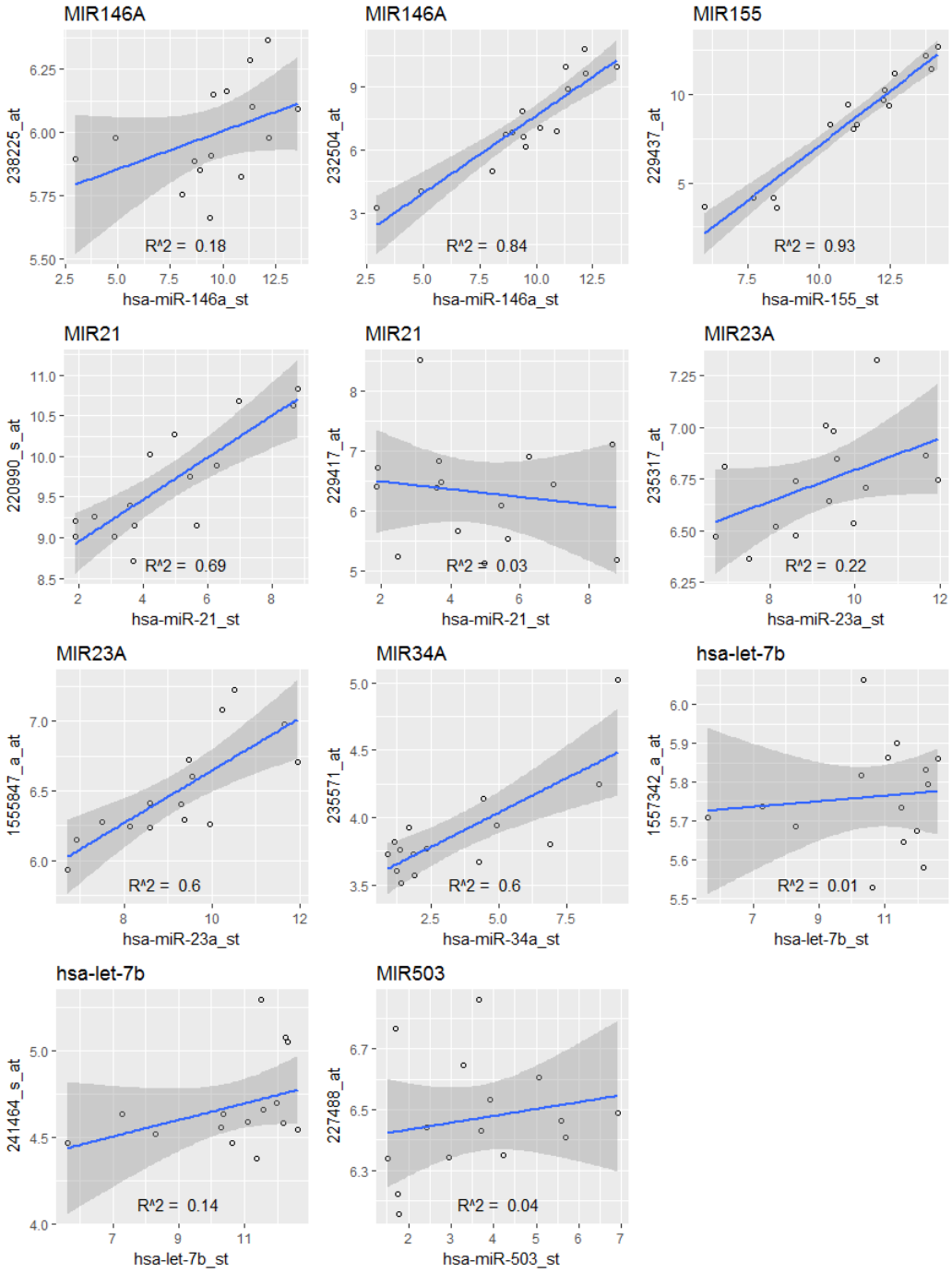

Correlation analysis between mature miRNA and miRNA encoding gene. In 15 DLBCL cell lines, the mature miRNA expression levels were measured by GeneChip miRNA 1.0.2 arrays and the precursors measured by Human Genome U133 Plus 2.0 arrays.

Supplementary figure 5:

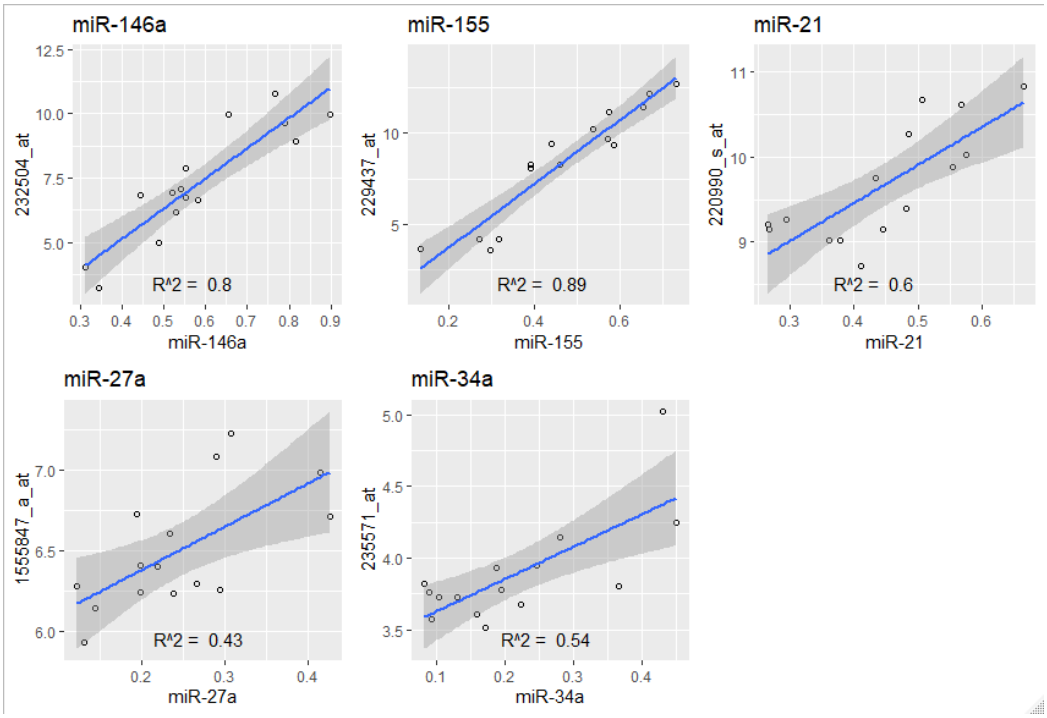

Correlation analysis between mature miRNA and miRNA encoding gene. In 15 DLBCL cell lines, the mature miRNA expression levels were measured by ddPCR and the precursors measured by Human Genome U133 Plus 2.0 arrays.

ISSN (online): 2246-1302
ISBN (online): 978-87-7210-690-8

AALBORG UNIVERSITY PRESS